Fondo Sociale Europeo - FSE
Programma Operativo Nazionale 2000/06
"Ricerca, Sviluppo tecnologico ed Alta Formazione nelle regioni dell'Obiettivo 1" - Misura 1.1 (F.S.E)

University of Calabria

PhD Course in Chemical Engineering and Materials

Thesis

Membrane Contactors for Water Purification and Recovery Factor Increase in Desalination Plants

Settore Scientifico Disciplinare CHIM07 – Fondamenti Chimici delle Tecnologie

Supervisor
Ch.mo Prof. Enrico DRIOLI

PhD Student
Francesca MACEDONIO

Ciclo XXI

PhD Coordinator
Ch.mo Prof. Raffaele MOLINARI

A.A. 2007-2008

INDEX

Summary

The 21st century has been named as "*The Century of Water Shortage*" and its first and second decades have been called as "*The Water Crisis Decades*".
The world's potable water supply, available to support the human, agriculture and industrial needs, is being depleted at an alarming rate and the forecasts are for an increased water scarcity in many regions around the globe by the year 2020 due to: (i) the continuous growth in population, tourist infrastructure and industrial development, (ii) the deterioration of water quality as a consequence of indiscriminate discharge of both domestic and industrial effluents without adequate treatments. Water usage is globally increased by *six* times in the past 100 years and will *doubl*e again by 2050.
Water scarcity, however, encouraged the development of alternative water resources and, because 97% of planet available water is represented by *salty water*, unavoidable was the recourse to sea for alleviating worldwide shortage water problem.
Nowadays, the global installed desalination capacity stands at 52 million m^3/d and it is expected to increase until to 107 million m^3/d in 2016. Among the desalination technologies, membrane based systems are becoming the most widely used processes, whose installations account for close to 80% of all desalination facilities and provide about 50% of the total capacity of desalination plants.
On the other hand, seawater desalination plants cause locally some negative impacts on the environment due to the dumping of their concentrate waste streams, often into surface waters or into the oceans. It is therefore necessary to develop alternative methods to ensure a more sustainable grow of desalination processes.
Ensuring *safe* future worldwide water supplies demands, today, for advanced and environmentally acceptable processes addressed to preserve water and to reduce its consumption. The way to satisfy the increasing water demand under the constrains imposed by the concept of *sustainable development* is a complex problem. The solution can be found in the innovative, low-cost, non-polluting, defect-free and perfectly safe industrial production processes pointing towards *Process Intensification Strategy*, avant-garde cycles whose design support the reduction of pollutant emissions and a more rational use of natural resources. An interesting and successful possibility to more sustainable fresh water production is one more time offered by *Membrane Engineering*, whose basic aspects satisfy the requirements of *Process Intensification.* In particular, the possibility to couple different membrane operations in integrated systems provides unprecedented opportunities in order (i) to develop more cost effective and environmentally acceptable processes, (ii) to use their synergic effects in terms of better performance of the overall system, (iii) to increase the recovery factor of the water treatment system thus reducing brine disposal problem and approaching the concept of "*zero-liquid-discharge"*, *"total raw materials utilization"* and "*low energy consumption*". The integration of diverse but complementary membrane units in the Reverse Osmosis (RO) pre-treatment and post-treatment steps, from the more traditional pressure driven units (as Nanofiltration (NF), Ultrafiltration (UF), Microfiltration (MF)), to the membrane contactors (as Membrane Distillation (MD) and Membrane Crystallization (MCr)), offers the possibility of overcoming the limits of the single operations and is able to solve problems from water quality, to brine disposal, to water cost, to the increasing of the recovery factor, etc.

In this work, the possibility of using integrated membrane desalination systems for improving the current design and operation practices of membrane operations used for water desalination/purification has been investigated. The proposed approach is based on the coupling of different membrane systems in RO pre-treatment and post-treatment stages.
In the pre-treatment steps, the selection of the most appropriate pre-treatment processes leads to the minimisation of membrane fouling problem thereby reducing the operating costs. Moreover, the recourse to NF as RO pre-treatment process has implications on the desalination process itself and not only on the quality of feed water because it decreases the osmotic pressure of the RO feed. In the post-treatment stages, the presence of MCr and/or MD, thanks to their intrinsic characteristic of temperature driven membrane processes, allow to produce fresh water also from highly concentrated feeds (such as the brine streams) with which RO cannot operate due to the osmotic phenomena. Therefore, the introduction of a MD/MCr unit downstream RO and/or NF retentate allows to increase the overall recovery factor, thus reducing the volume of concentrated streams usually discharged by the desalination plants and, in the case of MCr, recovering the dissolved salts in the form of high-quality crystals. Moreover, since MD/MCr technology operates on the principles of vapour-liquid equilibrium, only volatile components are transferred through the membrane. This means that MD can be also used for the treatment of waters containing non-volatile pollutants, in order to convert them into pure waters. Therefore, part of the present research activity has been addressed to study the potentialities of MD and of various integrated membrane systems for boron (B) and arsenic (As) removal from polluted waters.

Since various combinations are possible, different flow sheets (FS), for water purification before and for seawater desalination after, have been analyzed and compared in the present work.

For what concerns the problem of boron and arsenic removal, it is difficult to bring their concentrations down their maximum recommended values (0.3 mg/L and 10 μg/L, respectively) due to their small sizes and neutral charge. Therefore, it becomes of great importance the selection of a proper membrane unit. The obtained results have shown that: only RO membranes or tight NF membranes are really efficient if arsenic is mainly present as As(III); As(V) can be effectively treated by both RO and NF; the boron rejection of the current RO membranes ranges from 89% to 96%, high values but not sufficient for lowering the boron concentration until 0.3 mg/L; a membrane process that allows to achieve the total boron and arsenic (both As(III) and As(V)) removal from waters is instead MD; an integrated system RO+MD, in which a fraction of the RO permeate is treated in a MD module, has been proved to be able not only to reduce the concentration of these contaminants below their maximum recommended values, but also to produce fresh water at a cost competitive with that of the used conventional processes.

For what concerns seawater desalination, the following seven membrane systems have been considered: FS1, constituted by RO preceded by conventional pre-treatment; FS2, in which RO operates on NF permeate; FS3, in which MF and NF have been introduced as pre-treatment and load reduction to the following RO unit. In the remaining four flow

sheets, at the basis scheme represented by FS3, a MCr has been added: MCr operates on NF brine in FS4, on RO brine in FS5, both on RO and NF brine in FS6. In FS7, MCr has been introduced on NF brine while MD operates on RO brine.
The proposed desalination systems have been compared on the basis of their energetic requirement, exergetic efficiency, water cost, amount of discharged brine, fresh water and salts produced. Moreover, the use of the so-called *Sustainable Metrics* has allowed to compare the processes with respect to their size, modularity, plant efficiency and environmental impact. The achieved results have shown that:

- ✓ the introduction of a MCr unit, on one or on both retentate streams, increases plant recovery factor so much to reach 92.8% in FS6, higher than that of a RO unit (about 40%) and much higher than that of a typical Multistage Flash (MSF, about 10%).
- ✓ The presence of a MCr unit (in FS4, FS5, FS6 and FS7) introduces a thermal energy requirement for heating the brine stream and which increases the global energy demand and the water cost. However, in MD/MCr processes the required operating temperatures are lower than that of conventional evaporation processes because it is not necessary to heat the process liquids above their boiling temperatures. Therefore, low-grade, waste and/or alternative energy sources can be coupled with MD/MCr systems. In this condition, energy consumption and desalted water cost of the systems with MD/MCr units decrease reaching competitive values with those of the other processes.
- ✓ Among the desalination systems without MCr unit, FS3 is that to prefer because of the lowest cost and better quality of the produced desalted water.
- ✓ Among the desalination process with MCr unit, FS6 (which means the system with MCr operation on NF and RO retentate streams) is the one to prefer when thermal energy is available in the plant *or* the gain for the salts sale is considered because it is characterized by:
  - the highest recovery factor (92.8%),
  - the lowest amount of drained off retentate stream,
  - the lowest specific energy consumption and desalted water cost,
  - the highest modularity (M),
  - *productivity/size* ratio higher than FS7 and slightly lower than FS4 and FS5.
- ✓ If thermal energy is *not* available in the plant *or* if the gain for the salts sale is *not* considered, FS5 (which means MCr operating only on RO brine) is the desalination system with MCr unit to prefer for what concerns specific energy consumption, desalted water cost and *productivity/size* ratio. However, FS6 remains the best process for what concerns recovery factor, waste production and modularity.

As a consequence, the choice of the most convenient and suitable membrane desalination system depends by many parameters, first of all by the possibility to use alternative energy sources (solar, wind, geothermal, etc.) and by seawater composition, the latter of extreme importance because it influences the amount and the quality of the produced salts. In fact the carried out experimental tests have proved that the crystallization kinetics, the sizes and the shape of sodium chloride and magnesium sulphate heptahydrate (the salts that can be formed from the crystallization of NF and RO brine) are linked to the nature and amount of other ions and foreign substances present in the crystallizing solutions. For example, in the concentration and crystallization of NF retentate, the growth rate of NaCl is accelerated by the presence of

other ions while it is inhibited by the presence of humic acid (the main component of the Natural Organic Matter contained in waters). From here the necessity to control the composition of the MCr feed through the selection of the most suitable RO pre-treatment, because humic acid as well as some other substances present in seawater, besides causing fouling on RO membranes, can lead to the deceleration of growth and to the production of salts exhibiting undesired sizes.
The produced crystals have been characterized by means of crystals size distribution (CSD), middle diameter (d_m), cumulative function and coefficient of variation (CV); the distribution of crystal dimensions, nucleation and growth rate have been studied as a function of the retention time and slurry density; the kinetic parameters have been joined in a power law relation describing the nucleation rate as a function of the growth rate and magma density. Moreover, the experimental tests have also allowed to test fluid-dynamic effect on solvent trans-membrane flux and crystals growth rate.
The achieved results have shown that rising retentate flow rate and temperature, trans-membrane flux increases while the time for reaching supersaturation and crystals formation decreases. The values of the obtained coefficient of variations are lower than those from conventional equipments (equal to about 50%) and are therefore characteristic of narrow crystal size distributions and of qualitatively better products. The achieved kinetic parameters are in substantial agreement with those reported in literature for conventional crystallizers; the small discordances are due to the differences in the hydraulic characteristics of the compared crystallizers and to the presence, in the MCr, of a membrane that improves the nucleation process.
During the carried out experimental tests special focus has been placed on the stability and control of the MCr process by avoiding crystals deposition inside the membrane module and/or on membrane surface.
In the built lab plant, this problem has been avoided in three different ways:

- ✓ by re-circulating the solution in order to remove particles eventually deposited on the membrane surface;
- ✓ by recovering the produced crystals through the “crystals recovery system”;
- ✓ by controlling the temperature of the solution flowing along the membrane module given that the solubility of solids in solution depends on temperature.

The achieved results have been encouraging: the trans-membrane flux is kept almost constant during all the experimental tests. This means no crystals deposition inside the membrane module and/or on membrane surface.
For what concerns the problem of membrane fouling in MCr operation, it has been controlled and managed by means of a proper membrane cleaning: rinsing of the fouled membrane with clean water and chemical solutions has given about 100% of flux recovery.

In conclusion, adoption of the integrated membrane desalination systems with MCr unit seems to have the potentiality of improving water desalination operations, by increasing plant recovery factor, producing valuable crystals for medical/domestic/agricultural use, reducing brine disposal problem and, above all, its negative environmental impact.

Sommario

Il XXI Secolo è stato definito come "*Il Secolo della Carenza di Acqua"* e i suoi primi due decenni come "*I Decenni della Crisi Idrica"*.
Le riserve di acqua potabile del pianeta, in grado di sostenere le esigenze umane, industriali e dell'agricoltura, si stanno esaurendo ad una velocità allarmante. Le previsioni sono per un ulteriore carenza di acqua in molte parti del mondo entro il 2020 a causa (i) della continua crescita della popolazione e (ii) della deteriorante qualità delle risorse idriche attualmente disponibili in seguito ai continui e spesso indifferenziati scarichi degli effluenti domestici e industriali senza adeguati trattamenti. Il consumo medio pro-capite è aumentato di circa sei volte negli ultimi 100 anni e si prevede raddoppierà entro il 2050.
La carenza di acqua, comunque, ha promosso lo sviluppo di fonti idriche alternative e, dato che il 97% della quantità di acqua utilizzabile nel pianeta è presente sotto forma di *acqua salata*, inevitabile è stato il ricorso al mare per alleviare il grave problema della mancanza di acqua nel mondo.
Oggigiorno la quantità di acqua dissalata in tutto il mondo si aggira intorno ai 52 milioni di m^3/d e ci si aspetta che aumenterà fino ad arrivare a 107 milioni m^3/d nel 2016. Per quanto riguarda poi la tecnologia adottata negli impianti di dissalazione, l'80% di questi utilizzano come tecnologia di separazione un processo a membrana e forniscono circa il 50% della quantità totale di acqua dissalata.
D'altra parte, però, il proliferare degli impianti di dissalazione causa impatti negativi sull'ambiente. Essi infatti producono correnti altamente concentrate (retentati o *brines*) che necessitano di essere smaltite e che, spesso, vengono direttamente scaricate nelle acque superficiali o negli oceani. E' necessario dunque sviluppare processi alternativi per assicurare la crescita *sostenibile* degli impianti di dissalazione.
Al momento, assicurare in futuro rifornimenti di acqua che siano *sicuri,* significa puntare ad utilizzare processi avanzati ed eco-compatibili, atti a preservare la qualità delle riserve idriche e a ridurne il consumo.
Il modo di soddisfare la crescente domanda di acqua sotto le limitazioni imposte dal concetto di *Sviluppo Sostenibile* è un problema complesso. Una possibile soluzione può essere trovata in quei processi innovativi, economici, non inquinanti e sicuri che soddisfano le richieste della strategia del "*Process Intensification"*, tecnologie all'avanguardia pensate per ridurre le emissioni inquinanti e per un più razionale utilizzo delle risorse naturali. Un'interessante e possibile soluzione per una più sostenibile produzione di acqua potabile è offerta ancora una volta dalla *Ingegneria delle Membrane*, le cui peculiarità soddisfano le richieste del *Process Intensification*. In particolare, la possibilità di accoppiare diverse operazioni a membrana in sistemi integrati fornisce rilevanti opportunità (i) per sviluppare processi economicamente più efficienti e con meno impatti sull'ambiente, (ii) per utilizzare i loro effetti sinergici in termini di migliore rendimento globale del sistema, (iii) per incrementare il fattore di recupero degli attuali sistemi di trattamento acque riducendo, di conseguenza, il problema di smaltimento del *brine* e accostandosi ai concetti di *"scarichi nulli", "totale utilizzo delle materie prime"* e "*basso consumo energetico"*. L'integrazione di diverse ma complementari unità a membrana negli stadi di pre- e post-trattamento alla Osmosi Inversa (RO), dai più tradizionali processi a membrana indotti dalla pressione (quali la Nanofiltrazione (NF), l'Ultrafiltrazione (UF), la Microfiltrazione (MF)), ai contattori a

membrana (come la Distillazione a Membrana (MD) e la Cristallizzazione a Membrana (MCr)), offre la possibilità di superare i limiti delle singole operazioni ed è in grado di risolvere problemi come il miglioramento della qualità delle acque, la riduzione del problema di smaltimento del *brine* e del costo dell'acqua, l'aumento del fattore di recupero, ecc.

Nel presente lavoro di tesi è stata analizzata la possibilità di utilizzare sistemi integrati a membrana per migliorare il rendimento degli attuali processi a membrana usati nella purificazione/dissalazione delle acque. L'approccio proposto si basa sull'accoppiamento di diversi sistemi a membrana negli stadi di pre-trattamento e post-trattamento alla RO. Un opportuno pre-trattamento riduce infatti i problemi di sporcamento delle membrane e, di conseguenza, i relativi costi operativi. Inoltre, l'introduzione della NF come step di pre-trattamento alla RO ha implicazioni sul processo stesso di dissalazione e non solo sulla qualità dell'acqua in alimentazione poiché essa riduce la pressione osmotica della corrente in alimentazione alla RO. Negli steps di post-trattamento la presenza della MCr e/o della MD, grazie alle loro caratteristiche intrinseche di processi a membrana promossi da una forza spingente di origine termica, consente di ottenere acqua ad elevato grado di purezza anche da soluzioni altamente concentrate (come le correnti di *retentato*) con le quali la RO non potrebbe operare a causa degli effetti osmotici. Pertanto, quando vengono inserite sulle correnti di retentato della RO e/o della NF consentono di incrementare il fattore di recupero dell'impianto riducendo, quindi, il volume delle correnti concentrate solitamente scaricate dagli impianti di dissalazione e, nel caso della MCr, recuperando i sali presenti in tali correnti sotto forma di cristalli di alta qualità. Inoltre, poiché la MD e la MCr operano sul principio dell'equilibrio liquido-vapore, solo i componenti volatili vengono trasferiti attraverso la membrana. Ciò significa che la MD può anche essere usata per la purificazione di acque contenenti sostanze inquinanti non-volatili. Pertanto, parte della presente attività di ricerca è stata rivolta a studiare le potenzialità della MD e di vari sistemi integrati a membrana per la rimozione di boro (B) e arsenico (As) dalle acque inquinate.

Dato che varie sono le combinazioni possibili, diversi flow-sheets (FS), per la purificazione dell'acqua prima e per la dissalazione dell'acqua di mare dopo, sono stati analizzati e confrontati nel presente lavoro.

Per quanto riguarda il problema della rimozione di boro e arsenico, è difficile abbassare le loro concentrazioni nelle acque al di sotto del limite massimo raccomandato (rispettivamente 0.3 mg/L e 10 μg/L) a causa delle loro piccole dimensioni e della carica neutra. E' pertanto di estrema importanza scegliere un opportuna operazione a membrana. I risultati ottenuti hanno mostrato che: soltanto moduli a membrana da RO o da NF con pori stretti sono realmente efficienti quando l'arsenico è presente nelle acque principalmente come As(III); As(V) può essere effettivamente rimosso sia tramite la RO che la NF; la reiezione del boro delle attuali membrane da RO varia tra l'89 e il 96%, valori molto alti ma non tali da abbassarne la concentrazione fino a 0.3 mg/L; un processo a membrana che consente, invece, di ottenere la totale rimozione di boro e arsenico dalle acque (sia As(III) che As(V)) è la MD; il sistema integrato RO+MD, in cui parte del permeato della RO viene trattato in un modulo MD, si è dimostrato in grado non solo di ridurre la concentrazione di tali componenti al di sotto del loro limite

massimo ma anche di produrre acqua a costi competitivi con quelli dei processi convenzionali attualmente utilizzati.

Per quanto riguarda la dissalazione delle acque di mare, i seguenti sette sistemi a membrana sono stati considerati: FS1, costituito dalla RO preceduta da un pre-trattamento di tipo convenzionale; FS2, in cui la RO opera sul permeato della NF; FS3, in cui MF e NF sono state introdotte come pre-trattamento e riduzione del carico al successivo stadio di RO. Nei restanti quattro flow sheets, allo schema di base rappresentato da FS3 è stata aggiunta la MCr: in FS4 è stata inserita sul retentato della NF, in FS5 su quello della RO, in FS6 sia sul retentato della NF che su quello della RO, in FS7 sul retentato della NF mentre su quello della RO è stato inserito uno stadio di MD. I sistemi di dissalazione proposti sono stati confrontati in base alla loro richiesta energetica ed efficienza exergetica, in termini di costo dell'acqua prodotta e in base alla quantità di retentato scaricato, di acqua dissalata prodotta e di sali ricavabili dalle unità di cristallizzazione a membrana. Inoltre, l'utilizzo dei così detti "*Sustainable Metrics*" ha permesso di confrontare i processi rispetto alla loro dimensione, modularità, efficienza e impatto ambientale. I risultati ottenuti hanno mostrato che:

- ✓ l'introduzione dei cristallizzatori a membrana, su una o su entrambe le correnti di retentato, fa aumentare considerevolmente il fattore di recupero globale fino a raggiungere il valore di 92,8% in FS6, ben più alto di quello ottenibile dalla sola unità di RO (circa il 40%) e, comunque, molto più alto di quello di un tipico impianto termico quale la Distillazione a Flash Multistadio (MSF, pari a circa il 10%).
- ✓ La presenza del cristallizzatore a membrana (in FS4, FS5, FS6 ed FS7) introduce una richiesta energetica termica, necessaria per riscaldare la corrente di retentato e che fa aumentare la domanda energetica globale e il costo dell'acqua. Tuttavia, nei processi di MD/MCr le temperature di esercizio sono più basse dei processi di evaporazione convenzionali perché non è necessario riscaldare i liquidi di processo al di sopra della loro temperatura di ebollizione. Pertanto, fonti di energia alternativa e/o di scarto possono essere accoppiate con i sistemi MD/MCr per sopperire ai fabbisogni energetici del processo. In tali condizioni il consumo di energia e il costo dell'acqua dissalata dei sistemi con unità di MD/MCr si abbassano notevolmente raggiungendo valori competitivi con quelli degli altri processi di dissalazione.
- ✓ Tra i sistemi di dissalazione senza MCr, FS3 è quello da preferire perché caratterizzato dal costo più basso e dalla migliore qualità dell'acqua dissalata prodotta.
- ✓ Tra i sistemi di dissalazione con unità di MCr, FS6 (ovvero il processo con MCr sulle correnti di retentato sia della NF che della RO) è quello da preferire quando energia termica è disponibile nell'impianto *o* quando si tiene conto del ricavo proveniente dalla vendita dei sali perché è quello caratterizzato
  - dal fattore di recupero più alto (92.8%),
  - dal più piccolo volume di retentato da scaricare,
  - dalla più bassa richiesta energetica e costo dell'acqua dissalata,

- il più modulare,
- il cui rapporto *produttività/dimensione* è maggiore di FS7 e leggermente inferiore di FS4 e FS5.

✓ Se energia termica *non* è disponibile nell'impianto *o* non si tiene conto del ricavo proveniente dalla vendita dei sali, FS5 (ovvero il processo con unità di MCr solo sul retentato della RO) è il sistema di dissalazione con unità di MCr da preferire per quello che riguarda il consumo specifico di energia, il costo dell'acqua dissalata e il rapporto *produttività/dimensione*. Comunque, FS6 rimane il processo migliore per quello che riguarda il fattore di recupero, la quantità di prodotto di scarico prodotto e la modularità.

Di conseguenza, la scelta del sistema di dissalazione a membrana più conveniente e adatto dipende da molti parametri, innanzitutto dalla possibilità di utilizzare fonti di energia alternativa (solare, eolica, geotermica, ecc.) e dalla composizione dell'acqua di mare, questa ultima di estrema importanza perché influenza la quantità e la qualità dei sali prodotti. Difatti gli esperimenti condotti hanno mostrato che le cinetiche di cristallizzazione, le dimensioni e la forma del cloruro di sodio e del solfato di magnesio eptaidrato (i sali che si possono formare dalla cristallizzazione del retentato della NF e della RO) sono legati alla natura e alla quantità di altri ioni e sostanze estranee presenti nelle soluzioni da cristallizzare. Per esempio, nella concentrazione e cristallizzazione del retentato della NF, la velocità di crescita del NaCl è accelerata dalla presenza di altri ioni mentre è inibita dalla presenza di acido umico (il componente principale del Materiale Organico Naturale contenuto nelle acque). Da qui la necessità di controllare la composizione della corrente in alimentazione della MCr attraverso la scelta del più adatto pre-trattamento alla RO, poiché l'acido umico e le altre sostanze presenti nell'acqua di mare, oltre a causare sporcamento nelle membrane da RO, possono provocare la decelerazione della crescita e la produzione di sali di dimensioni indesiderate.

I cristalli prodotti sono stati caratterizzati tramite la distribuzione della dimensione dei cristalli (CSD), il diametro medio (d_m), la funzione cumulativa e il coefficiente di variazione (CV); la distribuzione delle dimensioni dei cristalli, la velocità di nucleazione e crescita sono stati studiati in funzione del tempo di ritenzione e della densità di magma; i parametri cinetici sono stati uniti in una relazione di potenza che descrive la velocità di nucleazione in funzione della velocità di crescita e della densità di magma. Inoltre, le prove di laboratorio hanno anche permesso di testare l'effetto della fluidodinamica sul flusso di trans-membrana di solvente e sulla velocità di crescita dei cristalli.

I risultati ottenuti hanno mostrato che, aumentando la portata e la temperatura, il flusso di trans-membrana aumenta mentre il tempo per raggiungere la sovrassaturazione e la formazione dei cristalli diminuisce. I valori ottenuti per il coefficiente di variazione sono risultati più bassi di quelli dei cristallizzatori convenzionali (circa uguali al 50%) e sono pertanto caratteristici di distribuzioni delle dimensioni strette e di un prodotto cristallino qualitativamente migliore. I parametri cinetici ottenuti sono in sostanziale accordo con quelli riportati in letteratura per cristallizzatori convenzionali; ovviamente alcune discordanze sono presenti e sono dovute alle differenze nelle caratteristiche

idrauliche dei cristallizzatori confrontati e alla presenza, nel MCr, di una membrana che favorisce il processo di nucleazione.

Durante la conduzione delle prove sperimentali speciale attenzione è stata rivolta al controllo e alla stabilità del processo di MCr per evitare che si crei accumulo di cristalli sulla superficie della membrana e/o all'interno del modulo a membrana.

Nell'impianto di laboratorio, tale problema è stato evitato in tre diversi modi:

- ✓ ricircolando la soluzione in modo da rimuovere particelle eventualmente depositate sulla superficie della membrana;
- ✓ recuperando i sali prodotti attraverso un "*sistema di recupero cristalli*";
- ✓ controllando la temperatura della soluzione che fluisce lungo il modulo a membrana dato che la solubilità dei solidi in soluzione dipende dalla temperatura.

I risultati ottenuti sono stati incoraggianti: il flusso di trans-membrana si è mantenuto pressoché costante durante tutte le prove sperimentali. Questo significa che non si è verificato l'accumulo di cristalli all'interno del modulo a membrana e/o sulla superficie della membrana.

Per quanto riguarda poi il problema dello sporcamento delle membrane nel processo di MCr, questo problema è stato tenuto sotto controllo tramite un opportuno procedimento di pulizia delle membrane: pulendo la membrana sporca con acqua pulita e con soluzioni di alcune sostanze chimiche si è avuto un recupero del flusso di circa il 100%.

In conclusione, il ricorso a sistemi di dissalazione integrati a membrana con unità di Cristallizzazione a Membrana sembra avere le potenzialità di migliorare le operazioni di dissalazione dell'acqua di mare, incrementando il fattore di recupero dell'impianto, producendo cristalli di buona qualità per uso domestico/medico/agricolo, riducendo il problema di smaltimento del *brine* e, soprattutto, il suo negativo impatto sull'ambiente.

Introduction to the work

Together with the supply of energy and the environmental protection, fresh water is one of the three keys elements for the sustainable development of every society. Fresh water is needed in agriculture, as drinking water, and as process water in a large variety of industries. Where the availability of water cannot be carried out by using conventional sources, unavoidable appears the resort of the major water source: the sea. As a matter of fact, desalination processes represent a valid solution to the water shortage problem and their application has completely changed the situation in many arid zones in the world. The current global installed desalination capacity stood at 52 million m^3/d. The principal desalination processes are enclosed in two main categories: thermal and membrane separation methods. At present, Reverse Osmosis (RO) is the most widely used process, whose installations account for close to 80% of all desalination facilities and provide about the 50% of the total capacity of desalination plants.

Despite the great success of membrane technology, some critical problems still remain open, such as: improving the water quality, increasing the recovery factor of desalination processes, reducing the global costs and minimizing the brine disposal impact. In effect, seawater desalination processes are positively contributing to solve the problem of water shortage but, at the same time, they cause locally some negative impacts on the environment that need to be minimized. In particular, nowadays, the majority of desalination facilities discharge their concentrate waste streams into surface waters or oceans. Currently, this disposal method represents the most effective and least expensive option for both small and larger systems located near coastal regions. However, the promulgation of more and more stringent environmental protection regulations is reducing progressively this opportunity. It is therefore necessary to develop alternative methods not only for decreasing the water cost but also for ensuring a more sustainable grow of desalination processes.

At present, the most interesting development for industrial membrane technologies are related to the possibility of *coupling different membrane operations* for overcoming the limits of the single units and using their synergic effects in terms of better performance of the overall system. The *integration of various membrane units* may contribute *to decrease* in particular *problems related to water recovery factor, brine disposal, cost and quality of water*, and *for reaching* all the important benefits in the logic of *Process Intensification*. This is a new strategy which consists in the development of avant-garde techniques that, compared to those commonly used today, are expected to bring drastic improvements in manufacturing and processing, substantially decreasing equipment size/production capacity ratio, energy consumption, or waste production.

As a matter of fact, in the last years the reliability of RO is greatly increased also as a consequence of the development of other various membrane operations (such as microfiltration (MF), ultrafiltration (UF) and nanofiltration (NF)), that can be combined with RO in the *pre*-treatment steps: MF is an obvious technique for the removal of suspended solids and large bacteria thus providing a RO feedwater of good quality with consequent extension of membranes life time and reduction of their maintenance and replacement costs; the introduction of NF as pre-treatment step leads to significant improvement in the reliability of RO because it decreases the osmotic pressure of the RO feed stream thus allowing to the unit to operate at higher recovery factors without scaling problems.

In this logic well fit in also Membrane Distillation (MD) and Membrane Crystallization (MCr) techniques that can be combined with RO in the *post*-treatment steps. MD is a temperature-driven membrane operation which is not limited by concentration polarization phenomena as it is the case in pressure driven processes. This means that it allows to obtain fresh water also from highly concentrated aqueous solutions with which RO cannot operate. Therefore, when MD operates on RO brine, more fresh water can be produced thus increasing the recovery factor of the desalination plant. MCr has been recently proposed as one of the most interesting and promising extension of the MD concept, an innovative process for the quasi total recovery of the desalted water combined to solid salts production. As a matter of fact, this innovative technology uses evaporative mass transfer of volatile solvents through microporous hydrophobic membranes in order to concentrate feed solutions above their saturation limit, thus attaining a supersaturated environment where crystals may nucleate and grow. When a MCr follows an NF or an RO stage, the highly concentrate brine does not represent waste but the mother liquor in which crystals could nucleate and grow.
Membrane crystallizer has another advantage: reduces until to eliminate brine disposal problem.
In the concentration and crystallization process, the knowledge and the control of the composition of the feed solutions are of extreme importance in order to aim to the production of salts of high quality, whose structures and morphologies (size, size distribution, shape, habit) are adequate to represent a *valuable product*, thus transforming the traditional brine disposal cost in a new and profitable market.
Moreover, new problems are recently gaining wide attention in the water treatment community, such as those related to pollutants removal from water (like boron, arsenic and pharmaceuticals compounds) due to their adverse effects both on human health and on agriculture, and to their growing consumption in current industry, as in the case of arsenic whose use as an intermediary in the manufacture of electronic products has been growing with total use up 13% between 1990 and 1996. Since MD operation operates on the principles of vapour-liquid equilibrium, only volatile components are transferred through the membrane. As a consequence, MD or integrated membrane systems with MD units can be used for the treatment of polluted water in order to convert it into pure water and in a concentrate containing the substances present in the parent solution.

The work presented in this thesis has four main objectives. The first purpose is to propose and analyse different possible flow sheets for seawater desalination based on integrated membrane operations. In order to reach this goal, a good knowledge of each membrane unit is necessary in order to find the most convenient integration and for a systematic analysis of possible advantages or drawbacks due to the introduction of a membrane stage instead of a conventional unit.
The second purpose is the comparison of the proposed desalination systems on the basis of the quality and characteristics of the produced fresh water and salts, of the discharged brine, of the desalted water cost, of the energy requirement and exergy efficiency. The third and main purpose of the present work is to test, experimentally, the potentialities of membrane crystallization for the exploitation of some components contained in seawater, in terms of amount and characteristics of the produced crystals and in terms of control of the stability of the process. Finally, the fourth objective is related to the analysis of the efficiency of an innovative integrated membrane based process for water

purification. In the proposed system, conventional pressure driven membrane separation units are combined with membrane contactor technology for the production of water streams with boron and arsenic concentrations below the WHO (the World Health Organization) and EPA (the U.S. Environmental Protection Agency) maximum recommended values.

The thesis is composed of seven chapters. The First Chapter briefly emphasises the role of desalination technologies as reliable remedy to water shortage and gives an overview on the existing thermal and membrane desalination processes. Moreover, the various membrane operations are described in terms of membrane structure, separation mechanism, limits and potentialities in integrated desalination schemes. The different integrated desalination systems are presented and described in the Second Chapter, where energy and mass equations are applied in order to determine the composition of the different streams and the energy consumption of the various flow sheets. The comparison of the proposed desalination systems is realized in the Third Chapter.
The Fourth Chapter gives the off to the section addressed to the experimental study through the description of the built and utilized lab plant.
The evaporative crystallization of sodium chloride and magnesium sulfate heptahydrate from aqueous solutions has been used as vehicle for preliminary experimental study in the Fifth Chapter. The interest for NaCl and for $MgSO_4 \cdot 7H_2O$ crystallization is due to the fact that they are the salts naturally present in the highly concentrated streams of the desalination plants. Results of the crystallization tests carried out on NF and RO retentate streams, in terms of crystals quality, nucleation and growth kinetic rates, are presented and discussed in the Sixth Chapter. The Seventh Chapter is instead dedicated to the analysis of the efficiency of MD and of different integrated membrane processes for boron and arsenic removal from water.

CHAPTER 1: Desalination Technologies

Table of Contents

1. Introduction

Water is one of the simplest and most indispensable molecules in the world, whose growing scarcity and declining quality negatively affect the overall quality of human life and the industrial and *sustainable* development of our society.

On the other side, current *water increasing scarcity and deteriorating quality* are the expected outcomes of the continuous growth in population, tourist infrastructure and industrial development of our World: water usage is globally increased by *six* times in the past 100 years and will *double* again by 2050 [1], driven mainly by industry, irrigation and demands of agriculture. This caused a reduction in the *renewable* water resources per capita of up to about 80% in the last 10-15 years, particularly in some of the countries of the Mediterranean and Middle East area. The forecasts are for an increased water scarcity in many regions around the globe by the year 2020:

- ✓ US Filter is predicting *water stress* only 15 years from now in China, southeast and southwest Asia, India, the Middle East, North Africa, South Africa, and the western United States. Water stress is a global measure of water available for socio-economic development and agricultural production.

Mathematically, *water stress index* is the ratio of a country's total water withdrawal to its total renewable freshwater resources and can be expressed as volume per person per year [m^3/p/y] or as percentage [%]: with values less than 10% or below 1,700 m^3/p/y, water stress is considered low; a ratio in the range of 10–20% or between 1,700 and 1,000 m^3/p/y indicates that water availability is becoming a constraint on development and that significant investments are needed to provide adequate supplies; when the volume per person per year is below 1,000 m^3/p/y or the water stress index is above 20%, comprehensive management efforts to balance supply and demand are supposed to be necessary.

- ✓ Average per capita water availability in MENA regions is today ≈ 1,200 m^3/p/y and it is projected to become ≈ 500m^3/p/y by 2025 (WBO, 2004);
- ✓ moreover, approximately half of the European countries, representing almost 70% of the population, are facing water stress issues today [2]. Figure 1 ranks the European countries according to their water stress index.

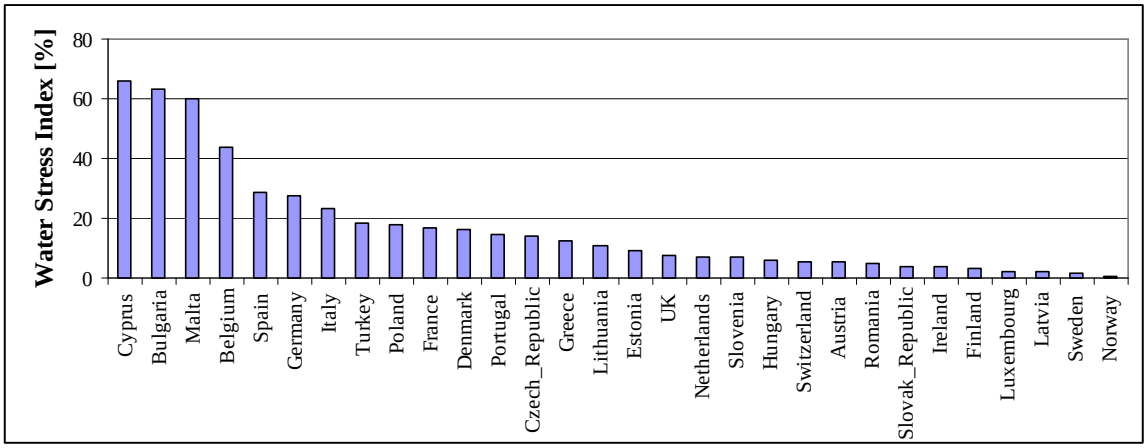

Figure 1: Water Stress Index for the European countries [2].

Water scarcity, however, encouraged the development of water production technologies. As can be seen in Figure 2, the planet's available water resources do not provide many alternatives: because much of this precious limited supply is either locked in the polar ice, or it is found in a limited number of lakes and rivers throughout the world, the largest potential source of alternative water is represented by *salty water* (97% of available water) and requires desalination.

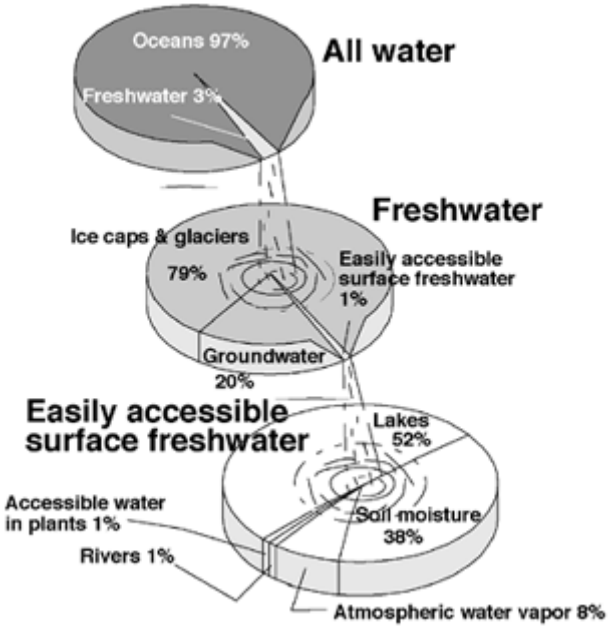

Figure 2: Distribution of the World's Water (Source: Lean & Hinrichsen 1994 (107) available on-line at http://www.infoforhealth.org/pr/m14/m14.pdf).

In a lot of the countries of the World, such as in China, Spain, California and Australia, the governments have already issued large-scale programs to desalinate sea-, brackish- and marginal-water sources (marginal water include industrial, agricultural and municipal effluents as well as contaminated surface and well waters). According to the International Desalination Association [3-5], through the first eight months of 2007 the year's new contracted capacity was 5 million m^3/d (a 28.9% increase over 2006) and the installed capacity was 3.8 million m^3/d (a 17% increase). The global installed desalination capacity stood at 46 million m^3/d in the first eight month of 2007 (representing an annual increase of 8.8% over 2006's total), and it is expected to increase from the current 52 million m^3/d to 107 million m^3/d in 2016 (Table 1). In the current and future sea-brackish water desalination plants, membrane based systems are the most widely used processes, whose installations account for close to 80% of all desalination facilities and provide about the 50% of the total capacity of desalination plants [6].

Table 1: How the desalination market is growing[I].

Year	Installed Capacity [million m^3/d]	Annual Increase [%]		Year	New contract capacity [Mm^3/d]	Annual Increase [%]	New capacity [Mm^3/d]	Annual Increase [%]
1997	22.6	8		1997	1.3		1.7	
1998	24	6.3		1998	1.6	17.4	1.4	-15.1
1999	25.2	4.7		1999	1.8	12.6	1.1	-20.9
2000	26.9	6.8		2000	2.6	46.2	1.7	53.1
2001	28.5	6.2		2001	3.0	15.6	1.7	-3.5
2002	31.6	10.8		2002	2.2	-25.9	3.1	86.8
2003	33.7	6.4		2003	3.5	59.1	2.0	-34.4
2004	36.9	9.7		2004	2.6	-24.5	3.3	61.2
2005	39.4	6.7		2005	4.6	75.1	2.5	-24.2
2006	42.6	8.1		2006	3.9	-16.4	3.2	29.6
2007 (8 months data only)	*46.4*	*8.8*		2007 (8 months data only)	*5.0*	28.9	3.8	*17.0*
2008*	52	12.1						
2016*	107	13.2						

*projections.

Without a doubt, the use of desalination is now rising around the world:

- ✓ in Algeria, the government is currently acting on the belief that the best way to jump-start the economy is to provide water for private consumption and for industry.
- ✓ According to a plant jointly issued by the State Development & Reform Commission, the National Bureau of Oceanography and the Ministry of Finance, desalinated seawater is expected to contribute 16 to 24% of the water supply in Chinese coastal areas in 2010, with a daily capacity of 800,000 to one million m^3 [7]. The daily capacity is expected to reach 2.5 to 3 million m^3 in 2020.
- ✓ The California Department of Water Resources (DWR), in November 2002, was authorized to administer a 50US$ million desalination grant program aimed to assist water utilities state-wide in the implementation of brackish and seawater desalination projects. The first round of this program was carried out in 2005 by awarding 24.75US$ million to 24 different desalination projects. The second round of the DWR program awarded another 21.5US$ million of grants to 23 projects in June 2006. The funded projects are planned to be completed by 2009 and are expected to yield practical solutions to key environmental, energy and cost challenges facing desalination today. The California desalination initiative is expected to yield over 20 new projects state-wide which would supply up to 10% of the total water demand along the coast by year 2020 and would produce approximately 2 million m^3 of new drinking water by 2030 [8].

In realty, since the biggest issue in the water industry is indeed *sustainability*, governments need to look at how their new desalination plants can be more efficient to

[I] Source: after *Water Desalination Report* and *IDAnews* [3-5].

reduce water usage, to conserve water supply and to reduce the environmental effects that often arise in term of both energy consumption and disposal of the residual brine. In fact, for every litre of water taken from the sea, less than half becomes desalted. The remaining brine has about twice the salinity of seawater and it is usually returned to the sea.

The way to satisfy the increasing water demand under the constrains imposed by the concept of *sustainable development* is a complex problem. An interesting and successful possibility to more sustainable fresh water production is one more time offered by *Membrane Engineering*, whose basic aspects satisfy the requirements of *Process Intensification*. In fact, as described with more details in the next paragraphs, some characteristics of membrane operations offer the possibility of completely redesigned water production, water treatments and water distributions systems, based on the concept of *Integrated Membrane Operations*, coupling several membrane processes in order to overcome the limits of the single units and to increase the performance of the overall system, for the optimization of water use, the minimization of water leaks and for its reuse in a timeframe much shorter than the one we are used today.

2. Process Intensification Strategy

Process Intensification is a strategy which refers to advanced and innovative technologies aiming to replace large-, expensive-, energy intensive-, polluting-equipments and/or processes, with avant-garde versions that are smaller, less costly, more efficient, less polluting, highly safe and automatized. Therefore, Process Intensification Strategy means pointing towards technologies and processes that are compact and that reduce energy consumption, material usage and waste production. In a few words, this strategy aims to *produce much more with much less* [9] for more *sustainable* industrial processes. This leads to select processes not only on an economic basis, but also aspects such as the *increased selectivity* and *environmental impact* linked to the process itself are important parameters to take into account. Therefore, nowadays, it is become necessary to promote innovative, low-cost, non-polluting, defect-free and perfectly safe industrial production processes; avant-garde cycles whose design could support the reduction of pollutant emissions and a more rational use of natural resources. This is particularly true when, for the human necessities and in the industrial cycles, water (and often high-purity water) is used in large amount.

Currently, advances in nano-scale science and engineering are providing unprecedented opportunities to develop more cost effective and environmentally acceptable processes. Membrane operations respond efficiently to the requirement of Process Intensification because they have the potential to replace conventional energy-intensive techniques (such as distillation and evaporation), to realize the selective and efficient transport of specific components, to reach advanced levels of automatisation and remote control. Nowadays, membranes techniques are essential operations to a wide range of applications, including the production of potable water, energy generation, tissue repair, pharmaceutical production, food packaging, and the separations needed for the manufacture of chemicals, electronics and a range of other products [10]. At the heart of every membrane processes there is an interface, which is clearly materialized by a nano-

structured/functionalised thin barrier that controls the exchange between two phases, not only by external forces and under the effect of fluid properties but also through the intrinsic characteristics of the membrane material itself. Membrane technology has already gained a huge importance in the last two decades and now is competing with other separation technologies in terms of energy efficiency, high separation capacity, selective separation and more investments. In a number of occasions, commercial *conventional* separation processes in industry were converted to *membrane* separation processes. This is what happened in water desalination. The oldest desalination methods were thermal technologies (that is Multi Stage Flash–MSF, Multi Effect Distillation-MED, Vapour Compression- VC), based on evaporating water and collecting the condensate. The newest desalination technologies are based on membrane treatment, in particular on Reverse Osmosis (RO) which now dominates the desalination market because more efficient, requiring less physical space and less energy consuming than vaporization or distillation [6].

At present, the most interesting developments for membrane technologies are related to the possibility of *integrating different membrane operations*, which means coupling several membrane processes in order (i) to overcome the limits of the single units and (ii) to use their synergic effects in terms of better performance of the overall system for decreasing water cost and brine disposal problem (see *section 4*). This offers new opportunities in the design, rationalization and optimization of industrial processes and it is recently emerging as an essential requisite for approaching the concept of *"zero-liquid-discharge", "total raw materials utilization"* and *"low energy consumption"* according to Process Intensification Strategy, transforming the traditional brine disposal cost in a new and potential profitable market.

3. Potentiality of membrane processes in desalination schemes

The idea that pure water could be made from seawater tantalized thirsty humans for hundreds, if not thousands, of years. In 1961, at an event to mark the start-up of the first seawater to freshwater conversion plant in the United States at Freeport (Texas), the then president of the United States, John F. Kennedy, commented: "*Today is an important step towards the achievement of one of man's oldest dreams, to secure freshwater from saltwater*" [11]. The original premise was based on the fact that boiling or evaporating water separates water from salt.

At the beginning, in the '60s, the only process for seawater desalination was the distillation.

The first large-scale desalination plants that sprouted in the desert areas in 1960s were thermal processes. These areas were lacking in water but with plenty of fuel to burn. In fact, energy requirements for thermal processes (in particular MSF and MEE) are high because they consume heating steam to drive the flashing and evaporation processes, and also they use a considerable amount of electrical power to drive the pumps. After about 10 years two new processes were developed: Multi Effect Distillation (MED) and Reverse Osmosis (RO).

Researchers began to study the possibility of using a membrane to separate salts from seawater since the early 1900s. The principle at the basis of the new strategy was the

osmotic nature of cell walls: semi-permeable membranes allow water to pass through, creating an equilibrium between a highly concentrated solution on one side of the membrane and a diluted solution on the other. With the right amount of pressure and with the correct membrane design, this natural phenomenon could be reversed: instead of flowing from the diluted to the concentrated solution, the concentrate can be forced to pass through the membrane. The first RO desalination membranes were developed in the second half of the 20th Century. Desalination by RO entered the commercial market in the late 1960s when the membrane manufacturing process became efficient enough to produce desalted water that was competitive with thermal processes. However, though more efficient than vaporization or distillation and requiring far less physical space for the same operation, the first plants demanded a high energy input. Over time, engineers developed Energy Recovery Systems (like Pelton turbine, Pressure Exchanger System, etc.) that take advantage of the high pressure of the RO waste brine streams. This led to sheer drops in the energy consumption and, as a consequence, in the desalted water cost. At the same time also the cost of the RO membranes dropped of about 50%. An example can be found in some SWRO elements developed by the Dow Chemical Company in the 1980s and 1990s. In 1996 the company introduced in the market the SW30HR-380 element as the improvement of its SW30HR-8040 element (another SWRO membrane of nine years older, with a nominal flux lower than 25% and a salt passage lower than 33%): the market price of a SW30HR-380 element in 1996 was about 50% that of an SW30HR-8040 in 1985 [11].

In 1996, the MSF total market share of sea and brackish water accounted for more than 54% while the RO process was slightly above 36%. At the end of 90s, these numbers became more close with 42.4% and 41.4% for MSF and RO, respectively [12]. In the middle of 2000s, the new MSF and RO contracts accounted for 32% and 54%, respectively. Today there are more than 15,000 desalination plants in the world and the number of membrane desalination installations accounts for close to 80% of all desalination facilities (90% of which use RO technology) [6]. These values represent an opposite trend with respect to the past period. Anyway, it should be noted that MSF projects are limited to seawater desalination; instead, RO contracts include various applications such as seawater, brackish water as well as river water treatment.

Table 2 summarizes the main advantages of membrane versus thermal desalination techniques.

Table 2: Conventional and membrane separation methods: comparison.

Thermal desalination processes for seawater (MSF, MED, VC)	**Membrane desalination processes for seawater (RO)**
Desalted water with low total dissolved solids concentrations (10-20 ppm)	Desalted water with total dissolved solids concentrations between 100 and 550 ppm
Energy consumption (MSF and MED) = 25.7÷26.4 kWh/m^3	Energy consumption = 2.2 ÷ 6.7 kWh/m^3 (6.7 kWh/m^3 using the steam cycle generation of electricity with an efficiency of only 33%) [14]
Recovery factor ≈ 10%	Recovery factor ≈ 40 % (using a 65 bar feed pressure)
High capital costs High operating costs	Low capital costs Low operating costs
Desalted water cost [13] ≈ *1.0÷1.4* \$/m^3 (MSF) ÷ *2.34* \$/m^3 (MED, TVC)	Desalted water cost ≈ *0.50 ÷ 0.70* \$/m^3 (in the most part of SWRO plants [15, 16]) and 0.36\$/m^3 (in the modern plants [17])

Table 3 shows some of the largest seawater desalination plants using reverse osmosis technology in the world.

Table 3: Some of the World's Largest SWRO Plants.

SWRO plant	Capacity [MGPD]
The Rongcheng of Shandong and Dalian Petrochemical,China	1.3
Tajura City, Libya	2.6
Gela, Sicily	4.4
Curacao, Antilles	4.8
Las Palmas, Telde	9.2
Dhekelia, Cyprus	10.6
El Coloso (Chile)	12
Alicante, Spain	13.2
Almeria, Spain	13.2
Madinat Yanbu Al-Sinaiyah (Red Sea)	13.3
Larnaca, Cyprus	14.3
Marbeilla, Spain	14.5
Jeddah (two plants), Red Sea	15
Palma de Mallorca	16.6
Cartagena, Spain	17.2
Murcia, Spain	17.2
Jubail, Red Sea	20
Tampa Bay	25
Trinidad and Tobago	28.8
Carboneras, Spain	32
Madina-Yanbu, Red Sea	33.3
Singapore	36
Campo de Mauricia	37
Fujairah, Emirati Arabi Uniti	45
Ashkelon (Tel Aviv)	84.4
Rishon Letzion (Israel)	100

The research and the experience developed over more than forty years, have brought that nowadays, only in China, there are about 20 desalination plants. In 2006, market analysts Global Water Intelligence put the online installed capacity (including Hong Kong and Macau) at about 380,000m^3/d, the most part of which through SWRO plants (see Table 4 which lists some large-scale SWRO today successfully operating in China [18, 19]). The daily capacity is expected to reach 2.5 to 3 million m^3 in 2020 (Table 5).

Table 4: Large-scale SWRO in China.

Year	Place	Yield of fresh water [m^3/d]
1997	Zhoushan Shengshan Island	500
1997	Shensi County of Zhejiang Province	500
1999	Changhai County of Liaoning	1000
1999	Da Changshan Island	1000
2000	Changdao County of Shandong Province	1000
2000	Changhai County of Liaoning Province	500
2000	Long Land of Shandong Province	1000
2000	The Rongcheng of Shandong and Dalian Petrochemical	5000
2001	Shensi County of Zhejiang Province	1000
2001	Weihai City of Shandong Province	2000
2001	Daliang City of Liaoning Province	2000
2001	Cangzhou County of Hebei Province	18,000*

* (for brackish water)

Table 5: Additional desalination in China by 2010 and 2020 [20].

Province/city	**2010 ('000 m^3/d)**	**2020 ('000 m^3/d)**
Dalian	80-100	150-200
Fujian	0-5	30-50
Guangdong	10-20	50-100
Guangxi	0-5	10-20
Hebei	150-180	200-250
Hainan	0-5	30-50
Jiangsu	0-5	10-20
Liaoning	60-80	150-200
Ningbo	10-20	100-150
Qingdao	180-200	350-400
Shandong	200-250	450-500
Shanghai	0-5	30-50
Shenzhen	10-20	30-50
Tianjin	200-250	450-500
Xiamen	0-5	30-50
Zhejiang	100-150	450-500
Total	**800-1,100**	**2,520-3,090**

Recent climatic changes and population growth throughout Australia have produced the state's first large-scale desalination facility: Perth Seawater Desalination Plant (PSDP), to be built at Kwinana and with a peak capacity of 144,000 m^3/day. The PSDP will also hold the title of the largest desalination plant in the southern and eastern hemispheres into the foreseeable future. But, most importantly, it will provide a secure supply of water that does not depend on rainfall. Also the new PSDP facility uses seawater reverse osmosis technology. Its low energy consumption (an overall 24MW requirement and a production demand of 4.0 kWh/kL to 6.0 kWh/kL) in comparison with those of the other conventional desalination technologies, allows that the electricity for the desalination plant will come from the new 80 MW Emu Downs Wind Farm (a wind farm which consists of 48 wind turbines). The power supply arrangement makes the desalination plant the largest facility of its kind in the world to be powered by renewable energy.

By November 2006, Gold Coast City, Sydney, Adelaide, Brisbane and Gosford-Wyong are among other coastal Australian cities considering seawater desalination.

3.1 Pressure driven membrane operation

Aim of this section is to give an overview on the pressure driven membrane technologies commonly used in desalination processes.

Pressure driven membrane operations can be divided into four overlapping categories of increasing selectivity: Microfiltration (MF), Ultrafiltration (UF), Nanofiltration (NF) and Reverse Osmosis (RO). In all four processes, a mixture of different components is brought to the surface of a semi-permeable membrane; under the driving force gradient, some components permeate the membrane while others are more or less retained. Thus, a feed solution is separated into a filtrate which is depleted of particles or molecules, and a retentate in which these components are concentrated.
As we go from MF through UF to NF and RO, the size (Molecular Weight) of the particles or molecules separated diminishes and, consequently, the pore size of the membrane becomes smaller. This implies that the resistance of the membranes to mass transfer increases and the applied pressure (which is the driving force) has to be increased to achieve the same flux.
A schematic drawing of the membrane process characteristics is given in Figure 3.

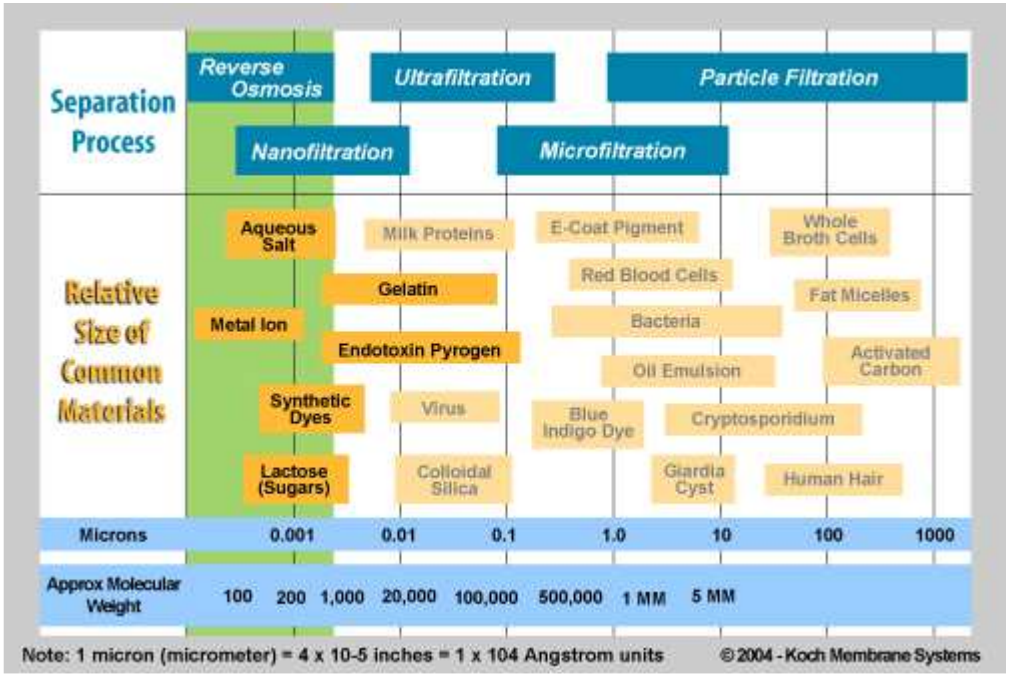

Figure 3: Membrane process characteristics [21].

The pressure-driven membrane processes differ each other for membrane structure, separation mechanism, applied pressure.

3.1.1 Microfiltration

The membranes used for MF are usually *symmetric* microporous structures with pore size in the range of 10-0.05 μm [22]. The membrane thickness can extend from 10 to more than 150 μm. MF is used in a wide variety of industrial applications where

particles with diameters in the range of 0.1 to 10 μm have to be retained from a solvent. Separation is accomplished by MF membranes via mechanical sieving and particles are separated solely according to their dimensions. The hydrostatic pressure difference used as driving force is low (less than 2 bar).
The flux J through the membrane can be described by Darcy'law:

$$J = A \cdot \Delta P \qquad (1)$$

where the flux is directly proportional to the applied pressure through the permeability constant A, parameter which contains structural factors such as viscosity, porosity and pore size distribution. In the case of convective laminar flux both Hagen-Poiseuille and Kozeny-Carmen equation can be used. If the membrane consists of straight capillaries, the following Hagen-Poiseuille equation can be used:

$$J = \frac{\varepsilon r^2}{8 \eta \tau} \frac{\Delta P}{\Delta x} \qquad (2)$$

where r is the pore radius, Δx the membrane thikness, η the dinamic viscosity, τ the tortuosity. When a nodular structure exists, the following Kozeny-Carmen equation can be employed:

$$J = \frac{\varepsilon^3}{K \eta S^2} \frac{\Delta P}{\Delta x} \qquad (3)$$

where K is a constant which depends from the geometry of the pore, S is the superficial area of the spherical particles per unit volume, ε the porosity. From equations (2) and (3) it appears that in order to optimize microfiltration is essential a porosity as high as possible and a pore size distribution as narrow as possible. MF membrane can be prepared from a large number of different materials, based on organic materials (polymers) or inorganic materials (ceramics, metals, glasses).
Two mode of process operation exist: dead-end (in which the feed flow is perpendicular to the membrane surface so that the retained particles accumulate and form a cake layer at the membrane surface) and cross-flow filtration (in which the feed flow is along the membrane surface so that part of the retained solutes accumulate). Moreover, hydrophobic MF membranes were observed to be more prone to foul than hydrophilic MF membranes, especially in the case of proteins, of hydrophilic neutral and colloidal components of the Natural Organic Matter (NOM) contained in sea/surface-waters [23].

3.1.2 Ultrafiltration

Ultrafiltration is used for the separation of suspended solids, colloids, bacteria and virus. This technique uses membranes with pore size between 1-100nm.
The most part of UF membranes used commercially are prepared from polymeric or inorganic (ceramic) materials. In UF, like in MF, the membranes can be considered as porous membranes, with rejection determined by the size and shape of the solutes relatively to the pore size in the membranes and where the transport of the solvent is directly proportional to the applied pressure. As a consequence, the flux through an UF membrane can be described with the same mathematical correlation (1) as for a MF membrane. However, an important difference between MF and UF is that ultrafiltration membranes are mostly asymmetrically structured: in UF the hydrodynamic resistance is

mainly determined within a small part of the total membrane thickness (generally less than 1μm) facing the feed solution, whereas in MF virtually the whole of the membrane thickness contributes towards the hydrodynamic resistance [22]. The hydrostatic pressures generally used in UF are in the range of 2 to 10 bars because the osmotic pressure of the feed solution is small.

UF membranes have originally been developed and proven for many years in a wide range of much more difficult liquid environments than seawater, such as highly polluted municipal and industrial wastewaters [24]. UF membranes provide a positive barrier to particulates, pathogens, macromolecules, colloids and smaller bacteria and not only towards suspended solids and large bacteria as in the case of MF membranes.

According to the dependence of permeate flux on the applied pressure, the operation of a pressure driven ultrafiltration process can be divided into three distinguishable pressure ranges: (1) linearly increasing flux (sufficiently low), (2) intermediate, (3) and limiting flux (sufficiently high) as shown in Figure 4.

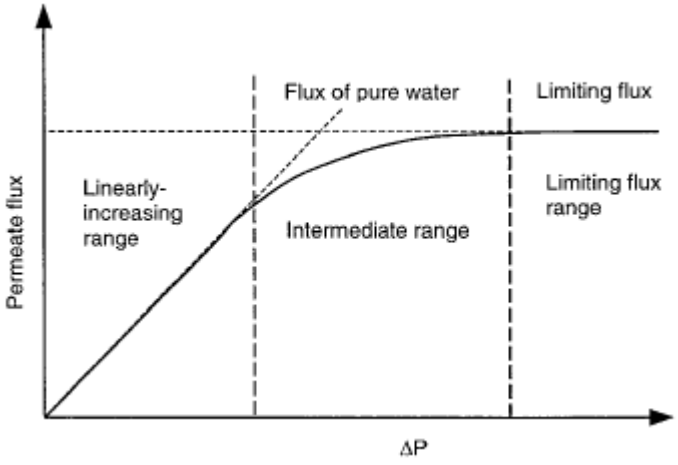

Figure 4: Three pressure ranges in the flux pressure curve: the linearly increasing flux, the intermediate, and the limiting flux ranges.

In the linearly increasing flux pressure range, the resistance to permeate flux comes only from the membrane because the concentration polarization layer is not significantly developed. On the other hand, permeate flux in the limiting flux pressure range is independent on the applied pressure. As in MF, these boundary layer phenomena mainly determine the process performance. As a consequence, the success of membrane operations and the number of their applications increased and will increase as much as they become more resistant (i) to the various kind of chemicals necessary for cleaning procedures and (ii) to a wide range of pH.

3.1.3 Nanofiltration and Reverse Osmosis

Nanofiltration and reverse osmosis are used for a wide range of applications, most of which are in the purification of water to produce potable water, mainly desalination of sea (TDS≈35,000ppm) and brackish water (TDS in the range of 1,000-5,000ppm). Another important application is in the production of ultra-pure water for the semiconductor industry.

Both the processes are based on the same principle: forcing a solvent through the molecular structure of a membrane, while trapping impurities and salts. In nature, when a semi-permeable membrane separates two compartments at different concentration, the water tends to flow from the lower to the higher concentrated compartment according to the natural osmosis phenomenon. Thus, the concentrated solution will be diluted until when the equilibrium between the compartments is reached and the trans-membrane flux becomes zero. Reverse Osmosis is when water flows through the membrane from the concentrated to the diluted solution. To obtain this an external pressure higher than the osmotic pressure has to be applied to the concentrated solution (Figure 5).

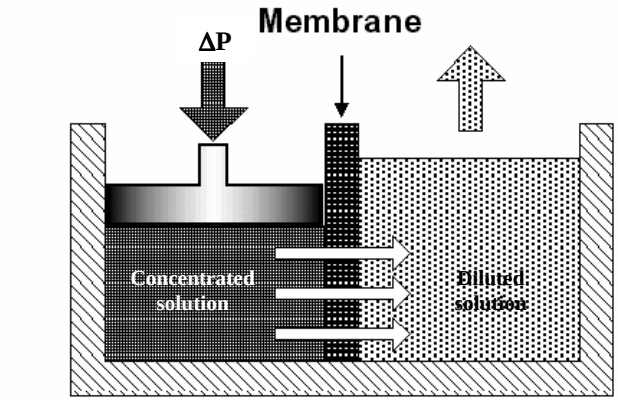

Figure 5: Reverse osmosis phenomenon.

During water transfer, the molecules and ions trapped by the membrane tend to accumulate along the membrane and increasing osmotic pressure. This reversible phenomenon, called "concentration polarisation", results in high energy costs and could cause precipitation if the solubility product of one of the cation-anion pairs is exceeded in the membrane layer.
The water flow J_w can be represented by the equation $J_w = A \cdot (\Delta P - \sigma \cdot \Delta\pi)$ (4)
while the solute flux can be described by $J_S = B \cdot \Delta c_S$ (5), where A and B are the water and solute permeability coefficients, respectively [22].
In NF and RO operations, in contrast to UF and MF, the choice of membrane material directly influences the separation efficiency through the constants A and B. In fact, in order to have high water recovery factor and solute rejections, the membrane material has to have a high affinity for the solvent (this means A high) and a low affinity for the solute (which means B low). The difference with UF/MF, based on sieving mechanisms, where the dimensions of the pores determine the separation properties and the choice is mainly based upon chemical resistance, is obvious. Thus, whereas MF and UF are destined for raw water clarification/partial disinfection, RO and NF are used to remove environmental micro-pollutants, organic matter and dissolved salts.

3.1.4 Membrane materials and module for NF/RO

For efficient processes, membranes should display high flux and high rejection. NF and RO membranes are similar with the exception that the second have a tighter structure. This means that NF membranes is generally used in softening, disinfection, removal of

organic materials, metals and bivalent ions whereas monovalent species (like Na^+ and Cl^-) are retained only by 10-50% depending on the membrane properties.
Not all the materials are suitable for every NF/RO operation because the constant A and B must have optimal values for a given application. Moreover, solvent flux through the membrane is approximately inversely proportional to the membrane thickness. Therefore, NF/RO membranes have an asymmetric structure, with a thin dense top layer (thickness $\leq$ 1μm) supported by a porous sub-layer (thickness in the range of 50-150μm). The selectively permeable layer is reduced to a very fine skin in order to limit the resistance to transfer related to the layer thickness. This layer rests upon another thicker substrate that has much larger pores which intends to provide the membrane with satisfactory mechanical properties without significantly impeding the flow of water.
In the early 1960s the first asymmetric reverse osmosis membranes were produced by Loeb and Sourirajan [25]. These membranes showed up to 100 times higher flux than any symmetric membranes known. This development paved the way for the commercial success of reverse osmosis.
On the basis of the internal structure, there are two main types of asymmetric membranes for NF/RO: asymmetric homogeneous membranes and composite membranes.

- ✓ In asymmetric homogeneous membranes both top-layer and sub- layer consist of the same material. Cellulose esters (especially cellulose diacetate and triacetate) were the first commercially used materials, in particular for water desalination due to their high permeability towards water and low solubility towards salts. Unfortunately, these material have poor chemical stability and tend to hydrolyse over time depending on temperature and pH operating conditions. They are also subjected to biological degradation. Other material frequently used for RO/NF membrane are aromatic polyamides, polybenzimidazoles, polybenzimidazolones, polymidehydrazide and polyimides [22].
- ✓ Composite membranes are made by assembling two distinct parts composed of different polymeric materials: a very fine layer (0.05 μm to 0.5 μm), representing the salt barrier of perm-selective material (i.e.: polyamide) obtained through interfacial polymerisation of the microporous layer (30 to 50 μm) made, for example, in polysulphone, which is itself often asymmetrical and all of which is attached to a support medium (100 to 150 μm).

Composite membranes can combine various materials and provide optimum properties depending on their use, therefore most RO membranes are actually of this type.
The application, efficiency and economics of an RO process also depends on the packaging of the membranes. There are four possible membranes geometries:

1. *Spiral wound membrane* (Figure 6), which consists of consecutive layers of large membrane and support material in an envelope type design rolled up around a perforated steel tube. This design tries to maximize surface area in a minimum amount of space. It is the less expensive but more sensitive to pollution due to its manufacturing process. Spiral membranes are only used for NF and RO applications.

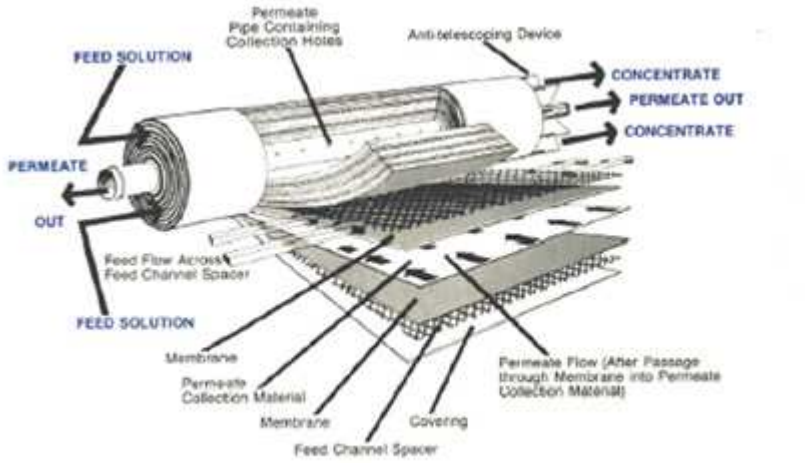

Figure 6: Spiral wound module [26].

2. *Plate and frame module*, which is normally used for bad quality water. They are set up with a stack of membranes and support plates.

3. *Tubular membrane* (Figure 7). Generally used for viscous or bad quality fluids, tubular membranes are not self-supporting membranes. They are located on the inside of a tube, made of a special kind of microporous material. This material is the supporting layer for the membrane. Because the feed solution flows through the membrane core, the permeate passes through the membrane and is collected in the tubular housing. The main cause for this is that the attachment of the membrane to the supporting layer is very weak. Tubular membranes have a diameter of about 5 to 15 mm. Because of the size of the membrane surface, plugging of tubular membranes is not likely to occur. Therefore, these modules do not need a preliminary pre-treatment of the water. The main drawback is that tubular membrane is not very compact and has a high cost per m^2 installed.

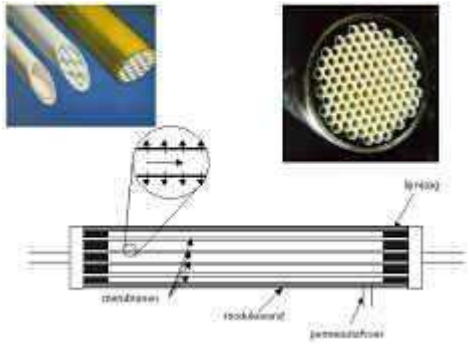

Figure 7: Tubular membranes [27].

4. *Hollow fiber membrane*. The modules contain several small tubes or fibers (diameter of below 0.1 µm), consequentially the chances of plugging of a hollow fiber membrane are very high. The membranes can only be used for the treatment of

water with a low suspended solids content. The packing density of a hollow fiber membrane is very high. Hollow fiber membranes are nearly always used merely for NF and RO.

Table 6 presents some general characteristics of the four basic membrane-module types, Table 7 shows examples of some RO industrial membranes.

Table 6: Qualitative comparison of membrane configurations [22].

Module type / **Characteristics**	*Tubular*	*Plate-and-frame*	*Spiral-wound*	*Hollow-fibre*
Packing density	low	⟶	⟶	very high
Investment	high	⟶	⟶	low
Fouling tendency	low	⟶	⟶	very high
Ease to cleaning	good	⟶	⟶	poor
Operating cost	high	⟶	⟶	low

Table 7: Examples of RO industrial membranes [21, 28].

Product	Description	Element Size			Flow	Stabilized Rejection
		Diameter inches (mm)	Length inches (mm)	Active Surface Area ft^2 (m^2)	gpd (m^3/d)	%
FILMTEC SW30-2514	SWRO elements for marine systems	2.4 (61)	14 (356)	6.5 (0.6)	150 (0.6)	99.4
FILMTEC SW30-2521	SWRO elements for marine systems	2.4 (61)	21 (533)	13 (1.2)	300 (1.1)	99.4
FILMTEC SW30-2540	SWRO elements for marine systems	2.4 (61)	40 (1016)	29 (2.8)	700 (2.6)	99.4
FILMTEC SW30-4021	SWRO elements for marine systems	3.9 (99)	21 (533)	33 (3.1)	800 (3.0)	99.4
FILMTEC SW30-4040	SWRO elements for marine systems	3.9 (99)	40 (1016)	80 (7.4)	1950 (7.4)	99.4
FILMTEC SW30HR LE-4040	SWRO element	3.9 (99)	40 (1016)	85 (7.9)	1600 (6.1)	99.75
Koch Membrane Systems, MegaMagnum® RO Element	Membrane element for: • Brackish Water Treatment • Municipal Water Reuse • Seawater Desalination	18 (457)	61 (1549)			
TM820-370	Standard RO element for sea water applications	8			(23)	99.75
TM820-400	High productivity RO element for sea water applications	8			(25)	99.75
TM820L-370	High flow RO element for sea water applications	8			(34)	99.7
TM820L-400	High flow RO element for sea water applications	8			(37.9)	99.7
TM820H-370	High pressure resistant RO element for sea water applications	8			(21)	99.75
TM820A-400	High Boron Rejection RO element for sea water applications	8			(22.5)	99.75

3.1.5 Limits of membrane processes

Membrane fouling together with concentration polarization phenomena are some of the major problems in membrane separation systems, which can considerably affect the economy of the processes and whose control is an important problem in the design of membrane systems.

When in a mass separation procedure a molecular mixture is brought to a membrane surface, some components will permeate the membrane under a given driving force while others are retained and accumulated at the membrane/solution interface. Thus, a concentration gradient between the solution at the membrane surface and the bulk is established which leads to a back transport of the material accumulated at the membrane surface by diffusion. This phenomenon is referred to as *concentration polarisation*. The adverse effects of the concentration polarisation are intensified when a deposition and/or an adsorption of certain feed constituents occurs at the membrane surface, causing a decline in flux over time when all operating parameters, such as pressure, flow rate, temperature and feed concentration are kept constant. This phenomenon is referred to as *membrane fouling*. Membrane fouling may be the results of concentration polarization but it may also be only the consequence of adsorption of feed solution constituents at the membrane surface and, especially in microfiltration, also within the membrane structure.

For what concerns concentration polarization, while the causes are identical in MF, UF and RO, the consequences are rather different. In reverse osmosis mainly low weight materials are separated from a solvent such as water. The feed solutions often have a considerable osmotic pressure. For example, seawater has an osmotic pressure of about 24 bar. In reverse osmosis, concentration polarisation leads to an increase in the osmotic pressure which is directly proportional to the solute concentration at the membrane surface, and thus a decrease in the trans-membrane flux at constant applied hydrostatic pressure. Furthermore, the quality of the filtrate is impaired since the solute leakage through the membrane is also directly proportional to the solute concentration at the membrane feed side surface.
In MF and UF only macromolecules and particles are retained by the membrane. The osmotic pressure of the feed solution is generally not as high as in solutions treated by reverse osmosis. However, the applied hydrostatic pressure is also quite low and, under certain conditions, the increased osmotic pressure due to concentration polarisation phenomenon could effect the trans-membrane flux. Due to the rather high molecular weight of the components separated in UF and MF, their diffusion from the membrane surface back, into the bulk solution, is relatively slow. Therefore, the retained components often are precipitated and form a solid layer at the membrane surface. This layer, which often exhibits membrane properties itself, can affect the membrane separation characteristics significantly by reducing the membrane flux and by changing the rejection of the lower molecular weight components. This is especially problematic in the fractionation of different molecular weight materials.
As described in detail in the following paragraphs, a membrane operation in which, on the contrary, concentration polarization hasn’t the same limiting effect is membrane distillation. Therefore, in this type of process fresh water can be recovered also from highly concentrated solutions with which RO would not be able to operate due to the osmotic effects. On the contrary, in MD temperature polarization, similar to concentration polarization, arises from heat transfer through the membrane and it is often the rate limiting step for mass transfer.
While concentration polarisation can be minimised by hydrodynamic means, such as the feed flow velocity and the membrane module design, the control of membrane fouling is more difficult.

Membrane foulants can be classified into four categories depending on the material deposited on membrane surface [29]:
a. Chemical foulants, which cause scaling.
b. Physical foulants or particulate matter, which are related to deposition of particles and colloidal matters on the membrane surface.
c. Organic foulants, which can interact with the membrane.
d. Biological foulants, which can either deteriorate the membrane or form a biofilm layer, which inhibits flux across the membrane due to growth of bacteria on the membrane surface.

Although for the first three foulants exist well-established, chemically-based and membrane-based pre-treatments, biofouling remains one of the most tenacious and least understood forms of membrane fouling.

Chemical foulants. Scaling of a reverse osmosis membrane occurs if concentrations of sparingly soluble salts, i.e. divalent and multivalent ions exceed their solubility level. Concentrations in the feed channel inside a module increase, and with increasing recovery, the risk of scaling grows. However, solubility levels only define the minimum concentration level at which scaling might occur. In practical operation, even at higher concentrations, scaling may not occur due to the long induction times of crystallisation. However, it is common practice not to exceed solubility limits [29].
Dissolved inorganic most likely to cause scaling are Ca^{2+}, Mg^{2+}, CO_3^{2-}, SO_4^{2-}, silica and iron. If solubility limits are exceeded, $CaCO_3$, sulphates of calcium, strontium and barium, CaF_2 and various silica compounds are the most likely compounds found as scaling on the membrane surface. Hydroxides of Al, Fe and Mn are normally precipitated before contact with the membrane. Most natural surface and groundwater display high $CaCO_3$ concentrations close to saturation. Therefore, the scaling tendency of a given feed water is often evaluated using the Langelier saturation index (LSI) for brackish waters and the Stiff and Davis Stability index (S&DSI) for seawaters [29].
Carbonate, sulphate and calcium fluoride scaling can be avoided by addition of antiscalants such as organic polymers, surface active agents, organic phosphonates and phosphates, e.g. polyhexametaphosphate (Calgon), which interfere with the kinetics of crystal nucleation, formation and/or growth. The presence of silica greatly complicates an RO desalting process. Threshold limits of silica scale precipitation are difficult to predict as they are influenced by a large number of parameters. Another difficulty is the lack of a silica anti-scalant that can be confidently used to extend water recovery limits. Moreover, silica scales deposited on a membrane are difficult and costly to remove. In the presence of silica it is customary to restrict the recovery limits below the silica saturation limit of about 120 mg/L.
Antiscalants may allow operation to a silica concentration of at most 220 mg/L [43].

Physical foulants or particulate matter. Particulate fouling is the deposition of suspended solids, colloidal and micro−organisms matters on the membrane surface originating from the raw water. Whereby, the suspended solids and colloidal matter are

clay minerals, organic materials, coagulants such as $Fe(OH)_3$ and $Al(OH)_3$, algae, extra cellular polymer substance (EPS) and transparent exopolymer particles [29].
Particulate matter in natural waters can be classified into four different categories depending on particle size:

- ✓ settable solids > 100 μm,
- ✓ supra-colloidal solids 1 - 100 μm,
- ✓ colloidal solids 0.001 - 1 μm,
- ✓ dissolved solids < 10 A°.

The most problematic feeds are those containing colloidal particles not easily removed by granular beds either because of their minute size or because of electrostatic repulsion effects of the media. In such cases it is necessary to add a coagulant or flocculating agent (such as ferric chloride, alum and cationic polymers, the latter can cause membrane fouling difficulties). Particles larger than > 25 μm can be easily removed by various pre-treatment prior to RO unit such as screens, cartridge filters, dual-media filters etc., whereby the presence of suspended solids can be monitored by the silt density index (SDI) test, turbidity analysis, zeta potential measurement and particle counting. Membrane manufacturers require a turbidity NTU (Nefelometric Turbidity Units) < 0.2, zeta potential > - 30 mV and SDI < 3 - 5 to prevent membranes from particulate fouling. Indeed, beach well raw waters are much less loaded with colloidal material and often no further reduction of colloid content is needed [29].
Additional source of colloidal matter in systems may arise from corrosion products from carbon steel pumps, piping and filters prior to the membrane filtration system. Analysis of the colour of the filter after filtration is also interesting for the identification of sticky or particular deposit. Table 7A gives some examples of the filter appearance and the indications about the possible corresponding fouling origin. This is essential to determine whether only suspended solids were in the water or whether it was adsorbed organic matter .

Table 7A: Origin of the fouling compounds according to SDI membrane appearance.

Color	**Identification**
Yellow/brown	Organics
Red/brown	Iron
Dark/grey	Activated carbon
Particles	Suspended solids

(Source: Mosset et al., *The sensitivity of SDI analysis: from RO feed water to raw water*, Desalination 222 (2008), 222**,** 17-23.)

Organic foulants can be defined as interaction between organic compound present in the feed water with the membrane surface. Organic matters components consist of proteins, carbohydrates, fats, oil and greases and aromatic acids such as humic acids. In reality, the humic substances represent the organics in natural waters, whose concentrations range from 0.5 and 20 mg/L in brackish water and up to 100 mg/L in surface seawater [29].
Dissolved organics, e.g. humic acids, proteins, carbohydrates and tannins are the most serious foulants and they are difficult to remove via conventional treatment.

Organic matter present in natural waters is undesirable because it is responsible for colour in the water, formation of carcinogenic disinfection by-products (DPB's) during water disinfection, complexation with heavy metals and calcium, etc. Moreover, the adsorption of organics on the membrane surface results in permeability decline, which even can be an irreversible process. It was found that mainly the hydrophobic humic substances are deposited on the membrane surface and that the adsorption process is favoured with positively charged, high molecular mass compounds. Similarly, the most hydrophilic membranes have been found less prone to fouling by organic colloids, i.e. humic acids [29].
In recent years membrane processes have been advanced for the removal of natural organic matter (NOM) for potable and other water uses. Several aspects of such processes have been the subject of intense research efforts with emphasis on NOM removal efficiency and on the inevitable fouling of the membranes, which limits their performance and lifetime. Important NOM properties relating to membrane performance are the nature of organic compounds, their hydrophilicity and charge, and the molecular weight distribution. Equally, important membrane properties are their pore size or MWCO, surface charge and hydrophilicity. In addition, water properties such as pH and ionic strength, as well as the presence of specific ions such as calcium, have been recognized to play a prominent role in NOM adsorption and fouling of membranes. Natural organic matter compounds are divided into humic substances or poly-hydroxy aromatics, and non-humic such as proteins, polysaccharides and amino-sugars. Humic substances are more hydrophobic than non-humic and constitute a significant fraction of surface water NOM. NOM is regarded as a carbon skeleton to which various functional groups are attached. The main components of this skeleton are Aliphatic units “straight chained or branched carbon units” and Aromatic units “based on benzene ring”.

Biological foulants. The presence of micro-organisms is ubiquitous. All raw waters contain micro-organisms such as bacteria, algae, fungi, viruses, and higher organisms such as protozoa, living or dead, or biotic debris such as bacterial cell wall fragments. The difference between micro-organisms and non-living particles is the ability of micro-organisms to reproduce and form a biofilm under favourable conditions. Consequently, biofouling is due to the growth of biofilm (bacterial) on the membranes surfaces. Micro-organisms entering a RO/NF system find a large membrane surface where dissolved nutrients from the water are enriched due to concentration polarization, thus creating an ideal environment for the formation of a biofilm. Biological fouling of the membranes may seriously affect the performance of the RO system. The symptoms are an increase in the differential pressure from feed to concentrate, finally leading to telescoping and mechanical damage of the membrane elements and a decline in membrane flux. Sometimes, biofouling develops even on the permeate side, thus contaminating the product water. A biofilm is difficult to remove because it protects its micro organisms against the action of shear forces and biocide chemicals. In addition, if not completely removed, remaining parts of a biofilm lead to a rapid re-growth.

Therefore, enhance pre-treatment process and microbiological activity control lead to biological fouling prevention.

In conclusion, fouling adversely affects membrane systems for the following reasons:

- *membrane flux decline* resulting from the formation of a permeability-reducing film on the membrane surface;
- *membrane biodegradation* due to the production of acidic by-products by micro-organisms, which are concentrated at the membrane's surface where they can cause the most damage;
- *increased salt passage* thereby *reducing the quality of the product water*;
- *increase in energy consumption.* To maintain the same production rate differential pressure and feed pressure must be increased to counteract the reduction in permeability brought on by the increase in resistance that the fouling causes. But damage to the membrane elements may occur if the operating pressure exceeds the manufacturer's recommendations.

Fouling can be prevented through the following means: *pre-treatment of the feed solution; modification of membrane surface; hydrodynamic optimisation of the membrane module; recourse to proper chemical agents for the cleaning; back-flushing.*
Particulate fouling in current practice is inhibited by mechanical pre-treatment of the RO feed water by use of screens, sand filtration and cartridge filters or membrane pre-treatment. Biological fouling, caused by microorganisms sticking to the membrane producing a gel like layer, is a serious problem to operation of a RO plant and has to be prevented by chlorination in pre-treatment prior to the actual RO stage.
Fouling can never fully be prevented even with optimised pre-treatment. Therefore, periodical membrane cleaning has to be performed. Complete removal is not possible and fouling has to be tolerated up to a decrease of mass flux down to 75% of original flux [30].
Good operating practice calls for chemical cleaning of the membranes if either normalised permeate flow decreases by 10%, feed channel pressure loss increases by 15% or normalised salt rejection decreases by 10% from initial conditions during the first 48 h of plant operation [31].

3.1.6 Reverse osmosis desalination process: technical description

Reverse osmosis is by far the most widespread type of membrane based desalination process. It is capable of rejecting nearly all colloidal or dissolved matter from an aqueous solution, producing a concentrate brine and a permeate which consists of almost pure water. Although reverse osmosis has also been used to concentrate organic substances, its most frequent use lies in seawater desalination applications.
The core of the process is based on Reverse Osmosis Membrane technology, but stand alone, it doesn't provide safe drinking water:

- ✓ Pre and Post-treatment steps are required to condition water before and after the RO membrane process to make it suitable to the application;
- ✓ Brine disposal can be an environmental and economical issue in some areas where the fauna and flora are sensitive to local seawater salinity increase. Brine disposal should be studied and engineered case by case.

- ✓ Energy consumption is one of the term which more influences desalted water cost and the application of energy recovery systems is currently usual in desalination plants.

A typical flow sheet of a simplified RO desalination plant with energy recovery system and open seawater intake is shown in Figure 8.
The process includes the following stages:

1. Water abstraction
2. Pre-treatment
3. Pumping system
4. RO membrane unit
5. Energy Recovery Devices
6. Post-treatment

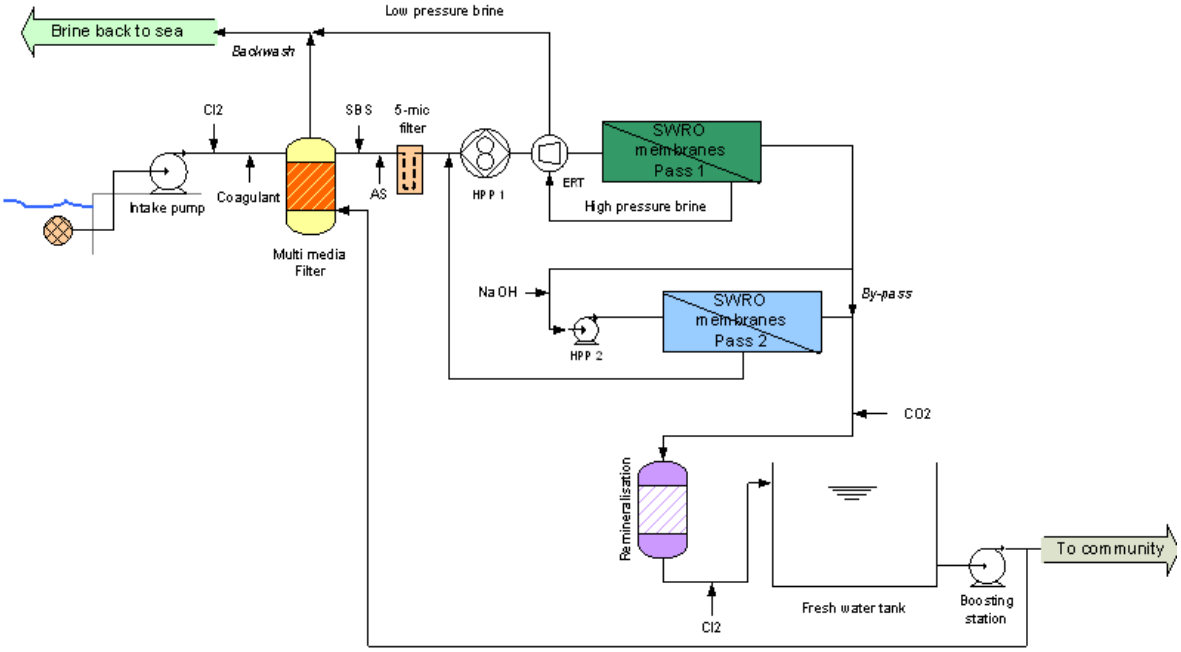

Figure 8: Simplified reverse osmosis scheme with energy recovery system.

1. The abstraction of feed water can be realised through open seawater intake systems or coast- and beach wells.
2. Pre-treatment step includes all activities to adjust intake water in order to reduce membrane fouling and deterioration.
3. Before entering the SWRO membrane, clarified seawater has to be pressurized by the High Pressure Pump, typically between 55 and 85 bars, depending on the temperature and the salinity of the water (Figure 9).

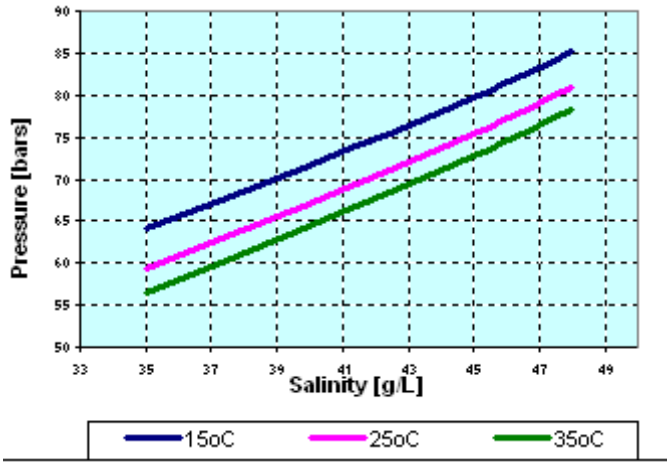

Figure 9: Pressure variations vs. salinity at different water temperatures [27].

4. The RO membrane is capable of separating salt from water with a rejection of 98–99.5%, depending on the membranes in use. Generally, desalination can be carried out by a single pass configuration or double-pass RO arrangements.

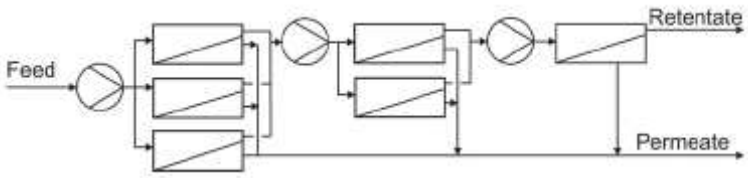

Figure 10: Double-pass RO process.

In a single pass configuration, one o more modules containing highly rejecting membranes are installed in parallel to give permeate water that can be directly utilised.
In double-pass operation each stage is fed by the reject of the previous stage. This arrangement is shown in Figure 10.

5. The pressure drop over the RO membranes is about 0.5 to 1 bar, depending on the number of element per pressure vessel, so the concentrate is released at high pressure. Thanks to Energy Recovery Devices (ERD), it is possible to reuse the energy from the concentrate flow.
The concentrate is directed to the ERD, where it directly transfers its energy to part of the incoming feed water which otherwise would be wasted. Depending on overall recovery and efficiencies of ERD and pumps, this can substantially reduce the specific energy consumption (SEC) of an RO plant.
The specific energy consumption of a RO plant is largely dominated by two factors: the amount of trans-membrane pressure difference required in order to achieve the necessary permeate flow rate at various mass transfer conditions, and the design and efficiency of the feed water pump in combination with the respective energy recovery system. For a given recovery rate, the required feed pressure is determined by the feed water properties, mostly temperature and feed salinity, which may vary significantly throughout the year due to seasonal influences. Feed water properties together with hydraulic losses from feed to brine also determine the outlet pressure of the membrane array, i.e. the inlet pressure for the energy recovery device.

While the operating conditions for larger seawater RO plants clearly indicate a centrifugal type feed pump, the selection of a suitable energy recovery device (ERD) for such a plant is not so obvious [32].
There are two main energy recovery concepts:
- Energy Recovery Turbine (ERT), which mostly are either Pelton wheel or turbocharger systems (Figure 11). These systems convert potential energy from the brine to mechanical energy either supplied to the feed pump as auxiliary power supply or directly to the feed water [29]. Turbine systems are the older option of the two types of ERD and work at efficiencies in the range of 91 - 93% [33].
- Pressure Exchanger (PX) which directly transfers pressure from the brine to part of the feed water achieving efficiencies of around 96%–98% [32] (Figure 12).

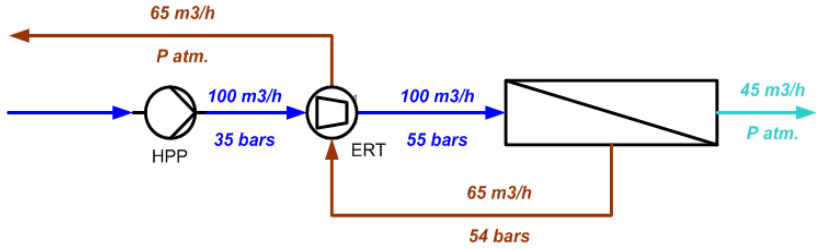

Figure 11: Process scheme with Energy Recovery Turbine [27].

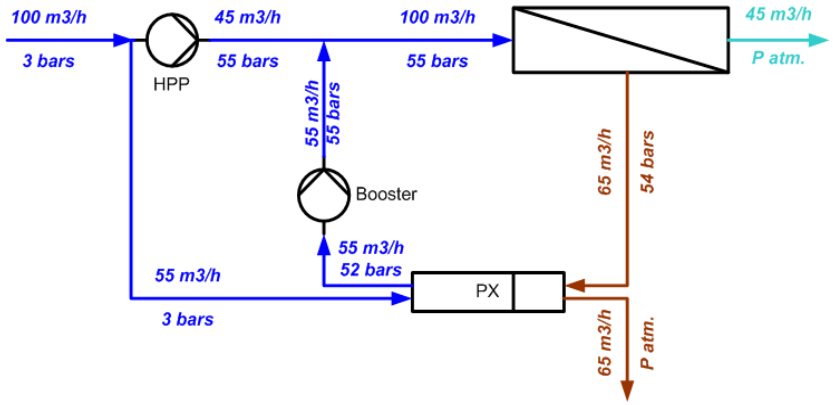

Figure 12: Process scheme with Pressure Exchanger [27].

6. In post-treatment the permeate is re-mineralised, re-hardened, disinfected by chlorination and adjusted to drinking water standards.

3.2 Membrane Contactors

Among the large variety of membrane operations, membrane contactors (MCs) represent relatively new membrane-based devices that are gaining wide consideration. Membrane contactors are systems in which microporous hydrophobic membranes are

used not as selective barriers but to promote the mass transfer between phases on the basis of the principles of phase equilibrium. All traditional stripping, scrubbing, absorption and liquid–liquid extraction operations, as well as emulsification, crystallization and phase transfer catalysis, can be carried out according to this configuration.
Starting from the description of the basic principles of this technology, the most promising perspectives in membrane distillation and membrane crystallizers in water treatment processes are addressed in the following paragraphs.

3.2.1 Membrane Distillation Technology

Membrane distillation (MD) is a relatively new process, introduced in the late 1960s, and it is investigated worldwide as a potential low cost, energy saving alternative to conventional separation processes such as distillation and reverse osmosis (RO).
The defining phenomenon of MD is relatively simple. A heated, aqueous feed solution is brought into contact with one side (feed side) of a hydrophobic, microporous membrane. The hydrophobic nature of the membrane prevents penetration of the aqueous solution into the pores, resulting in a vapour-liquid interface at each pore entrance (Figure 13).

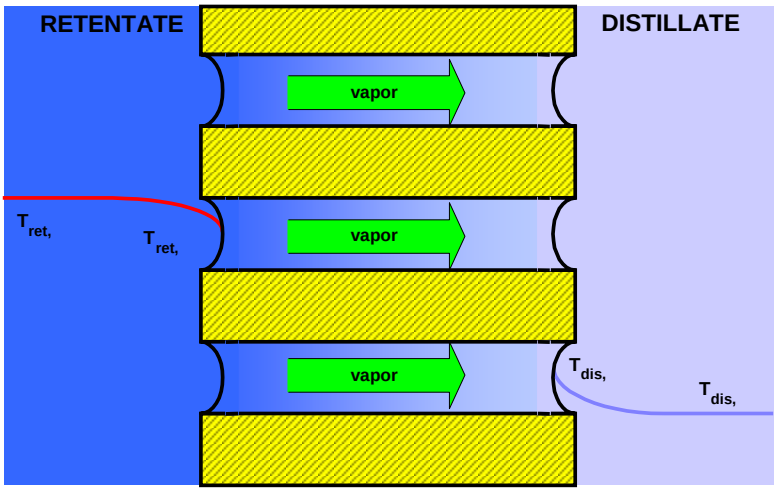

Figure 13: Membrane distillation process.

The driving force for the process is linked to both the partial pressure gradient and the thermal gradient between the two membrane sides.
A variety of methods may be employed to impose the vapour pressure difference across the membrane to drive flux and, according to the nature of the permeate side of the membrane, MD systems can be classified into four configurations (see Figure 14):

(1) direct contact membrane distillation (DCMD), in which the membrane is in direct contact only with liquid phases (saline water on one side and fresh water on the other, for example);
(2) vacuum membrane distillation (VMD), in which the vapour phase is vacuumed from the liquid through the membrane, and condensed, if needed, in a separate device;
(3) air gap membrane distillation (AGMD), in which an air gap is interposed between the membrane and the condensation surface; and
(4) sweeping gas membrane distillation (SGMD), in which a stripping gas is used as a carrier for the produced vapour instead of vacuum as in VMD.

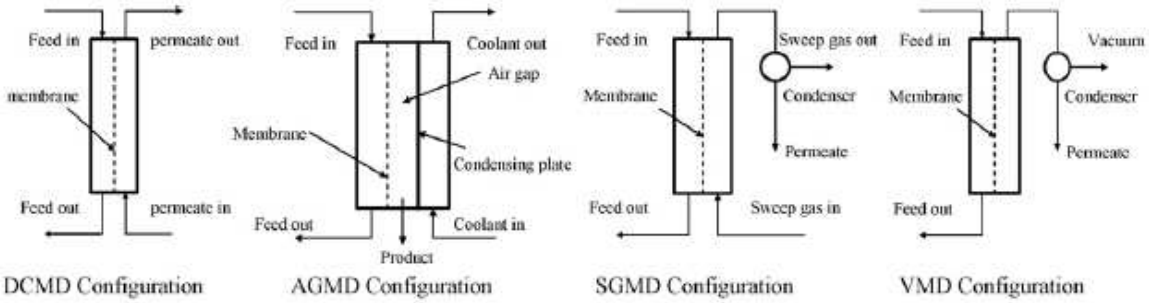

Figure 14: Common configurations of the Membrane Distillation process that may be utilized to establish the required driving force [34].

The type of employed MD depends upon permeate composition, flux, and volatility:

- SGMD and VMD are typically used to remove volatile organic or dissolved gas from an aqueous solution;
- Because AGMD and DCMD do not need an external condenser, they are best suited for applications where water is the permeating flux;
- the DCMD configuration, which requires the least equipment and is simplest to operate, is best suited for applications such as desalination or the concentration of aqueous solutions (orange juice), in which water is the major permeate component;
- AGMD, which is the most versatile MD configuration, can be applied to almost any applications.

Regardless of the MD configuration used, water and solute (if the solute is volatile) evaporate from the liquid-vapour interface on the feed side of the membrane, diffuse and/or convect across the membrane, and are either condensed or are removed from the membrane module as vapour on the permeate side.

The documented and expected benefits resulting from MD application are as follows:

1. The nature of the driving force, coupled with the hydro-repellent character of the membrane, allows, at least theoretically, the complete rejection of non-volatile solutes such as macromolecules, colloidal species, ions, etc.
2. The required operating temperature is much lower than that of a conventional distillation column because it is not necessary to heat the process liquids above their boiling temperatures. Typical MD processes can be conducted at temperatures below 70°C and driven by low temperature difference (20°C) of the hot and the cold solutions, thus permitting the efficient recycle of low-grade or waste heat streams, as well as the use of alternative energy sources (solar, wind or geothermal) for a cost and energy efficient liquid separation system.
3. Since MD is a thermally driven process, operating pressure are generally on the order of few hundred kPa, relatively low compared to pressure driven processes such as RO. Lower operating pressures translate to lower equipment costs and increased process safety.
4. Membrane fouling is less of a problem in MD than in other membrane separations because the pores are relatively large compared to the pores in RO and UF.
5. MD permeate flux is only slightly affected by the concentration of the feedwater, and thus, unlike other membrane processes, productivity and

performance remain roughly the same for high concentration feed-waters. This means that, by membrane distillation, pure water can also be obtained from highly concentrated feeds with which RO cannot operate. Therefore, MD can be preferentially employed whenever high permeate recovery factors or retentate concentrations are requested.

6. Robust membranes: since the membranes in MD act merely as a support for a vapor-liquid interface, they do not distinguish between solution components on a chemical basis, do not act as a sieve and do not react electrochemically with the solution, then they can be fabricated from almost any chemically resistant polymers with hydrophobic intrinsic properties. This characteristic increases membrane life.
   Polypropylene (PP), polytetrafluoroethylene (PTFE) and polyvinylidenefluoride (PVDF) are preferentially used in the preparation of membranes for such applications. PP in isotactic configuration exhibits excellent solvent resistant properties and high crystallinity. PTFE membranes are highly crystalline and show very good thermal stability and chemical resistance (they have low solubility in practically all common solvents); PVDF polymer, soluble in aprotic solvents such as dimethylformamide (DMF), dimethylacetamide (DMAc) and triethylphosphate (TEP), also demonstrates good thermal and chemical resistance [35, 64]. New amorphous perfluoro polymers (as Hyflon, Teflon, etc.) can be also utilized neglecting their still high costs.
7. The high flexibility of MD operations offer the attractive opportunity to integrate them in various important industrial production cycles with consequent benefits due to the synergic effects that can be reached.

Table 8 shows some MD applications reported in literature.

Table 8: Membrane Distillation applications reported in literature.

Reference	Application	Configuration
Calabrò et al. [53]	Wastewater treatment	DCMD
Nene et al.[54]	Concentration of raw cane sugar	DCMD
Calabrò et al. [55]	Concentration of orange juice	DCMD
Bandini et al. [56]	Concentration of must	VMD
Laganà et al. [57]	Concentration of apple juice	DCMD
V.D. Alves, I.M. Coelhoso [58]	Concentration of a sucrose solution, used as a model fruit juice	DCMD
Corinne Cabassud, David Wirth [59]	Seawater desalination	VMD

MD has been applied for separation of non-volatile components from water like ions, colloids, macromolecules [35-42], for the removal of trace volatile organic compounds from water such as benzene, chloroform, trichloroethylene [35, 43 -48] or the extraction of other organic compounds such as alcohols from dilute aqueous solutions [35, 49-52]. As a consequence, MD is suited for both concentration of aqueous solutions and water production. In fact, MD has been applied for biomedical applications (such as water removal from blood and treatment of protein solutions), water desalination, wastewater treatment and food processing (concentration of juice and raw cane sugar) [34].

Some of the technologies conventionally used to perform similar operations are: multi-effect distillation (MED), multi-stage flash (MSF), reverse osmosis (RO), electrodialysis/electrodialysis reversal (ED/EDR). In comparison with conventional MSF process, a MD plant is more compact and estate saving: the height of the MSF stage usually is in the range of 4-6 m, high compared with the ≈ 1 cm height of a MD cell. 1 m^2 of MD membrane has a volume of 0.01 m^3 and produce, with current generation configurations, up to 129 kg/m^3h, yielding a volumetric production rate of 12,900 kg/m^3h. The corresponding production rate per m^2 of plant surface area for MSF is 306.7 kg/m^2*h, and considering a 4-m stage height, the MSF process has a volumetric production rate of 76.6 kg/m^3*h, about 40 times lower [60]. The dimensions of a conventional distillation column are orders of magnitude larger than those of a comparable MD plant because the large vapour space required by a distillation column is replaced in MD by the pore volume of a microporous membrane, which is generally on the order of 100 μm thick [35]. Moreover, where conventional distillation relies on high vapour velocities to provide intimate vapour-liquid contact, MD employs a porous membrane to support a vapour-liquid interface. As a result, MD process equipment can be much smaller, which translates to a saving in terms of real estate [35].

The most interesting perspectives for the development of MD technology in desalination are related to the possibility of coupling MD with other processes, such as NF and RO, (i) for reducing the amount of oxygen or carbon dioxide dissolved in water streams, and (ii) for increasing both the quality and (iii) the recovery factor of the water treatment plants:

(i) In desalination, the content of oxygen and carbon dioxide in the seawater considerably affects the performance and the material life of the desalination plants. Carbon dioxide also affects the pH and the conductivity of the water and could influence the salts precipitation. Removal of these gases is usually made by stripping in a packed column and the final water pH is adjusted by means of caustic soda. This operation is difficult to fine control - due to the very low dosing rates- and is not well accepted by end users who do not prefer chemically treated waters. Membrane contactors working on the reverse osmosis permeate and/or feed can efficiently lead to the desired control of the oxygen and carbon dioxide content avoiding the final use of chemicals. Membrane contactors can be also applied for achieving a bubble-free efficient water ozonation.

(ii) Since MD operation operates on the principles of vapour-liquid equilibrium, then only volatile components are transferred through the membrane. As a consequence, MD process can be used for the treatment of polluted water to convert it into pure water and in a concentrate containing the substances present in the parent solution. For example, as described in *Chapter 7*, MD can and has been also used for boron and arsenic removal from water, in order to obtain substantial pollutants reduction in the permeate streams of the water treatment plants [61].

(iii) Because MD is not limited by concentration polarization phenomena as it is the case in pressure driven processes, when it operates on NF/RO brine, more fresh water can be produced.

3.2.1.1 The Membrane Distillation Process: vapor-liquid equilibrium, negative flux and membrane wetting

The driving force in MD is a vapour pressure difference across the membrane, which can be imposed by a temperature difference across the membrane, or by a vacuum or a sweep gas on the permeate side of the membrane.
One of the first assumptions made when modelling MD process is that kinetics effects at the vapour-liquid interface are negligible. In other words, the vapour and liquid are assumed to be in the equilibrium state corresponding to the temperature at the membrane surface and the pressure within the membrane pores. Further, the curvature of the vapour-liquid surface is assumed to have negligible effect on the equilibrium as compared to the flat surface state. A measure of the effect of curvature is given by the Kelvin equation [35]:

$$P^0 = P_\infty^0 \exp\left(\frac{2 \cdot \gamma_L}{r \cdot c \cdot R \cdot T}\right) \quad (6)$$

where P^0 is the pure liquid saturation pressure above a convex liquid surface with radius of curvature r, P_∞^0 is the pure liquid saturation pressure above a flat surface, γ_L is the liquid surface tension, c is the liquid molar density, R is the gas constant, T is the temperature. Generally, the effect of curvature doesn't overcomes 2%, then it can be considered negligible. As a consequence, there aren't significant influences on vapour-liquid equilibrium and it can be mathematically described by the equality between the fugacity of i-component in vapour phase and fugacity of the same i-component in liquid phase according to the following well-known thermodynamic equations:

$$\hat{f}_{i,L} = \hat{f}_{i,V}$$

$$\hat{f}_{i,L} = x_i \cdot \gamma_i \cdot P_i^0 \quad (7)$$

$$\hat{f}_{i,V} = y_i \cdot \pi$$

where x_i and y_i are, respectively, the molar fraction of i-component in liquid and vapor phase, π is the total pressure, γ_i the activity coefficient of i in solution (which is function of temperature and composition, can either be estimated from available experimental data or it can be calculated from one of a large variety of available equations -such as Van Laar or Wilson or UNIQUAC or NRTL equations), P_i^0 is the vapour pressure of pure i. In the equations (7), the effects of the pressure on the liquid (poyting factor) and the non-ideality of gas phase are neglected. These hypothesises are acceptable in the range of temperature and pressure usually used in membrane distillation process.

In MD the phenomenon of *reversed or negative flux* has been also observed. Negative flux results from a negative pressure drop across the membrane $(p_{fi} - p_{pi}) < 0$ caused by a difference between the feed and the permeate. Since a DCMD feed must be an aqueous solution and the permeate is generally pure water, the permeate has a higher osmotic pressure than the feed. As a results, a threshold temperature difference ΔT^0 must be overcome before positive flux is observed in MD process. Fortunately, ΔT^0 is generally on the order of 1°C or less for typical MD solution concentrations and operating temperatures [35]. The ΔT^0 can be calculated by the equality of the partial

pressures at the two membrane sides (condition of void flux), using Clausius-Clapeyron equation to simplify the vapour pressure-temperature relationship:

$$\frac{\Delta P}{\Delta T} \approx P^0 \frac{\Delta H}{RT^2} \quad (8)$$

$$\Delta T^0 = \frac{RT^2}{\Delta H}\left[\frac{x}{(1-x)}\right] \quad (9)$$

where (8) is Clausius-Clapeyron equation. Equation (9) is obtained when the following approximation for ideal dilute solutions is introduced in (8):

$$p_i = P_i^0(1-x) \quad (10)$$

where x is the molar solute concentration.

Another problem in MD is the *membrane wetting* which occurs when the liquid penetrates into and through the membrane pores. Once a pore has been penetrate it is said to be "wetted" and the membrane must be completely dried and cleaned before the wetted pores can once again support a vapor-liquid interface.

The Laplace (Cantor) equation provides the relationship between the membrane's largest allowable pore size (r_{max}) and the related operating conditions [35, 65]:

$$P_{liquid}\text{-}P_{vapor} = \Delta P_{interface} < \Delta P_{entry} = \frac{-2\,B\,\gamma_L\cos\theta}{r_{max}} \quad (11)$$

where B is a geometric factor determined by pore structure, γ_L the liquid surface tension and θ is the liquid/solid contact angle.

When the hydrostatic pressure on the feed side of a MD membrane exceeds ΔP_{entry}, liquid penetrates the pores and is able to pass through the membrane.

As stated earlier, in MD process membrane fouling is not a relevant problem such as in other membrane separations but fouling particles/molecules attached to the membrane surface might cause plugging of the membrane pore entrances causing first some flux decay and, then, may lead to membrane pore wetting. In fact, the increased deposition of the fouling species at the membrane surface might eventually lead to an increase in the pressure drop to levels that the hydrostatic pressure may exceed the ΔP_{entry}.

3.2.1.2 Heat transfer in membrane distillation process

Figure 15 illustrates the possible heat transfer resistances in MD with an electrical analogy.

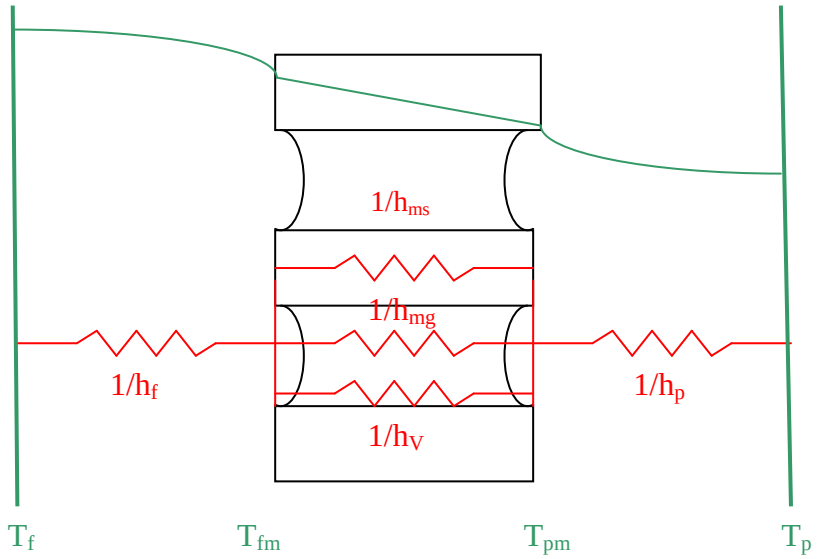

Figure 15: Heat transfer resistances in MD.

Heat is first transferred from the heated feed solution of uniform temperature T_f across the thermal boundary layer to the membrane surface at a rate $Q = h_f \cdot \Delta T_f$. At the surface of the membrane liquid is vaporized and heat is transferred across the membrane at a rate $Q_V = h_V \cdot \Delta T_m = N \cdot \Delta H_V$ (where N is the rate of mass transfer and ΔH_V is the heat of vaporization). Additionally, heat is conducted through the membrane material and the vapour that fills the pores at a rate $Q_m = h_m \cdot \Delta T_m$ where $h_m = \varepsilon \cdot h_{mg} + (1-\varepsilon) h_{ms}$ (ε is the membrane porosity, h_{mg} and h_{ms} represent the heat transfer coefficients of the vapor within the membrane pores and the solid membrane material, respectively). Conduction is considered a heat loss mechanism, because no corresponding mass transfer takes place. Total heat transfer across the membrane is $Q = Q_V + Q_m$. Finally, as vapour condenses at the liquid-vapor interface, heat is removed from the cold-side membrane surface through the thermal boundary layer at a rate $Q=h_p \cdot \Delta T_p$.

The overall heat transfer coefficient of the MD process is given by:

$$\frac{1}{U} = \frac{1}{h_f} + \frac{1}{h_m + h_v} + \frac{1}{h_p} = \frac{1}{h_f} + \frac{1}{\left(\frac{K_g \cdot \varepsilon + K_m(1-\varepsilon)}{\delta}\right) + \left(\frac{N \cdot \Delta H_V}{T_{fm} - T_{pm}}\right)} + \frac{1}{h_p} \qquad (12)$$

where each *h* and each *T* represent the corresponding heat transfer coefficients and temperatures shown in Figure 15.

The total heat transferred across the membrane is given by:

$$Q = U \cdot \Delta T \qquad (13)$$

Equation (12) illustrates the importance of minimizing the boundary layer resistances (maximizing the boundary layer heat transfer coefficients). A commonly used measure of the magnitudes of the boundary layer resistances relative to the total heat transfer resistance of the system is given by the temperature polarization coefficient (TPC):

$$TPC = \frac{T_{fm} - T_{pm}}{T_f - T_p} \quad (14)$$

- ✓ if $TPC \to 1$, the MD system is well designed and it is limited by mass transfer;
- ✓ if $TPC \to 0$, the MD system is poorly designed and it is limited by heat transfer through the boundary layers.

In literature, the recommended range of TPC is from 0.4 to 0.7 for well designed systems [35].

The boundary layer heat transfer coefficients are almost always estimated from empirical correlations such as the followings:

- Sieder-Tate correlation for turbulent liquid flow inside circular tubes

$$h = \frac{Nu \cdot K^T}{d}, \; Nu = 0{,}023 \cdot Re^{0,8} \cdot Pr^{1/3} \cdot \phi_\mu^{0,14} \text{ or}$$

$$\frac{hd}{K^T} = 0{,}023 \cdot \left(\frac{dG}{\mu}\right)^{0,8} \cdot \left(\frac{c_p \mu}{K^T}\right)^{1/3} \cdot \left(\frac{\mu}{\mu_w}\right)^{0.14} \quad (15)$$

where d is the tube diameter, K^T is the thermal conductivity of the liquid, G is the mass velocity equal to w/S = <ρv>, μ is the bulk liquid viscosity, μ_w is the liquid viscosity at the wall, c_p is the liquid heat capacity, ϕ_μ is the heating/cooling correction factor.

Equation (15) should be used for Re > 6000 and for tubes with large ratios L/d (where L is the tube length). For short tubes (L/d < 50), several corrections are available, including:

$\frac{h}{h_\infty} = 1 + \left(\frac{d}{L}\right)^{0,7}$ where h_∞ is the heat transfer coefficient given by eq. (15).

For the case of a non-circular flow channel, these correlations can still be used if the equivalent diameter d_e of the flow channel is substituted:

$$d_e = 4 \cdot r_H = 4 \cdot \frac{S}{L_P} = 4 \cdot \frac{\text{across - sectional area of the flow channel}}{\text{lenght of the wetted perimeter of the flow channel}} \quad (r_H = \text{hydraulic radius})$$

- Sarti correlation for laminar liquid flow in circular tubes with constant wall temperature:

$$Nu = 3.66 + \frac{0.067 \cdot Gz}{1 + 0.04 \cdot Gz^{2/3}} \quad \text{where} \quad Gz = \frac{\dot{m} c_p}{K^T L} \quad (16)$$

where G_z is the Graetz number, $\dot{m}$ is the mass flow rate, c_p is the liquid heat capacity, K^T is the liquid thermal conductivity, L is the length of the tubes.

However, several empirical correlations exist which allow to estimate the boundary layer heat transfer coefficients for other geometries and heat transfer mechanisms.

The heat transfer across the membrane has been already described.

For what concerns the heat transferred by convection within the membrane pores, this can be also considered but is negligible because convection accounts for, at most, 6% of the total heat lost through the membrane and only 0.6% of the total heat transferred across the membrane [35].

3.2.1.3 Mass transfer in membrane distillation process

Figure 16 illustrates the possible mass transfer resistances in MD using an electrical analogy.

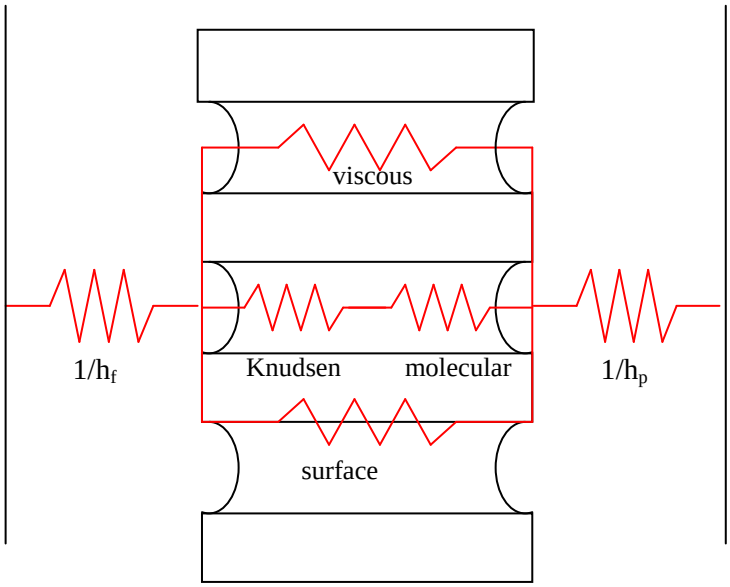

Figure 16: Mass transfer resistances in MD.

The resistances shown in Figure 16 are arranged as described by the dusty-gas model (DGM), which is a general model for mass transport in porous media.

✓ *Mass transfer across boundary layers*

A mass balance across the feed side boundary layer yields the relationship between molar flux N, the mass transfer coefficient k_x and the solute concentrations c_m and c_b at the interface and in the bulk, respectively [64 , 66]:

$$\frac{N}{\rho} = k_x \ln \frac{c_m}{c_b} \qquad (17)$$

where ρ is the solution density.

The method that is used in literature to determine the mass transfer coefficient is to employ an analogy between heat and mass transfer. Therefore, eqs. (15) and (16) can be used to estimate boundary layer mass transfer coefficients by substituting the Sherwood number for the Nusselt number, the Schmidt for the Prandtl, and the mass transfer Graetz number for its heat transfer form. In general, the used correlations are as follows:

$$Sh = \alpha \, Re^{\beta} \, Sc^{\gamma} \qquad (18)$$

where Sh = Sherwood number = $(k_x d_h)/D$ (d_h hydraulic diameter, D diffusion coefficient in the liquid), Sc = Schmidt number = $\mu/(\rho D)$ (μ is the bulk liquid viscosity, ρ is the solution density), Gz_M = mass transfer Graetz number = $Gz_M = \frac{\dot{m}}{\rho D_{AB} L}$ ($\dot{m}$ is the mass flow rate, L is the tube length).

As a result of the solvent trans-membrane flux across the membrane, when aqueous solutions containing non-volatile solutes are considered, the concentration of the

non-volatile solutes at the membrane surface (C_{Bm}) becomes higher than that at the bulk feed (C_{Bb}) with time as long as the separation process is taking place. Almost 100% of separation is obtained. In this case, care must be taken as supersaturation states may eventually be achieved affecting the efficiency of the membrane process. The term concentration polarization coefficient (CPC) is defined to quantify the mass transport resistance within the concentration boundary layer at the feed side as follows:

$$CPC = \frac{c_{Bm}}{c_{Bb}}. \quad (19)$$

The increased concentration of non-volatile compounds next to the membrane surface would have the influence of reducing the transmembrane flux due to the establishment of concentration polarization (CP) layer at the feed side that acts as a mass transfer resistance to the volatile molecule species (water). As stated earlier, in other membrane separation process (pressure-driven) such UF/NF/RO, concentration polarization is usually considered a major cause for flux decline [65] (see Figures 16 a) and b).

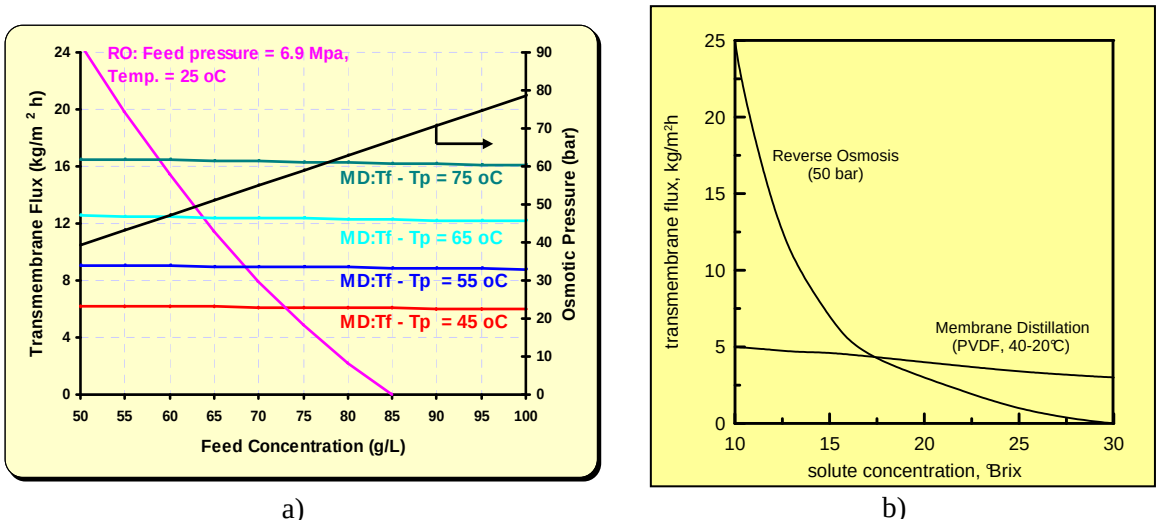

a) b)

Figure 16. Influence of feed concentration on RO and MD.

Fortunately, in MD process, the low to moderate flow rates and high heat transfer coefficients reduce the impact of concentration polarization, which is lower than that of the temperature polarization effect [57, 65, 67.]. In fact, boundary layers next to the membrane can contribute substantially to the overall transfer resistance: heat transfer across the boundary layers is often the rate limiting step for mass transfer in MD because a large quantity of heat must be supplied to the membrane surface to vaporize the liquid, and because the membrane fabrication technology has improved in the last decades so much that MD process has shifted away from being limited by mass transfer across the membrane to being limited by heat transfer through the boundary layers on either side of the membrane.

✓ *Mass transport through the membrane pores*

As stated earlier, the mass transfer process in MD is driven by the imposed vapour pressure gradient between both sides of the membrane. The mass transport

mechanism is governed by three basic mechanisms known as Knudsen-diffusion, Poiseuille-flow, Molecular-diffusion or the combinations between them known as transition mechanism (excluding surface diffusion, negligible in MD because, by definition of the MD phenomenon, molecule-membrane interaction is low and the surface diffusion area in MD membranes is small compared to the pore area).
The Dusty–gas model is usually used as a general model taking into account the latter basic mechanisms [35, 64, 65]:

$$\frac{N_i^D}{D_{ie}^k} + \sum_{j=1\neq i}^{n} \frac{p_j N_i^D - p_i N_j^D}{D_{ije}^0} = \frac{-1}{RT}\nabla p_i \qquad (20)$$

$$N_i^v = -\frac{\varepsilon r^2 p_i}{8 R T \tau \mu}\nabla P \qquad (21)$$

$$D_{ie}^k = \frac{2\varepsilon r}{3\tau}\sqrt{\frac{8RT}{\pi M_i}} \qquad (22)$$

$$D_{ije}^0 = \frac{\varepsilon}{\tau} D_{ij}^0 \qquad (23)$$

where N^D is the diffusive flux, N^V is the viscous flux, D^k is Knudsen diffusion coefficient, D^0 is the ordinary diffusion coefficient, p_i is the partial pressure of the component i, P is the total pressure, M_i is the molecular weight of component i, r is the membrane pore radius, ε is the membrane porosity (assuming the membrane consists of uniform cylindrical pores), μ is the fluid viscosity, τ is the membrane tortuosity. The subscript "e" is indicative of the effective diffusion coefficient function of the membrane structure.
There is only one problem with the application of the DGM to MD and that lies in the fact that MD is a non-isothermal process. The DGM was derived for isothermal flux, but has been successfully applied to non-isothermal systems via the inclusion of terms for thermal diffusion and thermal transpiration. However, it easily shown [35] that these terms are negligible in the MD operating regime, and T_{avg} in the membrane is used in place of T in the DGM equations.

Regardless of which mechanism is involved in the mass transportation process, the molar flux, N, must be proportional to the vapour pressure difference across the membrane:

$$N = C \cdot \Delta P$$

where ΔP is the vapour pressure difference across the membrane (function of temperatures and compositions at the membrane surface), C is the membrane distillation coefficient that can be obtained experimentally. C is a function of temperature, pressure and composition within the membrane as well as membrane structure and depends on the MD configuration employed as well as on the Knudsen number (Kn, ratio of the mean free path of the transported gas molecules (λ) through the membrane pores to the mean pore diameter of the membrane (d)). In fact, Kn number determines the physical nature of flow through membrane pores and, since the membranes used in MD exhibit pore size distribution, more than one mechanism may occur through the membrane.
Mass transfer in direct contact membrane distillation (DCMD, the configuration utilized in the following chapters) can also be separated into three steps (e.g. mass transfer in

feed boundary layer, mass transfer across the membrane and mass transfer in permeate boundary layer). The mass transfer in permeate boundary layer is not taken into account since the mole fraction of the transporting species in the permeate stream is approximately equal to one. For what concerns the mass transfer in boundary layers, it is general to neglect surface diffusion and viscous flow, and to employ a Knudsen-molecular diffusion transition model [35, 68].

3.2.2 Membrane Crystallization Technology

Membrane Crystallization (MCr) has been recently proposed as one of the most interesting and promising extension of the MD concept [62, 63], an innovative process for the quasi total recovery of the desalted water combined to solid salts production. As a matter of fact, this innovative technology uses evaporative mass transfer of volatile solvents through microporous hydrophobic membranes in order to concentrate feed solutions above their saturation limit, thus attaining a supersaturated environment where crystals may nucleate and grow.

One of the main characteristics of MCr is that the membrane does not act only as support for the solvent evaporation but also induces heterogeneous nucleation. As a matter of fact, a crystallizing solution can be imagined as a certain number of solute molecules moving among the molecules of solvent and colliding with each other, so that a number of them converge forming clusters. All the clusters larger than critical nuclei (r*) grow spontaneously. There is, anyway, an energetic barrier ΔG^* (nucleiation barrier) that must be crossed in order to induce the formation of stable nuclei [64].

The presence of the polymeric membrane in the crystallizing solution decreases the work required to create critical nuclei and will increase locally the probability of nucleation with respect to other locations in the system (this phenomenon is called heterogeneous nucleation). By considering the interactions between solute and solid substrate in terms of contact angle θ (which the crystallizing solution forms with the solid substrate), the reduction of ΔG due to heterogeneous nucleation is equal to:

$$\Delta G_{heter} = \Delta G_{homog}\left[\frac{1}{2} - \frac{3}{4}\cos\theta + \frac{1}{4}\cos^3\theta\right]$$

When a solution wets completely the solid substrate $\theta = 180°$ and $\Delta G_{heter} = \Delta G_{homog}$, for a contact angle equal to 90° (limit between hydrofobic and hydrofilic behaviour) $\Delta G_{heter} = \frac{1}{2}\Delta G_{homog}$. As a consequence, we can conclude that the presence of an hydrophobic membrane ($90° < \theta < 180°$) promotes the nucleation by decreasing the amount of energy required to form stable nuclei.

Because the relation between ΔG_{heter} and ΔG_{homog} depends by θ, different polymeric membranes exhibit dissimilar interactions with a liquid phase.

Another main feature of membrane with respect to conventional crystallizers is that the first one is characterized by an axial flux, in laminar regime, of the crystallizing solution through the membrane fibres. The laminar flow of the solution through tubular or capillary membranes improves the homogeneity of the mother liquor, reduces mechanical stress, and promotes an oriented organization of the crystallizing molecules.

As a consequence, crystals exhibiting good structural properties and narrow size distribution are generally produced in membrane crystallization devices.

The most interesting perspective for the development of MCr technology is probably related to the possibility of combining it with other conventional pressure-driven membrane processes such as NF and RO in order to reach the goals of *quasi total recovery of the desalted water combined to solid salts production* (see *Chapter 2* and *6).* Since MCr operation is not limited by concentration polarization phenomena as it is the case in pressure driven processes, when it operates on NF and/or RO brine, the highly concentrate brine does not represent waste but the mother liquor in which (i) the crystals, usually present in the concentrated streams of the desalination plants, could nucleate and grow and (ii) more fresh water can be produced. In this logic MCr allows to utilize the added value of the retentate streams usually discharged by the desalination plants, thus reducing brine disposal problem, producing valuable crystals and increasing plant recovery factor [62, 63, 69].

3.3 Membrane Bioreactor Technology

Membrane Bioreactor (MBR) is an emerging technology for (waste)water treatment and recycling combining membrane filtration with biological treatment. The reactor is operated similar to a conventional activated sludge process but without the need for secondary clarification and tertiary steps like sand filtration (Figure 17) [70, 71].

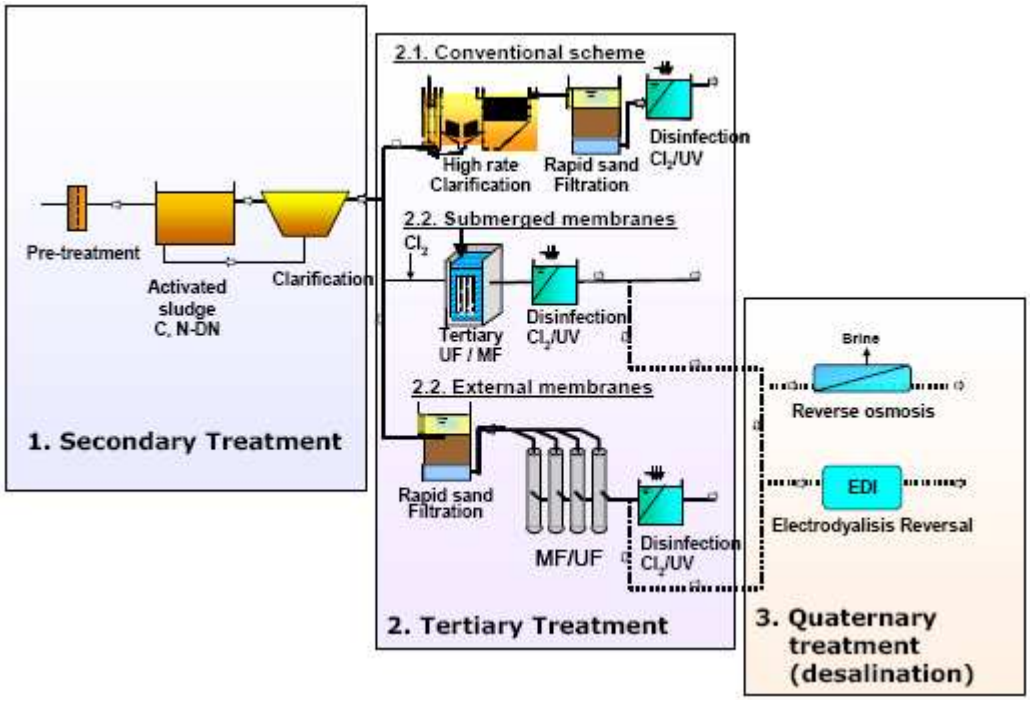

Figure 17: Typical treatment schemes used for tertiary treatment and further polishing of secondary effluents before urban water reuse [72].

To clarify what happens in a MBR, its advantages and drawbacks, it is better to describe how a typical waste-water treatment plant usually works. It generally involves four stages, called *primary*, *secondary*, *tertiary and, sometimes, quaternary treatment*:

1. first, the solids are separated from the wastewater stream;
2. in the secondary treatment (often also including nutrient removal) the dissolved biological matter is progressively converted into a solid mass by using indigenous, water-borne microorganisms. This treatment is characteristic of restricted agricultural irrigation (i.e. for food crops not consumed uncooked) and for some industrial applications such as industrial cooling (except for the food industry).
3. Finally, the biological solids are neutralized then disposed of or re-used, and the treated water may be disinfected chemically or physically (for example by lagoons and micro-filtration). The final effluent can be discharged into a stream, river, bay, lagoon or wetland, or it can be used for the irrigation of a golf course, green way or park. If it is sufficiently clean, it can also be used for groundwater recharge.
4. Quaternary treatment is a treatment producing a quality comparable to drinking water, often involving a "dual membrane" step to meet unrestricted residential uses and industrial applications requiring ultrapure water.

In an MBR, low-pressure membrane filtration, either MF or UF, is used to separate effluent from activated sludge.
Activated sludge is a sospension in water of active biological material (saprophytic bacteria, amoebae, Spirotrichs, Peritrichs and other microorganisms) that substantially removes the biodegradable organic material presents in waste-waters. An activated sludge process (Figure 18) has to include at least two stages: (i) an aeration tank where air (or oxygen) is injected in the mixed liquor to promote the growth of biological floc that substantially removes organic material and (ii) a settling tank to allow the biological flocs to settle, thus separating the biological sludge from the clear treated water.

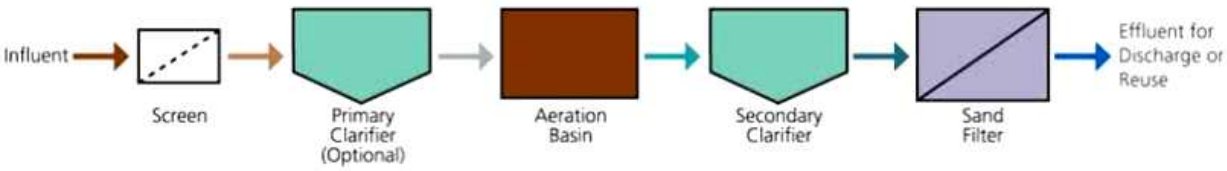

Figure 18: Schematic representation of conventional activated sludge process.

In the MBR, the membranes are typically immersed in the aeration tank (immersed configuration, Figure 19). However, in some applications, a separate membrane tank is utilized (external loop, Figure 20).

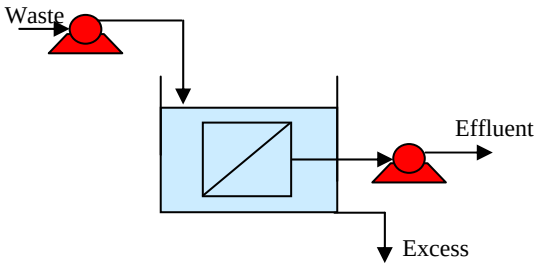

Figure 19: Schematic representation of membrane bioreactor: immersed membranes.

The first generation of membrane bioreactors operated with organic or

inorganic tubular membranes placed in external recirculation loops. To perform well, the external loop configuration requires very high liquid velocity**.** In fact, the biomass has to be pumped at high speed through the tubes (3 to 6 m/s) so as to slow the fouling of the membranes and reduce the frequency of chemical cleaning [70]. Therefore, the use of recirculation loops leads to increase energy costs (2 to 10 kWh/m^3 of water produced, depending on the internal diameter of the tubes used) [70, 73]. In addition the high shear stresses in the tubes and in the recirculation pumps can contribute to the destruction of biological flocs, which has been linked to the loss of biological activity [70].

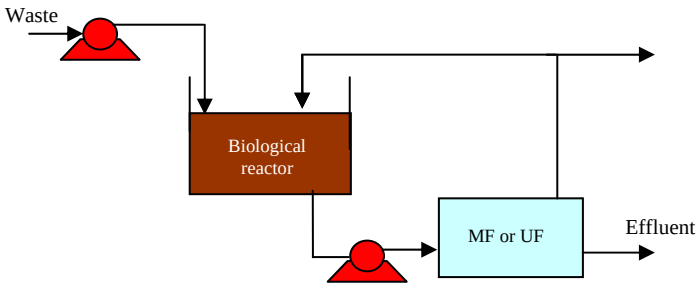

Figure 20: Schematic representation of membrane bioreactor: external loop.

Immersed membrane bioreactors have been developed out of a need to simplify the use of these systems and to operate more cost effectively than the external loops with respect to both energy consumption and cleaning requirements. In these configurations, the membranes are directly immersed in the tanks containing the biological sludge and the treated permeate is extracted. This operating mode limits the energy consumption associated with the filtration to 0.2 to 0.4 kWh/m^3 [70, 73, 74].

Membranes applied in submerged MBRs can be either hollow fibres or flat membranes [70, 71].

Feed water for MBR plants needs sufficient pre-treatment in order to prevent the damages related to membrane fouling. Membrane fouling is significantly influenced by the hydrodynamic conditions, by membrane type and module configuration and by the presence of higher molecular weight compounds, which may be produced by microbial metabolism or introduced into the sludge bulking process [71].

Because membrane is an absolute barrier for bacteria and in the case of UF also for viruses, the MBR process provides a considerable level of physical disinfection. The resulting high quality and disinfected effluent implies that MBR processes can be especially suitable for reuse and recycling of wastewater. Presently it has been applied at full scale on certain industrial wastewater treatment, domestic wastewater recycling [74] and is the configuration more often applied in municipal wastewater treatment.

One of the key benefits of a MBR is that it effectively overcomes the limitations associated with poor settling of sludge in conventional activated sludge (CAS) processes. The technology permits bioreactor operation with considerably higher mixed liquor suspended solids (MLSS) concentration than CAS systems, which are limited by sludge settling. The process is typically operated at MLSS in the range of 8,000–12,000 mg/L, while CAS are operated in the range of 2,000–3,000 mg/L. The elevated biomass concentration in the MBR allows for very effective removal of both soluble and particulate biodegradable materials at higher loading rates. Thus increased Sludge Retention Times (SRTs)—usually exceeding 15 days—ensure complete nitrification even under extreme cold weather operating conditions [75].

Another advantage in the use of MBR is its compactness: up to 5 times more compact than a CAS plant because the membrane module replacing the clarification tank, thus producing significantly less excess sludge. In developed urban areas where the footprint of the treatment plant is considered a limiting factor, MBR facilities can be considered a desirable option.
On the other hand, however, the energy consumption, because of pumping, can be significantly higher than with a CAS process. Also the cost of building a MBR is usually higher than conventional wastewater treatment. However, as the technology has become increasingly popular and has gained wider acceptance throughout the industry, the life-cycle costs have been steadily decreasing.
Since the early MBR installations in the 1990s, the number of MBR systems has grown considerably; projected total European revenue for the MBR market is around 40 million euro in 2005 with a steady growth rate of 9% [71]. One key trend driving this continue growth in the next 5-10 years is the use of MBR systems for decentralised treatment and water reuse. The majority of the currently operating and commissioned plants are small- to medium size. The entry of membrane bioreactors into large sized projects has been slow. It is only in the last couple of years that the use of MBRs for medium to large-scale domestic wastewater applications is beginning to grow. The main factors that contributed to their development were the experience gained with pilot/small-scale projects, the decrease in the cost of membranes and the improvements in their performance.
Membrane bioreactors are by now almost exclusively used in wastewater treatment. The great potential of MBRs to produce high quality effluent could also be of great interest in the removal of a variety of anthropogenic organic pollutants and fouling agents that are increasingly present in sea/brackish-water.
With respect to costs, MBR is considered a high tech process with high initial investment costs when applied to wastewater treatment. However, this is not the case when MBR is used to treat seawater, with a typical total organic carbon concentration in the range of 1.0-3.0 mg/L. Under such conditions the use of MBR technology, especially in the submerged configuration, could be a very cost-effective process.

4. Integrated Membrane Systems for Water Treatment

Over the last few decades more and more membrane technology has emerged as the most promising contributor to solve water shortage problems by *sea/brackish water desalination* and *wastewater treatment and reuse*. The success of membrane operations is due to their intrinsic characteristics of efficiency and operational simplicity, high selectivity and permeability for the transport of specific components, compatibility between different membrane operations in integrated systems, low energetic requirement, good stability under operative conditions, environment-compatibility, easy control and scale-up, large flexibility and lower water cost compared with conventional water treatment methods (Table 2).
At the beginning the research efforts were on reverse osmosis membranes for sea and brackish water desalination. These have had an impact on the progress of the whole membrane science and considerable advances in ultrafiltration and microfiltration

technologies in water purification processes for drinking water production have been also achieved:

- ✓ The growth in MF/UF systems installations in the past few years has been almost explosive. In 1995 it was estimated that less than 25 MGD installed capacity was in operation in North America [76]. Five years later that number has grown to over 400 MGD. MF systems have been installed in both the potable water markets and for water reuse applications treating municipal secondary effluent. UF systems have been gaining wide acceptance for potable water enhancement.
- ✓ Large NF plants have been put into operation in Florida for organic removal. Plantation has 18 MGD capacity and Palm Beach County is building a 30 MGD facility. Other large installations are planned in the future. The metropolitan Water District is evaluating membrane technology and looking at very large nanofilters plant to reduce TDS and lower hardness in addition to pathogen protection. These plants could exceed 200 MGD.

Today, for more and more increasing the reliability of membrane based water treatment processes (which means decreasing desalted water costs, increasing water quality, rising fresh water recovery factor and reducing the environmental impact of discharged brine streams), two different ways can be pursued:

- discovering new materials for making membranes more stable and resistant to chemicals in order to increase their performance and life-time and, then, to reduce the replacement and maintenance costs;
- coupling several membrane processes in order to overcome the limits of the single units and to use their synergic effects in terms of better performance of the overall system.

The possibility of redesigning overall industrial production by integration of various already developed membrane operations is becoming of particular interest and is growing rapidly with excellent results, because of the simplicity of the units and the possibility of reaching advanced levels of automatization and remote control. Moreover, the rationalisation of industrial production by integration of these technologies permits low environmental impact, low energy consumption, and high quality of the final product.

For example, microfiltration and ultrafiltration are more and more combined with RO in the pre-treatment steps for removing suspended solids and organic contaminants in raw seawater, thus providing an RO feedwater of good quality which results in the reduction of membrane fouling and, then, in capital and operating costs of the desalination plant.

In this logic also Membrane Distillation (MD) and Membrane Crystallization (MCr) techniques well fit in: since they are temperature-driven membrane operations not limited by concentration polarization phenomena, when MD and/or MCr operate on NF/RO brine as post-treatment step, more fresh water can be produced thus increasing plant recovery factor and decreasing the amount of the highly concentrated streams that the desalination plants usually discharged in oceans.

In conclusion, membrane technology offers today new opportunities in the design and optimization of industrial processes. The possibility of integrating the new membrane operations (MD, MCr) together with the well-assessed pressure driven membrane units (MF, UF, NF, RO) could contribute to reach the goals of better water quality, reduction of membrane fouling, lower fresh water cost, fewer brine production and, as a

consequence, reduction of the environmental problems related to its disposal.

A successful example of an integrated water treatment process is, instead, in the world's largest Integrated Membrane System put into operation by PWN Water Supply Company North Holland in the Netherlands. In this plant, UF and RO are the most essential process elements of this treatment plant, having a capacity of 18 million m^3/year (13mgd). Water abstracted from the Ijssel Lake is processed in the membrane plant. The treated obtained water is a drinking water which meets the most stringent water quality criteria regarding desired low salinity, minimal corrosion and optimal low hardness and organic matter content.

4.1 Pre-treatment strategies

Due to the fouling sensitivity of membrane units, high quality feedwater is required to ensure stable, long term performance. In particular RO membranes are susceptible to a wide variety of organic and inorganic foulants. A sufficient pre-treatment, supplying high quality feedwater, regardless of fluctuation of raw water quality, is therefore essential for an efficient plant operation.

Ineffective or unreliable pre-treatment can lead to problems with the RO system including high rates of membrane fouling, high frequency of membrane cleanings, lower recovery rates, high operating pressure, poor product quality and reduced membrane life; all having a direct impact on plant productivity and operational costs [24]. Accordingly, pre-treatment optimization is the key factor for a successful RO desalination system.

The type of pre-treatment depends on *feedwater quality*, which varies with the location of the plant, seasonal variations and intake system. While for feedwater from well sources cartridge filtration is usually sufficient, feedwater from open seawater intakes demands more extensive pre-treatment.

Pre-treatment operations can be divided into two main groups: (i) physical and (ii) chemical pre-treatment. The first is responsible for mechanical filtration through screening, cartridge filters, sand filters or membrane filtration. Chemical pre-treatment includes the addition of scale inhibitors, coagulants, disinfectants and polyelectrolyte [29]. While chemical pre-treatment is responsible for pH adjustment, increasing the solubility of salts and disinfection, the physical pre-treatment is responsible for the separation of dispersed particles from the feed water to prevent blocking, fouling and flux decreases in the membrane.

In the past, conventional RO pre-treatment (which is defined as chemical and physical pre-treatment without the use of membrane technologies) has been widely applied. With the cost of membranes constantly declining and the quality of feedwaters continually deteriorating, an increasing number of plant owners are nowadays considering the use of membrane based pre-treatments to replace less efficient, conventional pre-treatment systems, which do not represent a positive barrier to colloids and suspended solids and produce unsteady quality of RO feedwater [24].

Micro- and ultrafiltration membranes are considerable alternative options and it is estimated that membrane pre-treatment will rapidly grow in the coming years [29].

Looking at the available pre-treatment technologies for the clarification of seawater upstream RO, a quick and easy classification is as follows:

- ✓ conventional pre-treatment;
- ✓ membrane pre-treatment.

A rapid overview of the previously mentioned pre-treatment operations is proposed in the following paragraphs.

4.1.1 Conventional pre-treatment

A typical conventional RO pre-treatment is shown in Figure 21. Usually it consists of the following parts:

- ✓ seawater intake system;
- ✓ rotating screens for coarse pre-filtration;
- ✓ chemical additions (chlorination, acid and antiscalants addition, in-line coagulation, addition of flocculants);
- ✓ single- or double-stage sand filtration;
- ✓ cartridge filtration (mesh size 5–10 μm).

Chlorination is necessary to disinfect the feed water and to prevent biological growth which causes fouling for both filters and membranes and reduces treatment performance. Chlorine is added to the raw water as sodium hypochlorite (NaOCl) or chlorine gas (Cl_2).

As an alternative to chlorination, ultraviolet (UV) radiation is able to disinfect the raw water but so far is seldom applied.

Dechlorination has to be performed because residual chlorine in the feedwater to the reverse osmosis element may damage the membrane by oxidation and/or hydrolysis. Commonly, sodium metabisulphite is used for dechlorination due its high cost effectiveness [29]. Moreover, beside sodium metabisulphite, activated carbon is very effective to reduce residual free chlorine.

Sometimes it is necessary to adjust the pH of the feed water to prevent $CaCO_3$ scaling by adding acids such as hydrochloride acid (HCl) or sulphuric acid (H_2SO_4). In RO applications, the pH value is generally lowered to normalized value where RO membranes show better performance.

Coagulation and flocculation agents (such as $FeCl_3$, ferric salts $Fe_2(SO_4)_3$ or aluminium sulphate $Al_2(SO_4)_3$) are added to promote the adsorption of dissolved matter on hydroxides formed and the agglomeration of colloidal matter. A subsequent sedimentation and sand filtration remove those agglomerates from the feedwater. During coagulation alkalinity is reduced and CO_2 is produced.

Different scale inhibitors are used to prevent the precipitation of salts on the membrane surface caused by supersaturation.

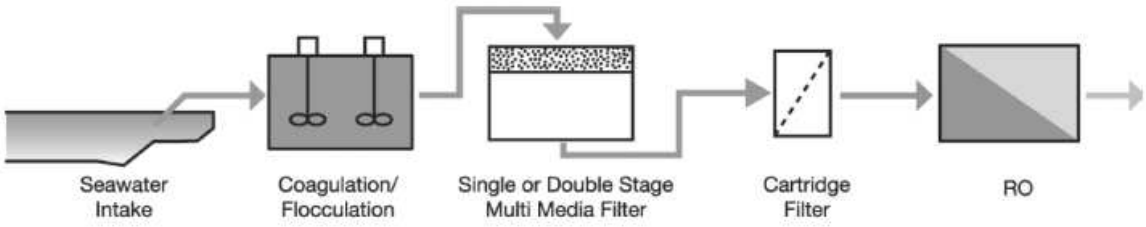

Figure 21: Typical conventional RO pre-treatment [24].

Filtration is either performed in pressurized lined steel vessels or gravity driven concrete chambers to remove a portion of the coagulated organic and inorganic particulate and colloidal matter present in the raw water.

The final step of pre-treatment is a cartridge- or bag type guard filter with a mesh size of 5 to 10 µm to protect the RO membranes. Accordingly, particles larger than 5µm only are removed. Conventional filter systems are backwashed with filtered water and air at least once a day. The filter replacement rate varies depending on the raw water quality and ranges between every two to eight weeks [24, 29].

The above described pre-treatment systems may produce feed water of an acceptable quality when properly tuned and with good and constant raw seawater quality: a single stage sand filtration or even a simple cartridge filtration is able to achieve SDI values well below 3 if the system is fed by water from beach well sources which provide good quality raw water. But, when open seawater intakes are used, poor raw water quality during storms or algae bloom can cause problems even in a properly tuned conventional pre-treatment system [29].

Wolf et al. [24] listed the major disadvantages of a conventional pre-treatment which contribute to higher rates of RO membrane fouling and shorter RO membrane lifetime expectancy of as:

- ✓ significant fluctuations of the quality of RO feed caused by changing raw water conditions;
- ✓ difficult to achieve a constant $SDI_{15} < 3.0$, especially during high turbidity feed water conditions;
- ✓ low removal efficiency of particles smaller than 10–15 microns;
- ✓ possibility of breakthrough during filter backwash;
- ✓ carry over of high concentrations of colloidal particles immediately following a filter backwash;
- ✓ coagulant influences membrane performance;
- ✓ large footprint due to slow filtration velocities. The footprint of a conventional pre-treatment is about 35–40 m^2/1000 m^3/day permeate [29].

In conclusion, conventional pre-treatment is generally complex, labour intensive and space consuming.

4.1.2 Membrane pre-treatment

Pressure-driven membrane operations are the new trend in designing pre-treatment systems because they are able to remove a wide range of contaminants including particulates, colloids and pathogens.

Microfiltration and ultrafiltration membranes have been successfully applied in pre-treatment of much more difficult raw waters than seawater, such as in industrial and municipal wastewater for many years.

In a process using membranes in pre-treatment, the raw water is usually roughly pre-filtered by a mechanical screen before it is fed to the membrane. Commercially available modules are: immersed plate-, pressure driven capillary-, pressure driven spiral wound- and immersed hollow fibre- modules. Most commonly, hollow fibre modules are applied for pre-treatment [29].

For what concerns MF, it generally provides an RO feedwater of good quality, with lower COD/BOD and a lower SDI in comparison to the untreated seawater. The total costs for the MF are lower than that a conventional pre-treatment because of:

- ✓ elimination of fine filters in the RO systems;
- ✓ less membrane replacement cost due to the lengthened membrane useful life;
- ✓ less chemical consumption and cost because less chemicals are needed for disinfection, coagulation and dechlorination (see Table 9);
- ✓ elimination of cartridge filters cost because no cartridge filters are needed before the RO step (see Table 10) [15];
- ✓ less maintenance cost for the high pressure pump and the measuring instruments;
- ✓ less labor cost because less manpower is needed to operate the conventional pretreatment system and to clean the membrane and maintain the system [77].

Table 9: Chemical cost comparison for different pre-treatment options [78].

Pre-treatment process	Conv.	UF/MF	UF/MF
RO cleans/y	3	2	1
Operating costs — chemicals	k,$	k,$	k,$
Dosing and UF/MF cleaning	61.4	24.1	24.1
RO cleaning	83.5	55.7	27.8
Total	144.9	79.8	51.9

Table 10: Total water cost comparison for different pre-treatment options [78].

Number of RO cleans per year →	RO + conventional pre-treatment		RO + UF/MF pre-treatment			
	3		2		1	
	$	cents/m^3	$	cents/m^3	$	cents/m^3
Electric power [A]	2,850,000	41.18	2,850,000	41.01	2,850,000	40.83
RO membrane replacement	243,000	3.51	162,000	2.33	162,000	2.32
UF membrane replacement	0	0	136,000	1.96	136,000	1.95
Chemicals	145,000	2.10	80,000	1.15	52,000	0.74
Cartridges	31,000	0.45	0	0	0	0
Maintenance and parts	415,000	6.00	415,000	5.97	415,000	5.95
Supervision and labor	265,000	3.83	265,000	3.81	265,000	3.80
Amortization [B]	2,284,000	33.01	2,354,000	33.87	2,354,000	33.72
Total	6,233,000	90.07	6,262,000	90.10	6,234,000	89.31
Operating days per year	346		347,5		349	
Plant capacity [m^3/y]	6920		6950		6980	

[A] Based on an unit electric cost of 0.10 $/KWh, a specific consumption of electric power of 4.1kWh/m^3 and, therefore, without the presence of currently adopted Energy Recovery Devices in the desalination process.
By considering a price more normally used with this type of project evaluation (0.07 $/KWh), the energy cost would be approximately 26 cent/m^3, reducing unit water cost from about 90 to 75 cents/m^3.
[B] Based on amortization of capital at 8% over 20 years.

Further improvement of the RO feedwater can be obtained by replacing MF by UF. In UF, not only suspended solids and large bacteria but also (dissolved) macromolecules, colloids and smaller bacteria are retained; turbidity and suspended solids are completely removed; SDI values are always well below 2 and the COD/BOD decreased by the removal of (large) dissolved organics. As a consequence, UF permeate (the RO feed) is significantly improved. Somewhat larger pressures than MF have to be applied (in the range of l-5 bar) so that the cost is higher than for MF, but competitive with conventional pre-treatment. Moreover, allowing higher RO membrane operating flux, fewer RO membranes, pressure vessels, manifolds, space and lower total water cost are expected [24]. Taking all factors into account, the total cost of a membrane desalination plant constituted by UF + RO will be 2-7% lower than the total cost of a SWRO plant based on conventional pre-treatment [79].
Membrane application in surface water treatment also provides many other advantages over conventional treatment including: capability of handling wide fluctuations in raw water quality, enabling operation with a high and stable permeate flux in long term operation even during storm events and algae blooms [23, 24, 29]; small footprint; low energy consumption.
A comparative overview of the influence of both membrane and conventional pre-treatment is given in Tables 11 and 12.

Table 11: Comparison of conventional and MF/UF pre-treatment [80].

	Conventional pretreatment	MF/UF pretreatment	Benefits
Capital costs	Cost competitive with MF/UF	Slightly higher than conventional pretreatment. Costs continue to decline as developments are made	Capital costs of MF/UF could be 0–25% higher, whereas life cycle costs using either of the treatment schemes are comparable
Foot print	Calls for larger footprint	Significantly smaller footprint	Foot print of MF/UF could be 30-50 % of conventional filters.
Energy requirements	Less than MF/UF as it could be gravity flow	Higher than conventional	MF/UF requires pumping of water through the membranes. This can vary depending on the type of membrane and water quality
Chemical costs	High due to coagulant and process chemicals needed for optimization	Chemical use is low, dependent on raw water quality	Less chemicals
RO capital cost	Higher than MF/UF since RO operates at lower flux	Higher flux is logically possible resulting in lower capital cost	Due to lower SDI values, RO can be operated at 20% higher flux if feasible, reducing RO capital costs
RO operating costs	Higher costs as fouling potential of RO feed water is high resulting in higher operating pressure. One experiences frequent cleaning of RO membranes.	Lower RO operating costs are expected due to less fouling potential and longer membrane life	The NDP (net driving pressure) is likely to be lower if the feed water is pre-treated by MF/UF. Membrane cleaning frequency is reduced by 10–100%, reducing system downtime and prolonged element life.

Table 12: Comparison of the impact of UF pre-treatment on an RO based sea water desalination plant [24].

	UF pretreatment: ZeeWeed® 1000 immersed hollow fiber	Conventional pretreatment: in-line coagulation and 2-stage sand filters
Treated Water:		
SDI_{15}:	<2.5, 100% of the time, usually <1.5	<4 for about 30% of the timer
Quality:	Consistent, reliable	Fluctuating
Barrier activity:	Positive barrier to particles and pathogens – no breakthrough	Not a positive barrier to colloidal and suspended particles
Turbidity:	<0.1 NTU	<1.0 NTU
Bacteria:	>5 log removal	N.A.
Giardia:	>4 log removal	N.A.
Virus:	>4 log removal	N.A.
Typical Lifetime:		N.A.
UF Membranes:	5–10 years	N.A.
Filter media:	N.A.	20–30 years
Cartridges:	often not needed	2–8 weeks
Average RO Flux:	~18 lmh	~14 lmh
SWRO replacement-rate	~10% per year	~14% per year
SWRO cleaning frequency	~1–2 times per year	~4–12 times per year
Pretreatment foot-print	~30–60% (of conventional)	100%

According to Wolf et al. [24], who compared conventional pre-treatment using inline coagulation and two stage sand filters with membrane pre-treatment using UF ZeeWeed® 1000 immersed hollow fibre based on sea water desalination plant (as illustrated in Table 12), the use of UF membrane showed a better RO performance than that with conventional pre-treatment.

However, the major limitation of membrane filtration is fouling caused by the deposition of materials on or within the structure of the membrane, which results in increase in hydraulic resistances, operational and maintenance costs, and deterioration of productivity and product quality [23]. Any species in the feed water is a potential foulant and its impact will depend on its characteristics and concentration as well as membrane properties (pore size, charge, and hydrophobicity), module properties, mode of operation and applied flux [23]. One of the most important identified foulants found in surface water filtration is natural organic matter (NOM). Bacteria can also adhere on the membrane surface and create a biofilms [23].
In terms of design and membrane fouling control, UF and MF are always protected by a screen from 500 to 50 μm according to the membrane supplier. Moreover, according to Bonnélye et al. [81], it can be necessary to add a coagulation and settling/flotation for the treatment of very bad water quality, to improve the permeate water quality feeding the RO or to optimize the design (filtration flux increase and membrane surface reduction, cleaning frequency reduction, membrane life-time increase). This coagulation and settling is considered "the pre-treatment of the pre-treatment", and interesting is the replacement of the settling technology by a flotation step.
In both cases, the full coagulation (i) allows a better removal of NOM; (ii) can face bad seawater quality, high turbidity, algae counts (red tide and blooms), hydrocarbon pollutions; (iii) presents a definitive advantage for the control of clarification-membrane fouling.

In a dissolved air flotation (DAF) process, about 10% of the raw water is taken from the raw water stream, pressurised and saturated with air, before it is released back through nozzles or valves into the raw water leaving the flocculation chamber. The sudden pressure release forms micro bubbles of about 60 microns in size onto which preformed flocs and particulate matter attach and are carried by the bubbles to the surface. DAF can achieve effluent turbidity <0.5 NTU, effectively removes high concentration of algae and shows advantages in treating very cold raw water [29]. Bonnélye et al. [81] reports some piloting tests performed by Degremont showing that dissolved air flotation (AquaDAF^{TM}, Figure 22) prior to immerged membrane filtration (GE/Zenon's product, Figure 23), improves the UF membrane filtration and optimizes the cost of the UF pre-treatment.

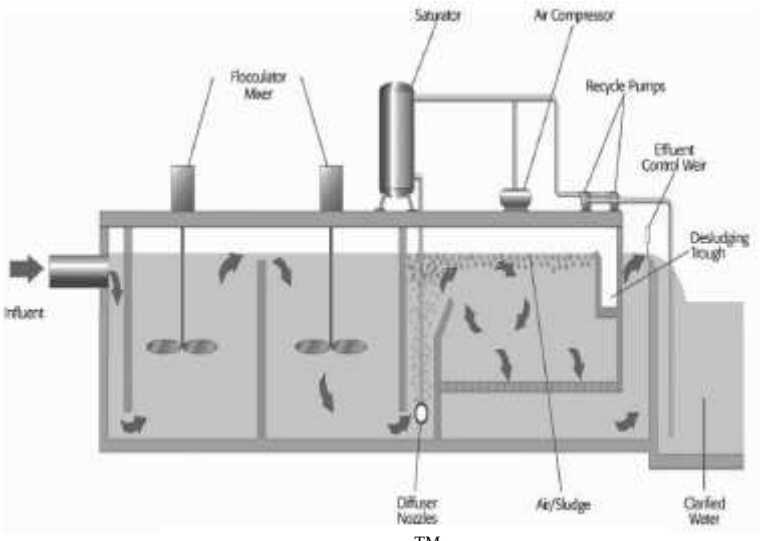

Figure 22: AquaDAF^{TM} technology [81].

Figure 23: Submerged UF membrane (ZW1000 V3 -GE/Zenon's product) [81].

It must be noted that the association pre-clarification plus UF/MF allows a significant reduction of costs mainly due to the increase of filtration flux in the case of difficult surface seawater [81]. But this process is still more expensive than conventional pre-treatment. UF/MF and pre-coagulation can only be justified if associated with a reduction of the RO cost. In fact, the challenge of dissolved air flotation (AquaDAFTM) prior to immerged membrane filtration is to produce a high-quality treated water which allows higher RO flux (and/or higher recovery), reaches an optimum RO power consumption and improves reliability regarding biofouling issue. Only RO flux higher than 10% would make this process a cost-effective solution.
In conclusion, the choice of the best pre-treatment strongly depends on raw water quality to treat and can extend the applicability of the RO treatment on a wider variety of sources.

Further improvements to RO flux and reliability can be achieved through the introduction of NF as pre-treatment process because it has implications on the desalination process itself: turbidity, microorganisms, hardness, the most part of multivalent ions and 10-50% of monovalent species (depending on NF membrane type) are retained through this operation. As a consequence, the osmotic pressure of the RO feed stream is decreased, thus allowing the unit to operate at higher recovery factors. In fact, according to Drioli et al. [67], coupling NF and RO for seawater desalination, a global recovery factor of 52% can been obtained, more higher than that of a typical RO operation which is in the range of 35-40%. Moreover, the integrated NF-RO process is more environmentally friendly, because less additives (antiscalants, acid) are needed [15].

4.2 Brine disposal strategies

Seawater desalination processes are positively contributing to solve the problem of water shortage but, at the same time, they cause locally some negative impacts on the

environment that need to be minimized. In fact, desalination plants supply water for municipal, tourist, agricultural and industrial use and they preserve natural water resources from exploitation providing water for recreational areas and forests. But, besides this environmental protection effect, they have several disadvantages concerning their impact on the environment: noise is emitted, energy is consumed and highly concentrated brine as well as waste membranes have to be discharged.

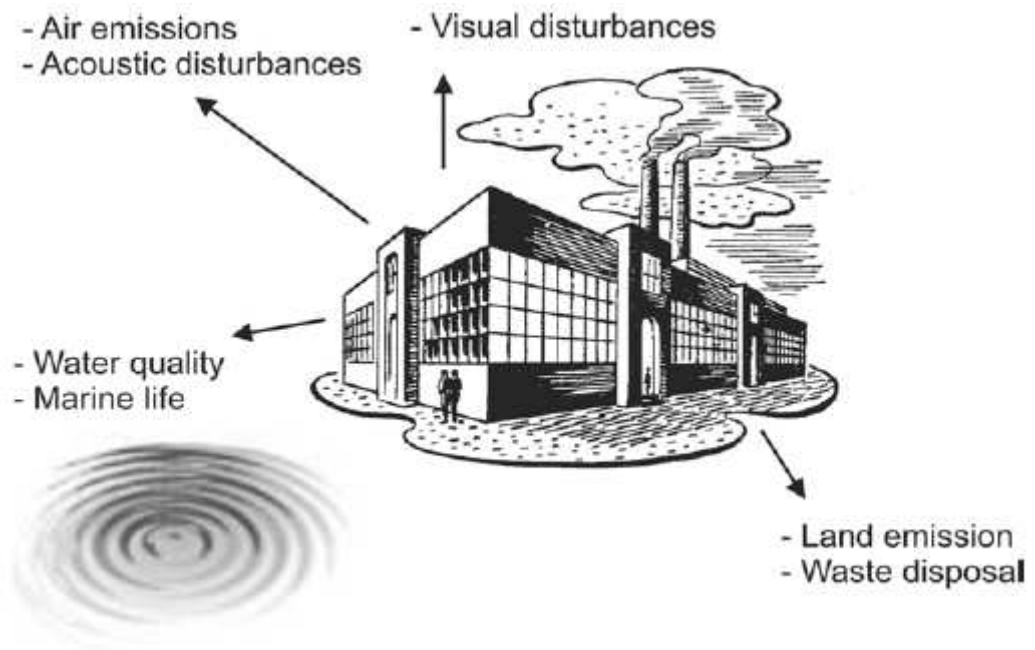

Figure 24: Environmental impact of RO desalination [29].

Special attention has to be paid to the way brine is discharged. At present, the majority of desalination facilities discharge their concentrate waste streams into surface waters or the oceans. This disposal method represents currently the most effective and least expensive option for both small and larger systems located near coastal regions. However, the promulgation of more and more stringent environmental protection regulations will reduce progressively this opportunity. Negative influences of the discharged brine may not only damage the environment or reduce public acceptance, but can also result in financial penalties if toxicity standards are not met.
Three aspects of the highly concentrated streams to be discharged are important: (1) temperature, (2) salinity and (3) chemicals discharged with the brine.
The temperature rise may have a negative influence on the oxygen level of the receiving water; the same effect is found for a salinity increase. The increased salinity resulted in a significant impact on marine organisms due to the natural osmosis phenomenon. This is the ability of water to move in and out of living cells (anything else that membranes) in response to a concentration of a dissolved material, until an equilibrium is reached. It was observed that, after three years of operation, higher salinity resulted in significant degradation on some macro-algal populations, while some other species completely disappeared within a distance of 100 m from the discharge point. Changes in the observed marine ecosystem are shown in Table 13 [29].

Table 13: Benthic community at the Dhekelia plant [29].

	Before Operation [%]	After three years of operation [%]
Polychaetes	27	80
Echinoderms	27	—
Scaphopods	26	—
Gastropods	20	—
Crustaceans	—	20

For what concerns chemical agents utilized during RO desalination process, these are a real contamination for the receiving water. Van der Bruggen et al. [15] classified chemicals into three major categories: (1) biocides, (2) scale control and (3) anti-foams. New trends are in the development of environmentally-friendly products (such as the use of polymeric additives based on maleic anhydride and biodegradable anti-foams).

Possible measures to mitigate environmental impact of the discharged brine are [29]:

- ✓ lower recovery rates and/or dilution of the brine with seawater prior to the discharge to reduce its salinity;
- ✓ discharge devices, such as multiple port diffusers, spreading the brine across a larger area and increasing dispersion velocity;
- ✓ dilution of the brine with water from other processes, e.g. with cooling water from power;
- ✓ discharge in an area with strong currents and at depth.

In the present work, membrane contactor technology has been applied in order to reduce pollutant emissions and to ensure a more rational use of natural resources. As described in details in *Section 3.2* and in *Chapters 2, 6 and 7*, when the NF/RO retentate streams of a desalination plant are processed in a MD and/or MCr unit, the added value of the retentate is utilized with several advantages:

1. the salts usually present in the highly concentrated streams of the desalination plants (sodium chloride, magnesium sulphate, calcium carbonate) are recovered in the form of valuable crystals for medical, domestic or agricultural use.
2. The recovery factor of the MD and MCr is, respectively, 77 and theoretically 100% [67], whereas the RO unit alone gives a recovery factor in the range of 35-40%. By coupling NF/RO with MD/MCr, more fresh water can be produced: the RO brine is ≈60% of the total feed while, in the integrated system “RO” plus “MD on RO brine”, the discharged brine is only 14% of the feed.
3. The higher recovery factor of the integrated system “NF and/or RO” plus “MD or MCr on the retentate streams” reduces the amount of discharged brine and, as a consequence, its environmental impact.

5. Conclusions

Water shortage problem is growing increasingly in the last decades due to the deterioration of water quality and to the growing human, agriculture and industrial needs. However, water scarcity and contamination have encouraged the development of desalination as an alternative and available water source. Actually, the challenge is to supply desalinated water at lower costs and of better quality through environmentally friendly industrial processes.

Membrane Engineering offers the possibility to more sustainable fresh water production through those integrated membrane-based desalination systems whose basic aspects satisfy the requirements of *Process Intensification Strategy*.

A typical RO seawater desalination process can be improved and optimized introducing in the pre- and post-treatment steps other and different membrane operations. The integration of various membrane technologies allows to overcome the limits of RO operation thus enhancing the performance of the overall system. In particular:

- the presence of MF/UF in the pre-treatment step provides a RO feedwater of good quality, decreasing membrane fouling and, then, capital and operating costs;
- the introduction of NF allows to decrease osmotic pressure of the water fed to the following RO unit which can operate at higher recovery factor without scaling problems;
- in this logic well fit in also Membrane Distillation and Membrane Crystallization: they allow to utilize the added value of the retentate, increasing plant recovery factor, reducing brine disposal problem and its environmental impact, and producing valuable crystals for medical, domestic or agricultural use.

The importance of future worldwide water availability has been also recognized by the Commission of the European Communities, by MERDC and by the Joint Water Reuse & Desalination Task Force (JWR&DTF) through the financial support of a series of research projects. For example, the projects funded during the Sixth Framework Programme of European Commission in Global Change and Ecosystems thematic area are 303; seventy-two (72) of these funded projects (equal to 24%) are related to *Water Problem.*

MEDESOL and MEDINA are two of the European funded projects in the FP6. In particular, in MEDINA project the research team is developing a work programme based on the integration of different membrane operations in pre-treatment and post-treatment stages according to the philosophy of *Process Intensification* and for the sustainable development of desalination processes.

It is expected that, in future, more and more research activities will be conducted to assess the existing limitations and issues related to water production and treatment processes, to improve their efficiency and reliability, to develop and propose innovative strategies in order to minimise environmental impacts and water cost, to optimise energy sources and consumption, to increase water quality.

Relevant Bibliography

[1] Cost of water shortage civil unrest, mass migration and economic collapse Special reports Guardian Unlimited.htm
[2] D. Bixio, C. Thoeye, J. De Koning, D. Joksimovic, D. Savic, T. Wintgens, T. Melin, *Wastewater reuse in Europe*, Desalination, 187 (2006) 89–101.
[3] Water Desalination Report, Monday 22 October 2007.
[4] Water Desalination Report, 7 January 2008.
[5]Water IDA news, January/February 2008, Volume 17, Issue 1-2.
[6] Dr Val Frenkel, *Brackish vs Seawater Desalination: Which one is for You?*, Desalination & Water Reuse, Vol.17/4, 2008.
[7] Desalination & Water Reuse, Vol. 15, No. 3, pag.58, 2007.
[8] Nikolay Vouchkov, *Drought-Proofing Californian's Water Future*, The International Desalination&WaterReuse, Nov./Dec. 2006, Vol. 16/No 3, p. 10-17.
[9] Jean-Claude Charpentier, *Modern Chemical Engineering in the Framework of Globalization, Sustainability, and Technical Innovation* , Ind. Eng. Chem. Res., 2007, *46*, 3465-3485.
[10] G. M. Rios, M.-P. Belleville, D. Paolucci-Jeanjean, *Membrane engineering in biotechnology: quo vamus?*, TRENDS in Biotechnology, Vol.25 No.6 (2007) 242-246.
[11] Ian Lomax, *Experiences of Dow in the field of seawater reverse osmosis*, Desalination, 224 (2008) 111–118.
[12] El-Dessouky, H., *Multistage Flash Desalination Technologies*, Sustainability Assessment of Water Desalination Technologies, Vilamoura, Portugal (2000) 1-13.
[13] H. M. Ettouney, H. T. El-Dessouky, R. S. Faibish, P. J. Gowin, *Evaluating the Economics of Desalination*, CEP Magazine, (December 2002), 32-39.
[14] W. J. Koros, *Evolving Beyond the Thermal Age of Separation Processes: Membranes Can Lead the Way*, AIChE Journal, Volume 50, Issue 10, October 2004, Pages: 2326-2334.
[15] B. V. der Bruggen, C. Vandecasteele, *Distillation vs. membrane filtration: overview of process evolutions in seawater desalination*, Desalination, 143 (2002) 207-218.
[16]http://www.water-technology.net/projects/israel/specs.html (2008).
[17] http://www.epwu.org/167080115.html.
[18] G.Congjie, *Growth and Prospect of Seawater Desalination Technology in China*, International Forum on Water Industry Qingdao 2005, China, July 2005, 1- 16.
[19] Lin Zhang, Lin Xie, Huan-Lin Chen, Cong-Jie Gao, *Why China needs seawater desalination*, The International Desalination&WaterReuse, Vol. 15 No 2 (2005) 49-50.
[20] Global Water Intelligence, Issue: 11, November, 2005.
[21] http://www.kochmembrane.com
[22] Marcel Mulder, *Basic Principles of Membrane Technology*, Kluwer Academic Publishers, London.
[23] Eun Kyung Lee, Vicki Chen, A.G. Fane, *Natural organic matter (NOM) fouling in low pressure membrane filtration — effect of membranes and operation modes*, Desalination, 218 (2008) 257–270.
[24] P. H. Wolf, S. Siverns, S. Monti, *UF membranes for RO desalination pretreatment*, Desalination, 182 (2005) 293–300.
[25] S. Loeb and S. Sourirajan, *High flow porous membranes for separation of water from saline solutions*, US patent 3,133,132, 1964.

[26] http://www.kochmembrane.com/prod_sr.html
[27] http://www.lenntech.com
[28] http://www.dow.com/
[29] C. Fritzmann, J. Löwenberg, T. Wintgens, T. Melin, State-of-the-art of reverse osmosis desalination, Desalination 216 (2007) 1–76.
[30] R. Rautenbach and T. Melin, Mebranverfahren (Grundlagen der Modul- und Anlagenauslegung), 2nd ed., 2003.
[31] Cleaning chemicals, DOW FILMTEC Membranes, Tech Manual Exerpt, Form No. 609-02091-704.
[32] Manth T., Gabor M., Oklejas E., *Minimizing RO energy consumption under variable conditions of operation*, Desalination, 157 (2003) 9-21.
[33] D. H. Hellmann, H. Rosemberg, E. F. Tusel, *Saving of energy and cost in seawater desalination with speed controlled pumps*, Desalination, 139 (2001) 7-19.
[34] M.S. El-Bourawi, Z. Ding, R. Ma, M. Khayet, *A framework for better understanding membrane distillation separation process*, Journal of Membrane Science 285 (2006) 4–29.
[35] K.W. Lawson, D.R. Lloyd, *Membrane distillation*, J. Membr. Sci. 124 (1997) 1–25.
[36] J.I. Mengual, L. Pena, *Membrane distillation*, Colloid Interf. Sci. 1 (1997) 17–29.
[37] K.W. Lawson, D.R. Lloyd, *Membrane distillation. I. Module design and performance evaluation using vacuum membrane distillation*, J. Membr. Sci. 120 (1996) 111–121.
[38] M. Khayet, M.P. Godino, J.I. Mengual, *Theoretical and experimental studies on desalination using the sweeping gas membrane distillation*, Desalination 157 (2003) 297–305.
[39] M. Khayet, J.I. Mengual, G. Zakrzewska-Trznadel, *Direct contact membrane distillation for nuclear desalination. Part II. Experiments with radioactive solutions*, Int. J. Nucl. Desalinat. (IJND) 56 (2006) 56–73.
[49] M. Sudoh, K. Takuwa, H. Iizuka, K. Nagamatsuya, *Effects of thermal and concentration boundary layers on vapor permeation in membrane distillation of aqueous lithium bromide solution*, J. Membr. Sci. 131 (1997) 1–7.
[41] E. Drioli, V. Calabrò, Y.Wu, *Microporous membranes in membrane distillation*, Pure Appl. Chem. 58 (12) (1986) 1657–1662.
[42] P.P. Zolotarev, V.V. Ugrosov, I.B. Volkina, V.N. Nikulin, *Treatment of waste-water for removing heavy-metals by membrane distillation*, J. Hazard. Mater. 37 (1) (1994) 77–82.
[43] S.H. Duan, A. Ito, A. Ohkawa, *Removal of trichloroethylene from water by aeration, pervaporation and membrane distillation*, J. Chem. Eng. Jpn. 34 (8) (2001) 1069–1073.
[44] F.A. Banat, J. Simandl, *Removal of benzene traces from contaminated water by vacuum membrane distillation*, Chem. Eng. Sci. 51 (8) (1996) 1257–1265.
[45] G.C. Sarti, C. Gostoli, S. Bandini, *Extraction of organic-compounds from aqueous streams by vacuum membrane distillation*, J. Membr. Sci. 80 (1993) 21–33.
[46] N. Qureshi, M.M. Meagher, R.W. Hutkins, *Recovery of 2,3-butanediol by vacuum membrane distillation*, Sep. Sci. Technol. 29 (13) (1994) 1733–1748.

[47] F.A. Banat, M. Al-Shannag, *Recovery of dilute acetone–butanol–ethanol (ABE) solvents from aqueous solutions via membrane distillation*, Bioprocess Eng. 23 (6) (2000) 643–649.
[48] F.A. Banat, J. Simandl, *Membrane distillation for propane removal from aqueous streams*, J. Chem. Technol. Biotechnol. 75 (2) (2000) 168–178, AGMD.
[49] M.C. Garcia-Payo, M.A. Izquierdo-Gil, C. Fernandez-Pineda, *Air gap membrane distillation of aqueous alcohol solutions*, J. Membr. Sci. 169 (2000) 61–80.
[50] F.A. Banat, J. Simandl, *Membrane distillation for dilute ethanol separation from aqueous streams*, J. Membr. Sci. 163 (1999) 333–348.
[51] S. Bandini, A. Saavedra, G.C. Sarti, *Vacuum membrane distillation: experiments and modeling*, AIChE J. 43 (2) (1997) 398–408.
[52] S. Bandini, G.C. Sarti, *Heat and mass transfer resistances in vacuum membrane distillation per drop*, AIChE J. 45 (7) (1999) 1422–1433.
[53] V. Calabrò, E. Drioli and F. Matera, *Membrane distillation in the textile wastewater treatment*, Desalination, 83 (1991) 209-224.
[54] S. Nene, S. Kaur, K. Sumod, B. Joshi and K.S.M.S. Raghavarao, *Membrane distillation for the concentration of raw cane-sugar syrup and membrane clarified sugarcane juice*, Desalination, 147 (2002) 157-160.
[55] V. Calabrò, B.L. Jiao and E. Drioli, *Theoretical and experimental study on membrane distillation in the concentration of orange juice*, Ind. Eng. Chem. Res., 33 (1994) 1803-1808.
[56] S, Bandini and G.C. Sarti, *Concentration of must through vacuum membrane distillation*, Desalination, 149 (2002) 253-259.
[57] F. Laganà, G. Barbieri, E. Drioli, *Direct contact membrane distillation: modeling and concentration experiments*, J. Membr. Sci., 166 (2000) 1-11.
[58] V.D. Alves, I.M. Coelhoso, *Orange juice concentration by osmotic evaporation and membrane distillation: A comparative study*, Journal of Food Engineering 74 (2006) 125–133.
[59] Corinne Cabassud, David Wirth, *Membrane distillation for water desalination: how to chose an appropriate membrane?*, Desalination 157 (2003) 307-314.
[60] A. M. Alklaibi, Noam Lior, *Membrane-distillation desalination: status and potential*, Desalination 171 (2004) 111-131.
[61] F. Macedonio, E. Drioli, *Pressure-driven membrane operations and membrane distillation technology integration for water purification*, Desalination, 223 (2008) 396-409.
[62] F. Macedonio, E. Curcio, E. Drioli, *Integrated Membrane Systems for Seawater Desalination: Energetic and Exergetic Analysis, Economic Evaluation, Experimental Study*, Desalination, 203 (2007) 260-276.
[63] E. Curcio, A. Criscuoli, E. Drioli, *Membrane Crystallizers*, Ind. Eng. Chem. Res., 40 (2001) 2679-2684.
[64] E. Curcio, E. Drioli, *Membrane Distillation and Related Operations-A Review*, Separation and Purification Reviews, 34 (2005) 35-85.
[65] M.S. El-Bourawi, Z. Ding, R. Ma, M. Khayet, *Review. A framework for better understanding membrane distillation separation process*, Journal of Membrane Science, 285 (2006) 4–29.

[66] C. Mya Tun, A. G. Fane, J. T. Matheickal, R. Sheikholeslami, *Membrane distillation crystallization of concentrated salts—flux and crystal formation,* Journal of Membrane Science , 257 (2005) 144–155.
[67] Drioli, E.,Lagana, F., Criscuoli, A., Barbieri, G., *Integrated membrane operations in desalination processes*, Desalination 122 (1999) 141-145.
[68] S. Srisurichan, R. Jiraratananon, A.G. Fane, *Mass transfer mechanisms and transport resistances in direct contact membrane distillation process*, Journal of Membrane Science, 277 (2006) 186–194.
[69] E. Drioli, E. Curcio, G. Di Profio, F. Macedonio, A. Criscuoli, *Integrating Membrane Contactors Technology and Pressure-Driven Membrane Operations for Seawater Desalination: Energy, Exergy and Cost Analysis*, Chemical Engineering Research and Design, 84 (A3) (2006) 209–220.
[70] P. Coté, H. Buisson, M. Praderie, *Immersed membranes activated sludge process applied to the treatment of municipal wastewater*, Wat. Sci. Tech., Vol. 38, No. 4-5, 1998, 437-442.
[71] T. Melin, B. Jefferson, D. Bixio, C. Thoeye, W. De Wilde, J. De Koning, J. van der Graaf and T. Wintgens, *Membrane bioreactor technology for wastewater treatment and reuse*, Desalination, 187 (2006) 271-282.
[72] http://www.iwaponline.com
[73] R. Rautenbach, K. Vossenkaul, T. Linn and T. Katz, *Waste water treatment by membrane process. New development in ultrafiltration, nanofiltration and reverse osmosis*, Desalination, 108 (1996) 247-253.
[74] S. Zhang, Renze van Houten, D. H. Eikelboom, H. Doddema, Z. Jiang, Y. Fan, J. Wang, *Sewage treatment by a low energy membrane bioreactor*, Bioresource Technology, 90 (2003) 185-192.
[75] http://en.wikipedia.org/wiki/Sewage_treatment#Membrane_bioreactors
[76] Truby, R., *Membrane Separation Markets in North America*, IDA News, January-February 2001, 4.
[77] S. Ebrahim, M. Abdel-Jawad, S. Bou-Hamad, M. Safar, *Fifteen years of R&D program in seawater desalination at KISR Part I. Pretreatment technologies for RO systems*, Desalination, 135 (2001) 141-153.
[78] G.K. Pearce, *The case for UF/MF pretreatment to RO in seawater applications*, Desalination 203 (2007) 286–295.
[79] F. Knops, S. van Hoof, H. Futselaar, L. Broens , *Economic evaluation of a new ultrafiltration membrane for pretreatment of seawater reverse osmosis*, Desalination 203 (2007) 300–306.
[80] C. V. Vedavyasan, *Pretreatment trends-an overview*, Desalination, 203 (2007)**,** 296-299.
[81] V. Bonnélye, L. Guey, J. Del Castillo, *UF/MF as RO pre-treatment: the real benefit*, Desalination 222 (2008) 59–65.

CHAPTER 2: Integrated Membrane Systems for Seawater Desalination

Table of Contents

1. Introduction

As stated in *Chapter 1*, membrane technology has emerged, in the last years, as the most promising contributor to solve water shortage problems by seawater/brackish water desalination and wastewater treatment and reuse.
Despite the great success and the potentialities of membrane technology, some critical problems still remain open: improving water quality, increasing the recovery factor of desalination processes, reducing the global costs and minimizing the brine disposal impact. For solving these problems, two different ways can be followed in the field of membrane operations:

- discovering new materials for making membranes more stable and resistant to chemicals in order to increase their performance and life-time and, then, to reduce the replacement and maintenance costs;
- coupling several membrane processes in order to overcome the limits of the single units and to use their synergic effects in terms of better performance of the overall system.

At present, the most interesting developments for industrial membrane technologies are related to the possibility of integrating various membrane operations with all the important benefits in the logic of *Process Intensification*.

The first purpose of the work presented in *Chapters 2* and *3* is to propose and analyse seven different possible flow sheets for seawater desalination. In each of them different membrane units have been integrated. The second purpose is the comparison of the proposed desalination systems, on the basis of the quality and characteristics of the fresh water produced and of the discharged brine, of the energy requirements and exergy efficiency, on the basis of the desalted water cost and of the so-called "*sustainable metrics*".

2. Conventional integrated membrane systems for seawater desalination: case study 1, 2 and 3

Figures 1, 2 and 3 show three possible flow sheets for seawater desalination. In each of them, except for the first (FS1) constituted only by the RO unit, different membrane units have been integrated: RO operates on NF permeate in FS2; both MF and NF have been introduced for the feed water pre-treatment and load reduction to the following reverse osmosis unit in FS3.

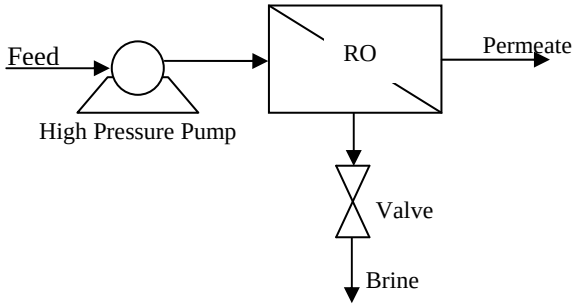

Figure 1. Flow sheet 1 (FS1): RO unit alone.

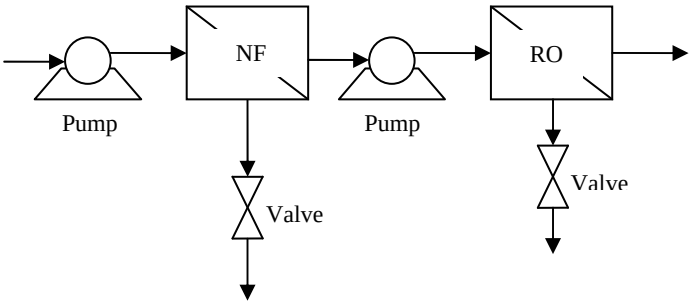

Figure 2. Flow sheet 2 (FS2): RO operating on NF permeate.

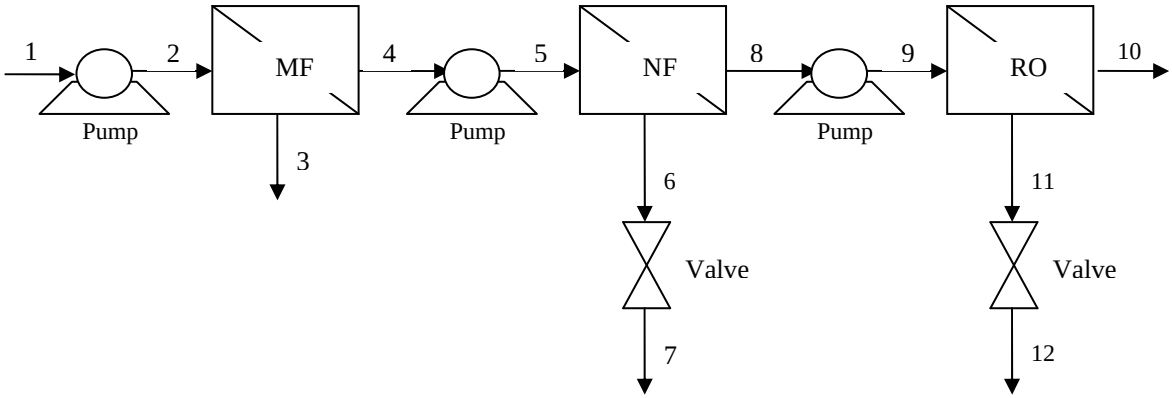

Figure 3. Flow sheet 3 (FS3): MF/NF/RO.

In all the proposed flow sheets, as feed water composition has been considered the standard seawater composition [1]. Seawater is a solution of more than 70 elements but only the following reported in Table 1 make up more than 99% of all the dissolved salts.

Table 1: Standard seawater composition.

TDS: 35,000 mg/L	pH: 8.1	
Chloride:	19,345 mg/L	55.03 wt %
Sodium:	10,752 mg/L	30.59 wt %
Sulphate:	2,701 mg/L	7.68 wt %
Magnesium:	1,295 mg/L	3.68 wt %
Calcium:	416 mg/L	1.18 wt %
Potassium:	390 mg/L	1.11 wt %
Bicarbonate:	145 mg/L	0.41 wt %

Table 2: Rejection values.

Ion	NF [%]	RO [%]
HCO_3^-	62.0	98.4
Na^+	22.0	98.9
Cl^-	12.8	99.0
SO_4^{2-}	90.0	99.6
Ca^{2+}	88.4	99.7
Mg^{2+}	89.0	99.6

The RO performance has been taken from a previous work reported in [2]. In all the flow sheets, the RO permeate water composition has been calculated considering the same rejection values (see Table 2) and which are referred to SW1 PA element with 7.3 m^2 of active surface area and flow equal to 3.7 m^3/d. The feed water flow rate and the operation conditions for the RO unit have been also taken from [2].
For the NF unit the rejection values are taken from [2] and are also reported in Table 2. They are referred to a NF300 PA element, with 6.8 m^2 of active surface area and flow equal to7.5 m^3/d. The NF acts on the feed seawater in FS2, on the MF permeate in all the other flow sheets. In all the cases its permeate is fed to the RO unit and has a water recovery of 75,3%. By introducing the NF unit for the feed water pre-treatment, the RO permeate increases due to the lower osmotic pressure of the water fed to the unit (related to the removal of bivalent ions by NF). In fact coupling the two units (FS2), a global recovery factor of 52% [2, 3] has been obtained (see Table 3).
In the third flow sheet, both MF and NF have been introduced in the feed water pre-treatment and load reduction to the following reverse osmosis unit. The MF unit acts on the feed seawater and has a recovery factor of 94,7% [4].
The MF introduction leads to benefits because it provides an NF/RO feedwater of good quality in view of lower capital and operating cost. A feed of high-quality means a reduction of membrane fouling with consequent extension of the life time of NF/RO membranes and reduction of their maintenance and replacement costs [4]. Moreover, MF introduction reduces chemicals cost (because no chemicals are needed for disinfection, coagulation and dechlorination) and labor cost (because less manpower is needed to clean the membrane and maintain the system).
Considering the same feed flow rate (1051 m^3/h) and rejection values for all the proposed systems, Table 3 shows the obtained results.

Table 3: Product characteristics for the first three analyzed flow sheets [3].

	FS1	FS2	FS3
Brine flow rate [m^3/h]	629.9	504.5	531.9
Brine concentration [g/l]	57.60	71.91	68.02
Fresh water flow rate [m^3/h]	421.2	547.0	517.6
Fresh water concentration [g/l]	0.3385	0.2699	0.2699
Fresh water recovery [%]	40.10	52.00	49.20

In FS3 and in FS2 the quantity of fresh water globally produced is higher and more pure with respect to FS1. The introduction of MF in FS3 decreases global recovery factor with respect to FS2 because the RO unit works at the same degree of efficiency of FS2 but on a lower NF permeate flow rate. As already said, the MF leads to benefits in term of reduction in capital and operating cost.

3. Chemical resources of the ocean waters

In the three flow sheets until now analyzed the quantity of brine globally produced is high and highly concentrated. Elements and compounds which are dissolved in the concentrated streams of the desalination plants represent a reserve of chemicals resources. If Waters of the World Ocean contain so many organic and inorganic elements that they are figuratively called "liquid polymetallic ore", all the more so this is true for the NF/RO retentate streams.

The main quantities of dissolved elements in marine waters are chlorine, sodium and magnesium. There are also insignificant concentrations of silver, zinc, copper, mercury, uranium, gold etc. Moreover, marine water is a reserve of raw material for the production of fertilisers, salts, acids, alkalis, various metals and a number of chemical products.

Reserves of chemical resources in the Ocean are practically unlimited, since the constant chemical composition of sea water is based upon continual deposition/solution from the environment. Only a small fraction of the large variety of chemical riches of the Oceans and seas is presently extracted, because the technology has not yet been developed to accomplish this in an economical manner. Constantly improving mining and recovery processes will make it possible in the future to extract chemical resources from the sea.

3.1 Production of magnesium, potassium, bromine and other salts from seawater

Figure 4 shows the method used to extract dolomite lime from sea water. The simplicity of production, successful selection of a site to construct a plant and proximity to power sources and raw materials determine the profitability of magnesium extraction. Magnesium was obtained from sea water for the first time in England in 1916.

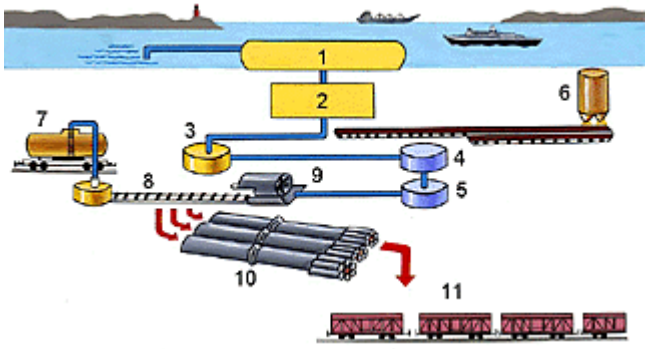

1) Distribution container; 2) water collection instruments; 3) Fresh water for washdown; 4) Fresh water; 5) Fresh water processing equipment; 6) Storehouse of burnt dolomite; 7) Crude yield; 8) Transporter; 9) Vacuum filter; 10) Drying furnaces; 11) Shipment magnesium oxide.

Figure 4. Method used to extract dolomite lime from sea water [5].

Simple magnesium and *its compounds* are widely used in the construction of rockets, aircraft and spacecraft. Textiles, building materials, paper, rubber, pharmaceuticals and agriculture are also customers. The Ocean provides more than 40% of all magnesium produced World-wide. Presently, only England and the USA have more than 20 plants producing a majority of magnesium from sea water, the most part of which is consumed within these countries.

In ancient times, people learned to use *cooking salt*. In countries with a hot and dry climate, salts are extracted by evaporation in special pools (or lagoons) under natural conditions, using energy of the sun and wind. At present, the same methods are used for obtaining some other salts. There is also the method whereby salt is deposited when sea water freezes, however this process is not widely used.
The best cooking salt contains not less than 96% NaCl (sodium chloride), and is used mainly for food preparation and seasoning. In industry, lower quality salt is used. Cooking salt is necessary for manufacture of soda, salt acid, plaster, glass, soup, papers, clearing of fats, smelting of metals, etc.
One-third of the World's supply of salts comes from the seas and Oceans.

Potassium salts represent the bases for various agricultural fertilisers. Usually they are received as a by-product of sodium chloride production. Potassium salts are used for refining, cleaning and dyeing fabrics, in the production of explosives and other items. The extraction of potassium from marine water was begun during the First World War in Japan and China.

Sea water and the precipitation of salts of dried up seas are basic sources also of bromine. Moreover, the possibility to extract compounds from marine organisms for pharmaceutical use is increasing in interest.
Bromine is practically unobtainable from land minerals. Although bromine concentration in sea water is rather minor (0.008%), it exceeds by 8 times the contents of an equal volume of land minerals. Current World-wide extraction of bromine is about 10,000 tons/year. Pharmacists have long used bromine for the preparation of medicines.

Interest in bromine increased after the discovery of two-bromide ethylene, a compound permitting to prepare fuels that do not explode in internal combustion engines. Bromine is also used in the production of dyes, photographic and film-materials, fire extinguishers, etc. Bromine is extracted, for example, from seawater at Freeport in Brazoria County [6].

The production of *iodine* from sea marine water is based on extracting it from the water with the help of activated charcoal, and also by processing of laminaria seaweed.

High hopes are laid to waters of the Ocean as a source of uranium, radium, gold, lithium, caesium and other trace-elements. Great obstacles lie in the path of extraction of these elements because the quantities are too small to efficiently extract them, thereby making technological methods very complex and the final yield extremely expensive. Prospective methods for their extraction by using synthetic, ion-exchanging resins are being studied, due to the tendency of some materials toward selective absorption of a required group of elements. These methods have been developed to some degree and Japan was the first to build a facility for obtaining uranium from marine waters.

Use of biological methods to extract rare elements is based on the fact that some marine plants and animals are capable of filtering them from water and storing these elements in their bodies. For example, in the bodies of marine crayfish (spiny lobsters) cobalt and radioactive plutonium^{239} have been found; holothurians and ascidians have vanadium in their bodies; the cellular tissue of oysters stores copper; there is gold in the bodies of jellyfish; and zinc, tin and lead have been noted. In some seaweeds the concentration of iron is 100,000 times greater than in marine water.

Waters of the seas and Oceans are the main storehouses of hydrogen and its heavy isotopes deuterium and tritium, and the latter is included in the structure of heavy water. The mass of the heavy water of the Ocean is estimated at 274,000 billion tons. The use of nuclear energy created by a reaction between deuterium and tritium opens a practically inexhaustible source of convenient and cheap energy to Mankind. Heavy water is presently used to decelerate reactions in nuclear reactors. The largest production facility for heavy water in the World (77% of the production from it goes to countries of Western nations) is in Canada.

Hydrogen is a natural fuel which is extractable from sea water by electrolysis. It is used in many industries and in transportation. World-wide more than 20 million tons of hydrogen is produced annually.

3.2 Geographical distribution of some of the main chemical compounds extracted from marine water

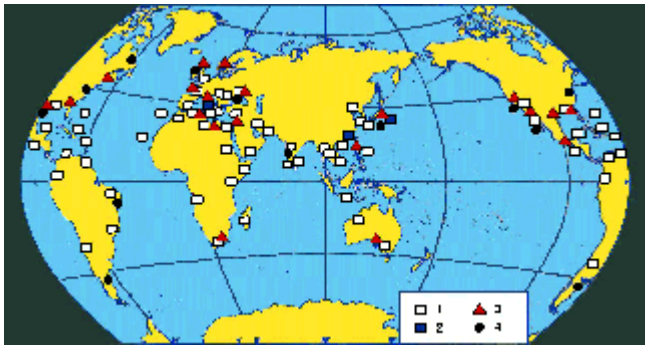

Places of extraction:
1.Cooking salts
2. Potassium
3. Magnesium
4. Bromine

Figure 5. Geographical distribution of the main chemical compounds extracted from marine water [5].

Figure 5 shows the places of extraction of some compounds from seawater.
Sodium chloride is the most important mineral obtained directly from seawater. Mexico leads the Pacific nations in salt extraction from the sea, mostly by solar evaporation. Bromine extracted from seawater is used in the food, dye, pharmaceutical and photo industries. Magnesium, recovered by an electrolytic process, is used in industrial metal alloys, especially with aluminium; Japan and California are the main sites for its extraction [7].
The supply of bromine, chloride, potassium and magnesium salts in Dead Sea is practically unlimited. These resources are widely used by private companies for the extraction of salts such as potash salts, industrial salts and food grade salts. As an example, in Table 4 is reported the salts production of the Dead Sea Works (DSW) industry.

Table 4. The DSW production of the different Dead Sea salts for the year 1994 [Source: HARZA & JRV, 1997].

ITEM	PRODUCTION RATE
Potash	2.3 Million tonnes
Industrial Salts	235,000 tonnes
Bromine	180,000 tonnes
Magnesium Chloride Flakes	74,000 tonnes
Table Salts	63,000 tonnes
Magnesium metal	2,500 tonnes
Bath salts	2,200 tonnes

4. Crystallization for the recovery of fresh water and salts from NF and/or RO retentate

Valuable compounds can be also extracted from the highly concentrated NF/RO retentate streams of the desalination plants. In literature, various studies can be found for the recovery of the compounds present in NF/RO retentate:

- ✓ the Murray-Darling Basin Commission (MDBC), in order to reduce the environmental problem of the salinity in the Murray Basin, converts the salts present in the water in commercial products addressed to the market: first the retentate is evaporated and then it is sent to a conventional crystallizer for the extraction of (NaCl) and epsomite ($MgSO_4 \cdot 7H_2O$). The fine quality salts are produced at a cost of 18.49 and of 329 $/t, respectively [8].
- ✓ Another example can be found in M. Turek [9]. He suggested dual-purpose desalination-salt production systems, namely: UF-NF-MSF-crystallisation and UF-NF-RO-MSF-crystallisation. In these systems, the high rate of water recovery is accompanied by salt obtainment. By assuming a cost of NaCl equal to $30/ton, he calculated water cost equal to $0.71/m^3 in UF-NF-MSF-crystallisation system and $0.43/m^3 in UF-NF-RO-MSF-crystallisation system respectively, competitive compared to those of potable water produced in thermal or RO seawater plants.

In this work, membrane crystallization units have been considered for the concentration and crystallization of NF and/or RO retentate streams of the desalination plants. Therefore, four other integrated membrane systems have been analysed. In each of them, at the basic process represented by FS3, a membrane crystallizer has been introduced: MCr operates on NF brine in FS4, on RO brine in FS5, both on RO and NF brine in FS6. In the last flow sheet (FS7), MCr has been introduced on NF brine while MD operates on RO brine (see Figs. 6-9).

In each MD/MCr process, the fresh water coming out from the RO has been used as cold water stream.

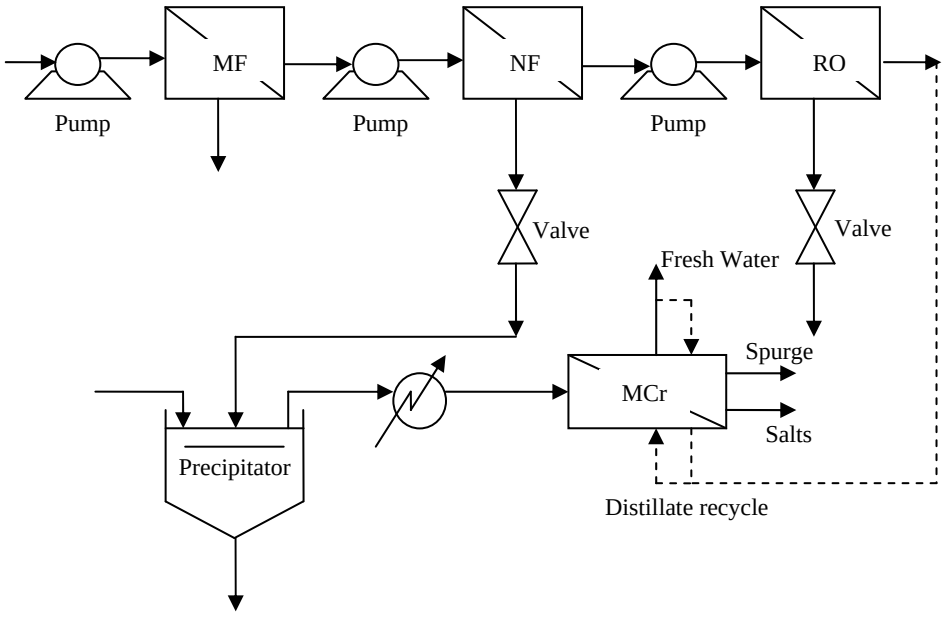

Figure 6. Flow sheet 4 (FS4): MF/NF/RO and MCr on NF retentate.

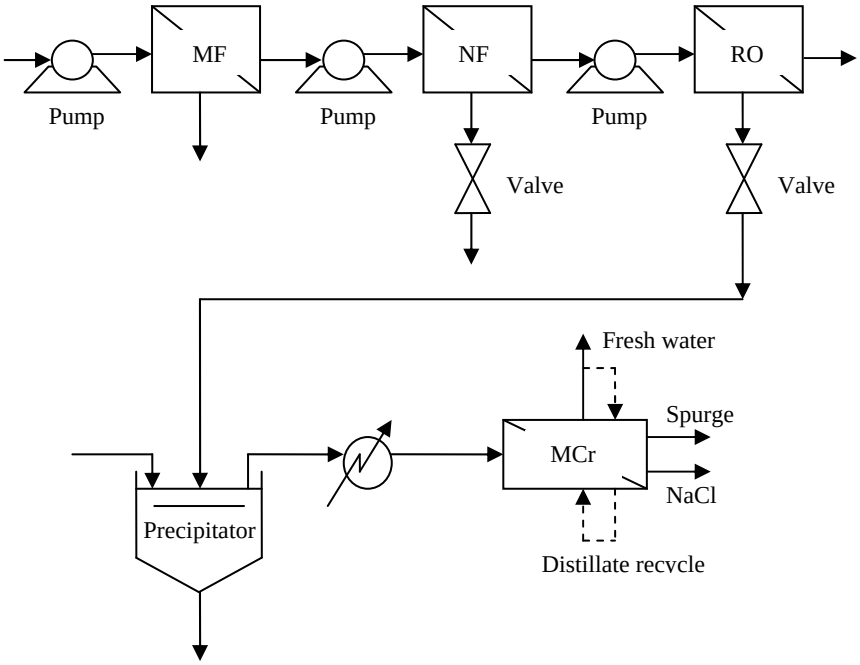

Figure 7. Flow sheet 5 (FS5): MF/NF/RO and MCr on RO retentate.

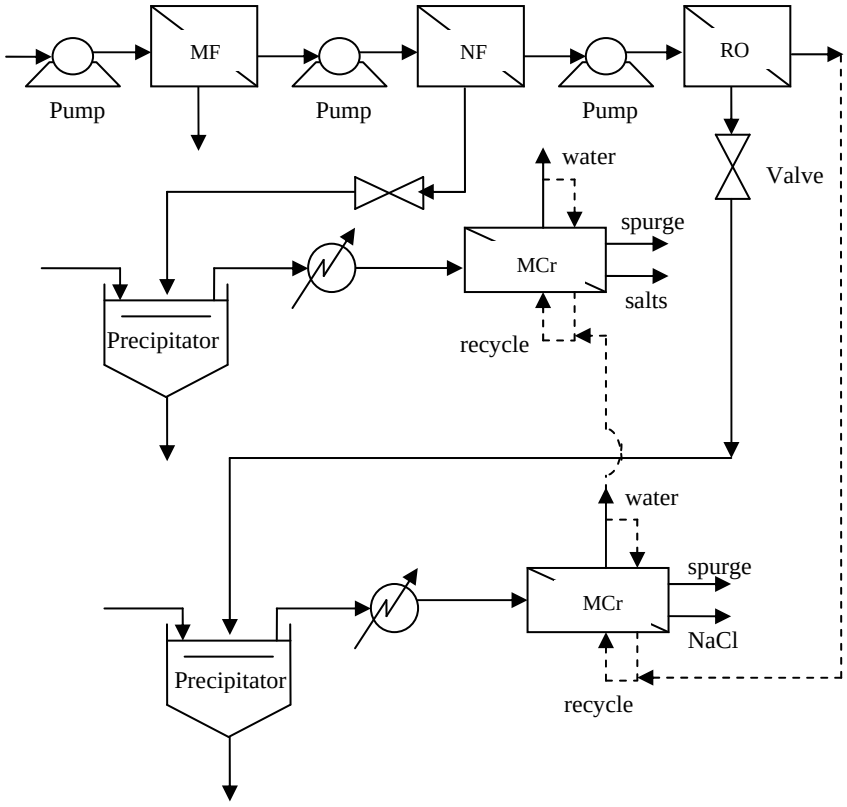

Figure 8: Flow sheet 6 (FS6): MF/NF/RO and MCr both on NF and RO retentate.

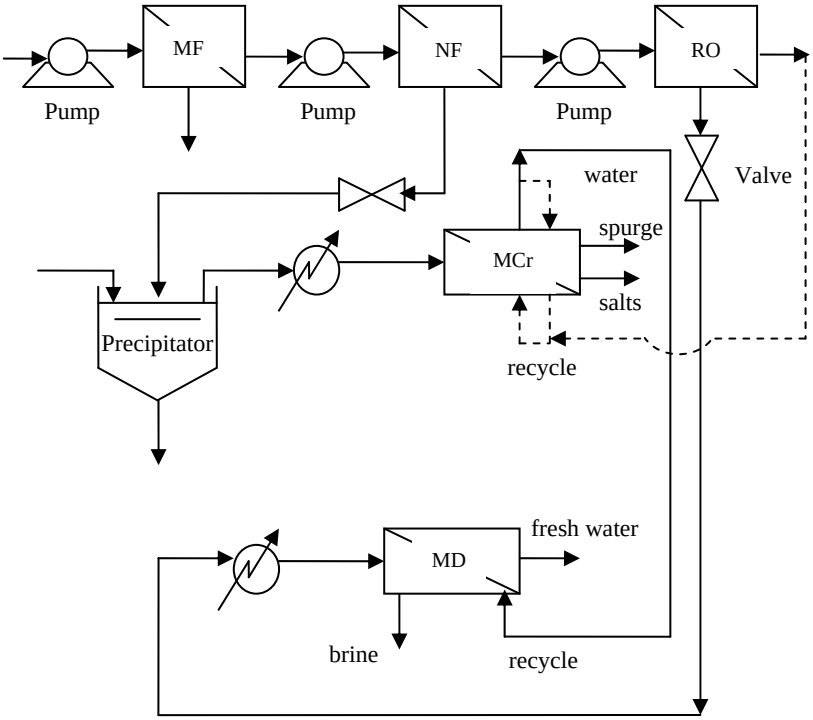

Figure 9: Flow sheet 7 (FS7): MF/NF/RO, MCr on NF retentate and MD on RO retentate.

4.1 Control of the Membrane Crystallization Process

In the concentration and crystallization process it is important to know the composition of the feed in order to aim to the production of valuable salts (such as sodium chloride and magnesium sulphate, the salts naturally present in the highly concentrated streams of the desalination plants).

The salts precipitation occurs when the solution is supersaturated. Unless a solution is supersaturated, crystals can neither form nor grow. Supersaturation refers to the quantity of solute present in solution compared with the quantity which would be present if the solution were kept for a very long period of time with solid phase in contact with the solution. The latter value is the equilibrium solubility at the temperature and pressure under consideration. As a consequence, the potential salts precipitation can be predicted by the comparison between the **solubility product** (K_{sp}) and the **ionic product** (IP):

- if $K_{sp} > (IP)$ the solution is not saturated and the precipitation doesn't occur;
- if $K_{sp} = (IP)$ the solution is saturated;
- if $K_{sp} < (IP)$ solid will precipitate until the saturation concentration is reached.

Table 5. Composition of each stream in FS3.

Stream N°	1	2	3	4	5	6	7 (NF brine)	8	9	10	11	12 (RO brine)
Cl^-	19.35	19.35	19.35	19.35	19.35	27.01	27.01	16.83	16.83	1.767E-01	54.00	54.00
Na^+	10.75	10.75	10.75	10.75	10.75	17.96	17.96	8.387	8.387	9.057E-02	26.90	26.90
SO_4^{2-}	2.701	2.701	2.701	2.701	2.701	10.11	10.11	0.2701	0.2701	9.994E-04	0.8707	0.8707
Mg^{2+}	1.295	1.295	1.295	1.295	1.295	4.809	4.809	0.1425	0.1425	6.268E-04	0.4590	0.4590
Ca^{2+}	0.4160	0.4160	0.4160	0.4160	0.4160	1.537	1.537	0.04826	0.04826	1.496E-04	0.1556	0.1556
HCO_3^-	0.1450	0.1450	0.1450	0.1450	0.1450	0.4191	0.4191	0.05510	0.05510	8.485E-04	0.1762	0.1762
Tot. [g/l]	34.65	34.65	34.65	34.65	34.65	61.85	61.85	25.73	25.73	0.2699	82.57	82.57
G[Kg/h]	1.048E+06	1.048E+06	5.554E+04	9.925E+05	9.925E+05	2.451E+05	2.451E+05	7.473E+05	7.473E+05	5.161E+05	2.312E+05	2.312E+05
P [MPa]	0.10	0.20	0.10	0.10	1.10	1.00	0.10	0.10	6.90	0.10	6.77	0.10
T[K]	293.2	293.2	293.2	293.2	293.2	293.2	293.2	293.2	293.2	293.2	293.2	293.2

Because NF and RO retentate streams of the proposed desalination systems are characterized by the composition reported in Table 5, sodium sulphate, magnesium sulphate and sodium chloride are the salts that can precipitate:

- ✓ for what concerns calcium sulphate, its solubility product (K_{sp}) at 25°C (temperature of the crystallization tank) is equal to $7.1 \cdot 10^{-5}$ [10].
  In the NF brine its ionic product is $4.04 \cdot 10^{-3}$, more than K_{sp}. In order to avoid $CaSO_4$ precipitation (which can cause scaling and limits the recovery of magnesium sulphate), according to previous experimental results [11], Na_2CO_3 is used to precipitate 95% of Ca^{2+} ions as $CaCO_3$.
  In RO brine, ionic product of $CaSO_4$ is $3.5 \cdot 10^{-5}$, then $CaSO_4$ doesn't precipitate. However, in order to avoid $CaSO_4$ precipitation during the concentration of the RO brine in the MCr, also this stream is treated with Na_2CO_3.

After the precipitation step, the so-treated retentate streams are sent to a MCr in order to recover sodium chloride and magnesium sulphate:

- ✓ for what concerns magnesium sulphate, its solubility increases with temperature (ΔH_{sol} = 3.18 kcal/mole) and at 25°C it precipitates as $MgSO_4*7H_2O$ (epsomite) if its concentration is higher than 710 g/L (see *Chapters 5 and 6* for further details regarding the crystallization process);
- ✓ sodium chloride solubility doesn't change much with temperature. In the range 0-100°C it increases from 35.7 to 39.8 g NaCl/100g H_2O [12], typical behaviour of a salt with small $\Delta H_{sol.}$ (ΔH_{sol} = 0.93 kcal/mole). Therefore, in the crystallization tank NaCl precipitates when its concentration is higher than 36.15 g NaCl/100g H_2O (see *Chapters 5 and 6* for further details regarding the crystallization process).

The crucial requirement of a membrane crystallizer is to guarantee crystals formation in the crystallization tank and not in the membrane module or on the membrane surface. Because the solubility of solids in solution is sensitive to changes in temperature (whose effect on salt solubility depends on its *enthalpy change of solution,* $\Delta H_{sol.}$), a suitable heating or cooling can guarantee that the temperature of the solution flowing along the membrane is high or low enough to be always under saturation condition.

For the crystals of interest in this work, both characterized by a positive enthalpy change of solution, a heating guarantees that the temperature of the solution flowing along the membrane is high enough to avoid crystals deposition or accumulation inside the membrane module.
In order to calculate the temperature of the MCr feed (T_f), it is necessary to consider that, along the membrane module, thermal exchange phenomena between cold and hot streams and the polarization effects cause a progressive reduction of temperature, depending on the fluid-dynamic regime (see *Chapter 1, section 3.2*).
The following iterative procedure has been put right for the calculation of T_f:

1. first T_f is hypothesized. Because thermal differences between input and output of the membrane module are very small (less than 3°C) [13], both for the feed and for the permeate side, middle temperatures can be easily determined.
2. The second step is the calculation of the temperature on membrane surface, both on the retentate (T_{mf}) and on the permeate side (T_{mp}). They cannot be measured experimentally but can be estimated from the flux and from the heat balance, at steady state, by the sequence of equations below:

$$T_{mf} = T_f - (T_f - T_p)\left[\frac{1/h_f}{\frac{1}{h_m + h_v} + \frac{1}{h_f} + \frac{1}{h_p}}\right] \quad (1)$$

$$T_{mp} = T_p + (T_f - T_p)\left[\frac{1/h_p}{\frac{1}{h_m + h_v} + \frac{1}{h_f} + \frac{1}{h_p}}\right] \quad (2)$$

where the temperatures are evaluated at the locations shown in *Figure 15 - Chapter 1*. Each h represents the corresponding heat transfer coefficient as shown in *Figure 15 - Chapter 1* and they are given by the following equations:

- $h_v = \frac{N \cdot \Delta H_V}{T_{fm} - T_{pm}}$ (3)
- $h_m = \varepsilon \cdot h_{mg} + (1-\varepsilon) h_{ms} = \frac{K_g \cdot \varepsilon + K_m (1-\varepsilon)}{\delta}$ (4)
- h_f and h_p are estimated from empirical correlations when the physical properties of the streams and the structural properties of the membrane module are known. Further, h_v is function of the molar flux N and of (T_{fm} - T_{pm}). As a result, simultaneous solution of the heat and mass transfer equations must be carried out via iteration, unless N is experimentally known.

3. When T_{fm} and T_{pm} are known, the total heat transferred across the membrane is given by:

$$Q = U \cdot \Delta T \quad (5)$$

where U represents the overall heat transfer coefficient of the process: $\frac{1}{U} = \frac{1}{h_f} + \frac{1}{h_m + h_v} + \frac{1}{h_p}$. (6)

4. To the MCr feed, before getting in the membrane module, a heat Q' equal to the sum of the total heat transferred across the membrane Q plus the heat necessary to dissolve the particles formed in the crystallizer has to be supplied:

$$Q' = G \cdot c_p \cdot (T_{in} - T_{crist}) = \sum_{i=1}^{n} m_i \cdot \Delta H_{sol,i} + U \cdot A \cdot \Delta T \qquad (7)$$

where G is the membrane module feed flow rate, c_p its specific heat, T_{crist} the temperature in the crystallizer tank, A the membrane area, ΔT the thermal difference between the retentate and the permeate side, m_i the amount of the precipitated salt i and $\Delta H_{sol,i}$ its enthalpy change of solution.
The temperature T_{in} obtained from the equation (7) has to be compared with the hypothesized T_f until convergence is reached.

In agreement with literature [11, 14, 15], the temperature of the retentate should have to range from 35 to 50 °C, and the temperature of the permeate from 15 to 20°C.
Because the cold stream utilized as permeate in the proposed systems is the RO permeate (≈20°C), a T_f equal to 50°C has been chosen as starting point of the planned iteration.
At the end of the described procedure, a $T_f \approx 34$°C is obtained, both for NF and RO retentate. However:

- ✓ since trans-membrane flux increases with temperature and high trans-membrane fluxes mean smaller membrane crystallizer modules and, then, reduction of their maintenance and replacement costs,
- ✓ since the solubility of the salts in question increases with temperature,
- ✓ because the aim is to avoid crystals deposition and accumulation inside the membrane module and on the membrane surface,

the temperature of MCr feed (T_f) has been chosen higher than 34°C and equal to 50°C.

4.2 Innovative integrated membrane systems for seawater desalination: Case study 4, 5, 6 and 7

Considering the same feed flow rate of the previous proposed systems, Figure 10 reports the results of the analysis for the last four flow sheets in terms of product characteristics and quantity of salts produced in the case in which crystallization tank operates at 25°C.
By introducing a MCr unit on NF brine (FS4), the quantity of fresh water produced is higher with respect to when it is on RO brine (FS5) because MCr works at the same degree of efficiency but, in FS5, on a lower brine flow rate. The introduction of a membrane crystallizer unit on both retentate streams increases plant recovery factor so much that it can reach 92.8% in FS6, value higher than that of a conventional membrane integrated desalination process (such as FS3 which has a recovery factor of about 50%) and higher than that of a typical MSF (about 10%). With respect to FS6, in FS7 the quantity of fresh water produced decreases because MD has a recovery factor of 77% [2, 3] while MCr of about 100%.

For what concerns salts, the highest production is when the membrane crystallizer unit operates on both retentate streams.

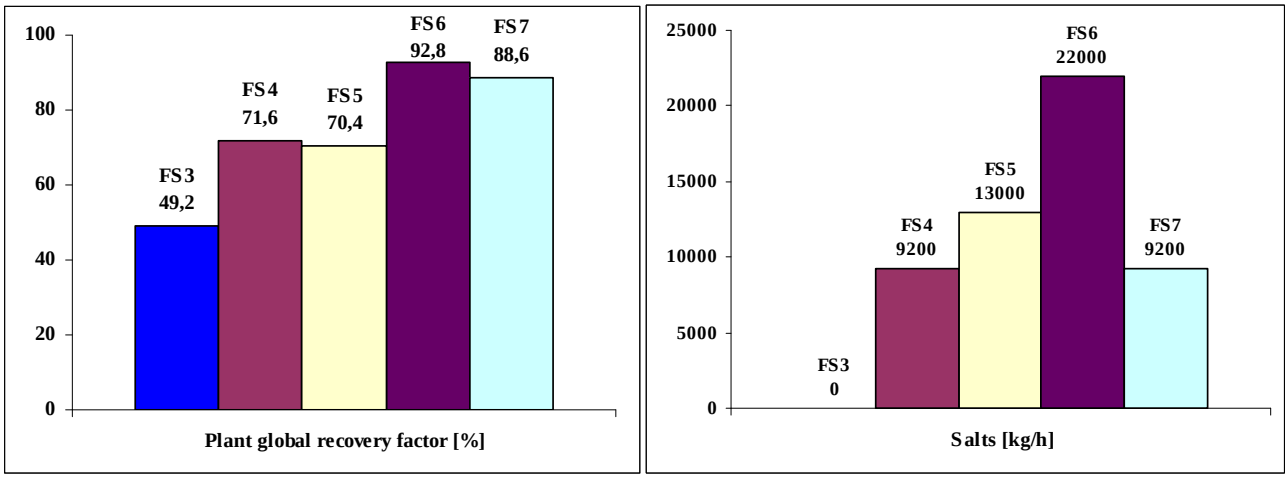

Figure 10. Plant global recovery factor and quantity of salts produced in the flow sheets with MCr unit.

Tables 6 reports a summary of the results of the analysis for the analysed flow sheets in terms of product characteristics and quantity of produced salts.

Table 6. Product characteristics for the analyzed flow sheets.

	FS1	FS2	FS3	FS4	FS5	FS6	FS7
Brine flow rate [m^3/h]	629.9	504.5	531.9	296.6	309.9	74.60	118.5
Brine concentration [g/L]	57.60	71.91	68.02	95.94	76.53	214.4	240.0
Fresh water flow rate [m^3/h]	421.2	547.0	517.6	753.0	739.6	974.9	931.5
Fresh water concentration [g/L]	0.3385	0.2699	0.2699	0.1856	0.1889	0.1433	0.1500
Fresh water recovery [%]	40.10	52.00	49.20	71.60	70.40	92.80	88.60
$CaCO_3$ flow rate [Kg/h]	-	-	-	893.9	85.37	979.3	893.9
NaCl flow rate [Kg/h]	-	-	-	7,371	12,470	19,840	7,371
$MgSO_4 \cdot 7H_2O$ flow rate [Kg/h]	-	-	-	938.6	-	938.6	938.6

5. Conclusions

The comparison of the achieved results shows a continuous improvement in the quality of the desalted water produced when membrane operations are used as RO pre-treatment (that means shifting from FS1 to FS3). The introduction of MCr operation, on one or on both retentate streams, as well as the presence of MD, increases plant recovery factor so much to reach 92.8% in FS6, higher than that of a RO unit (about 40%) and much higher than that of a typical MSF (about 10% [16]). Moreover, the use of MD and/or MCr allows exploiting brine added value, not only increasing plant

recovery factor, but also extracting the salts naturally present in the concentrated streams of the desalination plants and decreasing brine disposal problem and its negative environmental impacts. However, certainly the specific energy consumption of the systems with MCr will increase due to the retentate flow rate which has to be heated and which increases the global energy demand. As a result, only the balance among recovery factor, fresh water quality and cost, energy consumption and environmental impact can give information about the most convenient membrane desalination system.

Relevant Bibliography

[1] www.usask.ca/geology/classes/geol 206.
[2] A. Criscuoli, E. Drioli, *Energetic and exergetic analysis of an integrated membrane desalination system*, Desalination, 124 (1999) 243-249.
[3] E. Drioli, E. Curcio, G. Di Profio, F. Macedonio, A. Criscuoli, *Integrating Membrane Contactors Technology and Pressure-Driven Membrane Operations for Seawater Desalination: Energy, Exergy and Cost Analysis*, Chemical Engineering Research and Design, 84 (A3) (2006) 209–220.
[4] S. Ebrahim, S. Bou-Hamed, M. Abdel-Jawad, N. Burney, Desalination, 109 (1997) 165-175.
[5] http://www.oceansatlas.com/unatlas/-ATLAS-/chapter7.html
[6] Handbook of Texas Online MINERAL RESOURCES AND MINING.htm
[7] SOSTANZE ESTRATTE DAL MARE\FOSFATI\Pacific Ocean Minerals from seawater and alluvial deposits -- Britannica Concise Encyclopedia
[8] T. E. Borgate, *Value Adding to Salts Recovered from Saline Waters in Disposal Basins in the Murray-Darling Basin*, published by Murray-Darling Basin Commission, Canberra City, Australian Capital Territory (site Internet http://www.mdbc.gov.au).
[9] M. Turek, *Seawater desalination and salt production in a hybrid membrane-thermal process*, Desalination, 153 (2002) 173-177.
[10] P. Dydo, M. Turek, J. Ciba, *Scaling analysis of nanofiltration system fed with saturated calcium sulphate solutions in the presence of carbonate ions*, Desalination, 159 (2003) 245-251.
[11] E. Drioli, E. Curcio, A. Criscuoli, G. Di Profio, *Integrated system for recovery of $CaCO_3$, NaCl and $MgSO_4 \cdot 7H2O$ from nanofiltration retentate*, Journal of Membrane Science, 239 (2004) 27–38.
[12] J. H. Perry, *Perry's Chemical Engineers' Handbook*, McGraw-Hill Book Co., New York, 1987.
[13] K. Schneider, W. Holz, R. Wollbeck, *Membranes and modules for transmembrane distillation*, J. Mem. Sci., 39 (1988) 25-42.
[14] E. Curcio, A. Criscuoli and E. Drioli, *Membrane Crystallizers*, Ind. Eng. Chem. Res., 40 (2001) 2679-2684.
[15] C. M. Tun, A. G. Fane, J. T. Matheickal, R. Sheikholeslami, *Membrane distillation crystallization of concentrated salts—flux and crystal formation*, Journal of Membrane Science, 257 (2005) 144–155.
[16] A. M. Helal, A. M. El-Nashar, E. S. Al-Katheeri, S.A. Al- Malek, *Optimal design of hybrid RO/MSF desalination plants. Part II: Results and discussion*, Desalination, 160 (2004) 13-27.

CHAPTER 3: Integrated Membrane Systems for Seawater Desalination: Energetic and Exergetic Analysis, Economic Evaluation and *Sustainable Metrics*

Table of Contents

1. Introduction

Since the beginning of the 21st century, electronics, computer science, medicine, chemistry and the whole world of the related process industries (from oil, to pharmaceutical, agro, water and food, environment, textile, building materials, cosmetics, etc.) are continuously evolving, thanks to the increasing and unprecedented market demands, and to the emerging constraints from public concern over environment and safety issues. This led and leads to select processes not only on an economic basis, but also aspects such as the increased selectivity and savings linked to the process itself are important parameters to take into account.

In the past years several attempts have been made to quantify the progress of industrial processes towards *sustainability*, and to define and identify proper indicators to measure their impact on environment, economy and society.

In order to evaluate if the proposed membrane-based desalination systems can really represent an interesting alternative to the traditional processes and in order to establish which of the analyzed flow-sheets is the most *convenient, reliable* and *sustainable* process, the use of *Energetic and Exergetic Analysis, Substitution Coefficient, Economic Evaluation and* of the so-called *Sustainable Metrics* are discussed and utilized in the present chapter.

The use of *exergetic analysis* allowed to establish the quality of the obtained product and to identify the sites of greatest losses on which it was possible acting for improving the performance of the processes.

The *economic evaluation* has been made to determine the desalted water cost and the gain for the salts sale for all the proposed flow sheets.

The use of *metrics* have allowed to compare the proposed flow sheets with respect to their size and modularity, plant efficiency and environmental impact.

2. Energy and exergy analysis – basic criteria

In order to estimate the energy saving in the processes, a methodology based on energy and exergy analysis can be used for establishing, respectively, the energy requirements of the membrane integrated systems and their exergetic efficiency evaluated in terms of entropic losses [1], [2].

The total energy of a process is divided in two parts: exergy and anergy [2]. While anergy is the part of energy that is forced to be given to the environment as heat in conditions of complete degradation, exergy is the part of energy that can be completely converted from one form to another by reversible transformations. Therefore, the word “exergy” expresses the quality of energy and it can be defined as the maximum amount of work obtained by the evolution of a system with reversible transformations from the initial state to the equilibrium state with the environment.

Exergetic analysis is more time-consuming than an energetic analysis for the major complexity of the involved equations [1, 3], so it is used only in those cases where the contributions that cannot be evaluated with energetic analysis are important (e.g., exergy of solutions at different concentrations but at the same temperature).

In Table 1 the basic equations used to carry out exergetic analysis are reported. Table 2 shows the results of the analysis for the seven proposed flow sheets.

Table 1: Basic equations for exergetic analysis.

The mathematical definition of exergy for a fluid stream is given by the following equation [1, 2]:

$$Ex = G\left[c_p (T - T_0) - c_p T_0 \ln\left(\frac{T}{T_0}\right) + \frac{(P - P_0)}{\rho} - N_S R T_0 \ln x_1 \right] = Ex^T + Ex^p + Ex^c$$

where: Ex is the exergy;

G = mass flow rate and c_p = specific heat of the solution;

the subscript $_0$ indicates the reference state that, for the systems considered, is pure water at T_0 and P_0 (temperature and pressure of fed seawater, that is T_0 = 20 °C e P_0= 0.10 MPa);

N_s = moles of solvent per mass unit of the solution = $\dfrac{\left(1000 - \sum \frac{c_i}{\rho}\right)}{MW_S}$;

$$x_1 = \frac{N_S}{\left[N_S + \sum\left(\frac{\beta_i c_i}{\rho\, MW_i}\right)\right]};$$

β_i = number of particles generated from dissociation of species i; ρ = density of the liquid solution;

c_i = mass concentration of the i-th chemical component per liter of solution;

MW_s , MW_i = molecular weight of the solvent and of the i chemical component, respectively.

Exergetic balance: $\Delta E_x = -T_0 \cdot \dot{R}_S + \dot{W}_U + \dot{W}'_U$ where:

$T_0 \cdot \dot{R}_S$ = total exergy destroyed and transformed in the production of entropy;

$\Delta E_x = \sum_i E_{x,i} - \sum_k E_{x,k}$ = exergy variation between outlet and inlet streams;

$\dot{W}_U = E \cdot 3600$ electrical exergy;

$\dot{W}'_U = G_V[(h_V - h_C) - T_0(s_V - s_C)]$ thermal exergy supplied to the system. G_V is the required steam mass flow rate which can be calculated from the equation: $G_V = Q/\lambda_V$ where $Q = G \cdot c_p \cdot (T_2 - T_1)$ is the heat required to warm up the fluid G from temperature T_1 to temperature T_2.

Primary energy (PE) is the energy supplied by fuel combustion to produce thermal energy: $PE = G_V \cdot 0.8$ where 0.8 is the primary energy (Mcal) needed in the boiler for producing 1 kg of steam.

Table 2: Energy and exergy for the flow sheets analyzed.

	FS1	FS2	FS3	FS4	FS5	FS6	FS7
Elect. energy [KWh/h]	2206	1986	1913	1913	1913	1913	1913
W_u [KJ/h]	$7.942*10^6$	$7.148*10^6$	$6.886*10^6$	$6.886*10^6$	$6.886*10^6$	$6.886*10^6$	$6.886*10^6$
W_u' [KJ/h]	0	0	0	$7.129*10^6$	$6.640*10^6$	$13.77*10^6$	$13.77*10^6$
ΔE_x [KJ/h]	$-1.972*10^4$	$-3.454*10^4$	$-3.270*10^4$	$-7.876*10^5$	$-11.75*10^5$	$-17.78*10^5$	$-5.637*10^5$
$R_S T_0$ [KJ/h]	$7.962*10^6$	$7.183*10^6$	$6.919*10^6$	$14.80*10^6$	$14.70*10^6$	$22.43*10^6$	$21.22*10^6$
$R_S T_0$ [KJ/h] [(a)]	$7.962*10^6$	$7.183*10^6$	$6.919*10^6$	$7.674*10^6$	$8.061*10^6$	$8.664*10^6$	$7.450*10^6$
G_V [Kg/h]	0	0	0	13430	12510	25950	25950
PE [Mcal/h]	0	0	0	10750	10010	20760	20760

(a) if thermal energy is available in the plant or the stream is already at the operating temperature of the MCr unit.

From an energetic point of view (see Table 2), FS1, FS2 and FS3 processes use only electrical energy. The introduction of MCr and/or MD (in FS4, FS5, FS6 and FS7) introduces a thermal energy requirement (PE), due to the retentate flow rate which has to be heated and which increases the global energy demand.
FS1, FS2 and FS3 exergetic efficiencies are interesting because their entropic losses are moderate with respect to the other flow sheets. In the last four cases, instead, the presence of MCr and or MD increases exergy destruction: in FS5, where the RO brine has to be further concentrated in a membrane crystallization unit, the thermal energy necessary is reduced with respect to the other systems because a lower flow rate has to be heated; as a consequence, the entropic losses are also lower with respect to FS4, FS5, FS6 and FS7. In FS4, NF brine has been sent to the MCr: the thermal energy necessary and the entropic losses increase with respect to FS5 due to the higher flow rate which has to be heated. In FS6, where both retentate streams have to be heated, the total exergy destroyed and transformed in irreversible production of entropy is the highest. The same thing occurs in FS7. However, if the water streams are already available at the temperature needed for carrying out the MCr/MD operation or the thermal energy is available in the plant, than the entropic losses and the energy requirements of the integrated systems with MC (Membrane Contactor) decrease, reaching competitive values with those of the other desalination processes.

2.1 Exergy Destruction Distribution

The use of exergy for the analysis of real processes is of growing importance from a thermodynamic point of view. In fact, exergetic analysis allows not only to establish the quality of the obtained product, but also to identify the sites of greatest losses. As a consequence, changing system design, it will be possible to improve the performance of the processes [3]. For reaching this aim, the seven processes have been described in

detail and the exergies across the major components of each plant have been calculated in an attempt to assess the exergy destruction distribution.

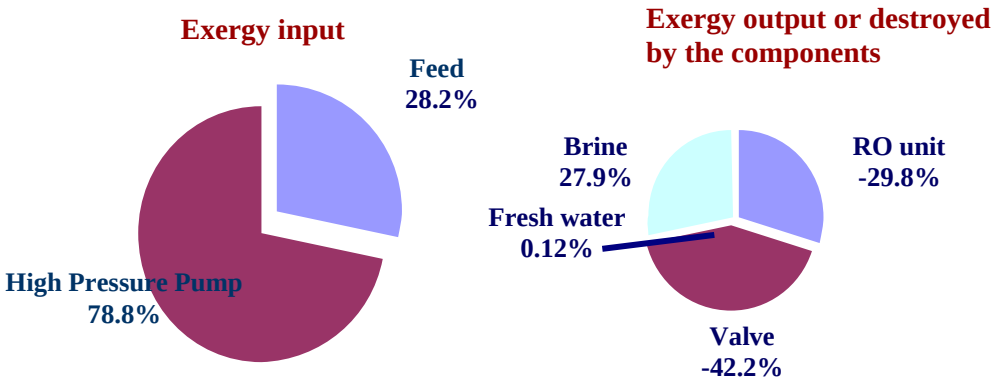

Figure 1: Exergy destruction distribution for FS1.

Figure 1 shows the results obtained for the first flow sheet (FS1). However, in each analysed desalination system, the achieved results demonstrate that the primary locations of exergy destruction are the membrane modules in which the saline water is separated into the brine and the permeate and the throttling valves where the pressure of liquid is reduced. Meanwhile there is nothing that can be done to eliminate or decrease the lost of exergy in the membrane module, the most reasonable and practical way to increase efficiency or reduce the power input of the plant significantly has been shown to be replacing the throttling valves on the brine stream by an energy recovery system (like a Pelton turbine or a pressure exchanger system) [3, 4]. In fact, the pressure of RO brine could be recovered by introducing a pressure exchanger system or a Pelton turbine which lead to a reduction of the energy consumption for all the analyzed systems transferring the brine pressure to the low-pressure feed water, while discharging the brine at low pressure [4].

The convenience of a process with an energy recovery device (ERD) with respect another without ERD can be evaluated also in terms of their exergetic efficiency ε, as following defined: $\varepsilon(\%) = \frac{\mathrm{Ex}_{\mathrm{output}}}{\mathrm{Ex}_{\mathrm{input}}} \cdot 100$. The analysis of the alternative design was based always on the exergetic analysis.

Diagrams in Figure 2 and 3 allow to compare exergetic efficiencies of the seven flow sheet in three different situations: 1) when the seawater desalination processes do not use any Energy Recovery Devices (ERDs), 2) when a Pelton turbine is introduced in order to minimize the Specific Energy Consumption (SEC), or 3) in the case in which a Pressure Exchanger System (PES) is used.

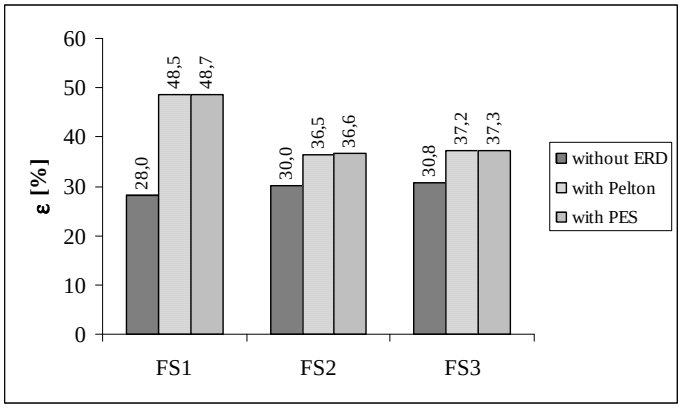

Figure 2. Exergetic efficiencies of FS1, FS2 and FS3 [5].

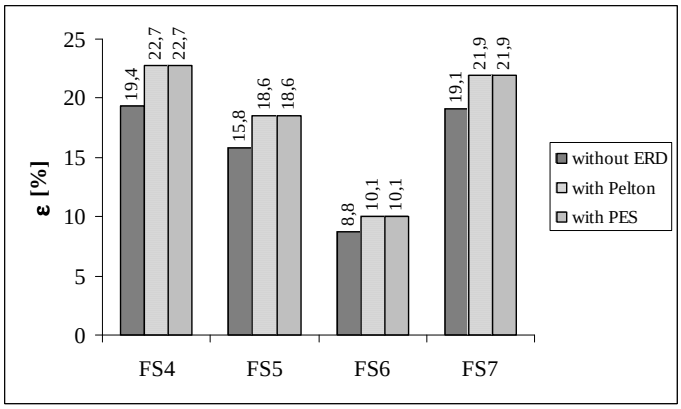

Figure 3. ε for the flow sheets with MCr unit [5].

In each case, the introduction of an energy recovery system allows to increase exergetic efficiency. The process that more gains profit from the use of an ERD is FS1 because is in this system that the turbine or the pressure exchanger, working with the highest RO retentate flow rate, permits to have the major reduction of energetic requirement. Exergetic efficiencies of the integrated systems with MCr unit are lower than those of the systems without MCr unit; this is due to the increase of exergy inlet because of the thermal exergy necessary to heat the retentate streams.

In any case, exergetic efficiency of membrane desalination systems is greater than that of thermal systems (such as MSF) which are highly irreversible and with exergetic efficiencies in the range 1.12 ~ 10.4% due to the high energy consumption [6].

Table 3: Quantity of energy required per m^3 of fresh water produced [KWh/m^3].

	MSF	**FS1**	**FS2**	**FS3**	**FS4**	**FS5**	**FS6**	**FS7**
without ERD	26.4 [1] 25.74[7]	5.24	3.63	3.70	2.54[a]/19.1	2.59[a]/18.3	1.96[a]/26.7	2.05[a]/28.00
with Pelton	-	2.69	2.87	2.93	2.02[a]/18.61	2.05[a]/17.79	1.56[a]/26.32	1.63[a]/27.54
with PES	-	2.58	2.84	2.90	1.99[a]/18.59	2.03[a]/17.77	1.54[a]/26.30	1.61[a]/27.52

(a) if thermal energy is available in the plant or the stream is already at the operating temperature of the MCr unit.

The estimation of energy saving can be an important but not a determining factor in the choice of the flow sheet to be used in the desalination operations. As already said, the fresh water production and the brine disposal are also two important factors to be taken into account. Referring to this, in Table 3 the quantity of energy required per m^3 of fresh water produced for the seven analyzed flow sheets and for a typical MSF plant is reported. As anticipated through the exergetic analysis, in each system the introduction of an energy recovery system allows to increase exergetic efficiency and to decrease the quantity of energy required per m^3 of fresh water produced. A comparison among the different membrane systems leads to the conclusion that, if the thermal energy is already available in the plant, then FS4, FS5, FS6 and FS7 become very attractive for carrying out the process also from an energetic point of view. Moreover, the results in the table show that all the proposed flow sheets present better performance with respect to the MSF process.

2.2 Substitution Coefficient

Since membrane operations utilize in prevalence electrical energy, the estimate benefit can be done using the method of the "substitution coefficient" (CS) introduced by Electricité de Francě; this coefficient compares the primary energy saved to the electrical energy consumed in cycles that utilize electricity-consuming operations in substitution of conventional thermal operations [2]: $CS = \frac{(C_1 - C_2)}{(E_2 - E_1)}$, where C is the consumption of thermal primary energy [MJ or Mcal], E the consumption of electrical energy [kWh], and 1,2 the relative index of the conventional and innovating process, respectively. An innovating process results convenient when the CS is greater than 10,5 MJ/kWh (2,5 Mcal/kWh).
The CSs calculated for FS1, FS2 and FS3 with respect to MSF and TVC indicate that all the three integrated membrane systems are more energetically convenient than thermal processes (Table 4).

	FS1	**FS2**	**FS3**
MSF	14.9	52.6	47.9
TVC	11.6	23.0	22.1

Table 4. Substitution Coefficient [MJ/kWh] for FS1, FS2, FS3 with respect to MSF and TVC [5].

Among flow sheets with MCr unit, FS5 is the most energetically convenient (CS like 99.3, 50.4 and 71.9 MJ/kWh with respect FS4, FS6 and FS7, respectively) [5]. Among the last three, FS4 is the most energetically convenient (CS like 47,6 and 70.0 MJ/kWh with respect FS6 and FS7, respectively).

3. Cost Analysis

The cost of desalination is continuously decreasing in the last decades as a result of advances in desalination technologies, process design, operating experience and due to the reduction in energy consumption. Desalination is now able to successfully compete

with other alternative water resources for potable water supplies such as wastewater treatment and recycling processes (see Table 5).
However, the cost of desalination depends on plant capacity and it is site-specific, mostly based on energy cost and on salinity and quality of the feed water available at the selected site. It is thus essential to select an appropriate desalination technology that produces desalinated water at a low cost for any site under consideration.

Table 5: Water production cost comparison from various water resources.

Water Plant	Capacity	Cost	REFERENCE
Ashkelon Seawater desalination treatment plant using RO technology	330,000 m3/d	0.53 $/m^3	http://www.water-technology.net/projects/israel/specs.html
Tampa Bay Seawater desalination treatment plant using RO technology	95,000 m^3/d	0.56 $/m^3	http://www.tampabaywater.org/watersupply/tbdesalprocess.aspx
Point Lisas (Trinidad) Seawater desalination treatment plant using RO technology	109,000 m^3/d	0.73 $/m^3	http://www.hbfreshwater.com/desalinationhistory.asp
El Paso brackish groundwater Desalination Plant, Texas, USA	104,000 m^3/d	0.36 $/m^3	http://www.epwu.org/167080115.html
Wastewater treatment plant for drinking water production using MF, RO and UV(Wulpen, Belgium)	8,560 m^3/d	0.66 EUR/m^3	https://archive.ugent.be/retrieve
Wastewater treatment plant using conventional pretreatment +RO	1,000 m^3/d 5,000 m^3/d 20,000 m^3/d	0.50-0.52 $/$m^3$ 0.49 $/$m^3$ 0.46 $/$m^3$	J.A. Redondo, Desalination 138 (2001) 29-40 - Data from the Devre Water Treatment Co
Wastewater treatment plant using CMF/UF +RO	1,000 m^3/d 5,000 m^3/d 20,000 m^3/d	0.46 $/$m^3$ 0.43 $/$m^3$ 0.40 $/$m^3$	J.A. Redondo, Desalination 138 (2001) 29-40 - Data from the Devre Water Treatment Co.

Generally, thermal desalination is more cost intensive than reverse osmosis desalination, with an average desalted water cost of 1.5 $/$m^3$ [8]. According to Helal et al. [9], the high water cost in thermal desalination plants is due to their higher investment and Operating and Maintenance (O&M) costs. In fact, land requirements and energy consumption for thermal processes are higher than those for membrane ones. Recent examples for MSF facilities are the Abu Dhabi's Taweelah desalination plants constructed in 2005 and having a water production cost of 0.7 $/$m^3$, and the Shuweihat plant having a capacity of 63,000 m^3/d and with a water cost of 0.73 $/$m^3$ [10]. However, these costs are given on a rudimentary basis and it is not clear if prices for fuel have been included in the calculation of water cost.
For what concerns water production cost in RO desalination plants, it is cheaper and in the range 0.50 ÷ 0.70 $/$m^3$ in the most part of SWRO plants [11, 12]: the world's largest reverse osmosis desalination plant in Ashkelon (Israel) achieves a product water price of 0.53 US$/m³; Tampa Bay SWRO desalination plant produces water at 0.56 $/$m^3$;

water production cost at Tuas plant (Singapore) is 0.48 $/m³. In the case of brackish water desalination, fresh water cost decreases considerably and it is usually in the range of 0.2-0.3 $/$m^3$. An example can be found at El Paso Desalination Plant (Texas), the site of the world's largest inland desalination plant (104,000 m^3/d) which uses RO technology to produce drinking water by treating previously unusable brackish groundwater with a recovery factor of about 83% and a water production cost less than 0.36 $/$m^3$.
On the other hand, thermal processes can deal with more saline water and can produce distillate water with very low TDS values: also these aspects have to be considered in the decision for one or the other option.

Aim of this section is to illustrate the factors affecting water production costs, to describe the cost elements for desalination processes, to introduce the equations generally used for the economic calculations of the desalination plants and to determine the desalted water cost and the gain for the salts sale for all the proposed flow sheets.

3.1 Project parameters which influence water cost

The cost of desalted water production depends by several factors, the main of which are as follows:

- ✓ *Plant capacity:* despite a higher initial capital cost, increasing plant capacity decreases desalted water cost due to economies of scale.
- ✓ *Energy cost:* energy consumption is one of the term which more influences water production cost, representing more than 40% of overall costs [4, 10, 13, 14]. Moreover, the electricity costs vary over a wide range: the higher energy costs are in the European countries while lower values can be found in the Gulf States and U.S. As a consequence, the availability of alternative energy sources (solar, wind or geothermal) or the recourse to Energy Recovery Device have a strong impact on the unit product cost.
- ✓ *Raw water characteristics:* due to the osmosis phenomena, low feed water salinity allows to reach high recovery factors. As a consequence, the specific energy consumption and the dosing of antiscalant chemicals decrease thus further reducing unit product cost. But raw water characteristics can change with seasonal variations and during storm events and algae blooms.

As a results, the costs of desalination plants are difficult to estimate accurately without specific information. Moreover, many systems are designed and built for specific applications thus increasing the number of variables for their univocal determination.

3.2 Elements and equations of economic calculation

In this section the main cost categories are briefly discussed in order to present for each of these a representative range of economic values.
The calculation of desalted water production cost is divided into annual operating costs, direct and indirect capital cost:

- ✓ *Direct capital costs (DC)* include the acquisition cost of land and process equipments as well as the costs for plant construction.
  For example, pumping and energy recovery system cost is given by $\text{Cost}_{\text{pump or turbine}} = 0.0141 \cdot G_e \cdot P$ [15] where P=pressure [atm], G_e= flow rate [kg/h]; heat exchanger cost is calculated as $\text{Cost}[\$] = \frac{M\&S}{280} \cdot 101.3 \cdot (2.29 + F_C) \cdot A^{0.65}$ [8, 9] where $F_c = (F_p + F_d) \cdot F_m = 1$, A= area [$ft^2$], M&S = Marshall & Swift index.

- ✓ *Indirect capital costs (A_{in})* include freight and insurance, construction overhead, owner's and contingency costs. These costs are usually expressed as percentages of the total direct capital costs.

- ✓ *Annual operating costs.* These costs incur during actual plant operation and include the following items:
  1. *Annual electric power cost*, calculated as $A_{\text{electric}} = c \cdot w \cdot f \cdot m \cdot 365$ where c=electric cost [$/KWh], w = specific consumption of electric power [KWh/m^3], f=plant availability, m = plant capacity [m^3/d];
  2. *Annual labour cost*, calculated as $A_{\text{labor}} = \gamma \cdot f \cdot m \cdot 365$ where γ =specific cost of operating labour [$/$m^3$]. This item is site-specific and it is strongly influenced by the pre-treatment technologies;
  3. *Annual membrane replacement cost*, A_{membrane}. Membrane replacement rate varies between 20% per year for membranes treating high-salinity seawater to 10 % per year for membranes treating low-salinity water supported by pre-treatment systems [8];
  4. *Annual maintenance and spare parts cost*, calculated as $A_{\text{maintenance}} = p \cdot m \cdot f \cdot 365$ where p= specific maintenance and spare parts cost [$/$m^3$].
     Maintenance of process equipment is necessary to guarantee stable and reliable operation throughout the lifetime of the desalination plant.
  5. *Insurance cost*, equal to 0.5% of the total capital cost;
  6. *Amortization or annual fixed charges*, calculated as $A_{\text{fixed}} = a \cdot DC$ where DC=direct capital cost [$], "a" is the amortization factor given by $a = \frac{i(1+i)^n}{(1+i)^n - 1} = [yr^{-1}]$; i = interest rate [%]; n = plant life [yr]. Design studies and experience in desalination industry indicate an amortization life of 30 years and an interest in the range of 5-10%.
  7. *Annual cost for chemicals*, calculated as $A_{\text{chemicals}} = k \cdot f \cdot m \cdot 365$ where k = specific chemicals cost [$/$m^3$].
     Chemicals are used in pre-treatment, cleaning operation and post-treatment. Chemical addition depends on raw water characteristics, membranes in use and pre-treatment technique in fact, as described in *section 4.1.2 - chapter 1*, membrane pre-treatment generally requires less chemical addition than conventional pre-treatment. Therefore, also this cost is site-specific and varies from plant to plant.

8. *Annual brine disposal cost*, calculated as $A_{brine} = b \cdot B \cdot f \cdot 365$ where b = specific cost of brine disposal [\$/m^3] and B = brine flow rate [m^3/d].
   The main factor influencing brine disposal cost are:
   a) the utilized discharge devices;
   b) the volume and the salinity of the brine stream to be discharged;
   c) the length of the pipeline systems to transfer the brine from the desalination plant to the disposal site;
   d) the costs associated with the control of the environmental risks caused by all types of land/sea disposal procedures.
9. *Annual steam cost*, calculated as $A_{steam} = s \cdot G \cdot f \cdot 365$ where s = heating steam cost [\$/lb] and G the required steam mass flow rate [lb/d].
10. *Annual Na_2CO_3 cost.* From the forth flow-sheet, the annual Na_2CO_3 cost has to be considered: $A_{Na_2CO_3} = Na_2CO_3 \text{ cost} \cdot \text{salt flow rate} \cdot f \cdot 365$.

Taking into account all the previous cost items, the *Total Annual Cost* and the *Unit Product Cost* are, respectively, given by:

$$A_{total} = A_{fixed} + A_{in} + A_{electric} + A_{chemicals} + A_{labor} + A_{steam} + A_{brine} + A_{maintenance} + A_{membrane} + A_{Na_2CO_3}$$

and $A_{unit,p} = A_{total}/(f \cdot m \cdot 365)$.

In literature there are many software packages for evaluating the cost of desalinated water, such as the DEEP (Desalination Economic Evaluation Program) and WTCost© software programs.
DEEP was issued by the International Atomic Energy Agency (IAEA). It is useful for preliminary economic evaluation for different combinations of various energy sources of fossil and nuclear power plants with different desalination processes [16]. It contains desalination models for MSF, MED, RO and possible hybrid combinations and enables side-by-side comparison of a large number of design alternatives, which help in identifying the lowest cost options for water and/or power production at a specific location.
WTCost© was developed by the US Bureau of Reclamation and I. Moch & Associates for comparison of different water treatment processes employing RO/NF, MF/UF, electro-dialysis and ion exchange [16]. It includes cost equations for estimating different pre- and post-treatment unit operations, chemical consumptions, intake infrastructures, disposal devices, labour, membrane replacements, amortization, rates, tanks, piping and instrumentations.
There are, moreover, some software packages developed by membrane suppliers, which are publicly available. However, these packages have an accuracy only 30% because they do not consider all the equipments and site parameters and many details are not available.
These packages are normally applied only for feasibility studies but not for project budgeting.

3.3 Economical evaluation of the proposed integrated membrane systems: results and discussion

Based on the analyses and equations illustrated in the previous paragraphs, the economic evaluation of the proposed integrated membrane systems for seawater desalination is presented in this section. All calculations are based on recent economic data extracted from actual field data and from design studies in literature. The calculations are based on the following assumptions:

- ✓ interest rate i = 5% [8];
- ✓ indirect capital costs = 10% of total direct capital costs [15];
- ✓ plant life n = 30 yr [8, 17];
- ✓ plant availability f = 0.9 [8, 18];
- ✓ electric cost c = 0,09 $/KWh [8, 19];
- ✓ heating steam cost s = 0,0032 $/lb [19];
- ✓ specific chemicals cost k = 0.025 $/$m^3$ [4, 8, 20] in the case of conventional pre-treatment, whereas k=0.018 $/$m^3$ [9, 14] by using membrane pre-treatment;
- ✓ specific cost of operating labour γ = 0.05 $/$m^3$ [8] in the case of conventional pre-treatment, whereas γ=0.03 $/$m^3$ [4] by introducing membrane pre-treatment;
- ✓ specific cost of brine disposal b = 0,0015 $/$m^3$ [8, 20];
- ✓ specific maintenance and spare parts cost p= 0,033 $/$m^3$ [4, 15];
- ✓ NF/RO membrane cost = 30$/$m^2$, MF/MD membrane cost = 90 $/$m^2$ [8];
- ✓ M&S = 1102.5 for 2002 [19];
- ✓ Na_2CO_3 market price= 0,068 $/kg [21];
- ✓ selling price for NaCl = 30$/t and for $MgSO_4 \cdot 7H_2O$ = 570 $/t [22], for $CaCO_3$ = 62 $/t [23].

That said, the economic evaluation for each proposed flow sheet has been made to determine the unit cost of fresh water produced and the gain for the salts sale.
Table 6 shows the achieved results for FS3.

Table 6: Summary of annual cost data for FS3.		
	without ERD	with Pelton turbine
Direct capital cost [$]	2,025,000	2,246,000
Plant capacity [m^3/d]	12,420	12,420
Specific consumption of electric power [KWh/m^3]	3.695	2.932
Annual fixed charges [$/yr]	59,230	73,580
Indirect capital cost [$/yr]	5,923	7,358
Annual steam cost [$/yr]	-	-
Annual electric power cost [$/yr]	1,357,000	1,077,000
Annual cost for chemicals [$/yr]	73,460	73,460
Annual brine disposal cost [$/yr]	6,290	6,290
Annual labour cost [$/yr]	122,400	122,400
Annual maintenance and spare parts cost [$/yr]	134,700	134,700
Annual membrane replacement cost [$/yr][1]	111,500	111,500
Total annual cost [$/yr]	1,871,000	1,606,000
Unit product cost [$/$m^3$]	0.46	0.39

[1] A membrane life of 10 years has been considered.

The desalted water cost in the most part of recently building SWRO desalination plants varies in the range 0.50 ÷ 0.70 $/$m^3$, not too much different from the one calculated (0.46$/$m^3$) with the above described equations and assumptions in the case of standard seawater composition.
Recently Borsani and Rebagli [24] estimated the unit water cost for an RO desalination plant for Arabian Gulf conditions. Their results and the comparison with the data reported by Dreizin [25] for Ashkelon seawater RO desalination plant are given in Table 7.

Table 7: Comparison between water price of Ashkelon RO plant and the one calculated by Borsani and Rebagliati [16].

Cost item	Ashkelon [$/$m^3$]	Borsani and Rebagliati [$/$m^3$]
Base fixed price	0.311	0.22
Energy	0.134	0.148
Chemical	0.21	0.078
Post-treatment	0.009	
Filters	0.005	/
Membranes	0.28	/
Others	0.17	/
Total water price	0.525	0.446

One can not be surprised of the higher water cost reported in Table 7 for Ashkelon plant, because it is characteristic of a RO desalination plant operating with high salinity feedwater.

For what concerns the membrane-based desalination systems with MCr unit, the salts production requires to add the following equation for the calculation of the profit for the salts sale: $\text{Annual profit} = \text{salt price} \cdot \text{salt flow rate} \cdot \text{plant availability} \cdot 365 \quad [\$/\text{yr}]$.
The results achieved when MCr operate on RO brine (FS5) are reported in Table 8.

Table 8: Summary of annual cost data for FS5.

	without ERD	with Pelton turbine
Direct capital cost [$]	5,539,000	5,763,000
Plant capacity [m^3/d]	17,750	17,750
Specific consumption of electric power [KWh/m^3]	2.586	2.054
Heating steam consumption [Kg/h]	12,510	12,510
Annual fixed charges [$/yr]	65,670	80,280
Indirect capital cost [$/yr]	6,567	8,028
Annual steam cost [$/yr]	689,300	689,300
Annual electric power cost [$/yr]	1,357,000	1,078,000
Annual cost for chemicals [$/yr]	105,000	105,000
Annual brine disposal cost [$/yr]	3,665	3,665
Annual Na_2CO_3 cost	51,020	51,020
Annual labour cost [$/yr]	174,900	174,900
Annual maintenance and spare parts cost [$/yr]	192,400	192,400
Annual membrane replacement cost [$/yr][A]	794,400	794,400
Total annual profit for the salt (NaCl and $CaCO_3$) sale [$/yr]	2,991,000	2,991,000
Total annual cost [$/yr]	3,440,000	3,177,000
Unit desalted water cost without considering the profit for the salt sale [$\$/m^3$]	0.59	0.54
Unit desalted water cost considering the profit for the salt sale [$\$/m^3$]	0.077	0.032

[A] The membrane life has been considered equal to 10 years for MF/NF/RO and to 5 years for MCr.

The possibility to use a crystallizer for increasing the recovery factor and for recovering the valuable salts usually present in the highly concentrated streams of the desalination plants has been also considered by M. Turek [26]. He analyzed two different hybrid systems: UF/NF/MSF/conventional crystallizer and UF/NF/RO/MSF/conventional crystallizer. In his systems the water cost is equal to 0.71 and 0.43 $/m^3$, respectively. The higher water price of the hybrid systems proposed by Turek is probably due to the presence of the thermal desalination process (MSF), more energy consuming than membrane processes.
A summary of the achieved results for the seven proposed flow sheets is reported in Table 9.

Table 9. Desalted water unit cost and profit for the salts sale for all the proposed flow sheets.

	FS1	FS2	FS3	FS4	FS5	FS6	FS7
Total profit for the salts sale[$/yr]	-	-	-	6,398,000	2,991,000	9,389,000	6,398,000
Total annual cost[$/yr]	2,040,000	2,005,000	1,871,000	4,024,000	3,440,000	5,593,000	5,445,000
Unit cost* [$/m^3]	0.61/0.40[a]	0.47/0.40[a]	0.46/0.39[a]	0.68/0.63[a]	0.59/0.54[a]	0.73/0.69[a]	0.74/0.71[a]
Unit cost*,[b] [$/m^3]	-	-	-	0.55/0.51[a]	0.47/0.43[a]	0.54/0.51[a]	0.55/0.51[a]
Unit cost** [$/m^3]	-	-	-	-0.40/-0.44[a]	0.077/0.032[a]	-0.49/-0.53[a]	-0.13/-0.16[a]
Unit cost**,[b] [$/m^3]	-	-	-	-0.52/-0.57[a]	-0.041/-0.086[a]	-0.68/-0.71[a]	-0.32/-0.36[a]

* Desalted water unit cost without consider the gain for the salts sale.
** Desalted water unit cost considering the gain for the salts sale.
(a) If Pelton turbine is used as energy recovery device.
(b) If thermal energy is available in the plant or the stream is already at the operating temperature of the MCr unit.

In all the examined flow sheets, the fresh water cost is lower than that of thermal desalination processes (about 1.5 $/m^3) [8] and ranges from 0.39 $/m^3 for FS3 with Pelton turbine like energy recovery system, to 0.74 $/m^3 for FS7. The higher water cost in the integrated system with MCr module is due to the thermal demand of the membrane crystallizer unit needed for heating the brine. If the water stream is already available at the temperature needed for carrying out the MCr operation or the thermal energy is available in the plant, the water cost is reduced until about 0.47÷0.55 $/m^3. However, it should be pointed out that in the integrated system with MCr unit there are two important advantages:

- the quantity of produced salts is high enough that the gain for the salts sale covers more than entirely the cost of desalination process (see Table 9). Therefore, the overall integrated desalination process becomes very attractive also from an economical point of view.
- The environmental problems related to the brine disposal are almost totally eliminated. These problems are more evident when the desalination plant has to be constructed away from a salt water body. Any existing ground or surface water has

to be prevented to the pollution with the salts of the concentrate streams. The transport by pipeline to a suitable disposal point could add up to the total costs.

3.4 Influence of temperature of the membrane crystallizer feed on fresh water cost

Membrane crystallization process is a temperature driven membrane operation in which the driven force increases with the temperature of the feed and/or with the temperature difference between the two membrane sides. Therefore, by growing the temperature of MCr feed, the trans-membrane flux increases while membrane crystallizer size and, as consequence, membranes purchase and replacement cost decrease.
Contemporarily, the thermal energy consumption of the desalination plant and the size of the heater before the MCr increase with the temperature of the MCr feed. Therefore, the cost of the desalted water is the result of the balance between these two opposite trends.
In Figure 4 a plot of the desalted water cost versus the temperature of the MCr feed is reported for the fourth and the fifth proposed desalination systems.

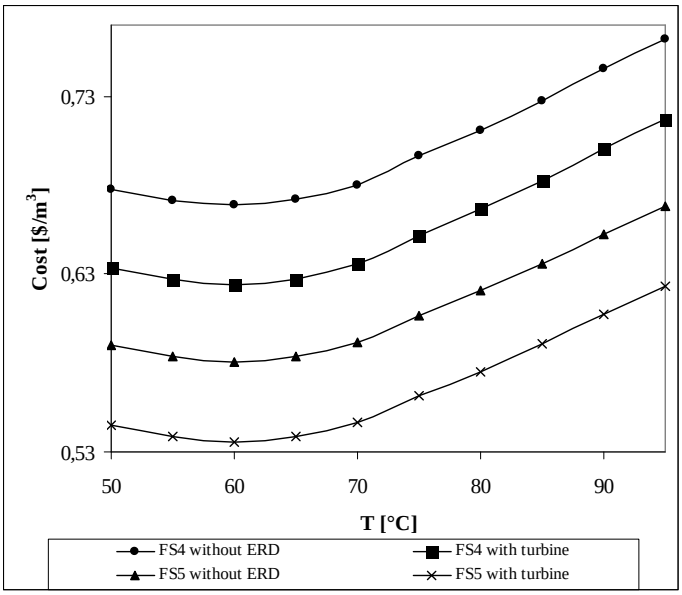

Figure 4: Desalted water cost vs. temperature of MCr feed.

Without considering the gain for the salts sale, it has been seen that, when the temperature of the MCr feed grows, the fresh water cost has a minimum due to the increase in annual steam cost and to the decrease in membrane replacement cost. This trend is another motivation for what concerns the choice to utilize a temperature higher than 35°C in the proposed flow sheets (*section 4.1, chapter 2).*
Moreover, from the linearization of the achieved results, both with and without energy recovery system (ERD), straight lines with slopes equal to 0.0021 for FS4 and to 0.0019 ($/m^3)/°C for FS5 have been obtained. This means that FS4 is more sensitive to variation in MCr temperature than FS5. In fact, a 10°C increase in the temperature of the MCr feed rises of 0.021 and 0.019 $ the cost of 1m^3 of desalted water in FS4 and FS5, respectively.

4. Sustainable Metrics

In a world more and more stressed by water scarcity and by the increasing water consumption for industrial/tourist development, another problem gains wide attention: the environmental protection and the environmental impact of each water treatment system. In a few words, it is important not only decreasing water cost but also, and above all, producing fresh water in a more *Sustainable Way*.

Since 1997, many chemical and allied industry companies that are a part of the American Institute of Chemical Engineers' Center for Waste Reduction Technologies (AIChE/CWRT) have been working to develop the so-called "*sustainable metrics*" [27-29]. It is generally agreed that metrics must be parameters clearly defined, simple, measurable, objective rather than subjective, and must drive business, government and communities towards more sustainable practices.

Over the past 5-10 years, a number of metrics have been proposed, some of which are reported in Table 10.

Table 10: Metrics.

Category	Metric	Unit
Mass	$\text{Mass intensity} = \frac{\text{Total mass}}{\text{Mass of product}}$	Kg/kg
Energy	$\text{Energy efficiency or intensity} = \frac{\text{Total process energy}}{\text{Mass of product}}$	MJ/kg
Ecotoxicity	$\text{Ecotoxicity} = \frac{\text{Total (mass persistent + bioaccumulative)}}{EC_{50}\text{material} / EC_{50}\text{DDTcontrol}}$ $\text{Waste Intensity} = \frac{\text{Total waste}}{\text{Mass of product (fresh water + salts)}}$	Kg Kg/kg
Safety	Thermal hazard Reagent hazard Pressure (high/low) Hazardous by-product formation	
Economic	Cost	$ or €

EC50: concentration at which 50% of the organisms in an acute toxicity test die during the fixed time period of the study.

Mass intensity takes into account yield, stochiometry, solvent, and reagents used in the reaction mixture, and expresses this on a weight/weight basis rather than a percentage. In the ideal situation, MI would approach 1. Total mass includes everything that is used in a process or process step.

Waste Intensity (or E Factor) draws attention to the quantity of waste that is produced for a given mass of product. It also exposes the relative wastefulness of different parts of the chemical processing industries that includes industries as diverse as petrochemicals, specialities and pharmaceuticals. This metric may certainly be used by industry and can, if used properly, spur innovation that results in a reduction of waste.

The mass indicators define both environmental impacts and raw material utilization (e.g., emissions and mass intensity), while the energy indicators evaluate energy consumption of the alternatives.

Clearly, wasted resources and energy consumption may have significant cost implications.
For the seven proposed flow-sheets some metrics have been calculated in the attempt to estimate the environmental impact of the systems and to show how green metrics can drive to the choice of the most convenient desalination process.
The selected green metrics are:

1) $\text{Mass intensity} = \frac{\text{Total mass (seawater + reagents)}}{\text{Mass of product (fresh water + salts)}}$;

2) $\text{Waste Intensity} = \frac{\text{Total waste}}{\text{Mass of product (fresh water + salts)}}$;

3) $\text{Energy Efficiency or Intensity} = \frac{\text{Total process energy (electrical + thermal)}}{\text{Mass of product (fresh water + salts)}}$.

Table 11 shows the value of the quantitative indicators for the integrated desalination membrane systems without membrane crystallization units.

Table 11: Comparison of metrics for FS1, FS2 and FS3.

		FS1	**FS2**	**FS3**
Mass Intensity	[kg/kg]	2.495	1.923	2.031
Waste Intensity	[kg/kg]	0.086	0.066	0.070
Energy Efficiency or Intensity	[MJ/kg]	0.019	0.0131	0.0133
Cost	[$/m^3 of fresh water produced]	0.614	0.465	0.458
Energy Efficiency with Pelton turbine	[MJ/kg]	0.010	0.010	0.011
Cost with Pelton turbine	[$/m^3 of fresh water produced]	0.398	0.400	0.394

From the Table 11 it is clear that:
1) desalination processes possessing high mass intensity and, then, waste intensity, will have also high environmental impact and cost because their plant efficiency will be low;
2) energy consumption is the term that more influences desalination cost. In fact, the presence of the Pelton wheel in the flow sheet reduces energy intensity and water desalination cost.
Table 12 and Figures 5-6 show the value of metrics for the integrated desalination membrane systems with MCr units (FS4-FS7).

Table 12: Comparison of metrics for FS4, FS5, FS6 and FS7.

		FS4	FS5	FS6	FS7
Mass Intensity	[kg/kg]	1.3804	1.3975	1.0556	1.1184
Waste intensity	[kg/kg]	0.0374	0.0316	0.0161	0.0303
Energy efficiency	[MJ/kg]	0.0484	0.0463	0.0650	0.0689
Energy efficiency[a]	[MJ/kg]	0.0091	0.0092	0.0069	0.0073
Energy efficiency with Pelton turbine	[MJ/kg]	0.0465	0.0444	0.0636	0.0674
Energy efficiency with Pelton turbine [a]	[MJ/kg]	0.0072	0.0073	0.0055	0.0058

(a) if thermal energy is available in the plant or the stream is already at the operating temperature of the MCr unit.

The achieved results confirm that the presence of MCr unit reduces significantly the brine disposal problem and that thermal energy is the term that more influences energy consumption, in fact the introduction of a Pelton wheel as Electrical Energy Recovery Device leads to a low reduction of the plant energy efficiency and water desalination cost (Figure 5). Only when thermal energy is already available in the plant it is possible to observe a higher reduction in plant energy efficiency and water cost (Figure 6).

Figure 5: Energy efficiency and cost for FS4, FS5, FS6 and FS7 with and without Pelton turbine as Electrical Energy Recovery Device. The cost is equal to dollar per kg of fresh water produced and it does not consider the gain for the salts sale.

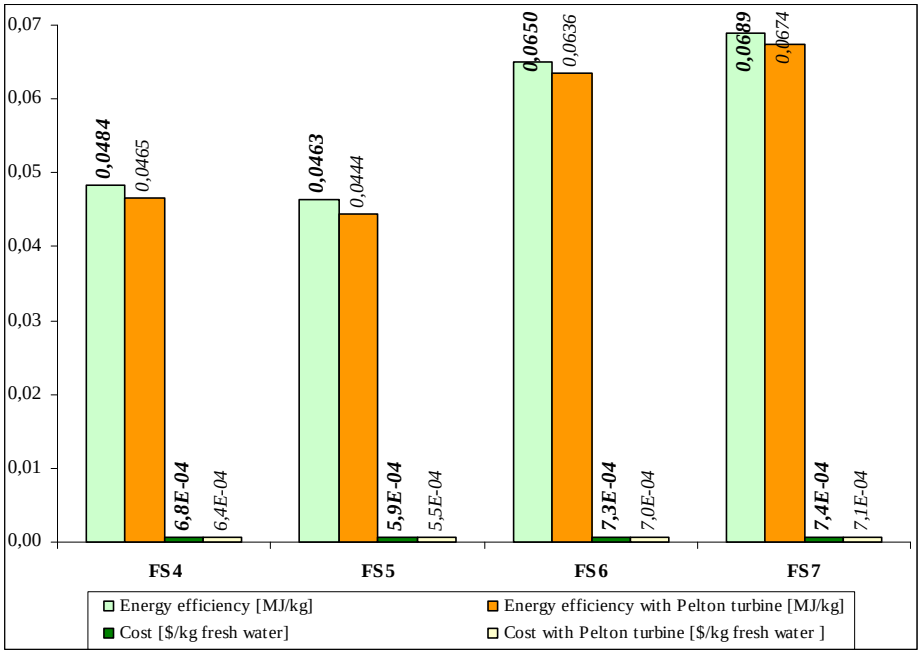

Figure 6: Energy efficiency and cost for FS4, FS5, FS6 and FS7 with and without thermal energy available in the plant. The cost is equal to dollar per kg of fresh water produced and it does not consider the gain for the salts sale.

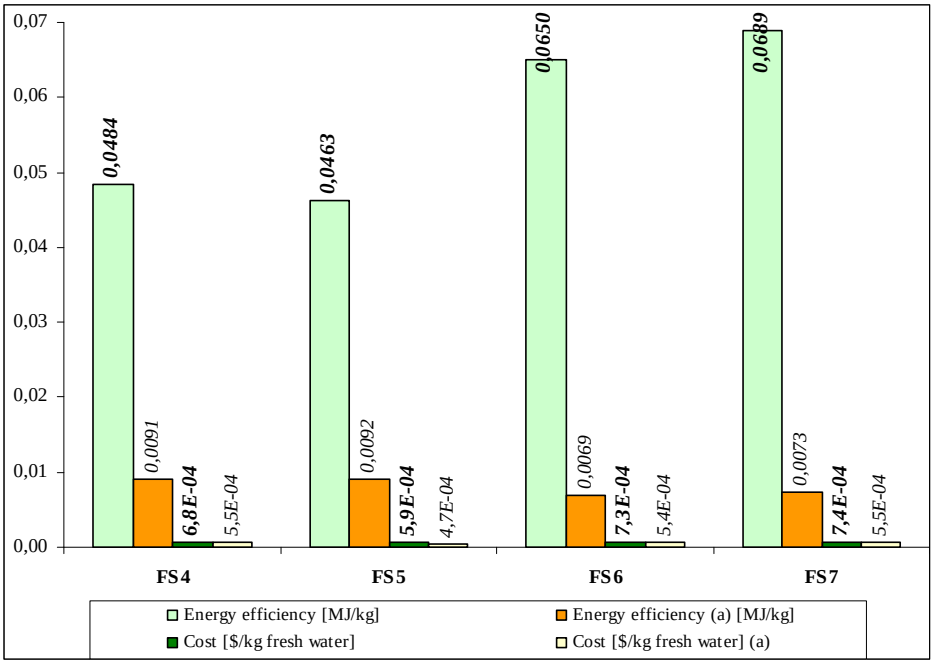

(a) if thermal energy is available in the plant or the stream is already at the operating temperature of the MCr unit.

It is important to underline that the results obtained with metrics agree with those obtained through exergetic and economic analysis of the proposed integrated membrane desalination systems. Therefore, the use of the principles of Sustainable Development can help to the choice of the best alternative for two reasons:
1) they allow to avoid risks from unsustainable business practices. These include risks from pollutants and toxic releases, greenhouse gas emissions taxes (energy, transportation), shipment of highly hazardous materials (reagents, intermediates, raw materials, solvents), etc.
2) A process that reduces costs by decreasing mass intensity or energy intensity will be more economic profitable and will have less environmental impact.

4.1 *New metrics*

Recently, other *new metrics* have been defined and utilized in the evaluation of membrane operations impact on the production lines (see Table 13).

Table 13: New proposed metrics [30].

PS (productivity/size ratio) = $\frac{\text{P/Size (membranes)}}{\text{P/Size (traditional)}}$
PW (productivity/weight ratio) = $\frac{\text{P/Weight (membranes)}}{\text{P/Weight (traditional)}}$
PW (productivity/weight ratio) = $\frac{\text{P/Weight (membranes)}}{\text{P/Weight (traditional)}}$
EI = $\frac{\text{P/Load of pollutant emissions (membranes)}}{\text{P/Load of pollutant emissions (traditional)}}$
Flexibility = $\frac{\text{Variations handled. (membranes)}}{\text{Variations handled (traditional)}}$
MI (modularity index) = $\frac{\text{Productivity}_2\text{ (scale up)}}{\text{Productivity}_1}$
M (modularity) = $\frac{\lvert \text{Area}_2/\text{Area}_1\text{ (membranes)- MI}\rvert}{\lvert \text{Volume}_2/\text{Volume}_1\text{(traditional)-MI}}$

With respect to the previous indicators, the new metrics take into account some other parameters of the industrial processes, such as size, weight, flexibility and modularity of the plants. Therefore, they can be coupled with the existing tools for comparing new and traditional processes with respect to other aspects of the production plants, always in the logic of the Process Intensification.

The chosen *new metrics* for the umpteenth comparison of the membrane-based desalination systems are PS and M indices (Tables 14-15).
PS was chosen because one of the most important characteristics of current and future plants is that to have high productivity and low size.
To compare the *productivity/size* ratio for the proposed membrane processes, the PS indicator has been re-defined as follows:

PS (productivity/size ratio) = $\frac{\text{P/Size (for flow sheet A)}}{\text{P/Size (for flow sheet B)}}$

PS value higher than 1 indicates that the process A should be preferred with respect to the process B.

Table 14: PS for FS4-FS7.

productivity/size (FS reported in the row) / productivity/size (FS in column)	**FS4**	**FS5**	**FS6**	**FS7**
FS4	1,00	0,97	1,26	1,23
FS5	***1,03***	***1,00***	***1,29***	***1,26***
FS6	0,80	0,77	1,00	0,98
FS7	0,81	0,79	1,02	1,00

The achieved results (Table 14) indicate that FS5 is, among the four analyzed flow-sheet, the one with the highest *productivity/size* ratio, meaning that this process is the one that provides the better compromise between the amount of fresh water and salts

produced and the size of the membrane process. Among FS4, FS6 and FS7, the process with the highest *productivity/size* ratio is FS4 (in agreement with the results achieved with the substitution coefficient CS).

The modularity metric M was chosen because a typical property of membrane operations is their modularity. The modularity takes into account the changes of the plant size due to variations of the plant productivity. To compare the modularity of the proposed membrane process, the modularity indicator was re-defined as follows:

$$\mathbf{M} = \frac{\left|\mathbf{area_2 / area_1 - MI}\right| \mathbf{(process_i)}}{\left|\mathbf{area_2 / area_1 - MI}\right| \mathbf{(process_j)}}$$

This metric compares the variations for the process i with those for the process j when the plant productivity varies from the condition 2 to the condition 1. The membrane process i has a higher modularity if the modularity metric is lower than 1; modularity values higher than 1 are in favour of the process j.
For the proposed flow sheets, $productivity_1$ is the one achieved when the pressure at the inlet of the RO unit is equal to 6.9 MPa, $productivity_2$ is the one achieved when the pressure at the inlet of the RO unit is equal to 6.7 MPa.

Table 15: Modularity metric for FS4-FS7.

$\frac{\left\|area_2 / area_1 - MI\right\| (FS\ reported\ in\ the\ row)}{\left\|area_2 / area_1 - MI\right\| (FS\ in\ column)}$	**FS4**	**FS5**	**FS6**	**FS7**
FS4	1,00	**0,96**	1,65	1,52
FS5	1,04	1,00	1,71	1,58
FS6	**0,61**	**0,58**	1,00	**0,92**
FS7	**0,66**	**0,63**	1,08	1,00

Among the four analyzed flow-sheet the obtained results indicate that FS6 and FS7 are more modular than FS4 and FS5.

5. Conclusions

In conclusion, the results achieved through the use of *Energetic and Exergetic Analysis, Substitution Coefficient, Economic Evaluation and* of the so-called *Sustainable Metrics* make realistic to affirm that adoption of membrane-based desalination systems appears an interesting possibility for improving desalination operations and meeting the increasing pure water demand.
In particular:

- the presence of MF provides a NF/RO feedwater of good quality. This results in a reduction of membrane fouling and, then, in capital and operating cost.
- The NF introduction allows to decrease osmotic pressure of the water fed to the following RO unit. As a consequence, coupling NF and RO units, plant global recovery factor increases up to 52%.
- The presence of MCr has three important advantages:
  1) increases plant global recovery factor so much to reach 92.8% when it operates on both retentate streams (higher than that of a RO unit -about 40%- and much higher than that of a typical MSF -about 10%);

2) it reduces, until almost to eliminate, brine disposal problem and its negative environmental impact.

3) By MCr, the quality and the quantity of produced crystals are high enough that the gain for the salts sale can cover more than entirely the cost of desalination process, particularly in the case of FS6 (see Table 9). Therefore, the overall desalination process becomes very attractive also from an economical point of view.

The comparison of the results achieved for the different flow sheets shows as follows:

- ✓ among the desalination systems without MCr unit, FS3 is the one to prefer because of the lowest cost and better quality of the produced desalted water (*Table 6-chapter 2*). The introduction of MF as pre-treatment in FS3 slightly decreases the plant recovery factor with respect to FS2 but it leads to benefits in term of reduction of membrane fouling (with consequent extension of the life time of NF/RO membranes) and chemicals dosage (because no chemicals are needed for disinfection, coagulation and dechlorination, with consequent reduction of the environmental impact of discharged NF/RO concentrated streams (see *Section 4.2 – chapter 1*).
- ✓ Among the desalination process with MCr unit, FS6 (which means the system with MCr operation on NF and RO retentate streams) is the one to prefer when thermal energy is available in the plant *or* the gain for the salts sale is considered because it is characterized by:
  - the highest recovery factor (92.8%),
  - the lowest amount of drained off retentate stream,
  - the lowest specific energy consumption (see Table 3) and desalted water cost (Table 9),
  - the highest modularity M (Table 15),
  - *productivity/size* ratio higher than FS7 and slightly lower than FS4 and FS5.
- ✓ If thermal energy is *not* available in the plant *or* if the gain for the salts sale is *not* considered, FS5 (which means MCr operates only on RO brine) is the desalination system with MCr unit to prefer for what concerns specific energy consumption, desalted water cost and *productivity/size* ratio. However, FS6 remains the best process for what concerns recovery factor, waste production and modularity.

As a consequence, the choice of the most convenient and suitable membrane desalination system depends by many parameters, first of all by seawater composition and by the possibility to use low-grade or waste heat streams, as well as alternative energy sources (solar, wind or geothermal) for a cost and energy efficient desalination system. What is undoubtedly is that *integrated membrane desalination systems* offer a reliable solution to the water shortage problem well approaching the concept of “zero-liquid-discharge”, “total raw materials utilization” and “low energy consumption”.

For what concerns the last point, currently, the total energy requirement of desalination processes (pretreatment of seawater + reverse osmosis) ranges between 3 and 4 kWh per cubic meter of desalinated seawater when optimized for large-scale plants (similarly to the results achieved in the first three proposed flow sheets – *see Table 3*). Recent demonstration studies performed in the United States by the Affordable Desalination Consortium demonstrated that energy requirements for the

RO desalination process alone could be lowered to 2 kWh/m^3 through optimization of conventional RO membrane and use of highly-efficient energy recovery device. A recent Request for Research Proposal issued by the US Defense Advanced Research Projects Agency has set an objective of 1.3 kWh/m^3, while the ADC (Affordable Desalination Collaboration) project in US (http://www.affordabledesal.com/index.html) and EWI in Singapore in collaboration with Siemens is aiming for a consumption of 1.5 kWh/m^3, not far from the theoretical inferior limit that remains around 0.6 kWh/m^3 due to the osmotic pressure and not so far from the energy consumptions of the proposed integrated membrane desalination systems with membrane crystallizer unit when thermal energy is available in the plant (*see Table 3*).

Relevant Bibliography

[1] A. Criscuoli, E. Drioli, *Energetic and exergetic analysis of an integrated membrane desalination system*, Desalination 124 (1999) 243-249.

[2] R. Molinari, R. Gagliardi, E. Drioli, *Methodology for estimating saving of primary energy with membrane operations in industrial processes*, Desalination, 100 (1995) 125-137.

[3] Y. Cerci, *Exergy analysis of a reverse osmosis desalination plant in California*, Desalination 142 (2002) 257-266.

[4] M. Wilf, *Fundamentals of RO-NF Technology*, International Conference on Desalination Costing, Cyprus, Dec. 2004, 18-31.

[5] F. Macedonio, E. Curcio, E. Drioli, *Integrated Membrane Systems for Seawater Desalination: Energetic and Exergetic Analysis, Economic Evaluation, Experimental Study*, Desalination, 203 (2007) 260-276.

[6] F. A. Al-Sulaiman, B. Ismail, Desalination, 103 (1995) 265-270.

[7] M.A. Darwish, F. Al Asfour, N. Al-Najem, Desalination 152 (2002) 83-92.

[8] H. M. Ettouney, H. T. El-Dessouky, R. S. Faibish, P. J. Gowin, *Evaluating the Economics of Desalination*, CEP Magazine, (December 2002), 32-39.

[9] A. M. Helal, A. M. El-Nashar, E. S. Al-Katheeri, S. A. Al-Malek, *Optimal design of hybrid RO/MSF desalination plants Part II: Results and discussion*, Desalination, 160 (2004) 13-27.

[10] C. Fritzmann, J. Löwenberg, T. Wintgens, T. Melin, State-of-the-art of reverse osmosis desalination, Desalination 216 (2007) 1–76.

[11] B. V. der Bruggen, C. Vandecasteele, *Distillation vs. membrane filtration: overview of process evolutions in seawater desalination*, Desalination, 143 (2002) 207-218.

[12] http://www.water-technology.net/projects/israel/specs.html (2008).

[13] J. Díaz-Caneja, M. Fariñas, *Cost Estimation Briefing for Large Seawater Reverse Osmosis Facilities in Spain*, International Conference on Desalination Costing, Cyprus, Dec. 2004, 120-139.

[14] J. A. Medina, *20 years Evolution of Desalination Costs in Spain*, International Conference on Desalination Costing, Cyprus, Dec. 2004, 293-309.

[15] A. M. Helal, A. M. El-Nashar, E. S. Al-Katheeri, S. A. Al-Malek, *Optimal design of hybrid RO/MSF desalination plants Part I: Modeling and algorithms*, Desalination, 154 (2003) 43-66.
[16] K.V. Reddy, N. Ghaffour, *Overview of the cost of desalinated water and costing methodologies*, Desalination 205 (2007) 340–353.
[17] B. M. Misra, *IAEA's Desalination Economic Evalutation Programme (DEEP)*, International Conference on Desalination Costing, Cyprus, Dec. 2004, 154-161.
[18] D. Manca, *Progettazione di Processo e Analisi dei costi*, Politecnico di Milano, www.chem.polimi.it.
[19] M. S. Peters, K. D. Timmerhaus, R. E. West, *Plant Design and Economics for Chemical Engineers*, Mc Graw Hill, 2002.
[20] E. Drioli, A. Criscuoli, E. Curcio, *Integrated membrane operations for seawater desalination*, Desalination, 147 (2002) 77-81.
[21] Data from *Sole 24 Ore, 2005*.
[22] T. E. Borgate, *Value Adding to Salts Recovered from Saline Waters in Disposal Basins in the Murray-Darling Basin*, published by Murray-Darling Basin Commission, Canberra City, Australian Capital Territory (sito Internet http://www.mdbc.gov.au).
[23] Data from *Retail Market Price Trends (Industrial Chemicals).*
[24] R. Borsani and S. Rebagliati, Fundamentals and costing of MSF desalination plants and comparison with other technologies, Desalination, 182(2005) 29–37.
[25] Y. Dreizin, Ashkelon seawater desalination project – off-taker's self costs, supplied water costs, total costs and benefits, Desalination, 190(2006) 104–116.
[26] M. Turek, *Seawater desalination and salt production in a hybrid membrane-thermal process*, Desalination, 153 (2002) 173-177.
[27] A. D. Curzons, D.J.C. Constable, D.N. Mortimer, V. L. Cunningham, *So you think your process is green, how do you know?—Using principles of sustainability to determine what is green–a corporate perspective*, Green Chemistry, 3 (2001) 1-6.
[28] D. J. C. Constable, A. D. Curzons, V. L. Cunningham, *Metrics to 'green' chemistry—which are the best?*, Green Chemistry, 4 (2002) 521–527.
[29] C. Jiménez-Gonzàlez, D. J. C. Constable, A. D. Curzons, V. L. Cunningham, *Developing GSK's green technology guidance: methodology for case-scenario comparison of technologies,* Clean Techn Environ Policy, 4 (2002) 44–53.
[30] A. Criscuoli, E. Drioli, *New index for evaluating the performance of membrane operations in the logic of process intensification*, Engineering Conferences International, Italy, June 11-15, 2006.

CHAPTER 4: Membrane Crystallizer: Avant-garde Technology for the Recovery of Water and Salts from the Concentrated Steams of the Desalination Plants. Description of the Lab Plant

Table of Contents

1. Description of the lab plan

In order to test the performance of a Membrane Crystallizer and to compare the experimental results with the theoretical ones, an experimentation phase has been carried out by using an existing lab plant, rehabilitated and improved in order to carry out the membrane crystallizer experimental activity with the control of the process.
The schematic representation of the experimental apparatus is depicted in Figure 1.

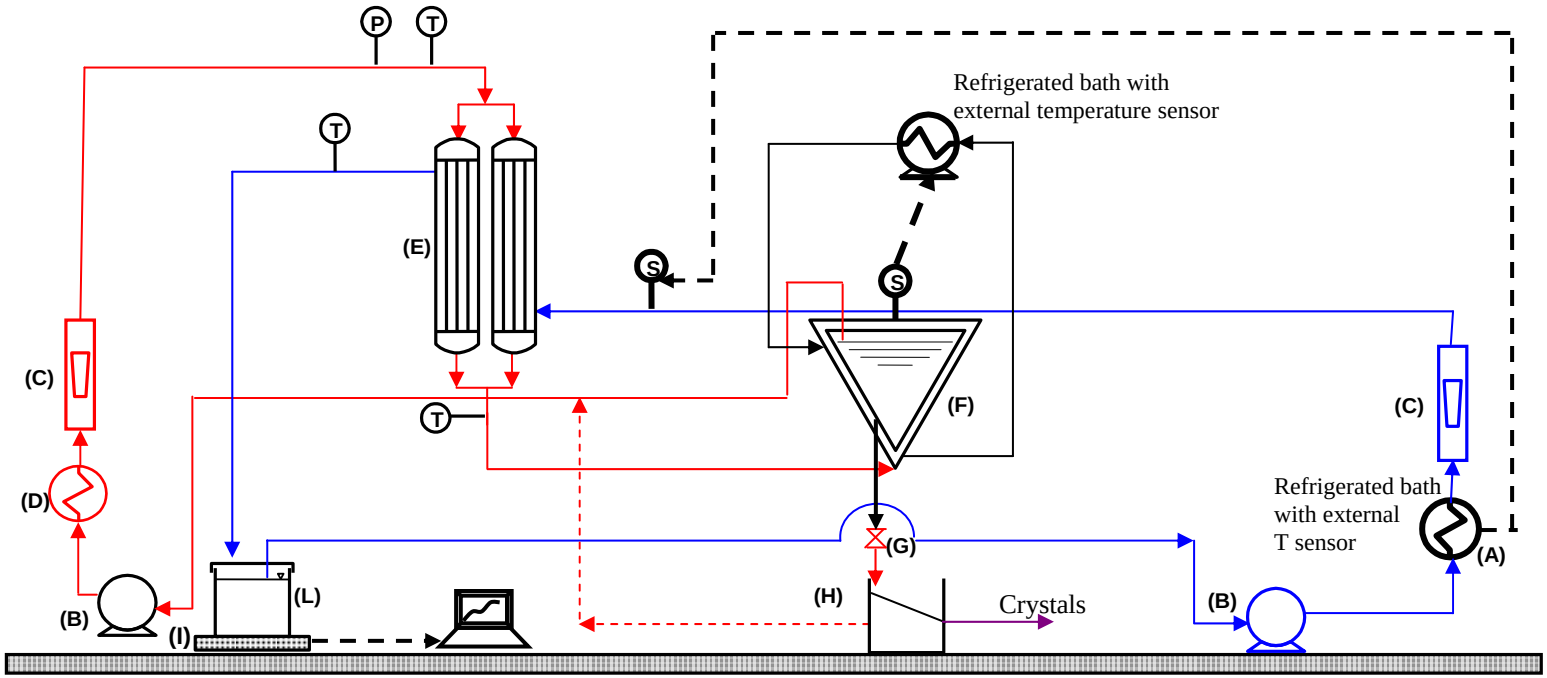

Figure 1: Schematic flow sheet of the lab plant: (A) cooler; (B) pump; (C) flow-meter; (D) heater; (E) membrane module; (F) crystallizer tank; (G) regulation valve; (H) crystals separation system; (I) balance; (L) distillate tank; (S) external temperature sensor.

The retentate (NF or RO brine) and the permeate streams (demineralized water) are the foremost lines: they converge in counter-current mode towards the membrane module containing microporous hydrophobic membranes, where the solution is concentrated by solvent evaporation. The employed MD020CP-2N membrane module, supplied by Enka Microdyn, contains 40 polypropylene (PP) hollow fibres (materials which guaranties the hydrophobicity typical in the membrane distillation process) packed in a shell of 2.1 cm diameter and 60 cm length. The nominal pore size of the PP membranes is 0.20 μm and the external diameter is 1.8 mm for 0.1m^2 of total membrane area.
The main characteristics of the membrane module are specified in Table 1.

Table 1: Structural Parameters of an Enka Microdyn MD020CP-2N Module

Material	Polypropylene (PP)
Type	Hollow fiber
No. of fibers	40
Packing density	70%
External diameter of the fibers	1.8 mm
Membrane thickness	120 μm
Length of the fibers	45 cm
Available area	0.1 m^2
Nominal pore size	0.2 μm
Shell diameter	2.1 cm

If during the tests too high pressure values are reached in the fibers, the liquid can penetrate into and through the membrane pores contaminating the permeate. Therefore, the flow rates to be used in the experiments have to be chosen to ensure that process pressure does not result in membrane wetting.
A variety of methods may be employed to drive flux according to the nature of the permeate side of the membrane. In literature, many publications show that direct contact membrane distillation (DCMD) is best suited for applications in which the major fluxing component is water, such as desalination or the concentration of aqueous solutions [1]. Also the lab plant is structured in order to satisfy the requirements of the direct contact.
Crystallization occurs inside a body where a CASTER MT7002PP centrifugal pump takes and sends the mother liquor to the membrane module on the retentate side.
The driving force in MD is a vapour pressure difference across the membrane which can be imposed by a temperature difference across the membrane. Because the major goal is to test the performance of the MCr for the concentration and crystallization of NF and RO retentate streams, the water removal from the retentate takes place only if its temperature is higher than that of the permeate. Therefore, the retentate line is heated by an ISCO GTR 2000 heater.
A crucial requirement for a MCr is to prevent crystals deposition inside the membrane: because the solubility of the solids of interest (sodium chloride and magnesium sulphate

heptahydrate) increases with temperature, a suitable heating must also guarantee that the temperature of the solution flowing along the membrane is high enough to be always under saturation condition. In this regard, it is necessary to consider that, along the capillary module, thermal exchange phenomena between cold and hot streams cause a progressive reduction of temperature, depending on the fluid-dynamic regime.
Moreover, once the crystals are formed, they are removed from the plant through a "*crystals recovery system*" constituted by two COLE PARMER - MASTERFLEX L/S pumps and a filtration unit. This system withdraws some of the solution through a hole close to the botton of the crystallization tank, sends it to the filtration unit, keeps on the filter the achieved salts and sends the filtered liquor to the membrane module in order to be further concentrated.
The solution coming out from the module is returned back to the magma reservoir, working at atmospheric pressure, whose admittance is placed on the bottom of the tank in order to create the elutriation of the crystals and to contribute to the reduction of the obstruction of the tubes during the pump draft. Also on the distillate line a CASTER MT7002PP centrifugal pump ensures the counter-current recycle of the cold stream that removes from the saline solution the water vapour passing across the membrane pores. The distillate coming out from the module is sent to a reservoir representing the drawing and picking tank for the permeate line. It is an adiabatic tank with thick and empty walls (like a honeycomb) in order to insulate the system.
The plant is also supplied with the necessary tools for the control of the most significant parameters of the system: flow rate, temperature, pressure and conductivity.
Flow rate control is achieved through Brooks Instruments mass flow-meters, with a capacity of up to 5.7 L/min, placed at the outlet of the pumps on the retentate and permeate lines; four platinum thermocouples (Pt100) disposed at the inlet and outlet of the module on the retentate and permeate lines allow a quantification of the thermal drop. The control of the crystallization temperature occurs through the use of NESLAB RTE 17 refrigerated bath supplied with external temperature sensor.
The estimation of the trans-membrane flux occurs by evaluating weight variations in the distillate tank with a Reflex HP 8200 balance. The control of the trans-membrane flux is realized through the use of a computer which acquires instantaneously the data from the balance. Therefore, the balance represents the system both for data acquisition and, connected to the computer, for the control of the stability of the crystallization process. In fact, the balance has the following functions:

- ✓ it records the time variations of the distillate volume that it is collected in the permeate tank;
- ✓ it transfers the weight data to the computer which, through the use of an appropriate software, estimates the trans-membrane flux and shows to the users its graphic trend vs time. An eventual precipitation and/or accumulation of crystals on membrane surface is immediately seen by the operators through a drop of the trans-membrane flux.

NESLAB RTE 17 refrigerated bath provides the maintenance of the inlet distillate temperature by removing the heat flux transferred from the retentate to the distillate side of the membrane modules.
The conductivity of the crystallizing solution and of the distillate is measured through the use of a HI 2300 bench meter supplied by Hanna Instruments.

2. Concentration tests: materials and methods

The experimental study has been conducted on the following synthetic solutions:

- aqueous solution of sodium chloride (initial concentration 267.8g/L);
- aqueous solution of $MgSO_4 \cdot 7H_2O$ (initial concentration 650g/L);
- aqueous solution of NaCl and $MgSO_4 \cdot 7H_2O$ (312.5g/L of NaCl and 10.2g/L of $MgSO_4 \cdot 7H_2O$). This represents the RO brine composition (4.57 times concentrated and after the precipitation of Ca^{2+} ions) of the integrated membrane desalination system constituted by MF/NF/RO-Precipitator-MCr and indicated with FS5 in the previous chapters;
- aqueous solution of NaCl (initial concentration 170.8 g/L), $MgCl_2 \times 6H_2O$ (initial concentration 179.7 g/L), $NaHCO_3$ (initial concentration 2.482 g/L), Na_2CO_3 (initial concentration 0.8306 g/L), KCl (initial concentration 5.352 g/L), KBr (initial concentration 0.5473 g/L), Na_2SO_4 (initial concentration 66.5022 g/L). It represents the NF brine composition (4.333 times concentrated and after the precipitation of Ca^{2+} ions) of an integrated membrane desalination system constituted by MF/NF-Precipitator-MCr /RO (such as FS4) in which NF and RO are characterized by the rejection values reported in Table 2 and using as feed a seawater with the composition shown in Table 3.

Table 2: NF/RO rejection values and recovery factors.

Ion	NF [%]	RO [%]
Cl	26.7	99.6
Na	26.7	99.6
SO4	93.3	99.6
Mg	87.7	99.6
Ca	80.7	99.6
HCO3	63.3	99.6
K	26.7	99.6
CO3	63..3	99.6
Br	10	99.6
Recovery factor [%]	75.3	69.1

Table 3: Seawater composition.

TDS: 33,540 mg/L	
Chloride:	19,000 mg/L
Sodium:	10,500 mg/L
Sulphate:	2,700 mg/L
Magnesium:	1,350 mg/L
Calcium:	400 mg/L
Potassium:	380 mg/L
Bicarbonate:	142 mg/L
Carbonate:	3.5 mg/L
Bromide:	65 mg/L

- Moreover, in order to evaluate the effect of organics on the crystallization process, several tests on synthetic NF brine solutions with different humic acid concentrations have been also carried out.

Different tests have been carried out changing:

(i) the temperature of the heater on the retentate line (from 40°C to 45°C)
(ii) the retentate flow rate (from 100 to 250 L/hr).

The permeate flow rate was kept constant and equal to 100L/hr. Planned the wished temperature and flow rate, the experimental data were read every ten minutes: from the computing of the weight variation in the permeate tank, the trans-membrane flux was estimated; from the electric conductivity measurements of the permeate, the absence of salts in the produced desalted fresh water stream is checked.

Since the crystals appeared, every 30 minutes, a suspension sample of them is extracted carefully and with alacrity. The particles are filtered, weighted, examined visually with

an optic microscope (ZEISS, model Axiovert 25) and pictures recorded with a video-camera module VISIOSCOPE Modular System equipped with optical head (10÷100X), in order to determine the crystal size distribution (CSD) at various time intervals.
CSD is one of the main characteristics of a crystalline product. The CSD is important for the product quality, but also influences the performance of the process, the separation of the crystals from the mother liquor, and the subsequent drying of the crystals. It is also essential for the storage and handling of the final product. For instance, small crystals contain more adhering mother liquor after filtration due to the relatively large surface area compared to a similar mass comprising larger crystals. This results in a less pure product after drying and a higher tendency towards caking. Although for many applications large crystals are preferred, there are also cases where the crystals are dissolved or digested in their final use. For those purposes, small crystals are required to reduce the dissolution time. In all cases, a narrow distribution around the mean crystal size is required. CSD allows to evaluate the cumulative percent function, a more significant parameter from an industrial point of view.
When the particle dimension is correlated to the cumulative percent function, the crystal distribution is generally characterized by the coefficient of variation [2]:

$$CV = \frac{\text{standard deviation}}{\text{mass based mean size}} = 100\frac{PD_{84\%} - PD_{16\%}}{2 \cdot PD_{50\%}}$$

where CV is the coefficient of variation, expressed as percentage, and PD is the crystal length at the indicated percentage.
By giving the coefficient of variation and the mean particle diameter, a description of the particle-size distribution is obtained which is normally satisfactory for most industrial purposes. If the product is removed from a mixed-suspension crystallizer, this coefficient of variation should have a value of approximately 50 percent [3].

3. Cleaning of the lab plant

The cleaning of the membrane module and of the overall plant is necessary at the end of each experimental test in order to avoid the deposition and the accumulation of the salts, and to restore the initial performance of the membrane.
The cleaning of the lab plant requires four different steps: (i) first of all it is necessary to empty the crystallization tank and the retentate line from the remainders of crystallizing solution; successively (ii) first an abundant washing with distillate water at ambient temperature, (iii) then a treatment with an aqueous solution of citric acid at pH 3÷4 for about 30 minutes, (iv) finally a second rinse with distillate water are required.
A different type of membrane cleaning has been used only for the crystallization tests with solutions containing organics (see *paragraph 5 – Chapter 6* for further details).
The pure water flux was measured after each step. Most of the fouling layer was swept out with the water stream. Besides, about 100% flux recovery was attained after recirculation of the citric acid solution. The trans-membrane flux measurements of pure water, first and after the tests, showed that the membrane performance after cleaning was similar to the one of the new membrane.

Relevant Bibliography

[1] E. Curcio, A. Criscuoli, E. Drioli, *Membrane Crystallizers*, Ind. Eng. Chem. Res., 40 (2001) 2679-2684.
[2] J. H. Perry, D. Green, *Perry's Chemical Engineers' Handbook*, McGraw-Hill international Editions, New York, 1987
[3] A. D. Randolph and M. A. Larson, *Theory of Particulate Processes*, Academic Press, New York (1971).

CHAPTER 5: Sodium chloride and magnesium sulfate heptahydrate crystallization. Experimental Study

Table of Contents

1. Introduction

As described in the previous chapters, in a Membrane Crystallizer, with respect to conventional crystallizers, additional factors intervene which influence crystals nucleation and growth rate. First of all, a membrane crystallizer apparatus is characterized by the dissociation of the two fundamental moments marking crystallization from the solution process: the solvent evaporation (occurring inside the membrane module) and the crystallization stage (performed in a separate tank on the retentate line). Thus, the produced crystals are expected to show improved size distribution and global quality. Secondly, the presence of the polymeric membrane in the crystallizing solution induces heterogeneous nucleation. Secondary nucleation, due to contact between crystals and (*a*) other crystals, (*b*) the walls of the container, and (*c*) the pump impeller, also occurs in a MCr. For what concerns crystals growth rate, it is correlated to the level of supersaturation and it depends by the diffusional resistance to the movement of molecules (or ions) to the growing crystal face, as well as by the resistance to integration of those molecules into the face. Moreover, the solvent trans-membrane flux modifies the level of supersaturation and it increases the concentration at membrane-solution interface.

The fundamental parameters of a membrane crystallizer device have been recalled because, as highlighted in the next paragraphs, they have to find confirmation in the experimental activity.

The evaporative crystallization of sodium chloride and epsomite from aqueous solution has been used as vehicle for preliminary experimental study. Even if NaCl represents a typical example of most inorganic crystallizing systems, interest for this salt and for $MgSO_4 \cdot 7H_2O$ are heightened since they are involved in sea and brackish water desalination process.

2. Concentration tests: control of the process

The crucial requirement of a MCr is to prevent crystals deposition on membrane surface and inside the membrane module.

In the built lab plant, crystal deposition inside membrane module is controlled by the following tools:

- ✓ by re-circulating the solution in order to remove particles eventually deposited on the membrane surface;
- ✓ by recovering the produced crystals through the “crystals recovery system”;
- ✓ by controlling the temperature of the solution flowing along the membrane module. For what concerns this aspect, known how the solubility of solids in solution depends on temperature, a suitable heating or cooling guarantees that the temperature of the solution flowing along the membrane is fairly high to be always under saturation condition.

Magnesium sulphate

Figure 1: Magnesium sulphate.

Magnesium sulfate is a chemical compound containing magnesium and sulfate, with the formula $MgSO_4$. Its solubility increases with temperature and, until to around 50°C, if the solution is supersatured, it is encountered as the heptahydrate, $MgSO_4 \cdot 7H_2O$, commonly called Epsom salts (Figure 2).

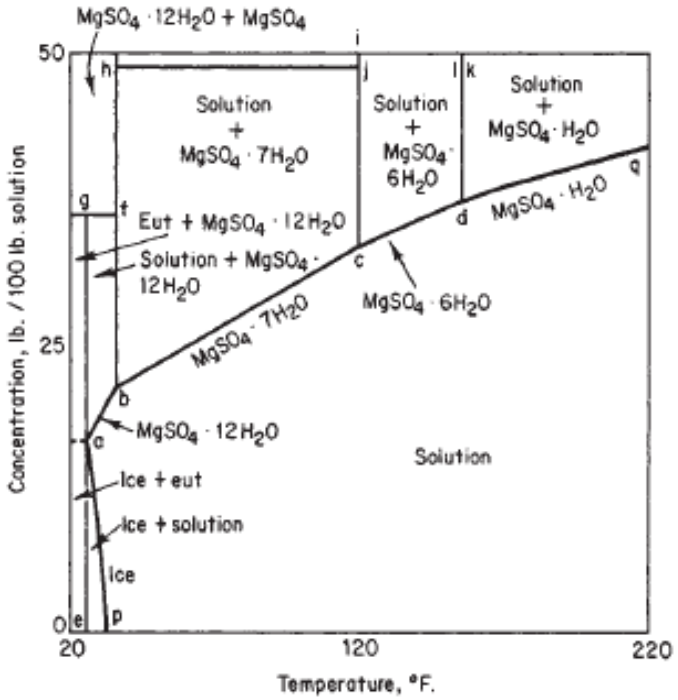

Figure 2: Phase diagram for magnesium sulphate in water [1].

Anhydrous magnesium sulfate is used as a drying agent. Since the anhydrous form is hygroscopic (readily absorbs water from the air) and therefore harder to weigh

accurately, the hydrate is often preferred when preparing solutions, for example in medical preparations. Epsom salts have traditionally been used as a component of bath salts.
The crystallization tank works at 25 °C and atmospheric pressure: if the solution is supersatured, magnesium sulphate precipitates as epsomite.

Sodium chloride

The solubility of sodium chloride doesn't change much with temperature. In the range 0-100°C it increases from 35.7 to 39.8 g NaCl/100g H_2O [2], typical behaviour of a salt with small $\Delta H_{sol.}$. According to Sparrow [3], solubility of pure sodium chloride (X_{sol}) can be also predicted, in the range $0 \leq T \leq 450$ °C, by the following equation:

$$(1) \qquad X_{sol} = 0.2628 + 62.75 \cdot 10^{-6} T + 1.084 \cdot 10^{-6} T^2$$

Equation (1), can be used for any concentration with increasing uncertainty above 0.26 sodium chloride mass fraction. Also this equation shows that sodium chloride solubility doesn't change substantially with temperature: it increases from 36.08 to 38.51 g NaCl/100g H_2O between 0 and 100°C.

Because the solubility of the salts of interest (NaCl and $MgSO_4 \cdot 7H_2O$ –naturally presents in the concentrated streams of the desalination plants) increases with temperature, a heating of the retentate solution before entering into the membrane module guarantees that the temperature of the solution flowing along the membrane is fairly high to be always under saturation condition.
According to literature [4] and to the following devised equation

$$(2) \qquad Q' = G \cdot c_p \cdot \left(T_{in} - T_{crist}\right) = \sum_{i=1}^{n} m_i \cdot \Delta H_{sol,i} + U \cdot A \cdot \Delta T ,$$

the temperature of the MCr feed has been chosen equal to 34°C (see *Section 4.1 – Chapter 2* for more details about the equation (2)).
A preliminary set of experimental tests has been carried out in order to check, by means of the trend of solvent trans-membrane flux, that the chosen MCr feed temperature is sufficient to avoid the accumulation and the deposition of the crystals on the membrane surface and inside the membrane module.

3. Concentration tests: trans-membrane flux measurements

In order to test the performance of a membrane crystallizer, water trans-membrane fluxes have been measured for aqueous solutions of sodium chloride or magnesium sulfate heptahydrate in a wide range of operative conditions.
Sodium chloride and magnesium sulfate heptahydrate in reagent grade was purchased from Sigma. Initial solutions were prepared by using bi-distilled water as solvent; water was also employed as condensing liquid on the distillate line. A filtration preceded the introduction of any fluid in the plant.
The experimental tests have allowed:

- to test fluid-dynamic effect on membrane crystallization operation and, in particular, on trend of solvent trans-membrane flux, on crystal size distribution, on their shape, dimension and growth rate, and
- to check the crystallization conditions in which there are no crystals deposition inside the membrane module.

For each solutions different tests have been carried out by using a permeate flow rate constant and equal to 100L/hr and changing the retentate flow rate from 250 to 100 L/hr. After a transitory state, the temperatures observed at the module entrance for retentate and permeate side were constant and equal to 35±1°C and 16±2°C respectively. As a consequence, for all the experiments, the temperature difference between the two membrane sides was almost unchanged ensuring the constancy of the process driving force. The crystallization tank worked at 25°C and atmospheric pressure.

3.1 Sodium Chloride Aqueous Solutions

Figure 3 shows the trend of sodium chloride concentration vs time at different retentate flow rates.

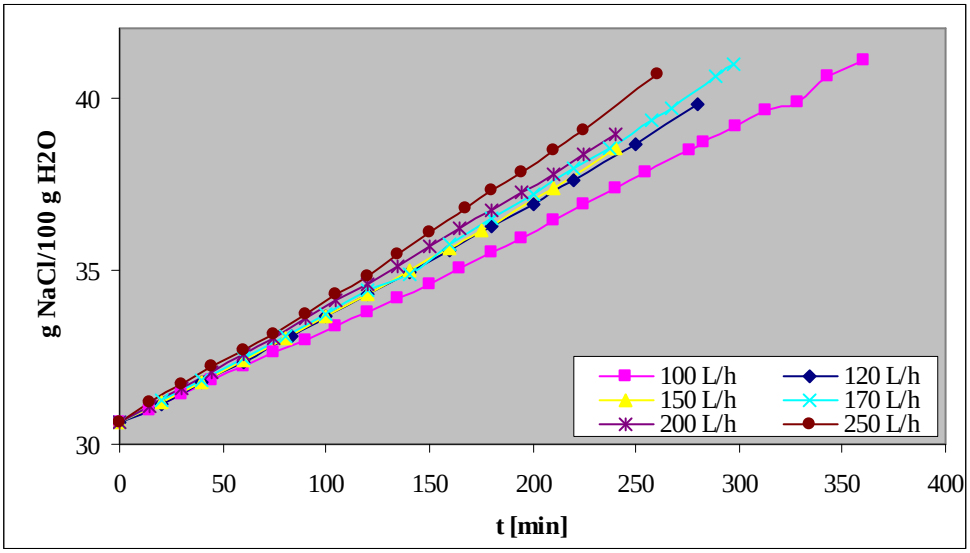

Figure 3: Concentration vs time at different retentate flow rates for the lab tests of aqueous solution of NaCl.

From an initial value of approximately 30.66 g NaCl / 100 g H_2O, an increase of the solution salinity with time is observed due to solvent recovery. The NaCl concentration growth is quite linearly, with increasing slope with feed flow rate (Table 1).

Table 1: Slope at different MCr feed flow rates.

MCr feed flow rate [L/h]	Slope (g NaCl / 100 g H_2O)/ min
100	0.0291
120	0.0326
150	0.0326
170	0.0345
200	0.0347
250	0.0381

Feed flow rate is an important parameter in membrane distillation operations. It influences both mass and energy transport phenomena: higher feed flow rate means higher Reynolds number and transport coefficients. As a consequence, polarization effects decrease and higher fluxes can be expected. However, the improvement of the performance of the system with the feed flow rate is low due to the high NaCl concentration (close to saturation point) and, therefore, to the low activity coefficient of NaCl-water solution. This, consequently, causes the growing of the viscosity and the reduction of the partial pressure difference between membrane interfaces. As a result, the trans-membrane flux decreases with sodium chloride concentration (Figure 4).

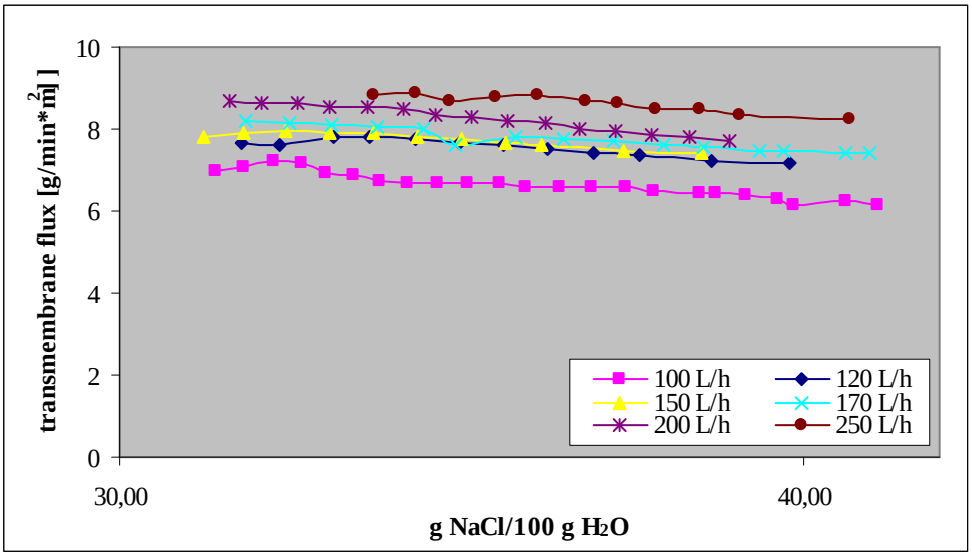

Figure 4: Trans-membrane flux vs concentration at different retentate flow rates for the lab tests of aqueous solution of NaCl.

However, the reduction of the trans-membrane flux is slow because the temperature of feed and the thermal difference between the two streams are high enough to contain the decrease in driving force due to concentration rise.
In Figure 5 is presented the trend of the trans-membrane flux vs time at different retentate flow rates. After a first stage corresponding to the settlement of the temperature profiles inside the membrane module, the flux is approximately constant:

this is characteristic of a good operation because means that there is no crystals deposition inside the membrane module.

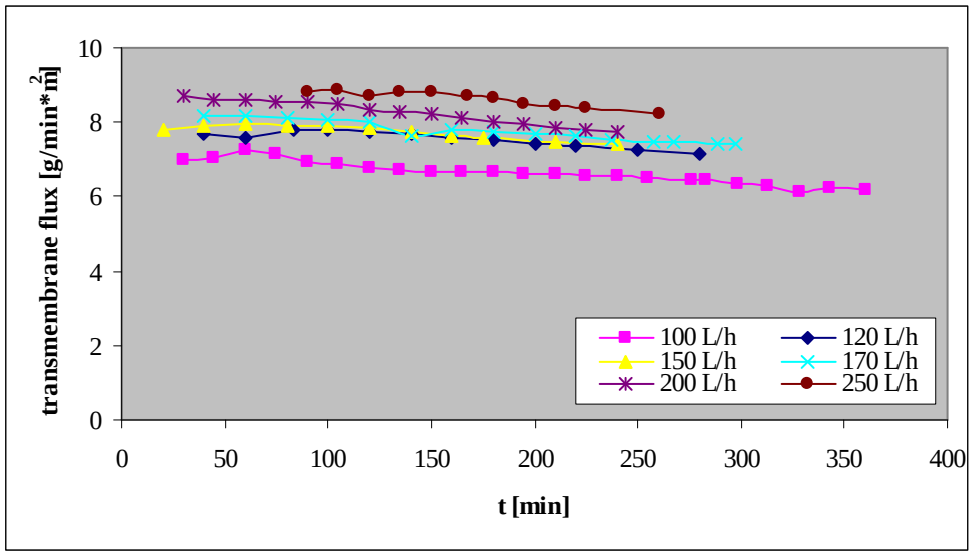

Figure 5: Trans-membrane flux vs time at different retentate flow rates for the lab tests of aqueous solution of NaCl.

In confirmation to the above reported for what concerns the influence of the feed flow rate on the transport coefficients, Figure 5 shows that water trans-membrane flux increases with retentate flow rate. Moreover, the assumption of constant temperature difference guarantees that any increase of the flux is exclusively due to the improvement of the polarization coefficients and, in particular, to the temperature polarization coefficient.
In addition, from Figure 3 and 5, it is expected that the time for reaching supersaturation and crystals formation decreases when the feed flow rate increases.
Finally, conductivity measurements carried out on samples of solution taken out from the distillate tank demonstrated that the infiltration of sodium chloride through the membrane pores was negligible; therefore, polypropylene membranes preserved the crucial requisite of hydrophobicity, at least during the operative time of these experiments.

3.2 Epsomite Aqueous Solutions

Similar results have been achieved with aqueous solution of epsomite (see Figures 6, 7, 8 and Table 2).

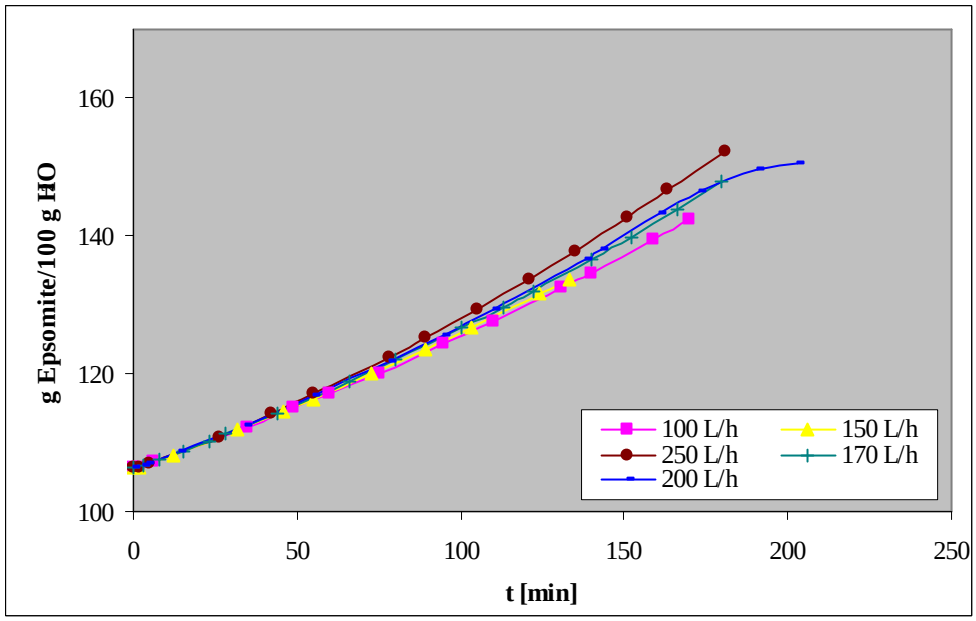

Figure 6: Concentration vs time at different retentate flow rates for the lab tests of aqueous solution of $MgSO_4 \cdot 7H_2O$.

Table 2: Slope at different MCr feed flow rates

MCr feed flow rate [L/h]	Slope (g Epsomite / 100 g H_2O)/ min
100	0.21
150	0.21
170	0.227
200	0.228
250	0.250

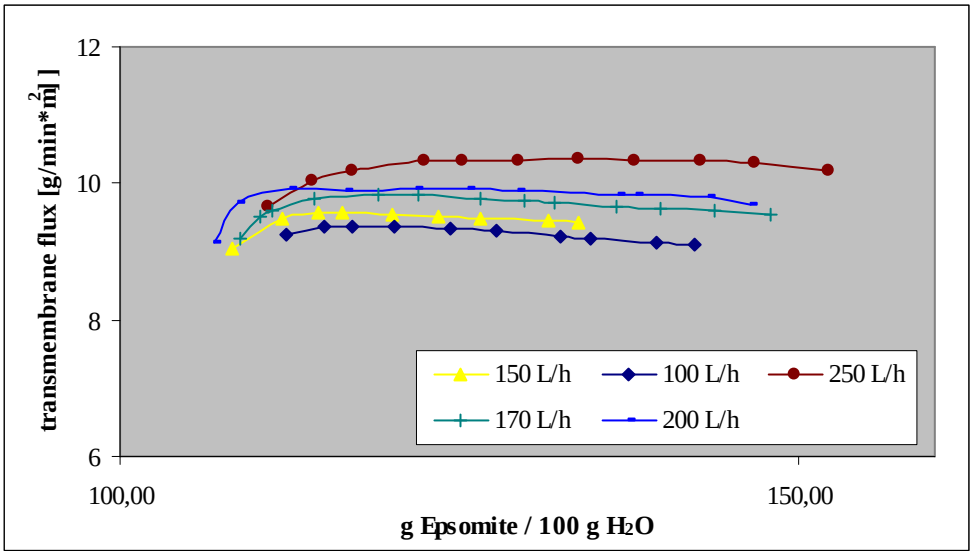

Figure 7: Trans-membrane flux vs concentration at different retentate flow rates for the lab tests of aqueous solution of $MgSO_4 \cdot 7H_2O$.

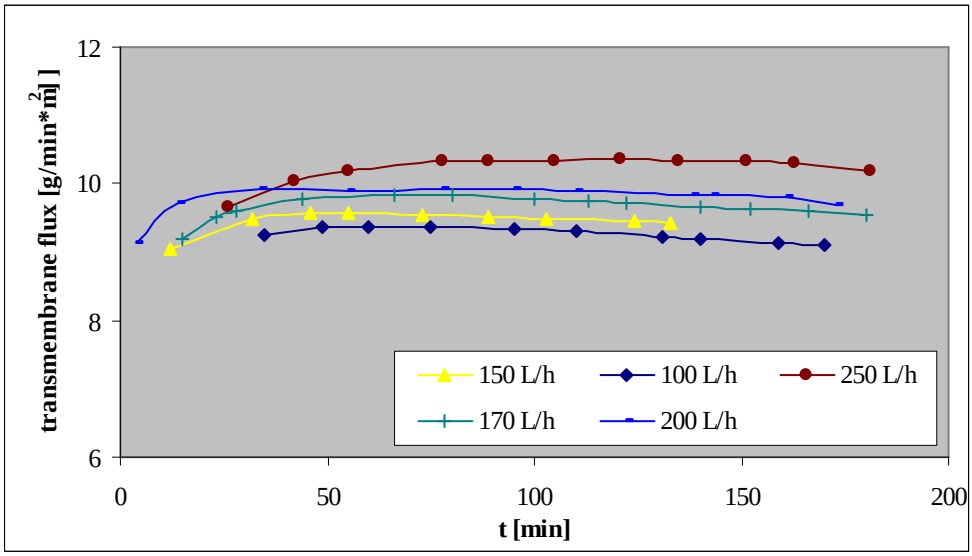

Figure 8: Trans-membrane flux vs time at different retentate flow rates for the lab tests of aqueous solution of $MgSO_4 \cdot 7H_2O$.

4. Crystallization tests: product characterization

During crystallization runs, suspension samples were withdrawn from the retentate tank every 30 minutes, particles filtered and examined visually in order to determine the crystal size distribution (CSD). Knowledge of the evolution of particle size distribution as function of time allows to evaluate quality, coefficient of variation (CV) and growth rate of the produced crystals and to test the fluid-dynamic effect on membrane crystallization operation and, in particular, on crystals shape, dimension and growth rate.

4.1 Aqueous solution of sodium chloride

The CSD of the total crystals contained in a known volume of magma was measured by a screen analysis performed via a video microscope. Figures 9-13 show the trend of CSD, at different MCr feed flow rates, for the tests carried out with synthetic aqueous solution of sodium chloride.

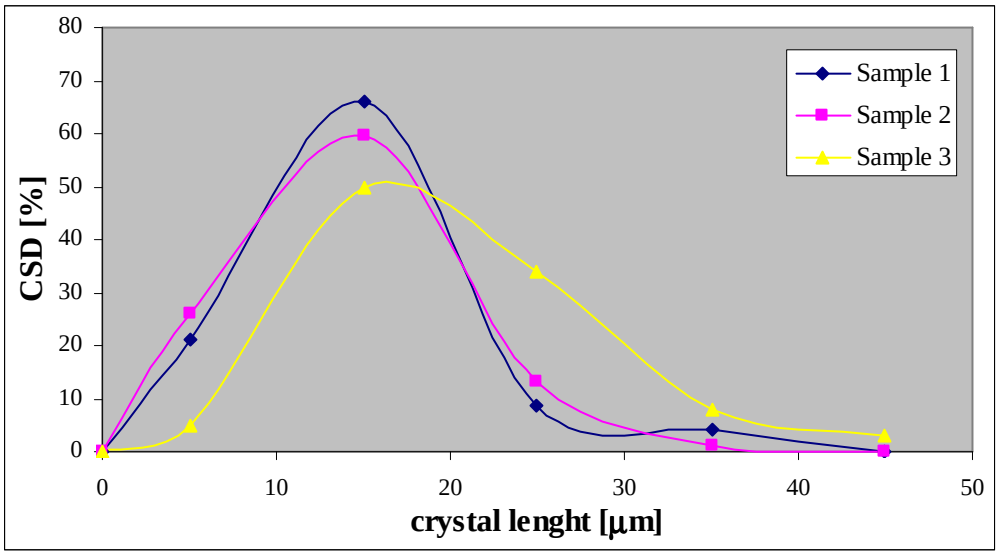

Figure 9: Crystal Size Distribution (CSD) obtained for the lab test with NaCl aqueous solution and retentate flow rate equal to 100 L/hr.

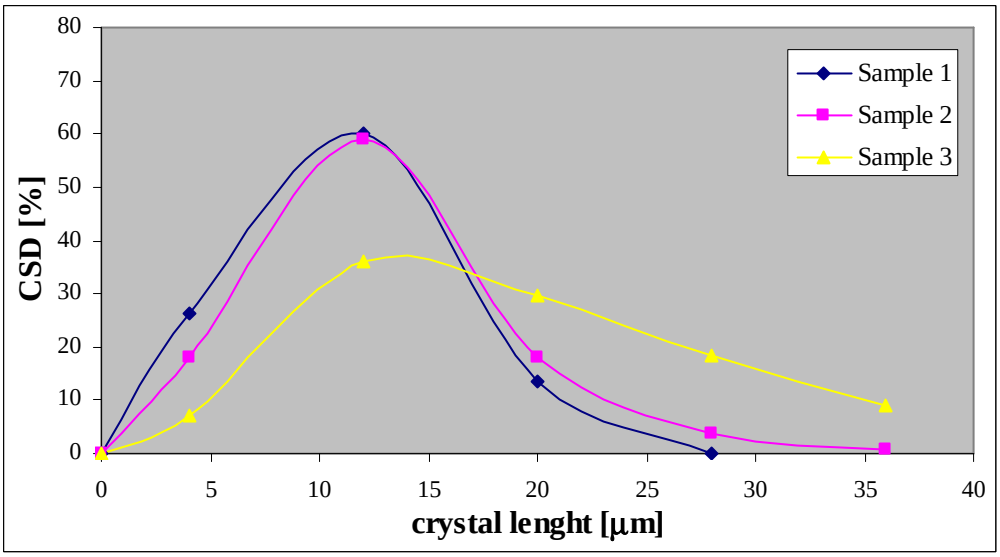

Figure 10: Crystal Size Distribution (CSD) obtained for the lab test with NaCl aqueous solution and retentate flow rate equal to 120 L/hr.

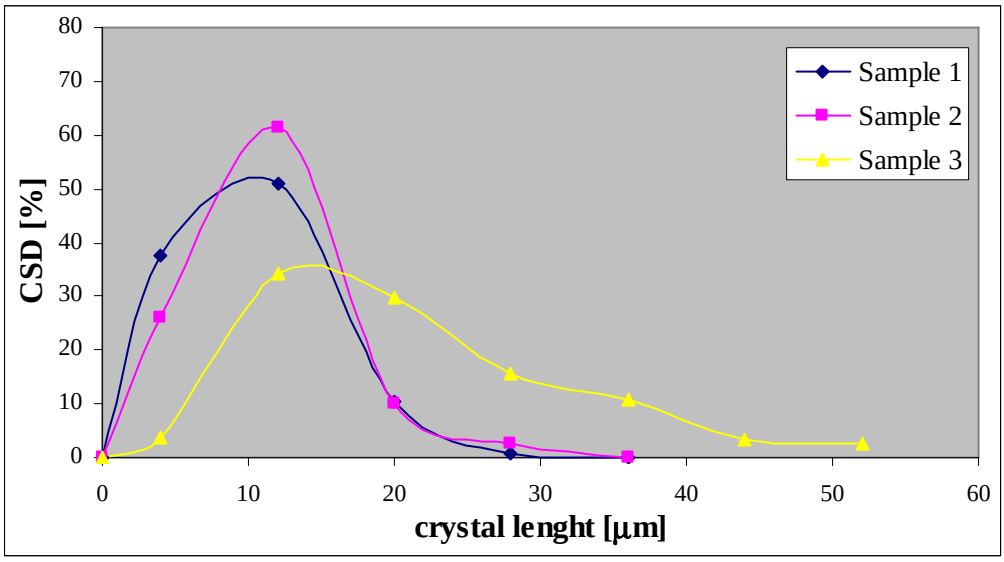

Figure 11: Crystal Size Distribution (CSD) obtained for the lab test with NaCl aqueous solution and retentate flow rate equal to 170 L/h.

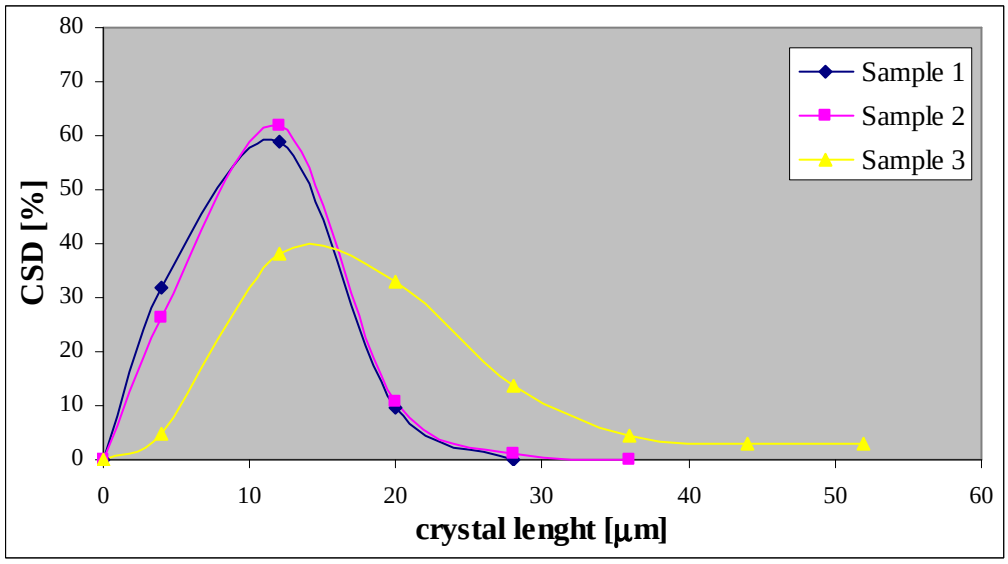

Figure 12: Crystal Size Distribution (CSD) obtained for the lab test with NaCl aqueous solution and retentate flow rate equal to 200 L/h.

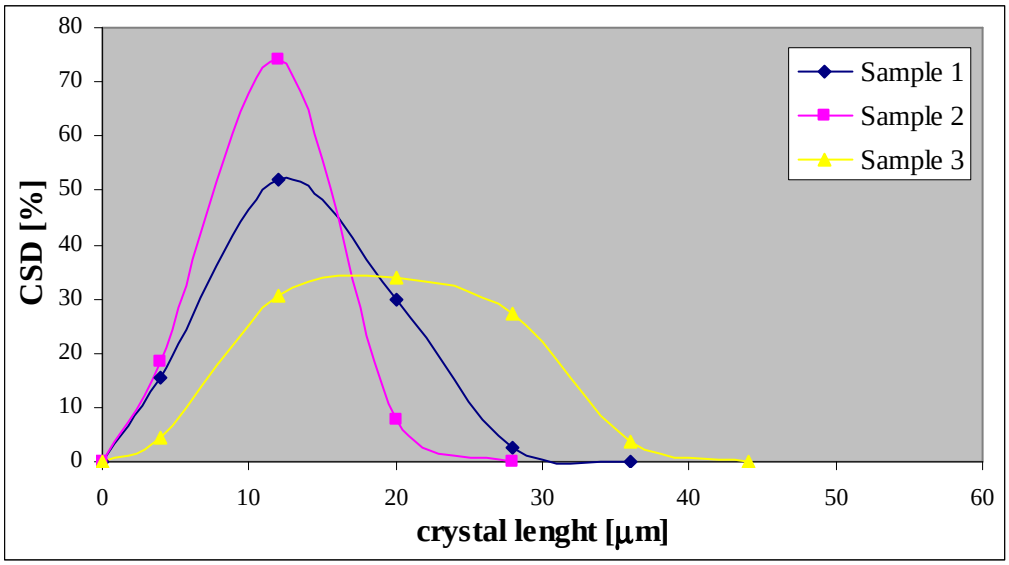

Figure 13: Crystal Size Distribution (CSD) obtained for the lab test with NaCl aqueous solution and retentate flow rate equal to 250 L/h.

The evolution of CDS shows that the initial peak of the distributions moves towards the larger dimensions as a consequence of the crystals growth.

As well as middle diameter d_m (determined from the crystal distribution), the dispersion of a distribution around the mean crystal size has been characterized with the coefficient of variation CV (see *Chapter 4* and Table 3).

Table 3: Evolution in function of time for the Coefficient of Variation (CV) and middle diameter (d_m). Parameters determined from the experimentally obtained CSDs at six different MCr feed flow rate.

Sample N° (time)	100 L/h		120 L/h		150 L/h		170 L/h		200 L/h		250 L/h	
	d_m [µm]	CV [%]	d_m [µm]	CV [%]	d_m [µm]	CV [%]	d_m [µm]	CV [%]	d_m [µm]	CV [%]	d_m [µm]	CV [%]
1 (0.5h)	14.57	**38.46**	14.87	**48.42**	11.94	**47.32**	9.85	**48.13**	10.11	**50.00**	13.24	**44.58**
2 (1.0h)	13.41	**47.01**	19.31	53.50	10.42	52.94	11.09	**45.11**	11.00	**45.11**	11.05	**36.70**
3 (1.5h)	20.24	**44.44**	26.06	51.47	17.78	52.22	21.14	58.76	19.71	52.40	19.88	**41.89**

If the crystal is removed from a mixed-suspension crystallizer, widely employed in the industrial crystallization, this coefficient of variation should have a value of approximately 50% [1]. Low CVs are characteristic of a narrow crystal size distribution and, therefore, of a better product [5]. Moreover, the values reported in Table 3 show that the CV increases with time: the second and third samples are always characterized by a higher CV than the first sample. This is due to the fact that between the first and

third sample there is a lapse of 60 minutes, period in which nucleation, crystallization and growth are subjected to some changes:

1. at the beginning of the crystallization process, the nucleation is primary and heterogeneous due to the presence of the polymeric membrane;
2. then, in the following samples, there is both the growth of the first crystals and the formation of the new ones. Moreover, also the secondary nucleation due to contact between crystals and (a) other crystals, (b) the walls of the plant, and (c) the pump impeller is present. For this reason, in each test, the last samples show a larger variety of crystals size.

The experimentally determined CVs agree with those found in literature and varying in the range 42.3 – 57.2 % [4]. In accordance with literature is also the experimentally determined density of the crystal slurries (Table 4).

Table 4: Density of the crystal slurries (M).

Retentate flow rate [L/h]	M [kg/m^3]
100 [4]	3.8
100	3.04
120	5.5
150	6.44
170	7.97
200	9.82
250	15.99

While the crystal size reflects the growth conditions rather than the periodic structure of the crystal lattice, the external appearance of a crystal (its shape) depends on its internal structure even if it can be influenced by the growing conditions. A crystal may be defined as a solid composed of atoms arranged in an orderly, repetitive array. The interatomic distances in a crystal of any definitive material are constant and are characteristic of that material. According to the external conditions, crystals can assume different shapes as long as the angles between two characteristic faces are always the same (the invariance of the angles between characteristic crystals faces is an universal property of the solids) [6].

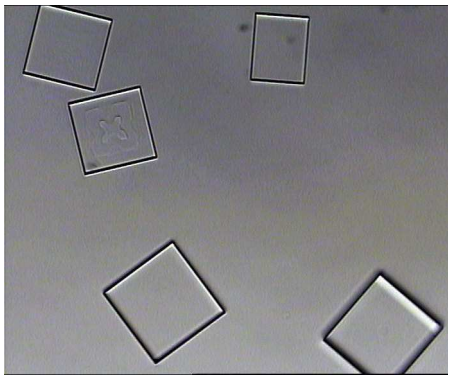

Figure 14: Crystalline habit of NaCl (picture from optical microscope, magnification: X20).

Crystals obtained by membrane crystallization showed the characteristic cubic block-like form in accordance with the expected geometry of the NaCl crystals (Figure 14).

However, in each sample, a small fraction exhibiting an elongated shape was present. Therefore, the length/width ratio of each produced crystal has been determined and the achieved results (presented in the histograms of Figures 15-20) showed that, in each analyzed sample, the most part of particles has a length/width ratio in the range 1.0 – 1.2, that is to have almost a cubic shape. Moreover, the number of crystals exhibiting a cubic block-like form increases when retentate flow rate decreases. This is probably due to the fact that high flow rates are expected to disturb the molecular organization which precedes the integration of molecules into the growing face.

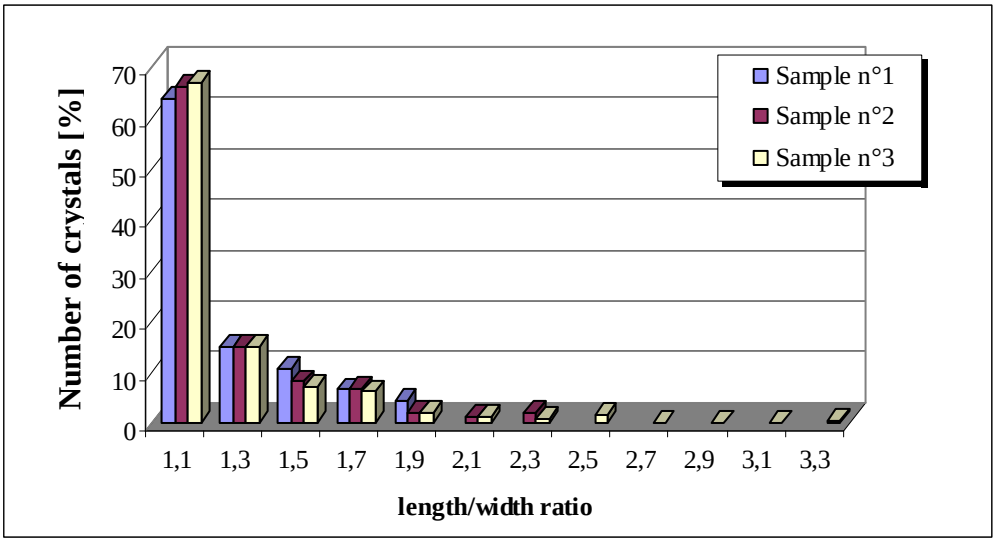

Figure 15: Number of crystals [%] vs length/width ratio at a retentate flow rate equal to 100 L/h.

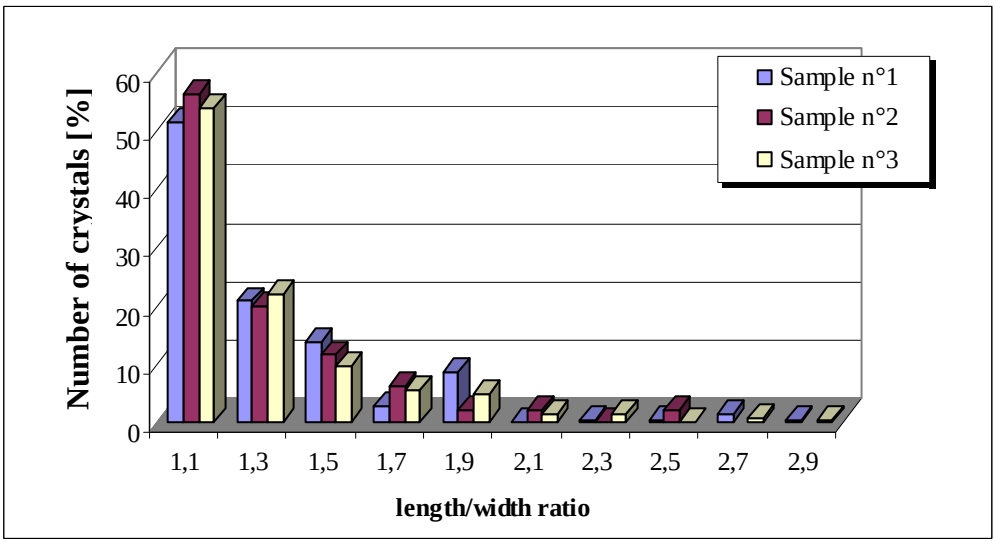

Figure 16: Number of crystals [%] vs length/width ratio at a retentate flow rate equal to 120 L/h.

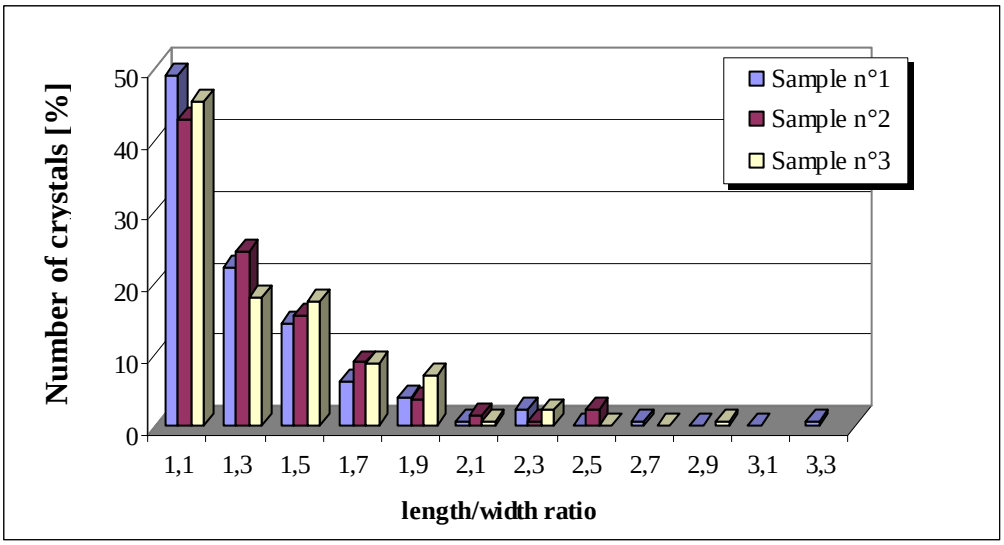

Figure 17: Number of crystals [%] vs length/width ratio at a retentate flow rate equal to 150 L/h.

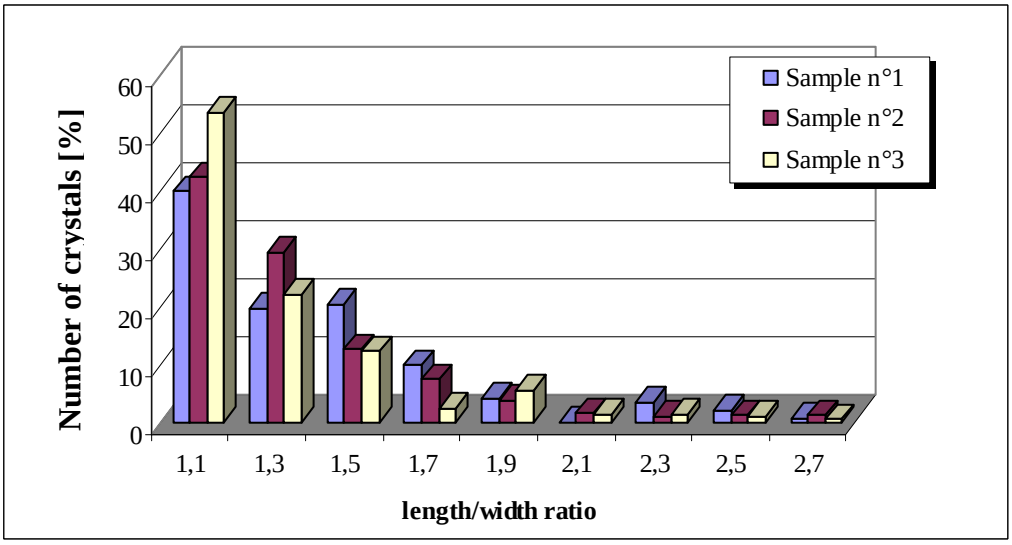

Figure 18: Number of crystals [%] vs length/width ratio at a retentate flow rate equal to 170 L/h.

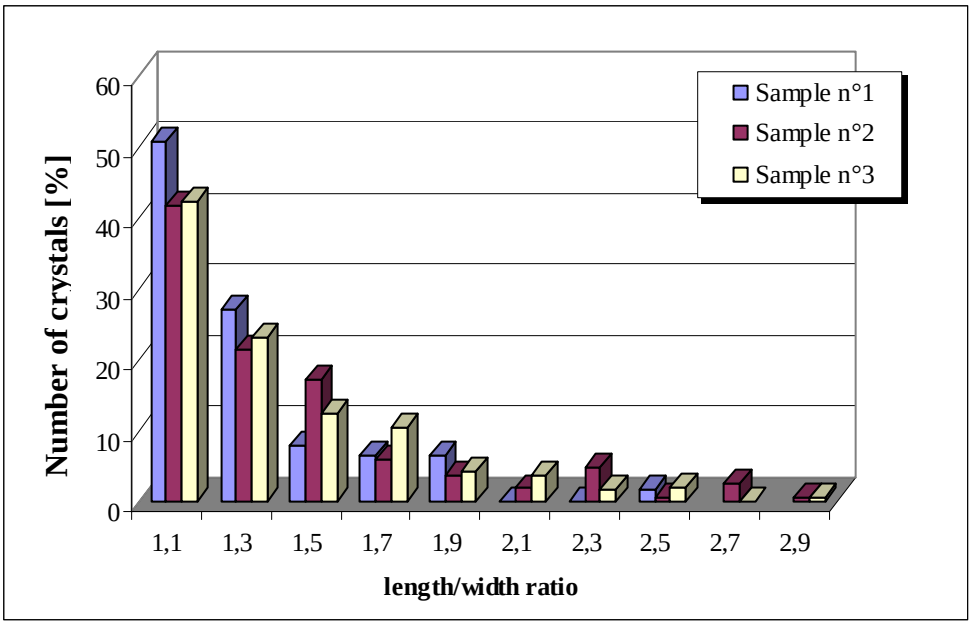

Figure 19: Number of crystals [%] vs length/width ratio at a retentate flow rate equal to 200 L/h.

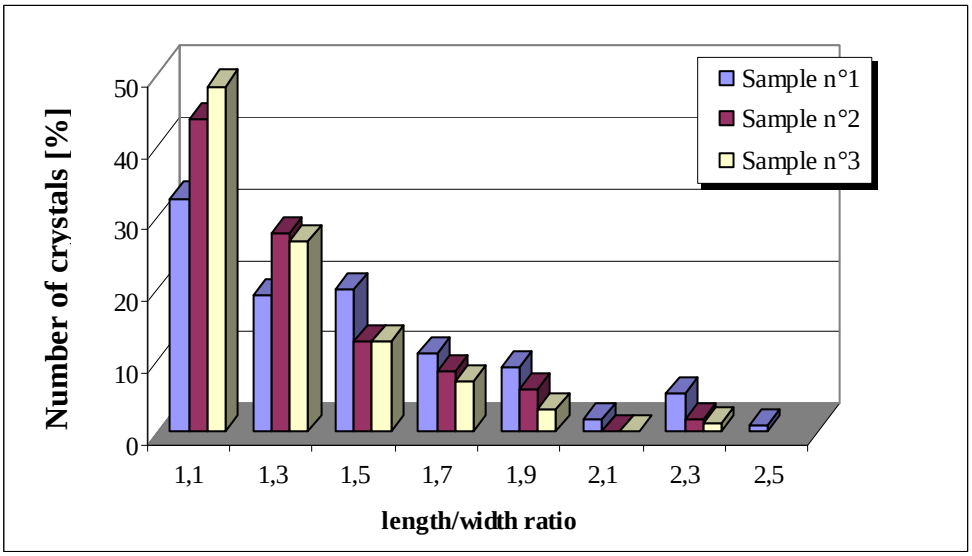

Figure 20: Number of crystals [%] vs length/width ratio at a retentate flow rate equal to 250 L/h.

4.2 Epsomite aqueous solution

Figures 21-26 and Table 5 show CSDs and density of the crystal slurries (M) achieved in the MCr experimental tests on aqueous solutions of $MgSO_4*7H_2O$. The results are similar to those obtained with NaCl aqueous solutions.

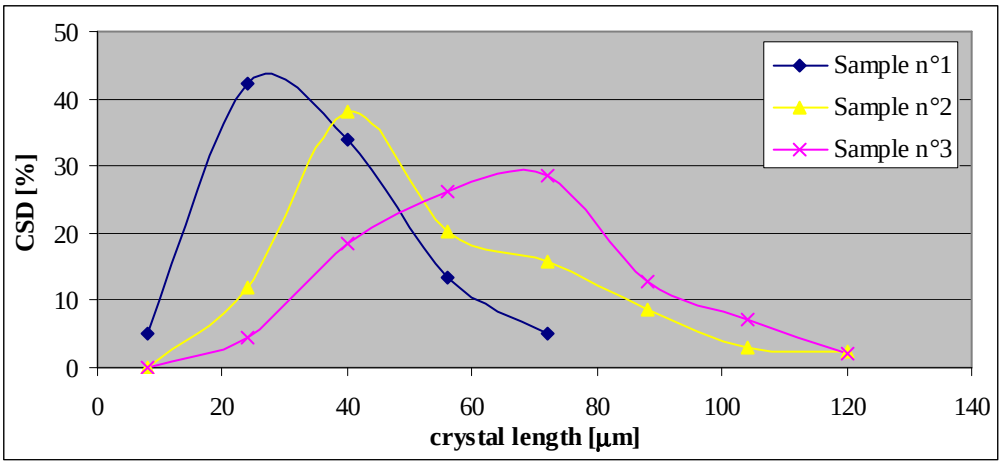

Figure 21: Crystal Size Distribution (CSD) obtained for the lab test with $MgSO_4*7H_2O$ aqueous solution and retentate flow rate equal to 100 L/h.

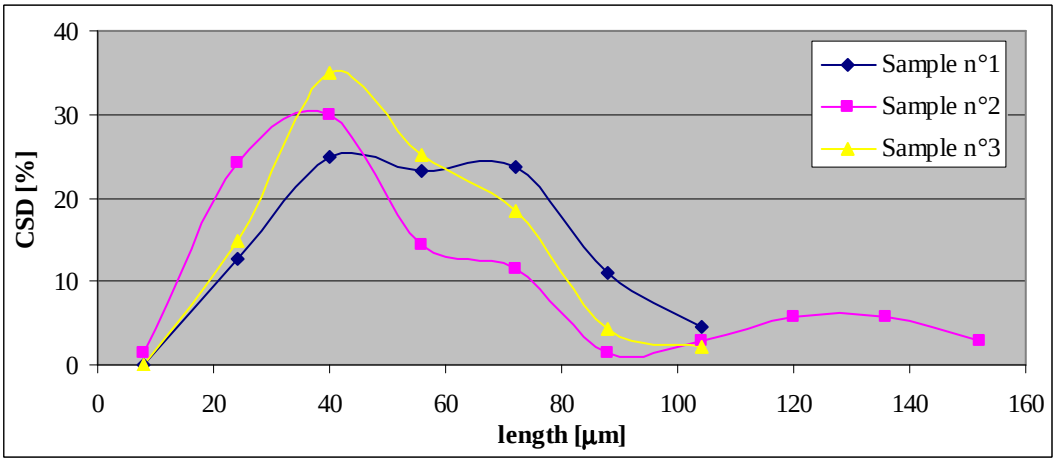

Figure 22: CSD obtained for the lab test with $MgSO_4*7H_2O$ aqueous solution and retentate flow rate equal to 120 L/h.

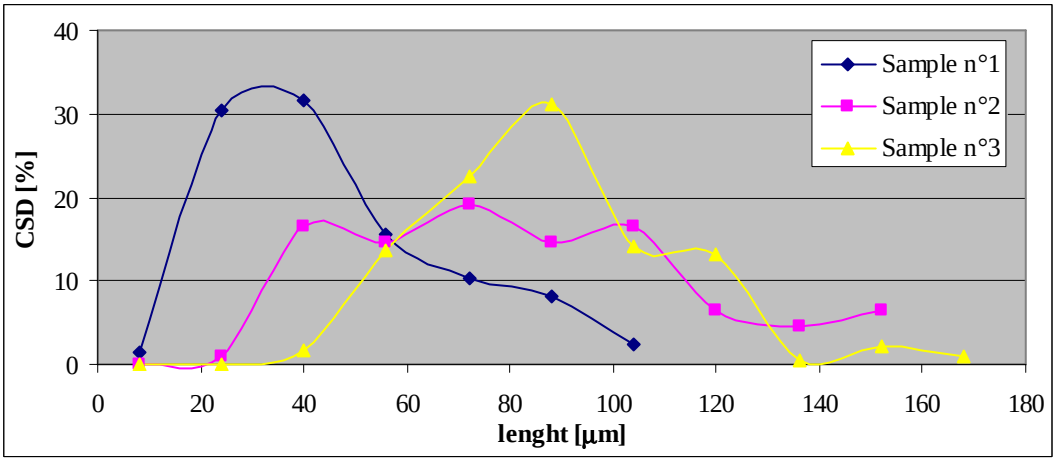

Figure 23: CSD obtained for the lab test with $MgSO_4*7H_2O$ aqueous solution and retentate flow rate equal to 150 L/h.

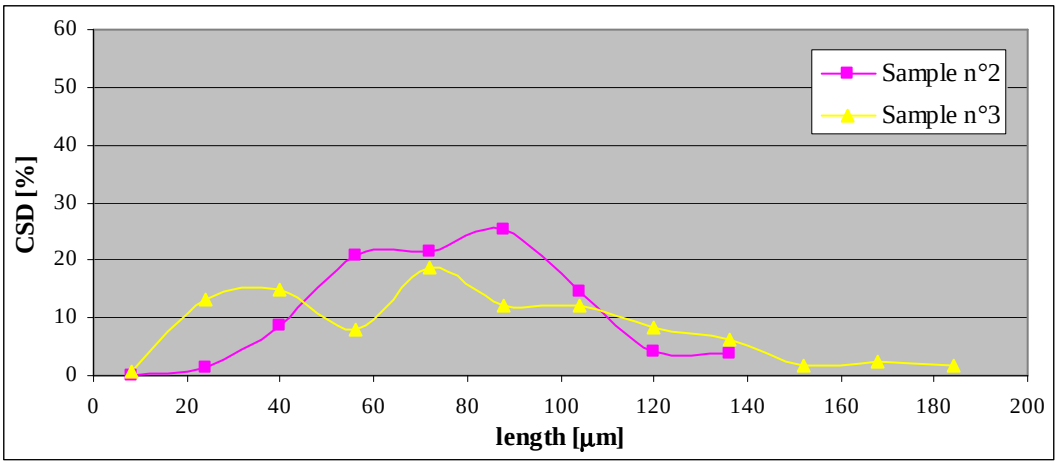

Figure 24: CSD obtained for the lab test with $MgSO_4*7H_2O$ aqueous solution and retentate flow rate equal to 170 L/h.

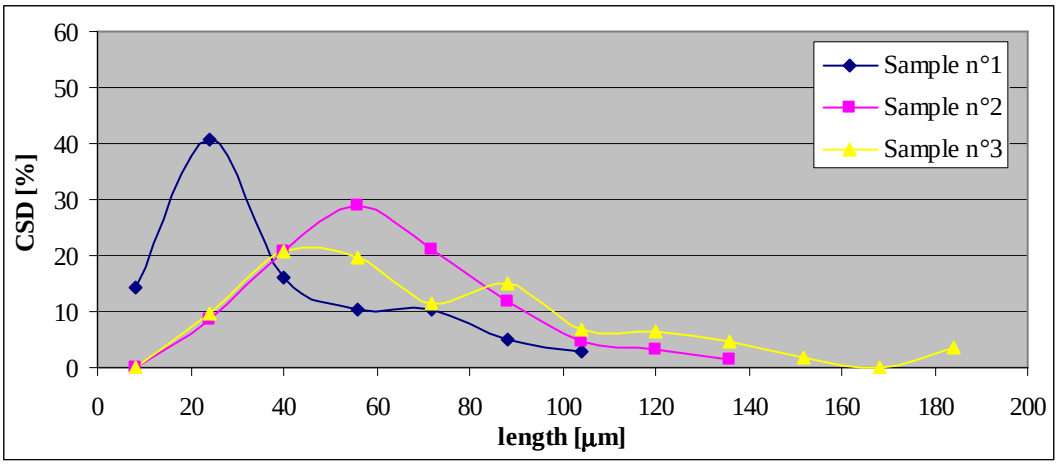

Figure 25: CSD obtained for the lab test with $MgSO_4*7H_2O$ aqueous solution and retentate flow rate equal to 200 L/h.

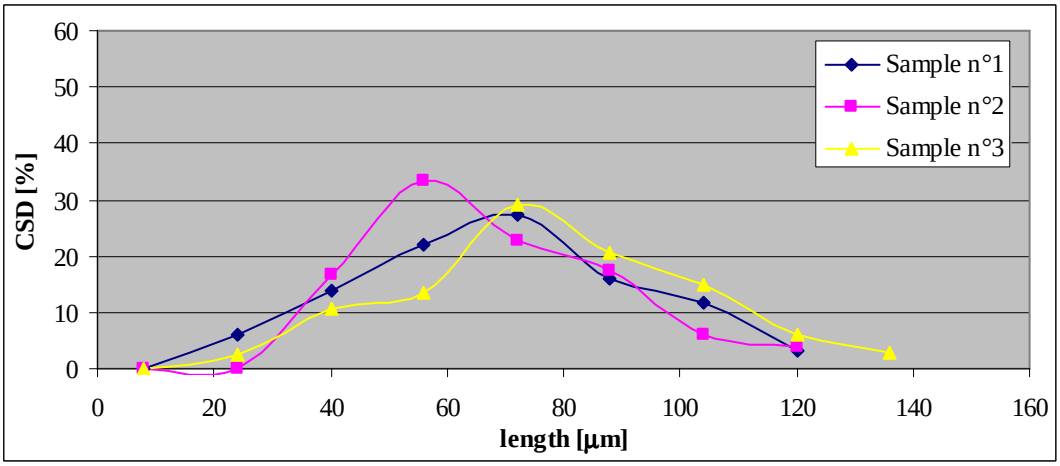

Figure 26: CSD obtained for the lab test with $MgSO_4*7H_2O$ aqueous solution and retentate flow rate equal to 250 L/h.

Table 5: Density of the crystal slurries M.

Retentate flow rate [L/h]	M [kg/m^3]
100	76.03
120	72.87
150	30.66
200	132.2

The obtained epsomite crystallizes in the orthorhombic system (in accordance with the expected geometry of $MgSO_4 \cdot 7H_2O$ crystals). Figures 27-29 show the epsomite crystals produced in three different times: the crystals growth is evident.

Figure 27: Crystalline habit of $MgSO_4 \cdot 7H_2O$ at retentate flow rate equal to 200L/h and time equal to 143 min (picture from optical microscope, magnification: X10).

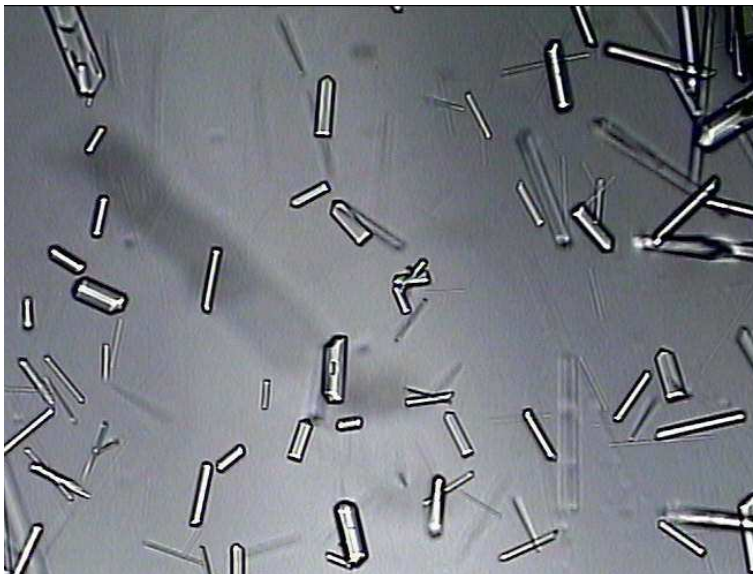

Figure 28: Crystalline habit of $MgSO_4 \cdot 7H_2O$ at retentate flow rate equal to 200L/h and time equal to 173 min (picture from optical microscope, magnification: X10).

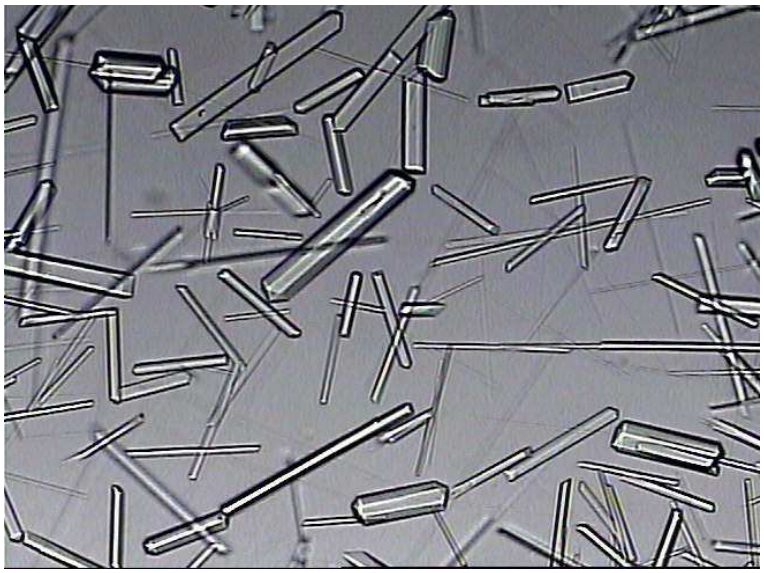

Figure 29: Crystalline habit of $MgSO_4 \cdot 7H_2O$ at retentate flow rate equal to 200L/h and time equal to 203 min (picture from optical microscope, magnification: X10).

The coefficients of variation and middle diameters (d_m) achieved in the carried out crystallization tests are reported in Table 6.

Table 6: Evolution in function of time for the Coefficient of Variation (CV) and middle diameter (d_m). Parameters determined from the experimentally obtained CSDs at five different MCr feed flow rates.

Sample N° (time)	100 L/h		150 L/h		170 L/h		200 L/h		250 L/h	
	d_m [µm]	CV [%]	d_m [µm]	CV [%]	d_m [µm]	CV [%]	d_m [µm]	CV [%]	d_m [µm]	CV [%]
1 (0.5h)	35.07	49.19	45.95	57.50	51.46	**30.39**	38.18	40.18	69.25	**34.64**
2 (1.0h)	45.06	**33.60**	82.30	44.23	79.05	**32.47**	62.64	42.81	67.24	**33.73**
3 (1.5h)	54.56	47.83	88.52	**27.46**	79.26	**36.00**	73.55	48.73	78.30	**33.99**

The obtained low CVs are characteristic of a narrow crystal size distribution and, therefore, of a qualitatively better product. As described in *Chapter 1*, this can be attributed to the fact that a membrane crystallizer, with respect to conventional crystallizers, is characterized by an axial flux, in laminar regime, of the crystallizing solution through the membrane fibres. This is expected to reduce mechanical stress, to improve the homogeneity of the crystallizing solution and to promote an oriented organization of the crystallizing molecules. As a consequence, crystals exhibiting good structural properties, narrow size distribution and low CVs are generally produced in membrane crystallization devices.

5. Crystallization kinetics: Nucleation and Growth

There are obviously two steps involved in the preparation of crystal matter from a solution. The crystals must first form and then grow. The formation of a new solid phase either on an inert particle in the solution or in the solution itself is called **nucleation.** The increase in size of this nucleus with a layer-by-layer addition of solute is called **growth.** Both nucleation and crystal growth have supersaturation as a common driving force.

The mechanism of crystal nucleation from solution has been studied by many scientists, and recent work suggests that—in commercial crystallization equipment, at least—the nucleation rate is the sum of contributions by (1) homogeneous nucleation and (2) nucleation due to contact between crystals and (*a*) other crystals, (*b*) the walls of the container, and (*c*) the pump impeller. If B^0 is the net number of new crystals formed in a unit volume of solution per unit of time,

$$B^0 = B_{ss} + B_e + B_c \qquad (3)$$

where B_e is the rate of nucleation due to crystal-impeller contacts, B_c is that due to crystal-crystal contacts, and B_{ss} is the homogeneous nucleation rate due to the supersaturation driving force. The mechanism of the last-named is not precisely known, although it is obvious that molecules forming a nucleus not only have to coagulate, resisting the tendency to redissolve, but also must become oriented into a fixed lattice. The number of molecules required to form a stable crystal nucleus has been variously estimated at from 80 to 100 (with ice), and the probability that a stable nucleus will result from the simultaneous collision of that large number is extremely low unless the supersaturation level is very high or the solution is supersaturated in the absence of agitation. In commercial crystallization equipment, in which supersaturation is low and agitation is employed to keep the growing crystals suspended, the predominant mechanism is contact nucleation or, in extreme cases, attrition.

In order to treat crystallization systems both dynamically and continuously, a mathematical model has been developed which can correlate the nucleation rate to the level of supersaturation and/or the growth rate. Because the growth rate is more easily determined and because nucleation is sharply nonlinear in the regions normally encountered in industrial crystallization, it has been common to assume

$$B^0 = k^* s^i \qquad (4)$$

where s, the supersaturation, is defined as (C − Cs), C being the concentration of the solute and Cs its saturation concentration; and the exponent i and dimensional coefficient k are values characteristic of the material.

While Eq. (4) has been popular among those attempting correlations between nucleation rate and supersaturation, recently it has become commoner to use a derived relationship between nucleation rate and growth rate by assuming that

$$G = k's \qquad (5)$$

whence, in consideration of Eq. (4),

$$B^0 = k''G^i \qquad (6)$$

where the dimensional coefficient k′ is characteristic of the material and the conditions of crystallization and $k'' = k/(k')^i$. Feeling that a model in which nucleation depends only on supersaturation or growth rate is simplistically deficient, some have proposed that contact nucleation rate is also a power function of slurry density and that

$$B^0 = k_n G^i M_T{}^j \qquad (7)$$

where M_T [g/L] is the density of the crystal slurry.

Although Eqs. (6) and (7) have been adopted by many as a matter of convenience, they are oversimplifications of the very complex relationship that is suggested by Eq. (3); Eq. (7) implicitly and quite arbitrarily combines the effects of homogeneous nucleation and those due to contact nucleation. They should be used only with caution.

In work pioneered by Clontz and McCabe [7] and subsequently extended by others, contact nucleation rate was found to be proportional to the input of energy of contact, as well as being a function of contact area and supersaturation. This observation is important to the scaling up of crystallizers: at laboratory or bench scale, contact energy level is relatively low and homogeneous nucleation can contribute significantly to the total rate of nucleation; in commercial equipment, on the other hand, contact energy input is intense and contact nucleation is the predominant mechanism. Scale-up modelling of a crystallizer, therefore, must include its mechanical characteristics as well as the physicochemical driving force.

It is therefore clear that no analysis of a crystallizing system can be truly meaningful unless the simultaneous effects of nucleation rate, growth rate, heat balance, and material balance are considered. The most comprehensive treatment of this subject is by Randolph and Larson [8], who developed a mathematical model for continuous crystallizers of the mixed-suspension or circulating-magma type [9] and subsequently examined variations of this model that include most of the aberrations found in commercial equipment. Randolph and Larson showed that when the total number of crystals in a given volume of suspension from a crystallizer is plotted as a function of the characteristic length, the slope of the line is usefully identified as the crystal population density, *n:*

$$n = \lim_{\Delta L \to 0} \frac{\Delta N}{\Delta L} = \frac{dn}{dL} \qquad (8)$$

where N = total number of crystals up to size L per unit volume of magma. The population density thus defined is useful because it characterizes the nucleation-growth performance of a particular crystallization process or crystallizer.

The data for a plot (ln n) vs (crystal size L) are easily obtained from a screen analysis of the total crystal content of a known volume (e.g., a liter) of magma.

In industrial practice, a mean value of the population density for any fraction of interest is determined directly as $\Delta N/\Delta L$, ΔN being the number of particles retained on a sieve and ΔL being the difference between the mesh sizes of the retaining sieve and its immediate predecessor. It is common to employ the units of $(mm*L)^{-1}$ for *n.*

For a steady-state crystallizer receiving solids-free feed and containing a well-mixed suspension of crystals experiencing negligible breakage, a material-balance statement degenerates to a particle balance (the Randolph-Larson general-population balance); in turn, it simplifies to:

$$\frac{dn}{dL} + \frac{n}{G\,t} = 0 \qquad (9)$$

if the delta *L* law applies (i.e., *G* is independent of *L*) and the retention time is assumed to be invariant and calculated as $t = V/Q$. Integrated between the limits n^0, the population density of nuclei (for which *L* is assumed to be zero), and *n*, that of any chosen crystal size *L*, Eq. (9) becomes:

$$\int_{n^\circ}^{n} \frac{dn}{n} = -\int_{0}^{L} \frac{dL}{G\,t} \quad \Rightarrow \quad \ln n = \frac{-L}{Gt} + \ln n^0 \quad \text{or} \quad n = n^\circ e^{-L/G\,t} \qquad (10)$$

A plot of ln *n* versus *L* is a straight line whose intercept is ln n^0 and whose slope is −1/Gt. Thus, from a given product sample of known slurry density and retention time it is possible to obtain the nucleation rate and growth rate for the conditions tested if the sample satisfies the assumptions of the derivation and yields a straight line.

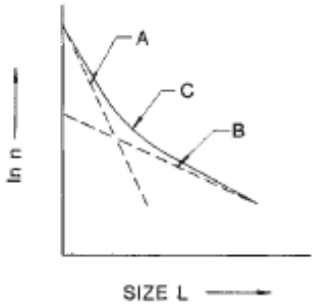

Figure 30: Population density of crystals resulting from Bujacian behavior.

If a straight line does *not* result (Figure 30), at least part of the explanation may be violation of the delta *L* law. The best current theory about what causes size dependent growth suggests what has been called growth dispersion or "Bujacian behavior" [10]: in the same environment different crystals of the same size can grow at different rates owing to differences in dislocations or other surface effects. The graphs of "slow" growers (Figure 30, curve *A*) and "fast" growers (curve *B*) sum to a resultant line (curve *C*), concave upward.

In Table 7, a number of derived relations which describe the nucleation rate, size distribution, and average properties are summarized.

Table 7: Common Equations for Population-Balance Calculations.

Name	Symbol	Units	Equation	References
Retention time	t	h	$t = V/Q$	
Growth rate	G	mm/h	$G = dL/dt$	
Population density	n	No. (crystals)/mm	$n = dN/dL = n^o e^{-L/Gt}$	9
Nuclei population density	n^o	No. (crystals)/mm	$n^o = K_M M^j G^{i-1}$	11
Nucleation rate	B_0	No. (crystals)/h	$B_0 = Gn^o = K_M M^j G^i$	12
Mass/unit volume (slurry density)	M_T	g/L	$M_t = K_v \rho 6\, n^o (Gt)^4$	9
Total number of crystals	N_T	No./L	$N_T = \int_0^\infty n\, dl$	9

5.1 Sodium Chloride Aqueous Solutions: Growth and Nucleation Rate

The procedure described in the previous paragraph has been applied to the carried out crystallization runs in order to estimate the crystals growth rate G and the nucleation rate B_0. The analysis has been made with data relative to the crystals dimensions distributions at different times. The procedure requires laborious calculations because of the number of samples needed.
In Figure 31 is shown the plot of ln n versus the length L for one of the carried out test with NaCl aqueous solution, at the conditions indicated in Table 8.

Table 8: Operative conditions for the crystals sample whose population-density plot is shown in Figure 31.

Retentate flow rate [L/h]	150
Permeate flow rate [L/h]	100
Temperature at the retentate entrance [°C]	35±1
Temperature at the permeate entrance [°C]	16±2
Time of withdrawal of the sample [min]	270

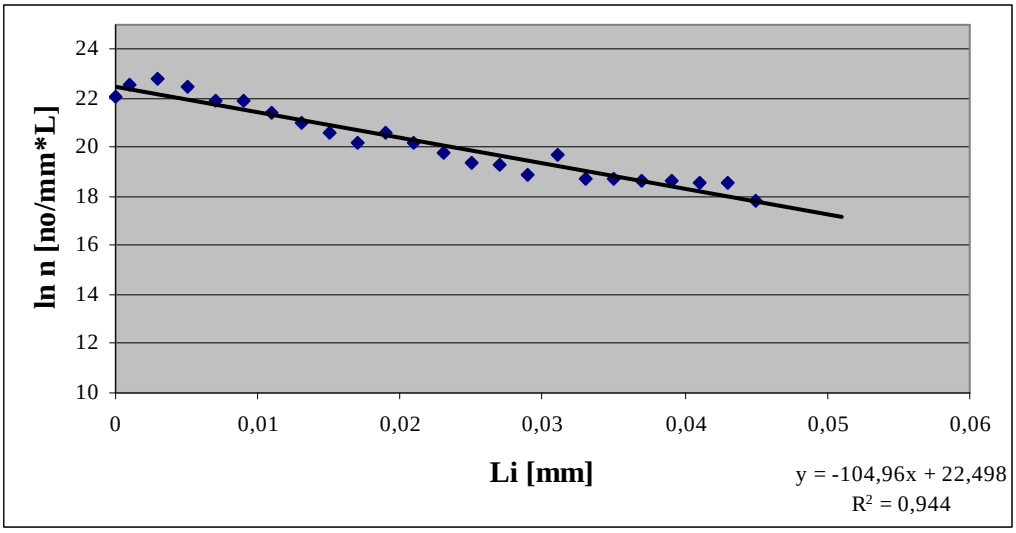

Figure 31: Population-density plot for NaCl crystals produced in the conditions indicated in Table 8.

The linear regression, with a correlation coefficient of 0.944, gives for the growth rate G a value of 0.03529 μm/min and for ln n^0 a value of 22.498. As a consequence, the nucleation rate B_0 will be:

$$B_0=G*n°=208147 \text{ no/L*min.}$$

From several other samples taken from the crystallizer during the same test, a plot of ln n^0 versus ln G can be constructed in order to calculate the quantity (i-1) of the equation $n^o = K_M M^j G^{i-1}$ or $B_0 = K_M M^j G^i$:

$$i-1=-1.0333 \quad \text{or} \quad i=2.0333.$$

A plot of ln n^0 versus ln M at corresponding G permits the determination of the power j:

$$j=-0.3511.$$

The same procedure has been applied at all the crystals samples withdrawn in each crystallization test. The results are shown in Table 9.

Table 9: Kinetic parameters for the NaCl crystallization tests at the indicated conditions.

Retentate flow rate [L/h]	G [mm/min]	B° [no/L*min]	i	j
100	0.0000572	102174	2.73	1.54
120	0.0000449	225124	1.98	0.669
150	0.0000330	297250	2.03	-0.351
170	0.0000254	273762	2.72	-2.64
250	0.0000403	262770	2.04	-2.78

For what concerns the exponent j of the density of the crystal slurry M, the relatively large scatter should be attributed to uncertainties associated with the inherent difficulty (often encountered in the crystallization literature) to measure and to estimate accurately this variable. For what concerns the value of relative kinetic order *i*, almost the same value has been obtained in the different tests. Moreover, it is in agreement with those usually reported in literature for some conventional crystallizers (about equal to 2) and reported in Table 10 [1].

Table 10: Kinetic equations for NaCl crystallized [1].

Scale of the plant	Range *t* [h]	Range M_T [g/L]	Temp. [°C]	Kinetic equation for B_0 [no./(L*s)]
Bench	0.2-1	25-200	50	$*B_0 = 1.92(10^{10})S_R^2 M_T G^2$
Pilot	0.6	35-70	55	$B_0 = 8*10^{10} N^2 G^2 M_T$

*S_R=rotation rate of the impeller [r/min].

Plotting growth rate G versus retentate flow rate it is possible to study the fluid-dynamic effect on membrane crystallization operation (Figure 32). Crystal growth rate is generally recognised as a layer-by-layer process and, since growth can occur only at the face of the crystal, material must be transported to that face from the bulk of the solution. Diffusional resistance to the movement of molecules (or ions) to the growing crystal face, as well as the resistance to integration of those molecules into the face, must be considered. In the first case, G increases with the feed flow rate due to the improvement of the transport coefficients; in the second case, G decreases when feed flow rate increases because a high flow rate disturbs the molecular organization which precedes the integration into crystal lattice.
As discussed earlier, different faces can have different rates of growth, and these can be selectively altered by the addition or elimination of impurities.

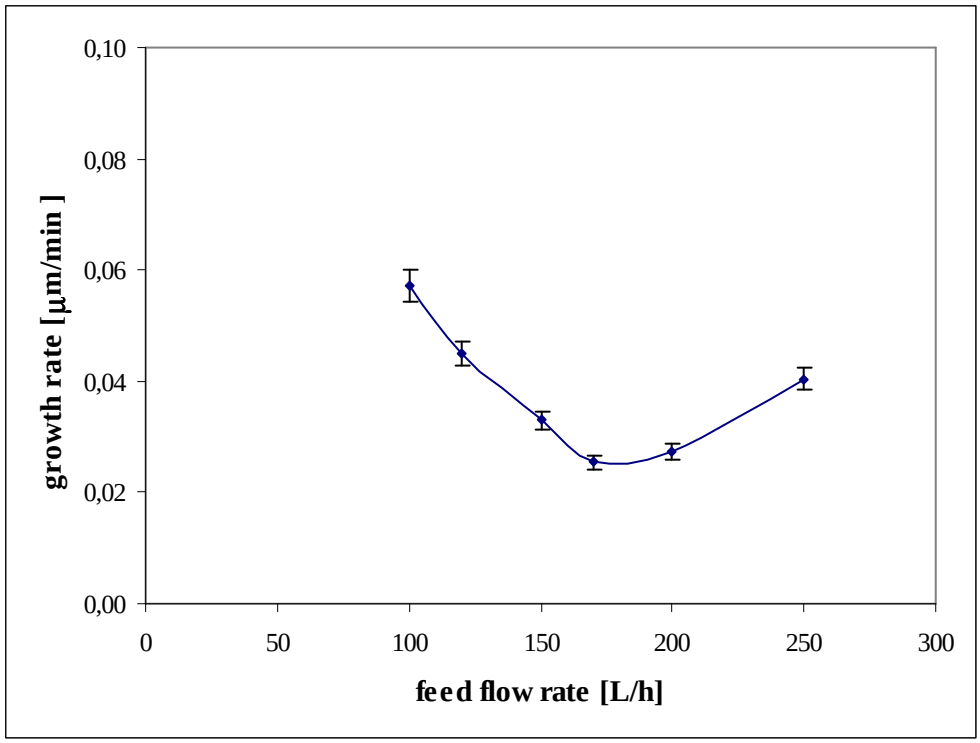

Figure 32: Growth rate vs retentate flow rate.

According to the experimental results (Figure 32), until a feed flow rate equal to about 150L/h crystal growth rate is limited by the integration of molecules into crystal lattice; then, for higher feed flow rate, the evidence of diminution of nucleation allows to justify the growth acceleration with the hypothesis that low salt concentrations in the boundary layer close to the solid/liquid interface, which is the case of a mass-diffusion control based mechanism, might promote the molecular organization which precedes the integration into crystal lattice, which in turn gives rise to an increase of crystal growth rate.

5.2 Epsomite Aqueous Solutions: Growth and Nucleation Rate

Table 11 shows some of the kinetic parameters achieved in the $MgSO_4 \cdot 7H_2O$ crystallization runs. The reached results are similar to the ones obtained with NaCl aqueous solutions.

Table 11: Kinetic parameters for the $MgSO_4 \cdot 7H_2O$ crystallization tests at the indicated conditions.

Feed flow rate [L/h]	G [mm/min]	B° [no/L*min]	i	j
100	***0.0002041***	***156359***	2.32	-0.242
150	***0.0004872***	***199410***	2.59	-0.126
170	***0.0003085***	***118426***	2.70	-0.223

For what concerns the exponents i and j, almost the same values have been obtained in the different tests. They can be checked against power law equations reported in Table 12 for conventional crystallizer configurations. The discordance is evidently due to the differences in the hydraulic characteristics of the crystallizers and due to the presence of a membrane in the MCr that improves the nucleation process.

Table 12: Kinetic equations for $MgSO_4 \cdot 7H_2O$ crystallized [1].

Scale of the plant	Range *t* [h]	Range M_T [g/L]	Temp. [°C]	Kinetic equation for B_0 [no./(L*s)]
Bench	/	/	25	$B^0 = 9.65(10^{12})M_T^{0.67}G^{1.24}$
Bench	/	Low	29	$*B^0 = f(N, L^4, N^{4.2}, S^{2.5})$

*S=supersaturation coefficient.

6. Conclusions

In this chapter membrane crystallizer has been employed to produce sodium chloride and epsomite crystals from aqueous solutions of these salts. The interest for NaCl and for $MgSO_4 \cdot 7H_2O$ crystallization is due to the fact that they are involved in sea and brackish water desalination processes.

The experimental tests have allowed to test fluid-dynamic effect on membrane crystallization operation and, in particular, on trend of solvent transmembrane flux and crystals growth rate. Crystals distribution has been characterized by the coefficient of variation (CV) and middle diameter d_m. Moreover, the distribution of crystal dimensions, nucleation and growth rate have been studied as a function of the retention time and slurry density. The kinetic parameters, investigated by using a mathematical model for continuous crystallizers of the mixed-suspension or circulating-magma type, have been joined in a power law relation describing the nucleation rate of the salts as a function of the growth rate and magma density.

The achieved results show that transmembrane flux increases with retentate flow rate. Therefore, the time for reaching supersaturation and crystals formation decreases when the feed flow rate is risen. The obtained CVs, in particular for epsomite, are lower than those from conventional equipments and are therefore characteristic of narrow crystal

size distributions and of qualitatively better products. For what concerns the achieved kinetic parameters, they are in substantial agreement with those reported in literature for conventional crystallizers. Of course, also some small discordances are present because of the differences in the hydraulic characteristics of the compared crystallizers and due to the presence, in the MCr, of a membrane that improves the nucleation process.
In conclusion, the results obtained in the carried out experimental tests confirm the interesting potentialities of the membrane crystallization strategy in redesigning traditional crystallizers.

Relevant Bibliography

[1] J. H. Perry, D. Green, *Perry's Chemical Engineers' Handbook*, McGraw-Hill international Editions, New York, 1987.

[2] J.A. Redondo, *Brackish-, sea- and wastewater desalination*, Desalination, 138 (2001) 29-40.
[3], B. S. Sparrow, *Empirical equations for the thermodynamic properties of aqueous sodium chloride*, Desalination, 159 (2003) 161-170.
[4] E. Curcio, A. Criscuoli, E. Drioli, *Membrane Crystallizers*, Ind. Eng. Chem. Res., 40 (2001) 2679-2684.
[5] E. Curcio, E. Drioli, *Membrane Distillation and Related Operation-A Review*, Separation and Purification Reviews, 34 (2005) 35-85.
[6] B. H. Mahan, R. J. Myers, *Chimica*, Casa Editrice Ambrosiana Milano, 1991.
[7] Clontz and McCabe, *Crystallization from Solution: Factors Influencing Size Distribution*, Chem. Eng. Prog. Symp. Ser., 67(110), (1971).
[8] A. D. Randolph and M. A. Larson, *Theory of Particulate Processes*, Academic Press, New York (1971).
[9] Randolph and Larson, *Am. Inst. Chem. Eng. J.*, 8, 639 (1962).
[10] Mullin (ed.), *Industrial Crystallization*, Plenum, New York, 1976.
[11] Timm and Larson, *Am. Inst. Chem. Eng. J.*, 14, 452 (1968).
[12] Larson, Timm, and Wolff, *Am. Inst. Chem. Eng. J.*, 14, 448 (1968).

CHAPTER 6: Crystallization of RO and NF retentate streams. Experimental Study

Table of Contents

1. Introduction

As described in *Chapter 1*, salty water represents 97% of the planet's available water resources so that, currently, the global installed desalination capacity is 52 million m^3/d. Moreover, marine water is also a practically unlimited reserve of chemical resources and it is the most abundant aqueous ionic solution on the earth: about 3% of its composition is represented by dissolved salts, with more than 70 elements present, but only seven of which (Cl, Na, SO_4, Mg, Ca, K, HCO_3) make up more than 99% of all the dissolved salts.

The first experimental work for an intensive exploitation of seawater was carried out by Nelson and Thompson in the Fifties and in the Sixties [1]. Their aim was to achieve the recovery both of the fresh water and of the dissolved components by freezing. In freezing, the dissolved salts are naturally excluded during ice crystals formation. Then, fresh water can be obtained when the produced ice is melted. According to their investigations, ice is the first solid phase precipitating at temperature of −1.9°C, followed by mirabilite ($Na_2SO_4 \cdot 10H_2O$) at −8.2 °C, hydrohalite ($NaCl \cdot 2H_2O$) at −22.9 °C, sylvite (KCl) and $MgCl \cdot 12H_2O$ at −36 °C, antarcticite ($CaCl_2 \cdot 6H_2O$) at −54 °C; in alternative pathways, gypsum ($CaSO_4 \cdot 2H_2O$) precipitation also occurs around −22 °C. In theory, freezing has some advantages with respect to the other desalination technologies such as: minor corrosion, precipitation and incrustation problems. Its disadvantage is correlated to the difficulty to handle ice, mechanically hard to move and process. As a result, this desalination and extraction technology never passed the experimental stage.

Completely different is the situation when evaporative and/or membrane operations are utilized for the recovery of fresh water and salts from seawater.

The aim of the work presented in this chapter is to test experimentally the performance of the membrane crystallizer for potable water production and crystals recovery from NF and RO retentate streams of an integrated membrane desalination process constituted by MF/NF/RO (the systems indicated as FS4 and FS5 in the previous chapters).

The experimental tests have allowed:

- ✓ to compare experimental results with theoretical ones, in terms of recovery factor of the system, type and amount of produced crystals,
- ✓ to check the crystallization conditions in which there are no crystals deposition inside the membrane module and on the membrane surface,
- ✓ to test temperature and fluid-dynamic effect on membrane crystallization operation,
- ✓ to verify that the "*crystals recovery system*" is able to remove the produced salts and, in particular, to avoid their deposition inside the membrane module and in the retentate line.

In a few words, the goal is to show that MCr allows to reduce the volume of concentrates discharged from the desalination plants by increasing plant recovery factor, reducing the environmental impact of discharged brines on the marine habitat and recovering the dissolved salts.

2. Test on RO retentate stream

Table 1 reports the *RO retentate* composition of the membrane based desalination system constituted by MF/NF/RO (stream N°12 of FS3 – *Chapter 2*). The possible salts that can be formed from its crystallization are sodium sulphate, magnesium sulphate and sodium chloride.

Table 1: RO retentate.

Ion	[mole/L]
Cl^-	1.52
Na^+	1.17
SO_4^{2-}	0.00910
Mg^{2+}	0.0189
Ca^{2+}	0.00390
HCO_3^-	0.00290

For what concerns $CaSO_4$, in order to avoid its precipitation (which can cause scaling and limits the recovery of magnesium sulphate), Ca^{2+} ions have been precipitated as $CaCO_3$ through reactive precipitation with anhydrous sodium carbonate. According to previous experimental results [2], Na_2CO_3 was added in appropriate parts (1:1 molar of Ca^{2+}/CO_3^{2-} ratio) in order to promote 95% precipitation of Ca^{2+} ions. After this precipitation step, the stream to be crystallized is characterized by the composition reported in Table 2.

Table 2: RO retentate composition after the precipitation of Ca^{2+} ions.

Ion	[mole/L]
Cl^-	1.52
Na^+	1.18
SO_4^{2-}	0.00906
Mg^{2+}	0.0189
Ca^{2+}	0.000194
HCO_3^-	0.00289
CO_3^{2-}	0.000194

For what concerns magnesium sulphate, SO_4^{2-} and Mg^{2+} concentrations are too low to promote the formation of the corresponding salt. As a consequence, the only salt that can be formed from the crystallization of the stream with the composition reported in Table 2 is sodium chloride, compound characterized by a positive enthalpy change of solution. Therefore, as stated in *Chapter 2*, a heating of the MCr feed guarantees that the temperature of the solution flowing along the membrane is high enough to be always under saturation condition, thus avoiding crystals deposition inside the membrane module. According to the procedure described in *Chapter 2*, a temperature equal to 35±1 °C has been chosen for the MCr feed.

A preliminary set of experimental tests has been carried out, at the operative conditions indicated in Table 3, in order to check the nature of the obtained salts and to confirm that the chosen MCr feed temperature is sufficient to avoid the crystals accumulation on the membrane surface and inside the membrane module.

Table 3: Operative conditions for the preliminary set of experimental tests.

Feed flow rate [L/h]	100-250
Permeate flow rate [L/h]	100
Temperature at the retentate entrance [°C]	35±1
Temperature at the permeate entrance [°C]	16±2

In Figure 1 is reported the trend of magnesium sulphate concentration vs time at different feed flow rates.

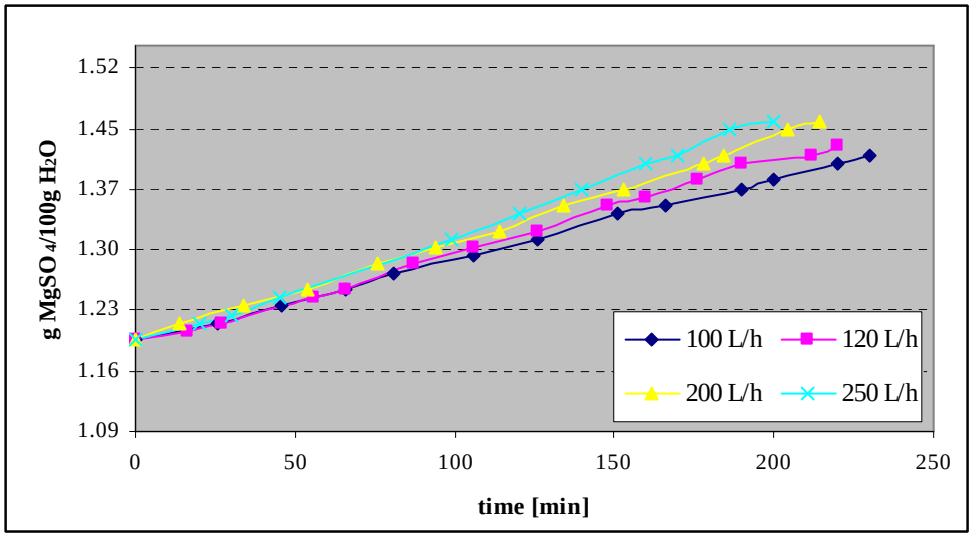

Figure 1: Magnesium sulphate concentration vs time at different feed flow rates for the lab tests of aqueous solution of NaCl.

The crystallization tank work at 25°C and atmospheric pressure. At this temperature, the solubility of magnesium sulphate in water is 25.6g/100g H_2O [3], much higher of $MgSO_4$ concentration in the carried out tests. As foreseen, only NaCl can be produced from the RO retentate crystallization.
The following step has been to check that heating the MCr feed until 35±1°C ensures that the solution, flowing along the membrane module, is under saturation condition. For reaching this aim, the procedure described in *Chapter 2 - Section 4.1* has been used.
During the carried out tests, the temperatures observed at the module entrance for retentate and permeate side were constant and equal to 35±1°C and 16±2°C respectively. At these temperatures, the physical properties of the streams together with the structural parameters of the membrane module (see *Table 1 – Chapter 4*) allow to estimate the transport coefficients:

- ✓ from K_g = 0.0203 W/m·K and K_s = 0.22 W/m·K, $h_m = \frac{K_g \cdot \varepsilon + K_m(1-\varepsilon)}{\delta}$ =668.4 W/m^2·K;
- ✓ the boundary layer heat transfer coefficients h_f and h_p have been estimated from the following empirical correlations for laminar liquid flow:

$$Nu = 1.86 \cdot \left(Re \cdot Pr \cdot \frac{d_h}{l} \right)^{0,33} \cdot \left(\frac{\mu}{\mu_w} \right)^{0.14} .$$

From μ_{H2O} = 1.16 cp, K_{H2O} = 0.609 W/m·K, c_p = 4.184 kJ/kg·K and permeate flow rate constant and equal to 100L/hr, h_p=429.6 W/m^2·K;

- ✓ from μ_{sale} = 3.288 cp, K_{sale} = 7.1 W/m·K, $c_{p,sale}$ = 0.837 kJ/kg·K, μ_{H2O} = 0.79 cp, K_{H2O} = 0.628 W/m·K, $c_{p,H2O}$ = 4.184 kJ/kg·K, h_f changes with retentate flow rate:
  h_f = 402.7 W/m^2·K for the test in which G=retentate flow rate= 100 L/h
  h_f = 427.6 W/m^2·K for G = 120 L/h
  h_f = 506.1 W/m^2·K for G = 200 Ll/h
  h_f = 544.8 W/m^2·K for G = 250 L/h.
- ✓ $h_v = \frac{N \cdot \Delta H_V}{T_{fm} - T_{pm}}$ (1)

where ΔH_V = heat of vaporization =9729 cal/mol. With knowledge of experimentally measured molar flux N, h_v and the difference (T_{fm} - T_{pm}) can be estimated by iteration using also the following equations (2) and (3):

$$T_{mf} = T_f - (T_f - T_p) \left[\frac{1/h_f}{\frac{1}{h_m + h_v} + \frac{1}{h_f} + \frac{1}{h_p}} \right] \quad (2)$$

$$T_{mp} = T_p + (T_f - T_p) \left[\frac{1/h_p}{\frac{1}{h_m + h_v} + \frac{1}{h_f} + \frac{1}{h_p}} \right] \quad (3)$$

- ✓ When T_{fm} and T_{pm} are known, the total heat Q transferred across the membrane can be estimated:

$$Q = U \cdot \Delta T \quad (4)$$

where U represents the overall heat transfer coefficient of the process.
As stated in *Chapter 2*, the following amount of heat Q' has to be supplied to the MCr feed before going in the membrane module:

$$Q' = G \cdot c_p \cdot (T_{in} - T_{crist}) = \sum_{i=1}^{n} m_i \cdot \Delta H_{sol,i} + U \cdot A \cdot \Delta T \quad (5)$$

where the variables have been already defined in *Section 4.1 – Chapter 2*.
The temperature of the membrane crystallizer feed (T_{in}) is obtained from the equation (5).

Figure 2 shows the trend of the obtained T_{in} at different retentate flow rate in the case in which the produced crystals are not removed from the lab plant through the "crystals

recovery system": as foreseen, if the crystals are not removed from the crystallization tank, the temperature of the MCr feed has to be increased with time due to the increase of the term $\sum_{i=1}^{n} m_i \cdot \Delta H_{sol,i}$. Moreover, when the flow rate increases, the transport coefficients rise, polarization effects decrease and lower T_{in} can be expected (at constant temperature at the permeate side). However, also if the crystals remain in the crystallization plant for a time interval equal to 60 minutes (time essential to study the crystals growth rate), T_{in} ranges from 28°C to 30°C, lower than the really utilized value (35±1°C).

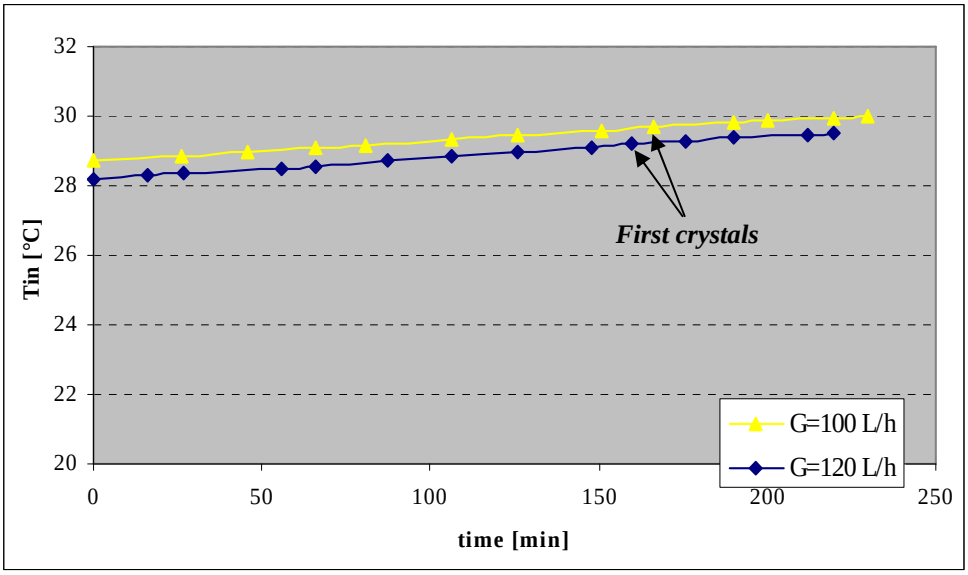

Figure 2: Temperature of the membrane crystallizer feed (T_{in}) versus time at different retentate flow rate.

Moreover, the conductivity measurements carried out on samples of solution taken out from the permeate tank demonstrated that the salts infiltration through the membrane pores was negligible; therefore, poly-propylene membranes preserved the crucial requisite of hydrophobicity thus ensuring the purity of the produced distillate stream.

2.1 Concentration tests: trans-membrane flux measurements

After the preliminary study, different tests have been carried out in order to test the performance of the membrane crystallizer for the concentration and the crystallization of RO retentate.

The experimental tests have been carried out at the same operative conditions of the crystallization experiments with aqueous solution of only one salt (see *Chapter 5*) in order to compare the achieved results.

Figure 3 shows the trend of sodium chloride concentration vs time at different retentate flow rates.

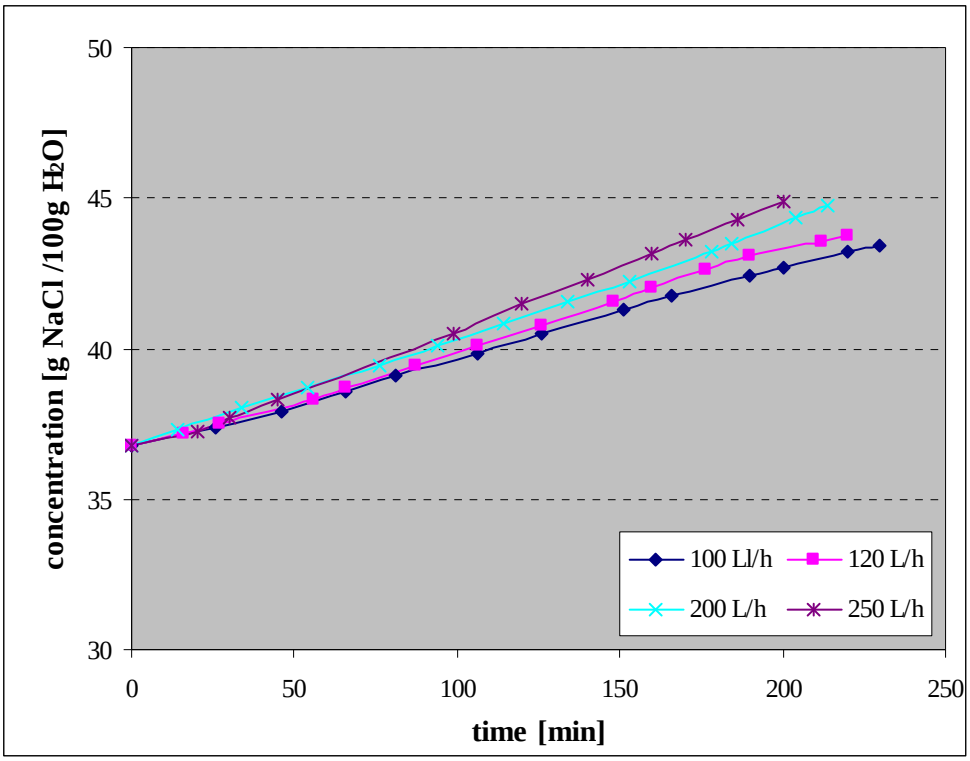

Figure 3: Concentration vs time at different retentate flow rates.

From an initial value of approximately 36.8 g NaCl / 100 g H_2O, an increase of the solution salinity with time due to solvent recovery is observed. The concentration increase is quite linearly, with increasing slope with feed flow rate (Table 4).

Table 4: Slope at the different MCr feed flow rate.

Feed flow rate [L/h]	Slope (g NaCl / 100 g H_2O)/ min
100	0.0301
120	0.0332
200	0.0369
250	0.0415

The achieved results are similar to the ones obtained by the crystallization of aqueous solution of only one salt (*Chapter 5)*: trans-membrane flux increases with flow rate (due to the highest transport coefficients – Figure 4) while it decreases very slowly with concentration (because the temperature of feed and the thermal difference between the two streams are high enough to contain the decrease in driving force due to concentration rise - Figure 5).
For what concerns the trend of the trans-membrane flux with time (Figure 4), it is approximately constant: this is the confirmation that no crystals deposition occurs inside the membrane module.

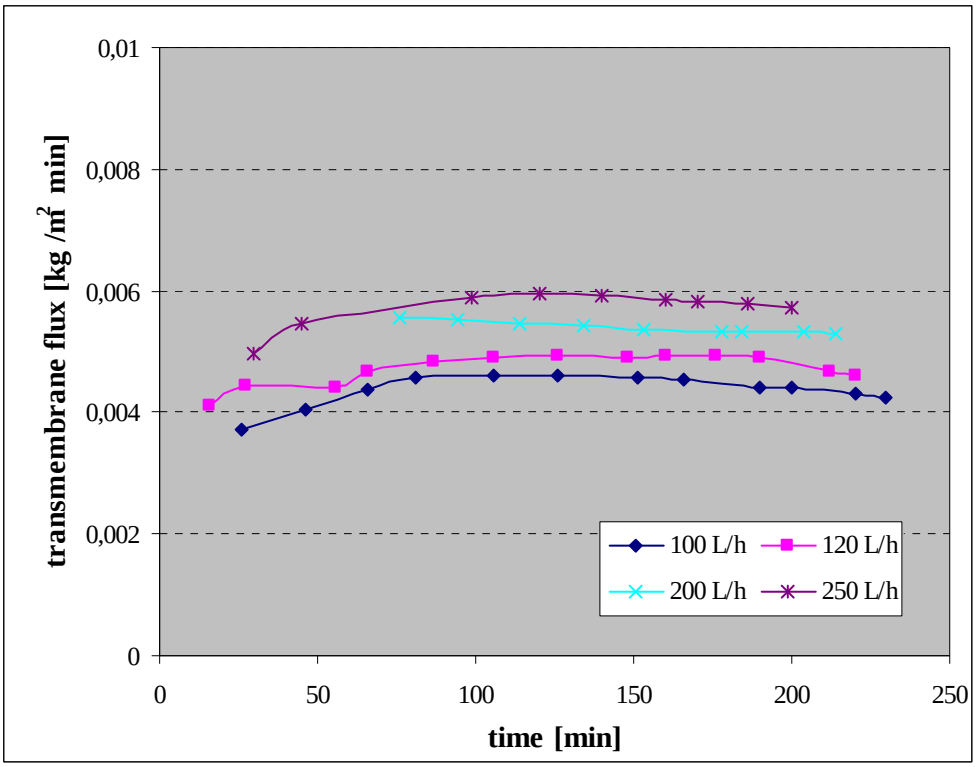

Figure 4: Trans-membrane flux vs time at different retentate flow rates.

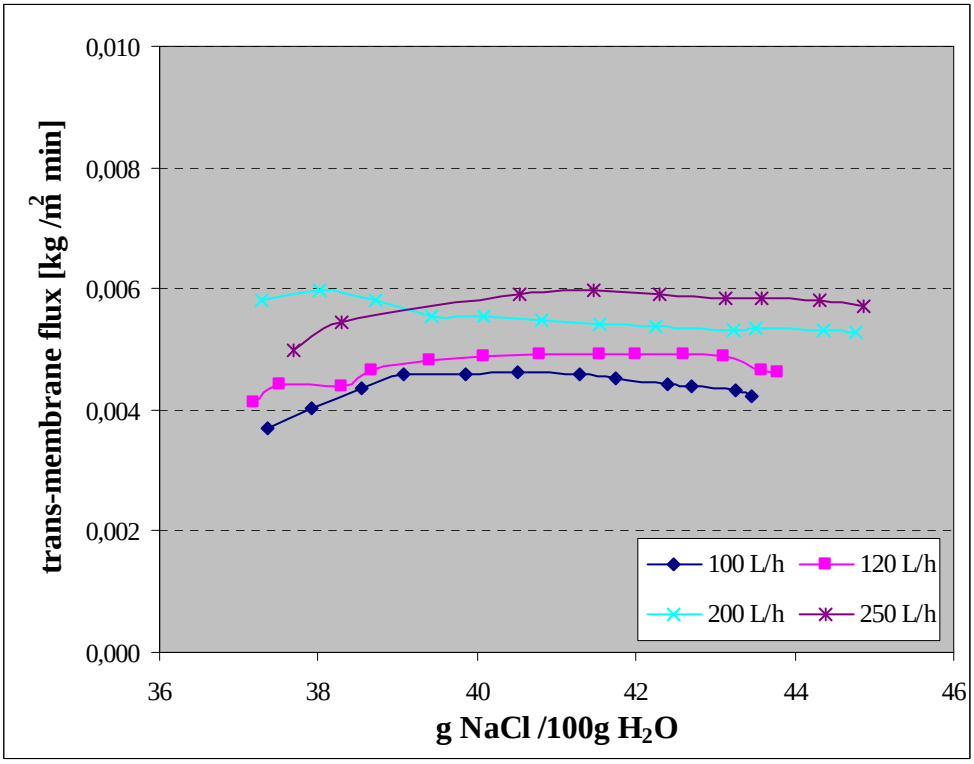

Figure 5: Trans-membrane flux vs concentration at different retentate flow rates.

Moreover, the trans-membrane fluxes obtained are about 62-79% lower than those achieved during the concentration tests of aqueous solution of a single salt (NaCl).

2.2 Crystallization tests: product characterization

Figures 6 - 9 show the crystal size distributions (CSD) for the carried out tests at different MCr feed flow rates. Knowledge of the evolution of particle size distribution as function of time allows to evaluate middle diameter, coefficient of variation (CV) and growth rate of the produced crystals, and to test the fluid-dynamic effect on membrane crystallization operation.

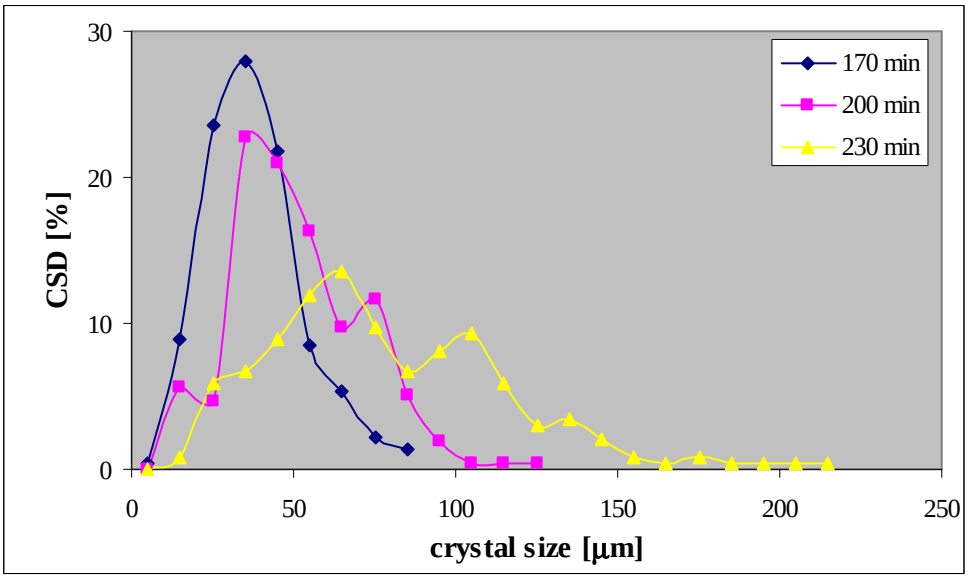

Figure 6: CDS for retentate flow rate equal to 100 L/h.

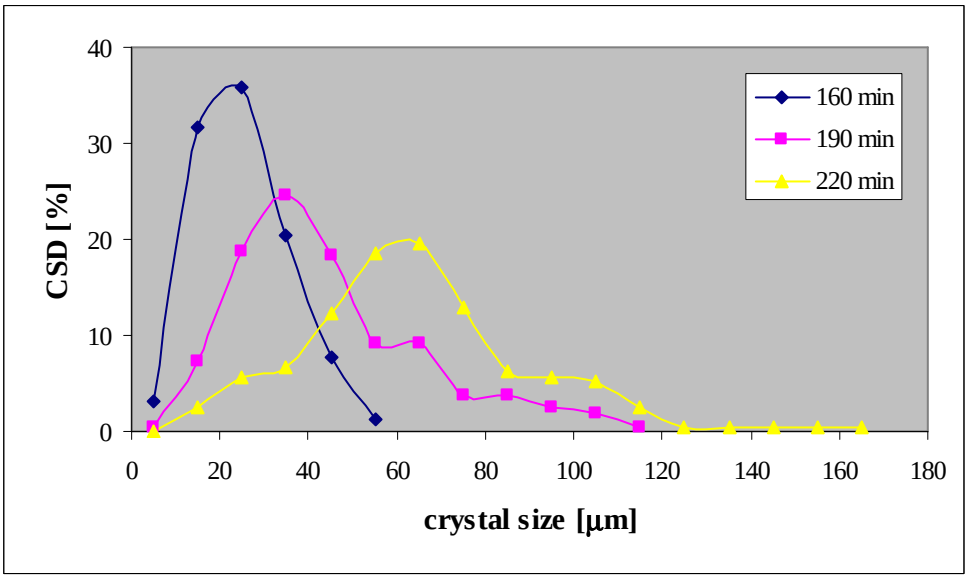

Figure 7: CDS for retentate flow rate equal to 120 L/h.

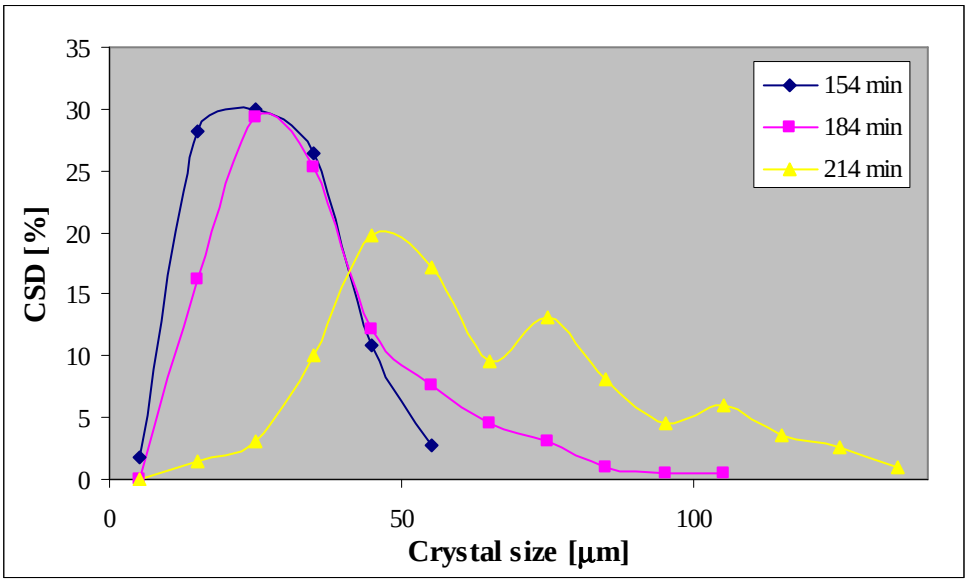

Figure 8: CDS for retentate flow rate equal to 200 L/h.

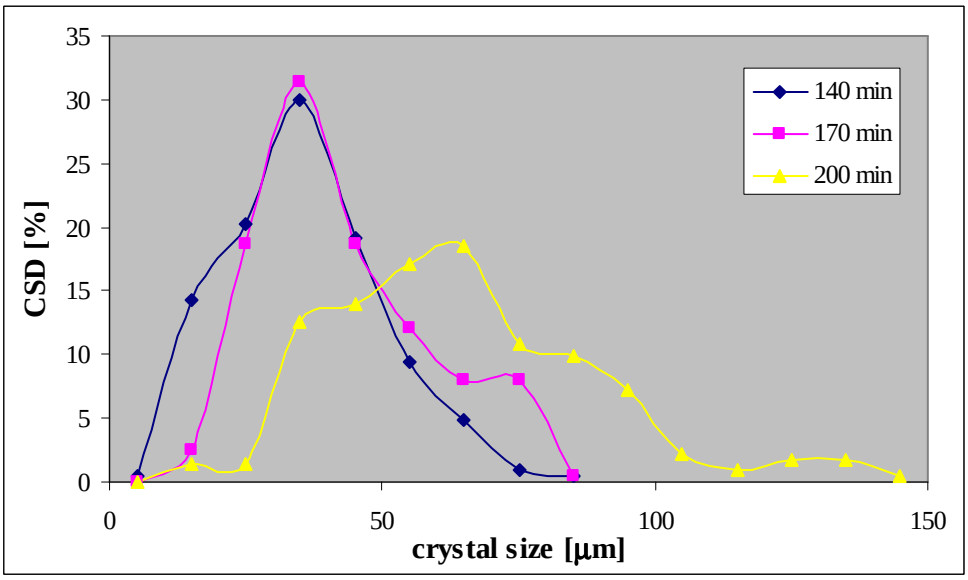

Figure 9: CDS for retentate flow rate equal to 250 L/h.

The evolution of CDS shows that the initial peak of the distributions moves towards the larger dimensions as a consequence of the crystals growth. Moreover, the influence of feed flow rate appears evident in the time for reaching supersaturation and crystals formation: it decreases when retentate flow rate increases due to the increase of trans-membrane flux, going down from 170 min when the feed flow rate is equal to 100 L/h, to 140 min when the feed flow rate is equal to 250 L/h.

The dispersion of the distributions around the mean crystal size has been characterized with the coefficient of variation CV. Table 5 reports the coefficients of variation (CV)

and the middle diameters (d_m) as obtained in the carried out RO retentate crystallization tests. Table 6 shows the experimentally determined density of the crystal slurries.

Table 5: Evolution in function of time for the Coefficient of Variation (CV) and middle diameter (d_m), parameters determined from the experimentally obtained CSDs at five different MCr feed flow rate.

100 L/h			120 L/h			150 L/h			200 L/h			250 L/h		
time [min]	d_m [µm]	CV [%]	time [min]	d_m [µm]	CV [%]	time [min]	d_m [µm]	CV [%]	time [min]	d_m [µm]	CV [%]	time [min]	d_m [µm]	CV [%]
170	37.8	45.97	160	25.5	58.4	151	28.7	66.7	154	27.7	55.2	140	36.0	49.2
200	51.1	45.98	190	44.7	57.1	182	44.0	50.7	184	35.3	58.3	170	42.8	50.0
230	78.9	52.6	220	64.7	42.6	211	56.3	36.8	214	65.1	49.1	200	64.8	42.3

Table 6: Density of the crystal slurries M.

Feed flow rate [L/h]	M [kg/m^3]
100	3.93
120	10.81
150	15.7
200	17.5
250	18.2

Table 7 reports the experimentally achieved recovery factor of the MCr lab plant and the recovery factor of the MCr in the analysed FS5 (the desalination system constituted by MF/NF/RO and MCr on RO brine), the latter obtained through the computer simulation when FS5 and the lab plant produce the same amount of salts. The comparison of the calculated with the experimentally determined MCr recovery factor shows a good agreement, with error less than 2%.

Table 7: MCr recovery factors.

Feed flow rate [L/h]	Experimentally determined MCr recovery factor [%]	MCr recovery factor in FS5 from the computer simulation [%]	Error [%]
100	78.47	81.19	1.70
120	78.61	81.60	1.87
150	79.41	81.85	1.51
200	79.00	81.97	1.84
250	79.04	82.01	1.84

The obtained NaCl crystals, examined visually with an optic microscope, showed the characteristic cubic block-like form in accordance with the expected geometry of the NaCl crystals. Their cubic shape has been also confirmed by the length/width ratio distributions (reported in the histograms of Figures 10-13).

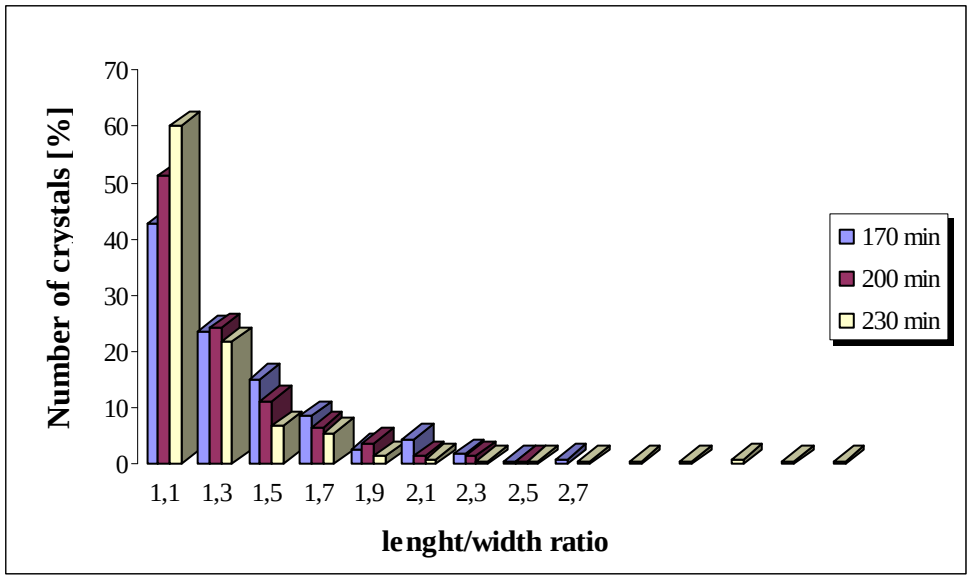

Figure 10: Number of crystals [%] vs length/width ratio at a retentate flow rate equal to 100 L/h.

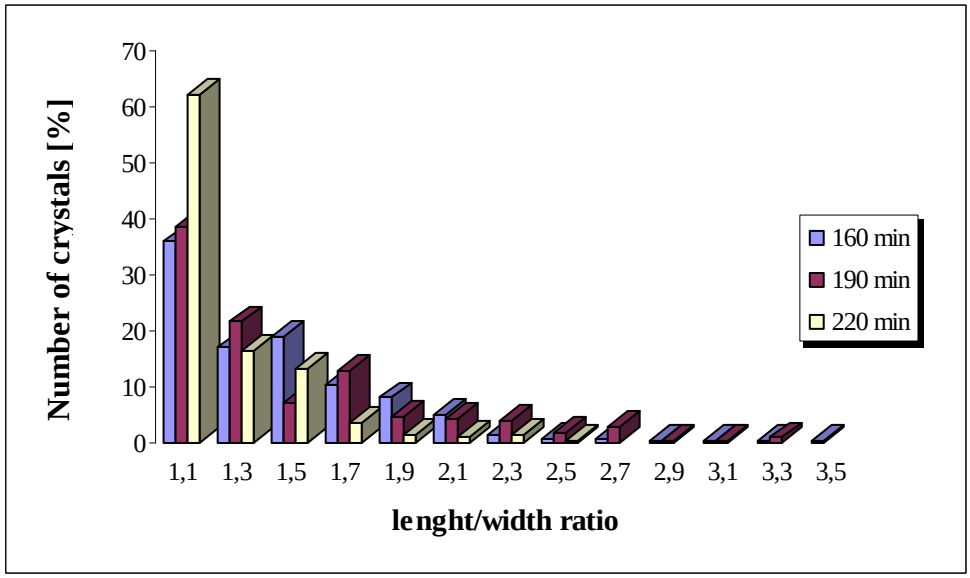

Figure 11: Number of crystals [%] vs length/width ratio at a retentate flow rate equal to 120 L/h.

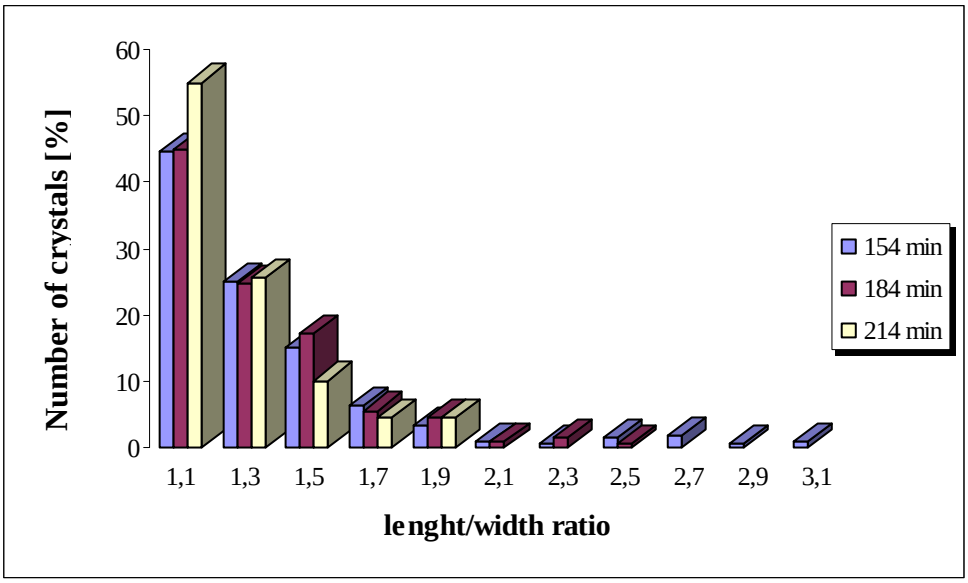

Figure 12: Number of crystals [%] vs length/width ratio at a retentate flow rate equal to 200 L/h.

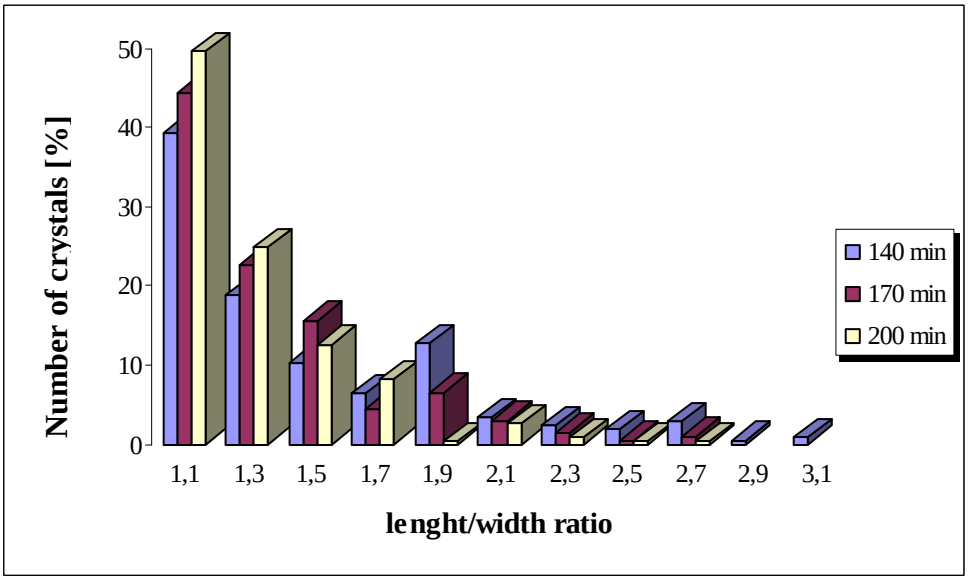

Figure 13: Number of crystals [%] vs length/width ratio at a retentate flow rate equal to 250 L/h.

The percentage of crystals exhibiting an elongated shape (in particular when feed flow rate decreases) is slightly higher with respect to the crystallization of solutions with only NaCl (see *Chapter 5)*. This is probable due to the presence, in the crystallization of RO brine, of the other components (such as Mg^{2+}, SO_4^{2-}, etc.) which might act as impurities. This phenomenon can be easily explained. Geometrically a crystal is a solid bounded by planes. The shape and size of such a solid are functions of the interfacial angles and of the linear dimension of the faces. As the result of the constancy of its interfacial angles, each face of a growing or dissolving crystal, as it moves away from or toward the center of the crystal, is always parallel to its original position. This concept is known as the

“principle of the parallel displacement of faces”. From the industrial point of view, the term *crystal habit* or *crystal morphology* refers to the relative sizes of the faces of a crystal. The crystal habit is determined by the internal structure and external influences on the crystal such as the growth rate, solvent used, and impurities present during the crystallization growth period. The crystal habit of commercial products is of very great importance. Long, needle like crystals tend to be easily broken during centrifugation and drying. Flat, plate like crystals are very difficult to wash during filtration or centrifugation and result in relatively low filtration rates. Complex or twinned crystals tend to be more easily broken in transport than chunky, compact crystal habits. Rounded or spherical crystals (caused generally by attrition during growth and handling) tend to give considerably less difficulty with caking than do cubical or other compact shapes.
Internal structure can be different in crystals that are chemically identical, even though they may be formed at different temperatures and have a different appearance. This is called *polymorphism* and can be determined only by X-ray diffraction. For the same internal structure, very small amounts of foreign substances will often completely change the crystal habit. For example, the selective adsorption of dyes by different faces of a crystal or the change from an alkaline to an acidic environment will often produce pronounced changes in the crystal habit. The presence of other soluble anions and cations often has a similar influence. For the same reason the presence of Mg^{2+}, SO_4^{2-}, etc. in the crystallizing solutions can have influenced the shape of the produced NaCl crystals.
In addition, there is another aspect to be considered. If a crystal is produced in a region of the phase diagram where a single-crystal composition precipitates, the crystal itself will normally be pure provided that it is grown at relatively low rates and constant conditions. With many products these purities approach a value of about 99.5 to 99.8 percent. The difference between this and a purity of 100 percent is generally the result of small pockets of mother liquor called occlusions trapped within the crystal. Although frequently large enough to be seen with an ordinary microscope, these occlusions can be submicroscopic and represent dislocations within the structure of the crystal. They can be caused by either attrition or breakage during the growth process or by slip planes within the crystal structure caused by interference between screw-type dislocations and the remainder of the crystal faces. To increase the purity of the crystal beyond the point where such occlusions are normally expected (about 0.1 to 0.5 percent by volume), it is generally necessary to reduce the impurities in the mother liquor itself to an acceptably low level so that the mother liquor contained within these occlusions will not contain sufficient impurities to cause an impure product to be formed.

Figures 14 - 16 show the NaCl crystals produced in three different times: the crystals growth is evident.

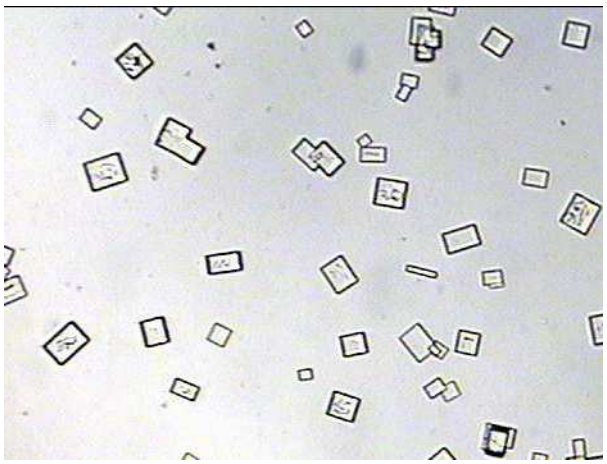

Figure 14: Crystalline habit of NaCl at retentate flow rate equal to 120L/h and time equal to 160 min (picture from optical microscope, magnification: X20).

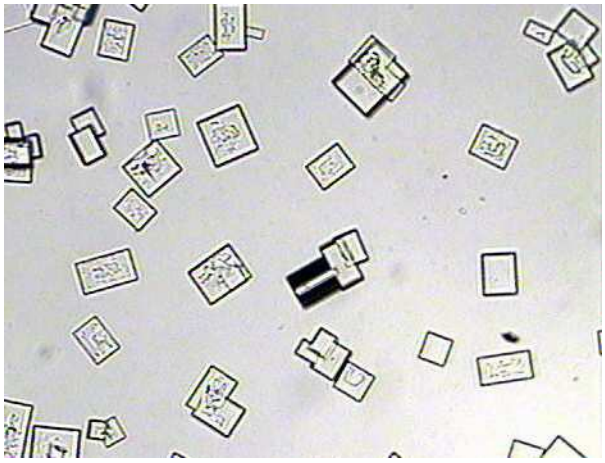

Figure 15: Crystalline habit of NaCl at retentate flow rate equal to 120L/h and time equal to 190 min (picture from optical microscope, magnification: X20).

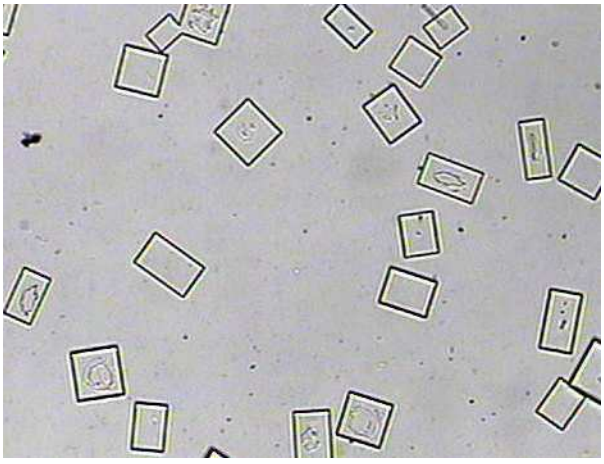

Figure 16: Crystalline habit of NaCl at retentate flow rate equal to 120L/h and time equal to 220 min (picture from optical microscope, magnification: X20).

2.3 Crystallization kinetics: nucleation and growth

The procedure described in the *Chapter 5 – Section 5* has been applied to the carried out crystallization runs in order to estimate the crystals growth rate G and the nucleation rate B_0.

In Figure 17 is shown the plot of ln n versus the length L for one of the carried out test with RO brine solution, at the conditions indicated in Table 8.

Table 8: Operative conditions for the crystals sample whose population-density plot is shown in Figure 17.

Retentate flow rate [L/h]	200
Permeate flow rate [L/h]	100
Temperature at the retentate entrance [°C]	35±1
Temperature at the permeate entrance [°C]	16±2
Time of withdrawal of the sample [min]	184

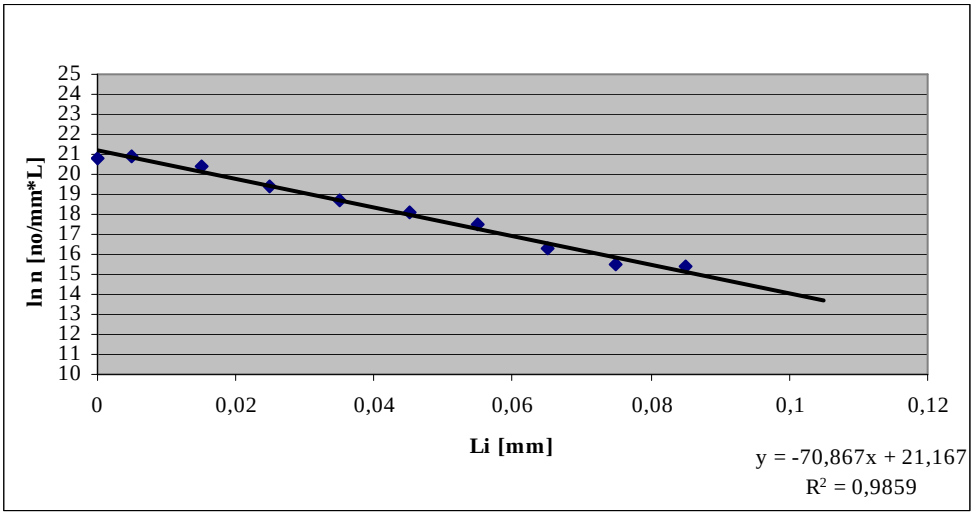

Figure 17: Population-density plot for NaCl crystals produced in the conditions indicated in Table 8.

The linear regression, with a correlation coefficient of 0.9859, gives for the growth rate G a value of 0.07669 μm/min and for ln n^0 a value of 21.167. As a consequence, the nucleation rate B_0 will be:

$$B_0 = G*n° = 119522 \text{ no/L*min.}$$

From several other samples taken from the crystallizer during the same test, a plot of ln n^0 versus ln G can be constructed in order to calculate the quantity (i-1) of the equation $n^o = K_M M^j G^{i-1}$ or $B_0 = K_M M^j G^i$

$$i-1 = -1.8698 \text{ or } i = 2.8698.$$

A plot of ln n^0 versus ln M at corresponding G permits the determination of the power j:

$$j = -1.1317.$$

The same procedure has been applied at all the crystals samples withdrawn in each crystallization test. The results are shown in Table 9.

Table 9: Kinetic parameters for the NaCl crystallization tests at the indicated conditions.

Retentate flow rate [L/h]	G [mm/min]	B° [no/L*min]	i	j
100	0.0001294	87,831	2.69	1.98
120	0.0001063	127,590	3.40	-2.92
150	0.0001017	115,511	4.54	-0.876
250	0.0001349	103,031	3.81	-0.951

For what concerns the exponent j of the density of the crystal slurry M, as in the case of the crystallization from aqueous solutions with only NaCl, the relatively large scatter should be attributed to uncertainties associated with the inherent difficulty to measure and to estimate accurately this variable.
Plotting growth rate G versus retentate flow rate it is possible to study the fluid-dynamic effect on membrane crystallization operation (Figure 18).

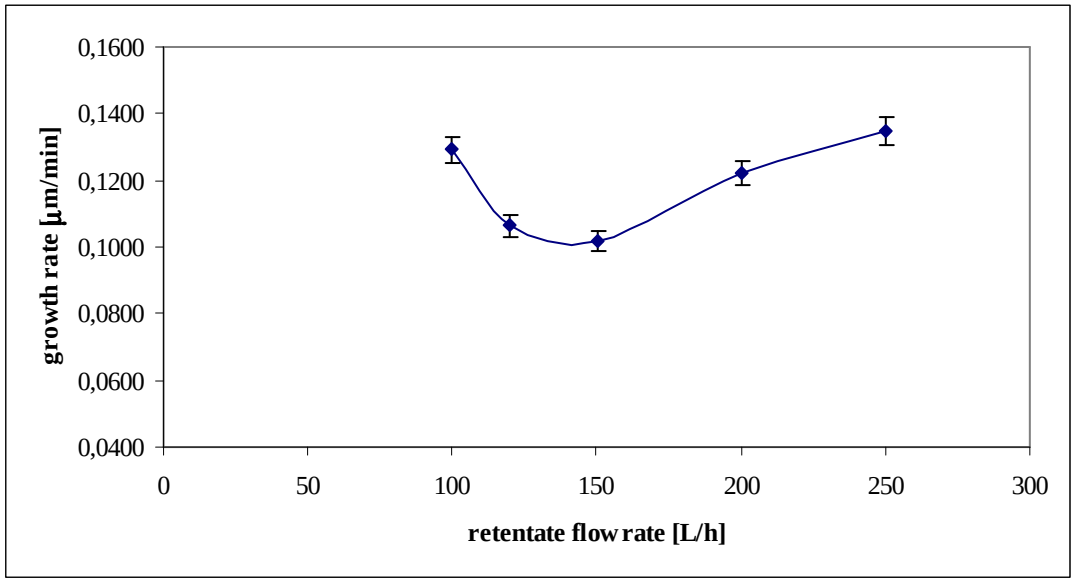

Figure 18: Growth rate vs retentate flow rate.

The obtained trend of the crystal growth rate versus retentate flow rate (Figure 18) and the evidence of diminution of nucleation for high feed flow rate allow to justify the growth acceleration after the minimum with the hypothesis that low salt concentrations in the boundary layer close to the solid/liquid interface, which is the case of a mass-diffusion control based mechanism, might promote the molecular organization which precedes the integration into crystal lattice, which in turn gives rise to an increase of crystal growth rate. The same trend has been also obtained through the crystallization of aqueous solution of NaCl pure.
Moreover, as reported in Figure 18, the experimentally determined crystal growth rate varies between 0.11 and 0.135 µm/min. It can be compared to the results obtained in the crystallization of NaCl pure in the same operative conditions (*Chapter 5*), showing that G values vary between 0.025 and 0.057 µm/min. The higher values obtained in tests on

RO brine can be explained by considering that kinetic rates and thermodynamic solubility equilibrium, as well as shape and purity of crystals, strongly depend on the presence of different components in the crystallizing solutions, degree of supersaturation, temperature and hydrodynamic conditions. In fact, [3] reports that NaCl growth rate and hardness increase in presence of other salts (range of concentration 0-100 ppm).

3. Test on NF retentate stream

The built lab plant has been also used in order to check, experimentally, the MCr performance for desalted water production and crystals recovery from a *NF retentate* stream of an integrated membrane desalination process constituted by MF/NF/RO.
In Table 10 the composition of the employed synthetic seawater is reported. With respect to the seawater until now utilized, also some other components (K^+, CO_3^{2+} and Br^-), present in small amount, have been considered.
In Table 11, the rejection values and recovery factor of the different units are summarized. Tables 12 shows the composition of NF and RO retentate.

Table 10. Seawater composition.

Ion	Concentration [g/L]
Cl^-	19.00
Na^+	10.50
SO_4^{2-}	2.700
Mg^{2+}	1.350
Ca^{2+}	0.4000
HCO_3^-	0.1420
K^+	0.3800
CO_3^{2+}	0.0035
Br^-	0.0650
Total	34.54
Flow rate [kg/h]	1.048 E+06
P [MPa]	0.10
T [K]	298.2

Table 11. Rejection values and recovery factor of NF/RO.

	NF [%]	RO [%]
Recovery factor	75.3	69.06
Ion	Rejection values	
Cl^-	26.7	99.6
Na^+	26.7	99.6
SO_4^{2-}	93.3	99.6
Mg^{2+}	87.7	99.6
Ca^{2+}	80.7	99.6
HCO_3^-	63.3	99.6
K^+	26.7	99.6
CO_3^{2-}	63.3	99.6
Br^-	10	99.6

Table 12. NF and RO retentate composition.

Stream	RO retentate	NF retentate
Ion	Composition [g/L]	
Cl^-	44.89	34.47
Na^+	24.81	19.05
SO_4^{2-}	0.5831	10.38
Mg^{2+}	0.5352	4.959
Ca^{2+}	0.2488	1.384
HCO_3^-	0.1680	0.4160
K^+	0.8978	0.6893
CO_3^{2-}	0.0041	0.0103
Br^-	0.1886	0.0848
Total	72.32	71.44

In order to avoid $CaSO_4$ precipitation, also in this case Ca^{2+} ions have been precipitated as $CaCO_3$ through reactive precipitation with anhydrous sodium carbonate and, in order to promote 98% precipitation, Na_2CO_3 was added in 1:1.05 molar ratio of Ca^{2+}/CO_3^{2-}.
SEM analyses carried out on the achieved solid products show the presence of Mg in the precipitated $CaCO_3$. Therefore, the Mg content in the precipitating solution slightly decreases because of its incorporation into carbonate phase.
Several studies agree with the generalization that Mg^{2+} in $CaCO_3$ is critically determined by the $[Mg^{2+}]/[Ca^{2+}]$ ratio [4 – 6]. The concentrations of Ca^{2+} and Mg^{2+} in NF retentate, first and after the precipitation step, have been measured with Optima 2100 DV Optical Emission Spectrometer supplied by PerkinElmer precisely. Under the investigated experimental conditions, the $[Mg^{2+}]/[Ca^{2+}]$ ratio in the NF retentate is 5.91 and the mole percent of Mg^{2+} incorporated in the precipitated particles varied between 4 and 12 mol% of the Mg^{2+} concentration in NF retentate; for artificial seawater (35 salinity) at 25 °C, with $[Mg^{2+}]/[Ca^{2+}]$ ranging from 1 to 20, Mucci and Morse [7] have found that carbonate precipitates contain 3–20 mol% of $MgCO_3$.
After this precipitation step, the so-treated NF brine is sent to the MCr where different tests have been carried out changing the temperature and the flow rate (from 100 to 250 L/h) of the MCr feed. The permeate flow rate and temperature have been kept constant and equal to 100 L/h and 16±2°C, respectively. Moreover, the system for crystals recovery described in *Chapter 4* was started up.

3.1 Concentration tests: trans-membrane flux measurements

Figure 19 shows the trend of trans-membrane flux with time obtained during lab tests at two different retentate flow rates and constant temperature. In both cases, apart an initial transitory stage, trans-membrane flux has shown almost a constant trend. The constant trend is characteristic of a good operation because means that there is no crystals deposition inside the membrane module. This is because the temperature of feed and the thermal difference between the two streams are high enough to contain the decrease in driving force due to concentration rise.
With respect to the previous tests, in the case of NF brine the experiments have not been stopped after 60 minutes from crystals formation (time essential to study the growth rate of the produced particles), but it has been decided to continue the runs to the point of exhaustion of the crystallizing solutions. The aim has been to evaluate the maximum amount of salts that can be recovered from the crystallization of NF brine. Therefore, in these tests, 60 minutes after crystals formation, the “crystals recovery system” has been started up in order to avoid crystals accumulation inside the membrane module. The almost costant trend of the obtained trans-membrane flux has also proved that this tool has allowed to separate the produced salts from the crystallizing solution: the crystals are kept on a paper filter while the remaining solution is re-send to the crystallization tank in order to be further concentrated.

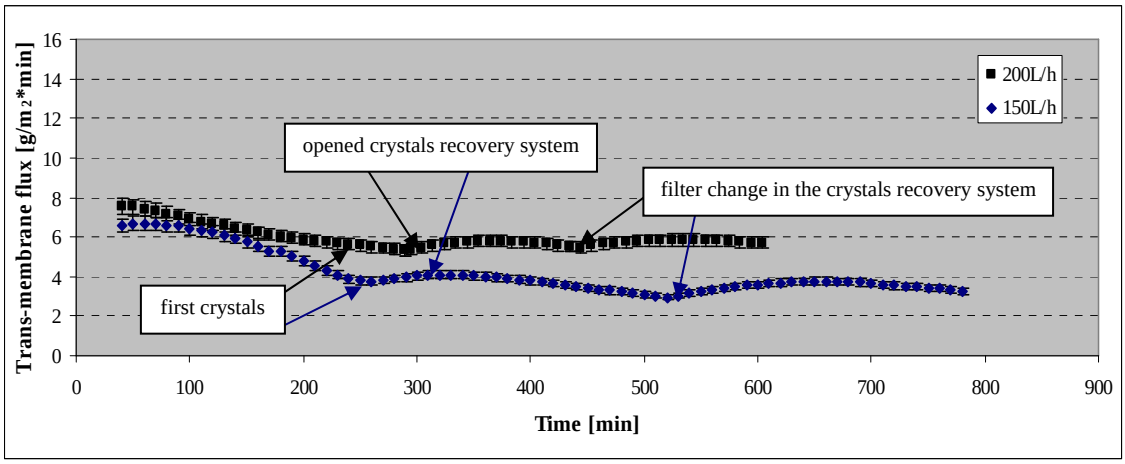

Figure 19: Trans-membrane flux vs time at different retentate flow rates and constant temperature ($T_{retentate}$ =34±1°C).

Figure 20 shows that trans-membrane flux increases with the temperature of the retentate. This trend is characteristic of a temperature driven membrane operation (as membrane crystallization) in which the driven force grows when the temperature of the feed and/or the trans-membrane temperature difference increase.

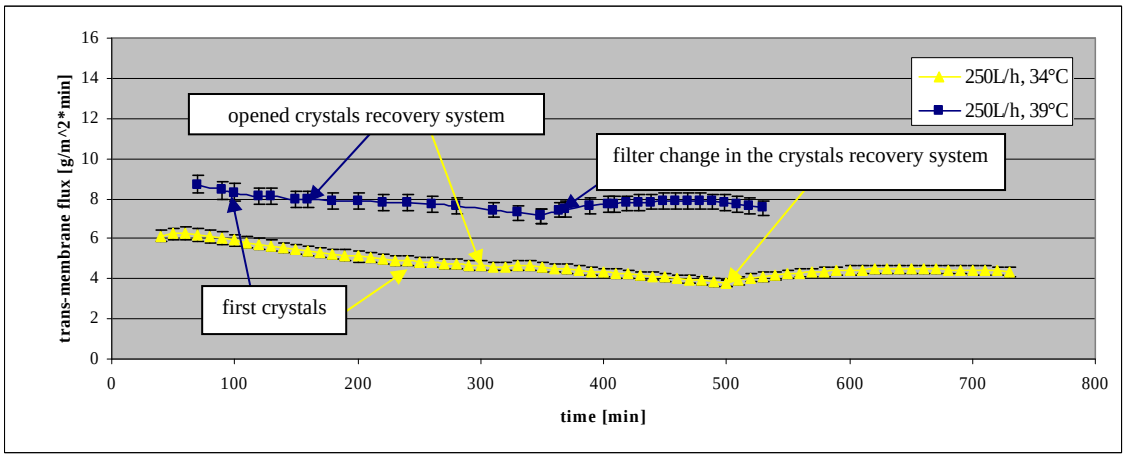

Figure 20: Trans-membrane flux vs time at different retentate temperature and constant flow rate (retentate flow rate=250 L/h).

Moreover, the influence of retentate flow rate and temperature appears evident in the time for reaching supersaturation and crystals formation: it decreases when these parameters increase (Table 13).

Table 13: Time for reaching crystals formation.

Flow rate [L/h] and temperature [°C] of the retentate	*Time for reaching crystals formation [min]*	Flow rate [L/h] and temperature [°C] of the retentate	*Time for reaching crystals formation [min]*
120 L/h and 34±1°C	*230*	120 L/h and 39±1°C	*150*
200 L/h and 34±1°C	*190*	200 L/h and 39±1°C	*140*
250 L/h and 34±1°C	*160*	250 L/h and 39±1°C	*100*

For what concerns the type of produced crystals, they have been analyzed by SEM (Scanning Electronic Microscopy), EDX (Energy Dispersive X-ray), low temperature DSC (Differential Scanning Calorimeters) and FT IR (Fourier Transform Infrared Spectroscopy) method:
1) the low temperature DSC measures on the achieved crystals (maximum temperature 250°C) clearly showed that no $MgCl_2*6H_2O$ was formed during the MCr tests of NF retentate;
2) the EDX (recorded using a Philips EDAX Analysis System) and FT IR analysis clearly showed the presence of NaCl and epsomite in the produced salts (Figures 21 and 22).

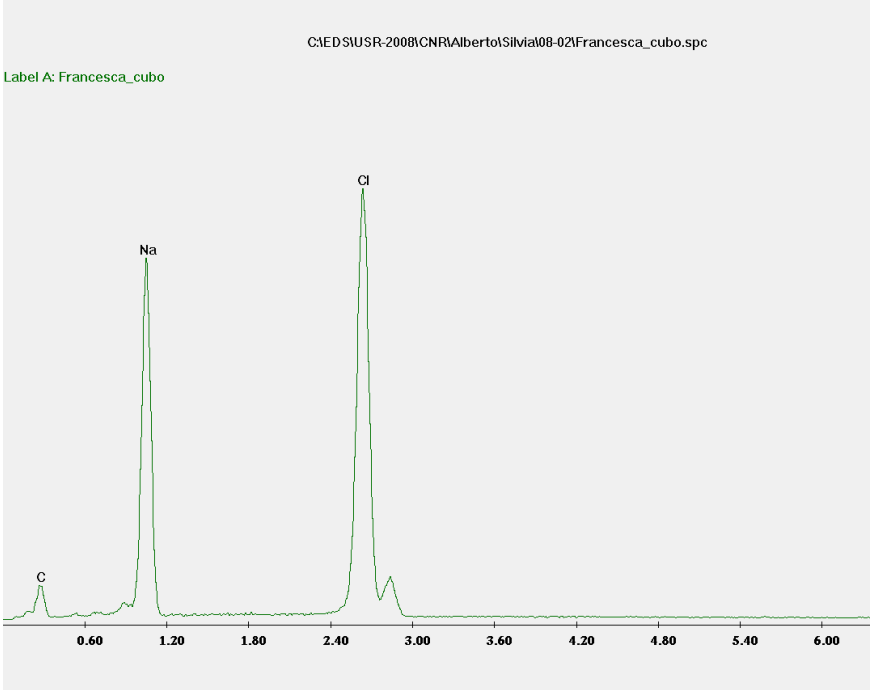

Figure 21: EDX spectrum of produced NaCl crystals.

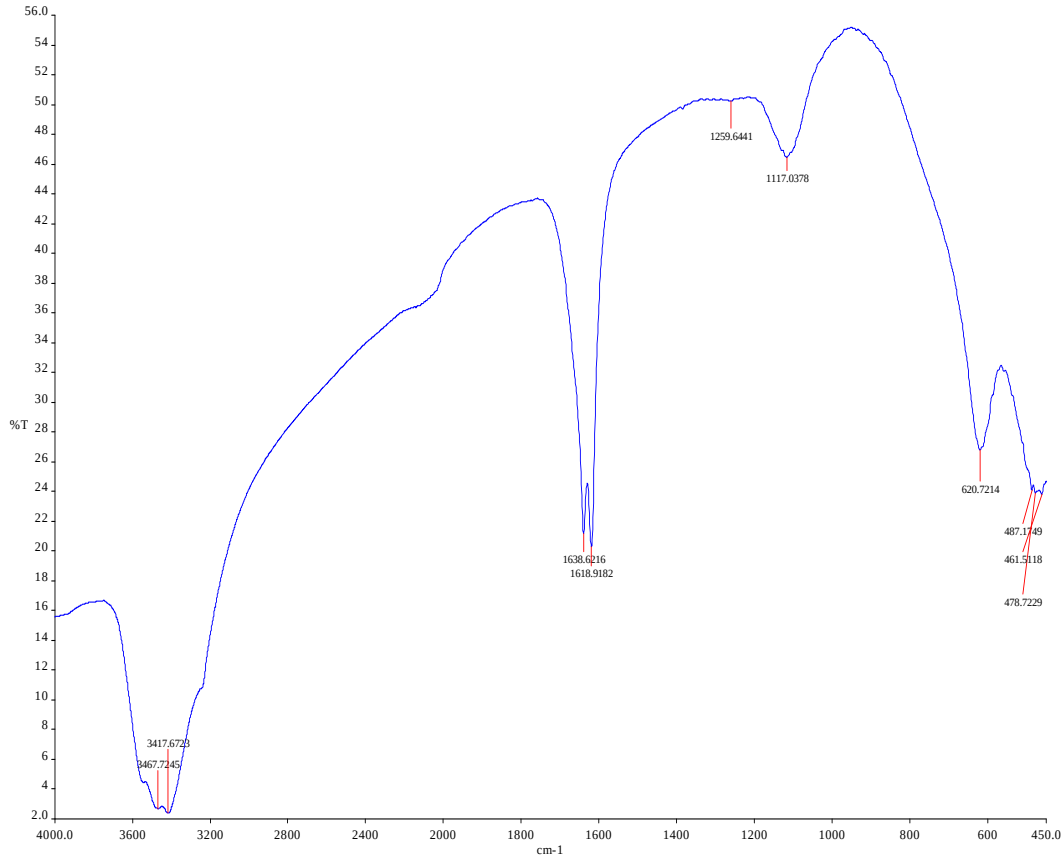

Figure 22: FT IR spectrum of some of the achieved epsomite crystals.

The Fourier transform infrared spectrum was recorded using a PERKIN ELMER – SPECTRUM ONE MODEL FTIR spectrometer in the range of 4000 – 450 cm-1 employing pellet technique. The FT IR spectrum of some of the achieved crystals completely agrees with the spectrum of epsomite found in literature. In fact, the broad envelope around 3400cm-1 indicates the presence of water (this envelope is due to the water involvement into the hydrogen bonding, the water stretching vibrations of free water). The asymmetric stretch of water (the water bendings) is observed at 1640cm-1. The out-of-phase-SO4 stretch appears at around 1120cm-1. The weak sharp band at 963cm-1 belongs to in-phase-SO4 stretch and points out that the oxygens of the anion are not in symmetrical equivalent environments. The bonding mode of sulphate is positioned at around 620cm-1.

3.2 Crystallization tests: product characterization

The product characterization has been performed only for the produced sodium chloride crystals.
The CSD of the total crystals contained in a known volume of magma was measured by screen analysis performed via the video microscope.
Experimental data relative to the cumulative fractional distribution of averaged slurry samples as a function of the particle size are shown in Figure 23 at three different operative conditions (details are reported in the Table 14).

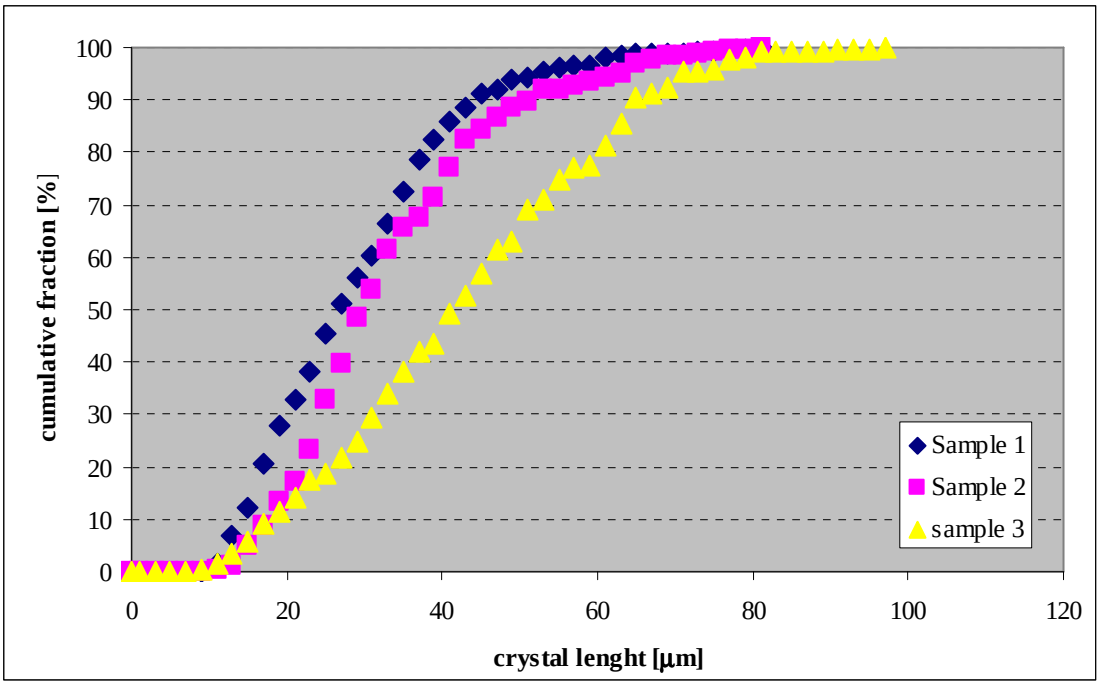

Figure 23: Cumulative distribution of crystals per unit of volume versus particle size at operative conditions indicated in Table 14.

Table 14: Operative conditions for the crystals samples whose cumulative distributions are shown in Figure 23.

Retentate flow rate =		150 L/h
Retentate temperature =		39±1°C
Permeate flow rate =		100 L/h
Permeate temperature =		16±2°C
	time [min]	M [g/L]
Sample 1	130	4.6
Sample 2	160	5
Sample 3	190	10.1

Some experimental evaluations of the coefficient of variation (CV) and of the middle diameter (d_m) as obtained in the carried out NF retentate crystallization tests are reported in Table 15.

Table 15: Evolution in function of time of the Coefficient of Variation (CV) and middle diameter (d_m), parameters determined from the experimentally obtained CSDs at three different MCr feed flow rate ($T_{feed,\ retentate\ side}$=39±1°C, $T_{feed,\ permeate\ side}$=16±2°C).

120 L/h			150 L/h			250 L/h		
time [min]	d_m [µm]	CV [%]	time [min]	d_m [µm]	CV [%]	time [min]	d_m [µm]	CV [%]
150	25.31	34.38	130	29.55	43.52	100	30.35	25.00
180	22.36	35.00	160	33.64	38.33	130	38.68	45.59
210	29.61	26.72	190	43.28	47.62	160	44.46	39.09

As can be seen in the Table 15, when crystals grown under milder conditions, CSDs are characterized by low CVs (characteristic of narrow distributions around the mean crystal size). In particular, for MCr feed flow rate equal to 120L/h, CVs less than 35% have been obtained.
With respect to the crystallization of RO brine, the produced NaCl crystals are characterized by lower coefficients of variation and middle diameters. This is probably due to the fact that, in the crystallization of NF brine, the temperature of the MCr feed is higher than that used in the crystallization of RO brine and this is expected to cause a higher dissolution of the smaller particles.
Table 16 reports the experimentally achieved recovery factor of the MCr lab plant and the recovery factor of the MCr in the proposed FS4, the latter obtained through computer simulation when FS4 and the lab plant produce the same amount of salts and using as seawater the composition reported in Table 10 and as rejections the values reported in Table 11. The comparison of the calculated with the experimentally determined MCr recovery factor shows a good agreement, with error less than 6%.

Table 16: MCr recovery factors.

Retentate flow rate [L/h]	Retentate temperature [°C]	Produced salts [g/L]	Experimentally determined MCr recovery factor [%]	MCr recovery factor in FS4 from the computer simulation [%]	Error [%]
120	39±1	6.16	76.71	87.13	6.36
150	39±1	12.22	79.83	88.81	5.32
200	39±1	17.05	80.84	90.15	5.45
250	39±1	21.90	81.22	91.49	5.95

The length/width ratio distributions of the obtained NaCl crystals confirmed their cubic block-like form examined visually with the optic microscope (Figure 24).

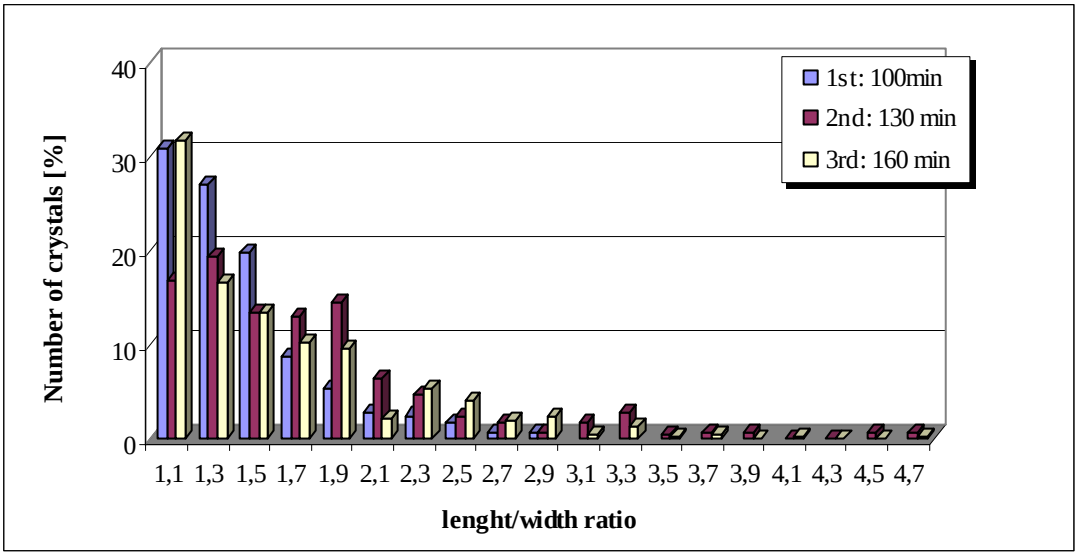

Figure 24: Number of crystals [%] vs length/width ratio at a retentate flow rate equal to 250 L/h.

The percentage of NaCl crystals exhibiting an elongated shape is higher in the crystallization of NF retentate than in the crystallization of RO retentate due to the presence of a bigger number of ions which may act as impurities.

3.3 Crystallization kinetics: nucleation and growth

Figure 25 reports the estimated population density data versus crystal size for a representative set of averaged samples at t = 130 min and M = 4.6 g/L; a linear regression of equation $n = n^0 \cdot \exp(-L/Gt)$ is used to determine both the crystals growth rate *G* and the nuclei population density n^0.

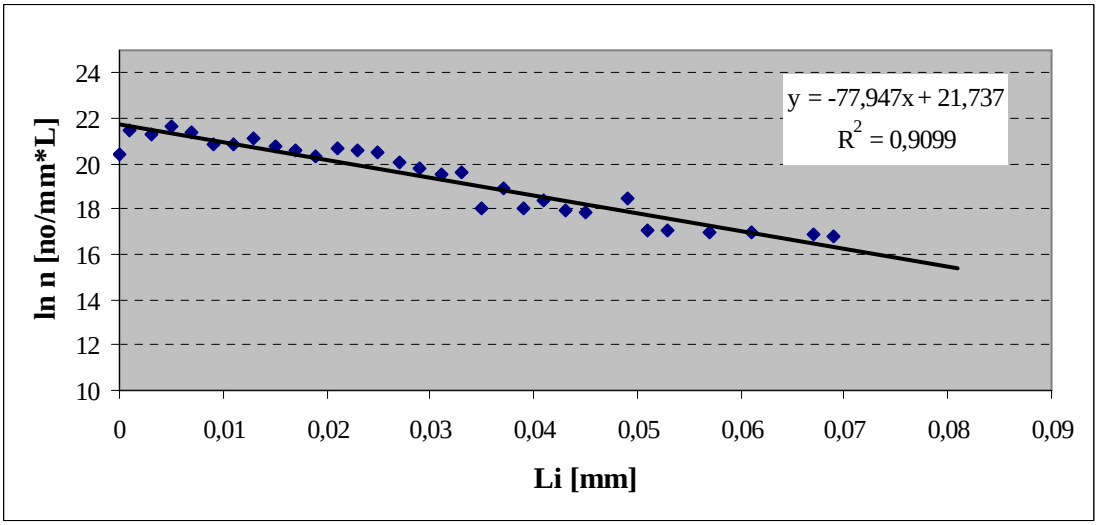

Figure 25: Population-density plot for NaCl crystals produced at retentate flow rate equal to 150 L/h and retentate temperature equal to 39±1°C.

From several other samples taken from the crystallizer during the same test and for each carried out run (Table 17), a plot of growth rate G versus feed flow rate can be constructed in order to study the fluid-dynamic effect on membrane crystallization operation (Figure 26).

Table 17: Crystals growth rate *G* and nucleation rate at different retentate flow rate.

Retentate flow rate [L/h]	G [mm/min]	B° [no/L*min]
120	0.0000585	200,200
150	0.0001142	194,110
200	0.0001235	168,714
250	0.0001639	199,914

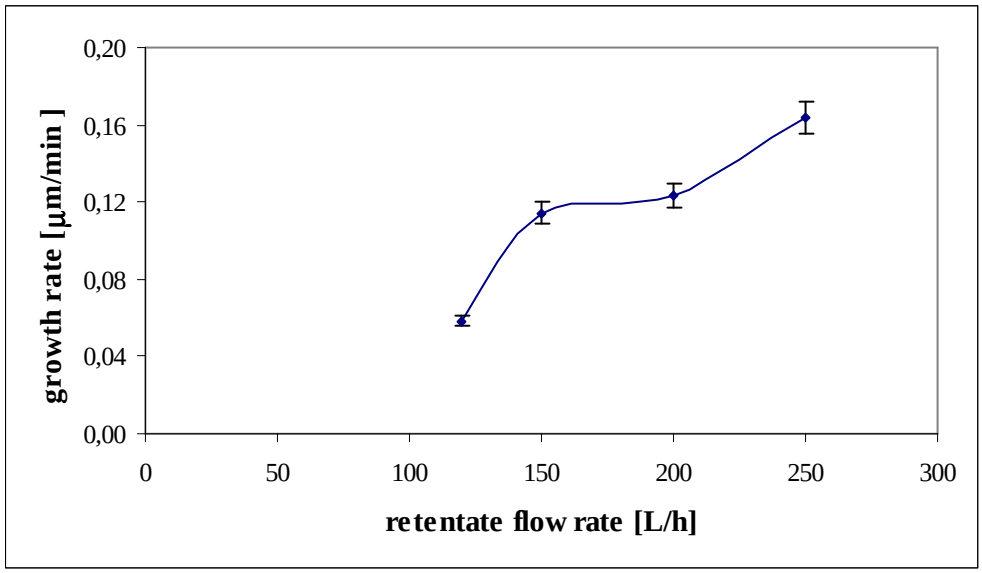

Figure 26: Growth rate vs retentate flow rate.

The obtained trend of the crystal growth rate versus feed flow rate (Table 19 and Figure 26) proves that crystal growth is limited by the diffusional resistance to the movement of molecules to the growing crystal face.

4. Effect of humic acid on membrane processes

Natural waters contain natural organic matter (NOM), largely composed of humic substances, which are macromolecular mixtures of humic acid (HA), fulvic acids and humin. Humic acids refer to the fraction of humic substances that is not soluble at pH<2. The removal of NOM from feed water is necessary in potable water production. Membrane processes have been shown to remove NOM effectively from water [8]: in the ultrafiltration of water containing humic acids, the retentions were in the range of 85-90%; NOM removal by nanofiltration membranes, quantified by total organic carbon (TOC) rejection, was found to be more than 90% at pH 8.

However, membrane fouling by NOM is one of major obstacles limiting the use of these processes. The observed fouling leads to a decrease of the membrane performance and subsequently to a reduction of the membrane life. The membrane surface characteristics (i.e. hydrophobicity, porosity, etc.), the hydrodynamic conditions (i.e. transmembrane pressure, crossflow velocity, temperature, etc.) and the chemical composition of feed liquid (i.e pH, ionic strength, type of NOM, etc.) exert significant effects on membrane fouling [9].

The flux decline observed during constant pressure microfiltration experiments [10] was caused by the formation of a humic acid deposit on the upper surface of the membrane with relatively low internal fouling. The rate and extent of fouling reduced by removing large humic acid aggregates proved that large aggregates were the main cause of flux decline. Yuan et al. [11] reported that the initial fouling of humic acids on MF membranes was due to deposition of large aggregates inside the pores that caused pore blockage. The cake layer was then formed on the region which had been blocked. It was

found that humic macromolecules are adsorbed more favourably onto hydrophobic membranes and the adsorption is greater at low solution pH [12].The deterioration of permeation flux during the ultrafiltration of humic acids was studied by Kabsch-Korbutowicz et al. [13]. They reported that the membrane with a higher degree of hydrophilicity was the least affected. The significant flux decline at low pH was attributed to the thick humic acid deposit layer contributed by the reduction of electrostatic repulsion between humic acid molecules and the strong tendency to sorption on the membrane surface [8].
Moreover, it was demonstrated that membrane fouling increases with increasing electrolyte (NaC1) concentration and with the addition of divalent cations (Ca^{2+}). Calcium and other multivalent cations are known to form complexes with NOM. The divalent cations interact specifically with humic carboxyl functional groups and reduce the humic charge and the electrostatic repulsion between humic macromolecules leading to enhanced aggregation [9].
Zuddas et al. [14] proved that dissolved organic matter influences the complex mechanism of calcite crystal growth from seawater: by a set of experiments at different humic acid concentrations (i.e. [HA] = 50, 500, 1000 μg/kg), they found that the rate of calcite precipitation from seawater solutions decreases as a function of the [HA] by at least one order of magnitude.

It is the interest of the work presented in this section to study membrane fouling in MCr process when applied to waters containing humic acids and inorganic salts similarly to NF brine of a seawater desalination plant. The effect of humic acids on crystal growth is also included.

4.1 Effect of humic acid on membrane distillation and membrane crystallization. Fouling and trans-membrane flux measurements

There are limited studies on fouling on MD/MCr process. Fouling in MD/MCr is generally less serious than that in other membrane processes [15, 16].
Apart from the scaling effect that can be produced on the membrane surface when high salts concentrations are used and the biological fouling or growth of bacteria on the membrane surface, particles or colloidal species may be trapped at both the membrane matrix and pores.
Gryta et al. [17] applied the DCMD system to concentrate a NaCI solution with dissolved organic matter and examined membrane fouling. The permeate flux decreased continuously with each consecutive series of experiments carried out without membrane cleaning. The membranes changed from a white to a brownish colour, and the membrane micrograph taken by scanning electron microscopy (SEM) confirmed fouling. Hsu et al. [15] reported flux decline in DCMD experiments using a NaC1 solution and seawater as feeds. The vapour flux of seawater decreased continuously from 10 kg/m^2h to 7 kg/m^2h within 160 h. The SEM micrograph of the membrane surface obviously showed signs of fouling. DCMD was also employed for the concentration of bovine serum albumin (BSA) aqueous solution [9]. It was found that membrane fouling was practically absent at low temperatures (i.e. 20°C-38°C), BSA concentration ranging between 0.4 and 1% w/w and solution pH of 7.4. It was argued

that the permeate fluxes are below the critical flux for fouling in DCMD. On the contrary, membrane fouling was observed during the concentration of tomato puree, which contains 3-4% carbohydrate, 0.5-1% protein and 0.1-0.3% fat [9]. It was indicated that the adhesion of fatty substances, including tomato pigments to the membrane surface blocks the membrane pores and therefore reduces the permeate flux. Membrane fouling in DCMD process was also observed during the treatment of wastewater originating from heparin production from intestinal mucous [9]. A permeate flux decline of about 43% was detected. It was found that protein and sodium chloride constituted the major components of the gel layer. 2 wt % of citric acid solution was used to restore the permeate flux close to its initial value.

Khayet et al. [9] investigated MD for the treatment of humic acid solutions containing sodium chloride and calcium chloride at concentrations typical of those found in natural waters. It was found that, compared to the pressure-driven membrane separation processes, higher rejection factors with very low permeate flux decline were observed in direct contact membrane distillation application when humic acid containing salts were considered.

Also Srisurichan et al. [8] investigated the extent of humic acid fouling during the membrane distillation process for water treatment. Flux declines were negligible (less than 6%) for the ranges of humic acid concentration (from 20 to 100mg/L), ionic strength (calculated by adding NaCl into the feed solution), and pH (from 3 to 7) studied. On the contrary, in MF of 2 mg/L HA solution, flux decline was significant. The differences in the results can be explained: in MD, the process liquid cannot wet the membrane. Therefore, HA is deposited only on the membrane surface but not in the membrane pores. Furthermore, due to the low operating pressure of the process, the deposition of HA aggregates on the membrane surface would be less compact and only slightly affect the transport resistance. A similar finding was recently reported in [18].

For what concerns the effect of divalent ions (such as Ca^{2+}), since HA contains negatively charged carboxyl groups, divalent ions act like binding agents of two carboxyl functional groups. The deposition can be increased by charge screening, as in the case of NaCI, and also by the complexation which contributes to the crucial increase in size of aggregates.

Srisurichan et al. [8] demonstrated that the coagulate of humic acids are the major cause of membrane fouling in MD. In fact, they proved that the addition of Ca^{2+} into the solution considerably reduces flux when Ca^{2+} concentration exceeds the critical coagulation concentration: Ca^{2+} affected flux by forming complexes with humic acids and resulted in coagulation on the membrane surface. The examination of the membrane surface by SEM confirmed the existence of a thin fouling layer.

On the contrary, in MF and NF, Ca^{2+} significantly accelerates the rate of flux decline also at low Ca^{2+} concentrations (0.5-1 mM) [8], while Ca^{2+} influences flux in membrane distillation when its concentration exceeded the critical coagulation concentration (2-3 mM of $CaC1_2$ [8]), the concentration at which coagulate occurs. Coagulation refers to a type of aggregation in which semi-solid particles of a suspension combine irreversibly into a cohesive mass or clot. As a result, the particles coalesce and precipitate. Agents which induce coagulation are usually electrolytes which neutralize the oppositely charged particles.

Figure 27 reports the effect of humic acid during membrane crystallization process of solutions containing HA and inorganics at concentrations typical of those found in NF retentate (Table 12). In particular, the tests have been carried out on solutions with the same composition of the NF brine after the precipitation with anhydrous sodium carbonate previously described, in which humic acid has been added.
Humic acid concentrations have been evaluated by using Total Organic Carbon Analyzer Shimadzu TOC-Vcsn.

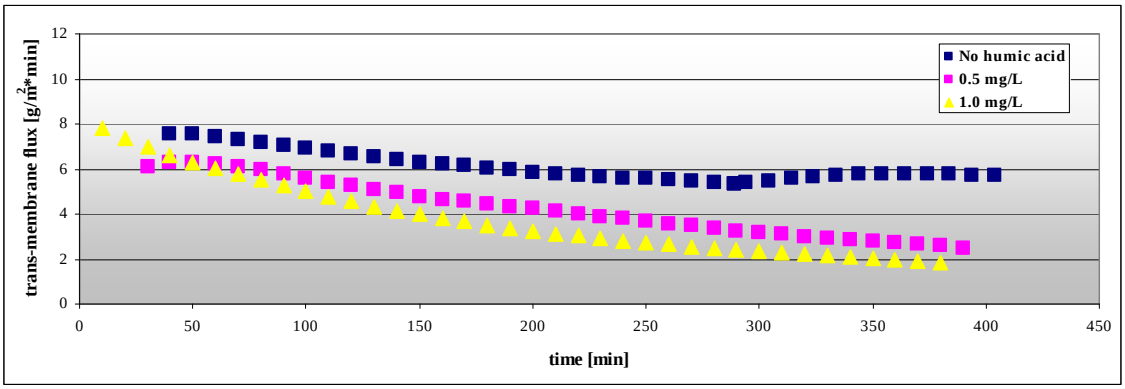

Figure 27: Trans-membrane flux vs time for NF retentate with different HA concentrations. ΔTin=11°C, ΔT_{out}=9°C, retentate flow rate = 207L/h, $T_{in,\ feed}$=39±1°C.

The achieved results have proven that trans membrane flux decreases when the concentration of humic acid increases due to the formation of a fouling layer. In fact, in agreement with what found in literature, the examination of the membrane surface confirmed the existence of a fouling layer which appeared dark brown (Figure 28).

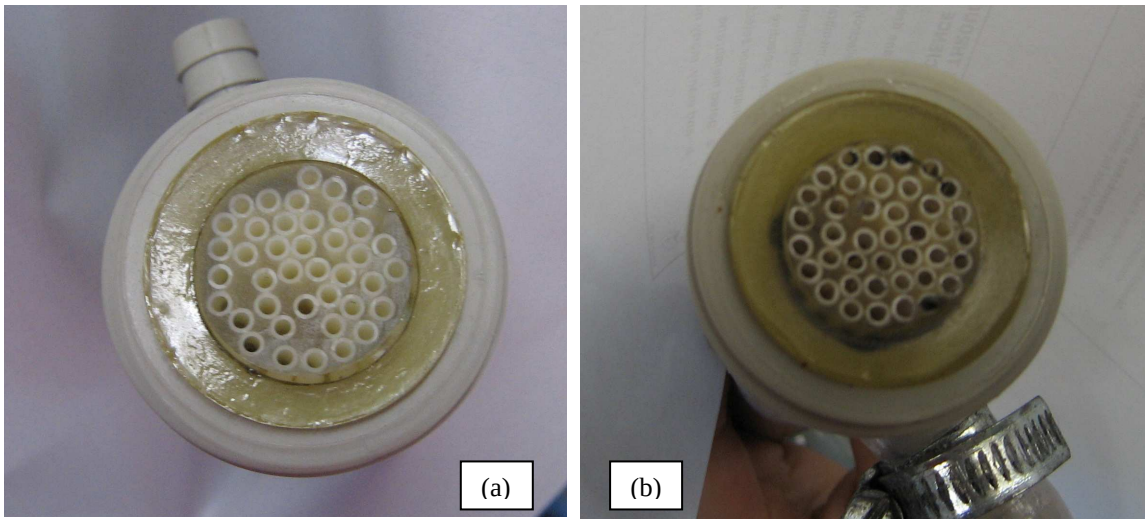

Figure 28: (a) New membrane module, (b) fouled membrane module after operation with humic acid.

The deterioration of flux due to the fouling layer may be attributed to two effects: first, the reduction of surface area available for vaporization as the fouling layer blocked the pore entrances; second, the fouling layer may decrease the heat transfer driving force.

Even though there has been no report on the heat transfer resistance of the fouling layer, it is expected that such a layer can reduce the temperature polarization coefficient [15, 17, 19]. As described in *Chapter 1 – Section 3.2*, the temperature polarization coefficient (TPC) reflects the heat transfer efficiency of the process, in fact it is the measure of the magnitudes of the boundary layer resistances relative to the total heat transfer resistance of the system:

$$TPC = \frac{T_{fm} - T_{pm}}{T_f - T_p}$$

Therefore, in order to obtain crystals, an increase of the driving force of the process with respect to the previous tests has been necessary. Figure 29 reports the effect of the temperature difference (ΔT) between the two membrane sides on MCr operation: crystals formation was not observed for ΔT equal or less than about 11°C.

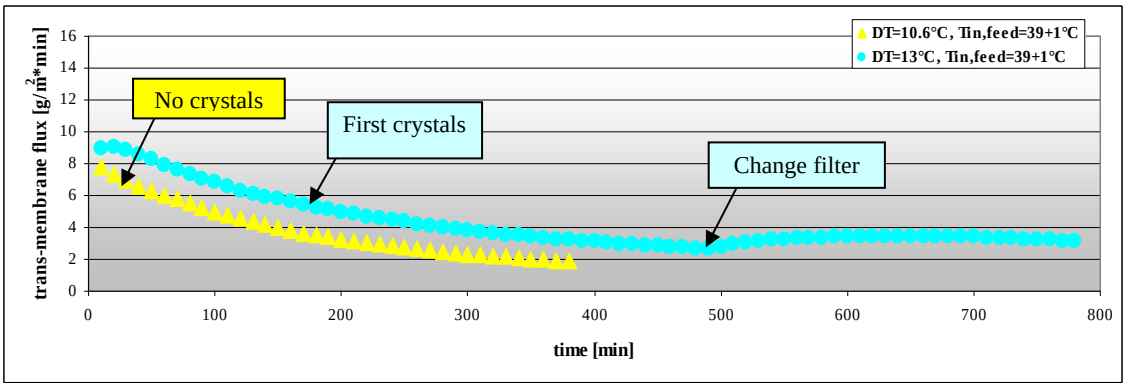

Figure 29: Trans-membrane flux vs time at different temperature difference between the two membrane sides. Humic acid concentrarion =1 mg/L; retentate flow rate = 207 L/h; $T_{in,\ retentate}$=39±1°C.

4.2 Influence of dissolved humic acid on the kinetics of salts precipitation from NF retentate

Figure 30 shows the experimental data relative to the cumulative fractional distribution of the obtained crystals as a function of their size at three different operative conditions (details are reported in the corresponding legend).

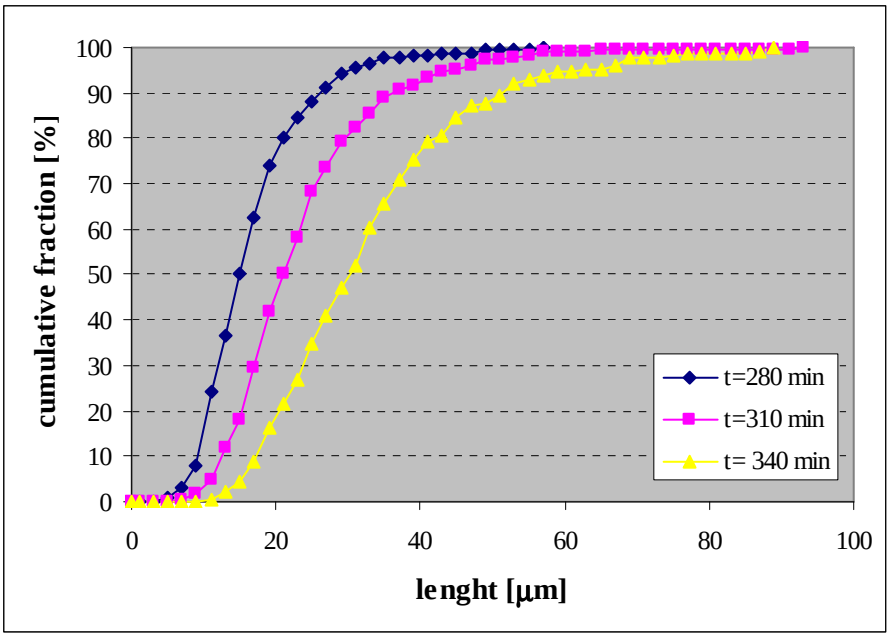

Figure 30: Cumulative distribution of crystals per unit of volume versus particle size. Retentate flow rate=207 L/h, humic acid concentrarion =0.5 mg/L; permeate flow rate = 100 L/h; $T_{in,\ retentate}$=39±1°C; ΔT_{in}=11.09°C.

Table 18 reports some experimental evaluations of the coefficient of variation (CV), the middle diameter (d_m) and the density of the crystal slurry (M) as obtained in the carried out NF retentate crystallization tests at different humic acid concentrations. They can be compared to the results obtained in the crystallization of NF retentate without humic acid in the same operative conditions (Table 15), showing that d_m values vary between 22.36 and 44.46 µm, and CV values vary between 25 and 45.59%.

Table 18: Evolution in function of time of the Coefficient of Variation (CV), middle diameter (d_m) and density of the crystal slurry (M). Parameters determined from the experimentally obtained CSDs at two different humic acid concentrations (Retentate flow rate=207 L/h; Permeate flow rate=100 L/h; $T_{feed,retentate\ side}$=39±1°C, ΔT_{in}=12±1°C).

Humic acid concentration [mg/L]							
0.5				1.0			
Sample n°	d_m [µm]	CV [%]	M [g/L]	Sample n°	d_m [µm]	CV [%]	M [g/L]
1	17.48	41.12	-	1	16.32	41.67	-
2	24.22	41.67	0.9	2	19.68	48.57	2.1
3	33.49	43.33	1.6	3	37.02	67.19	4

For what concerns the experimentally achieved recovery factors, they ranged from 74.9 to 78.1% in the carried out tests with humic acid concentrations equal to 0.5 and 1.0 mg/L, respectively.

Figure 31 reports the estimated population density data versus crystal size for a representative set of averaged samples at t = 250 min and M = 4.0 g/L. The linear regression of equation $n = n^0 \cdot \exp(-L/Gt)$ is used to determine both the crystals growth rate *G* and the nuclei population density n^0. A summary of the results achieved at different humic acid concentrations is reported in Table 19.

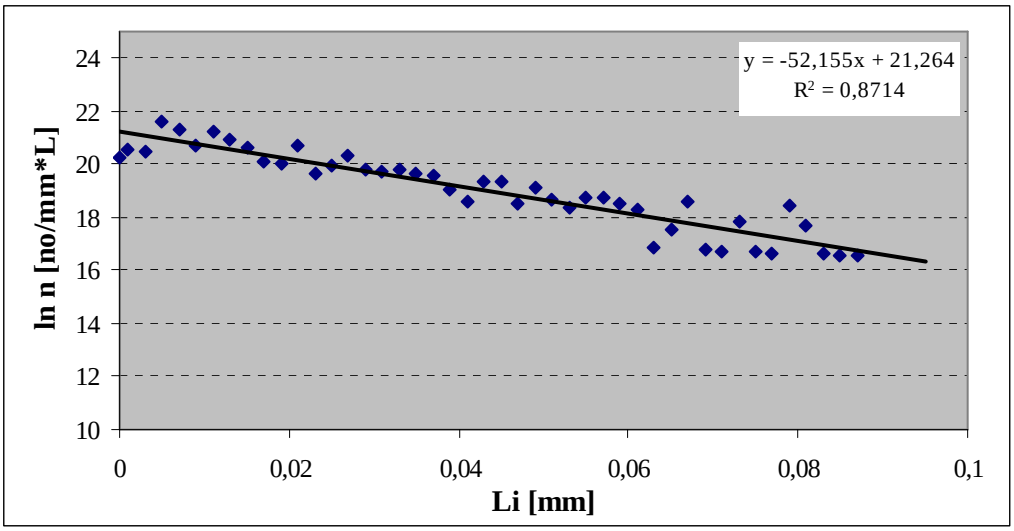

Figure 31: Population-density plot for crystals produced at retentate flow rate equal to 207 L/h, [HA]=1 mg/L, retentate temperature equal to 39±1°C, ΔT_{in}=12±1°C.

Table 19: Crystals growth rate *G* and nucleation rate at different humic acid comncentration.

Humic acid concentration [mg/L]	0.5	1.0
G [μm/min]	0.0407	0.0612
ln n°	21.75	21.87
B° [no/L*min]	116,200	197,000

In conclusion, the effect of humic acid is not only on membrane fouling but also on crystals size (smaller particles), on CV (higher CVs, characteristic of wider distributions around the mean crystal size) and on crystals growth rate which is at least one order of magnitude smaller than the one obtained from inorganic NF brine solutions (Table 17). The achieved results agree with Zuddas et al. [14] observations on calcite precipitation from seawater solution. It was found that the dissolved organic matter in the form of HA inhibits the rate of calcite crystal growth in strong electrolyte solutions of ionic strength like seawater. They proposed that the inhibition of crystal growth results from a decrease of active growth sites rather than a decrease in the amount of free-calcium resulting from complexation with HA. This might indicate that the growth inhibition is governed by large organic molecules able to adsorb to more than one growth site on the crystal surface.
These observations are in agreement with Mayer [20] and Troy et al. [21] where it was found that an incorporation of high levels of organic carbon in surface pore produces an increases of the surface area of at least two orders of magnitude.

5. Membrane cleaning

The cleaning of the membrane module and of the overall plant is necessary in order to try to restore the initial performance of the membrane fouled by humic acid and various inorganic components.

Cleaning was performed by re-circulating first of all pure water for 1 h, followed by 30 min of re-circulation of a citric acid solution (pH 3÷4), successively 30 min of pure water, then 30 min of a 0.1M NaOH solution. Finally, a third rinse with distillate water was performed. The pure water flux was measured after 1 h cleaning with pure water and after 1 h chemical cleaning. The obtained trans-membrane fluxes were compared with the water flux in a new module (Figure 32).

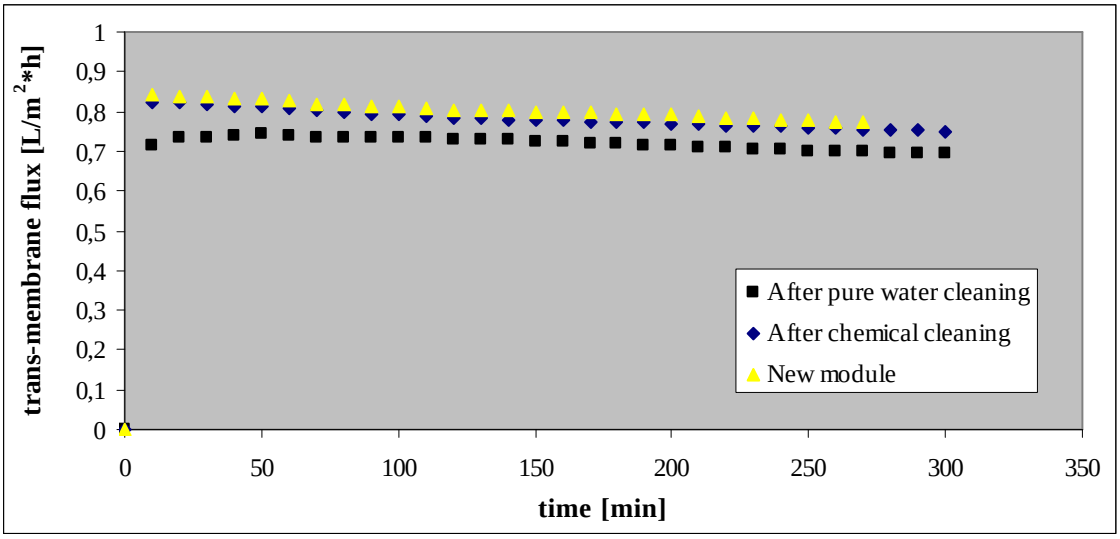

Figure 32: Tran-membrane flux of pure water at the conditions shown in the legend. Retentate flow rate = 200L/h, permeate flow rate = 100L/h, ΔT_{in}=9.5 °C, ΔT_{out}= 9°C.

The permeation flux recovery was 91% of the initial flux after water rinsing. Most of the fouling layer was swept out with the water stream. Besides, due to the good dissociation and dissolution of humic acid at high pH, 100% flux recovery was attained after chemical cleaning.

In conclusion, humic acid fouling in membrane distillation can be easily controlled and managed since the mechanism is physical. The achieved results are in agreement with [8] which proved that the deposit of humic acid coagulate on the membrane surface is loosely packed and is rather easily removed.

6. Conclusions

The results achieved in the carried out experimental tests show the interesting potentialities of membrane crystallizer for the exploitation of some components contained in seawater. In particular:

- ✓ around 98% of Ca^{2+} ions have been precipitated as $CaCO_3$ through reactive precipitation with anhydrous sodium carbonate by using a 1:1.05 molar ratio of Ca^{2+}/CO_3^{2-}. The Mg^{2+} content in the precipitating solution has been decreased

because of its integration into carbonate phase. Under the investigated experimental conditions, the mole percent of Mg^{2+} incorporated in the precipitated particles varied between 4 and 12 mol% of the Mg^{2+} concentration in NF retentate;

- ✓ cubic NaCl crystals obtained by membrane crystallization show narrow CSDs, with CVs lower than those from conventional equipments;
- ✓ the experimentally determined crystals growth rate shows that the presence of other ions accelerate kinetic rate of NaCl crystallization;
- ✓ the presence of humic acid in NF retentate inhibits crystals growth rate which is at least one order of magnitude smaller than the one obtained from inorganic NF brine solutions.

In conclusion, the integration of Membrane Crystallizers on NF and/or RO brine might offer the possibility of producing solid materials of high quality, whose structures (polymorphism) and morphologies (size, size distribution, shape, habit) can be adequate to represent a valuable by-product, transforming the traditional brine disposal cost in a potential new profitable market.

From here the necessity to optimize the pre-treatment step in order to control the crystallization kinetics that, as over described, are linked with the nature and the amount of the foreign species existing in the highly concentrated brines emerging from the NF and RO stages. These substances, besides causing fouling on RO membranes, would easily hinder the crystallization kinetics via the deleterious effects of surface poisoning of the growing crystals, thus leading either to the cessation of growth or to the production of a product exhibiting inferior, undesired properties. Moreover, small quantities of specific impurities can suppress the growth, while others, being crystallographic face-selective, might be used as habit modifiers. Selective crystallization of polymorphs requires control and manipulation of the nucleation and growth processes and may be influenced by the presence of additives. The manipulation of polymorphism, morphology, and crystal size at micro- and nano-scale levels is a very relevant challenge from an application point of view because of their strong influences on materials properties.

Relevant Bibliography

[1] K.H. Nelson, T.G. Thompson, *Deposition of salts from seawater by frigid concentration*, J. Mar. Res. 13 (1954) 166.

[2] E. Drioli, E. Curcio, A. Criscuoli, G. Di Profio, *Integrated system for recovery of $CaCO_3$, NaCl and $MgSO_4{\cdot}7H2O$ from nanofiltration retentate*, Journal of Membrane Science, 239 (2004) 27–38.

[3] J. H. Perry. D. Green. *Perry's Chemical Engineers' Handbook*. McGraw-Hill international Editions. New York. 1987

[4] D.M. Devery, A.J. Ehlmann, *Morphological changes in a series of synthetic Mg-calcites*, Am. Mineral. 66 (1981) 592.

[5] M.R. Howson, A.D. Pethybridge, W.A. House, *Synthesis and distribution coefficient of low-magnesium calcites*, Chem. Geol. 64 (1987) 79.

[6] T. Oomori, H. Kaneshima, Y. Mezato, Y. Kitano, *Distribution coefficient of Mg^{2+} ions between calcite and solution at 10–50 °C*, Mar. Chem. 20 (1987) 327.
[7] A. Mucci, J.W. Morse, *The incorporation of Mg^{2+} and Sr^{2+} into calcite overgrowths: influence of growth rate and solution composition*, Geochim. Cosmochim. Acta 47 (1983) 217.
[8] S. Srisurichan, R. Jiraratananon, A.G. Fane, *Humic acid fouling in the membrane distillation process*, Desalination 174 (2005) 63-72.
[9] M. Khayet, J.I. Mengual, *Effect of salt concentration during the treatment of humic acid solutions by membrane distillation*, Desalination 168 (2004) 373-381.
[10] W. Yuan, A.L. Zydney, *Humic acid fouling during microfiltration*, J. Membr. Sci., 157 (1999) 1-12.
[11] W. Yuan, A. Koeic, A.L. Zydney, *Analysis of humic acid fouling during microfiltration using a pore blockage-cake filtration model*, J. Membr. Sci., 198 (2002) 51-62.
[12] C. Jucker, M.M. Clark, *Adsorption of aquatic humic substances on hydrophobic ultrafiltration membranes*, J. Membr. Sci., 97 (1994) 37-52.
[13] M. Kabsch-Korbutowicz, K. Majewska-Nowak, T. Winnieki, *Analysis of membrane fouling in the treatment of water solutions containing humic acids and mineral salts*, Desalination, 126 (1999) 179-185.
[14] P. Zuddas, K. Pachana, D. Faivre, *The influence of dissolved humic acids on the kinetics of calcite precipitation from seawater solutions,* Chemical Geology 201 (2003) 91– 101.
[15] S.T. Hsu, K.T. Cheng, J.S. Chiou, *Seawater desalination by direct contact membrane distillation*, Desalination, 143 (2002) 279-287.
[16] J.M. Ortiz De Zarate, C. Rineon, J.I. Mengual, *Concentration of bovine serum albumin aqueous solutions by membrane distillation*, Sep. Sci. Technol., 33(3) (1998) 283-296.
[17] M. Gryta, M. Tomaszewska, J. Grzechulska, A.W. Morawski, *Membrane distillation of NaCl solution containing natural organic matte*r, J. Membr. Sci., 181 (2001) 279-287.
[18] M. Khayet, A. Velazquez, J.I. Mengual, *Direct contact membrane distillation of humic acid solutions*, J. Membr. Sci., 204 (2004) 123-128.
[19] K.W. Lawson, D.R. Lloyd, *Membrane distillation*, J. Membr. Sci., 124 (1997) 1-25.
[20] L.M. Mayer, *Surface area control of organic carbon accumulation in continental shelf sediments*, Geochim. Cosmochim. Acta 58 (4), 1271–1284 (1994).
[21] P.J. Troy, L. Yuan-Hui, F.T. MacKenzie, *Changes in surface morphology of calcite exposed to the oceanic water column,* Aquat. Geochem. 3 (1997) 1 – 20.

CHAPTER 7 : Pressure-Driven Membrane Operations and Membrane Distillation Technology Integration for Water Purification: Analysis and Comparison

Table of Contents

1. Introduction

The recent and worrying studies on the effects caused by the presence of some pollutants in the waters have stimulated the study and the analysis of other integrated membrane based systems for reducing the concentration of these contaminants below their maximum recommended value, as well as the possibility to use membrane distillation as an innovative technology for their removal.
In the wide spectrum of the harmful substances contained in the polluted waters, in the present work the attention has been focused on the analysis of different membrane systems for the elimination or the reduction of boron and arsenic concentrations.
In the last years, boron and arsenic are gaining wide attention in the water treatment community due to their adverse effects both on human/animal health and on agriculture, and to their growing consumption in the current industry.

For what concerns boron, although it is vital as a trace element for plant growth and is supplied in fertiliser, it can become detrimental at concentrations higher than 0.3 mg/L. Among the more sensitive crops are citrus trees, which show massive leaf damage at boron levels of more than 0.3 mg/L in the irrigation water [1]. Excess boron also reduces fruit yield and induces premature ripening on other species such as kiwi. Moreover, in the lab tests, it has been noticed that boron has toxic effects at concentrations as low as 0.5 mg/L, because it impairs animal growth and causes nerve damage. As a consequence, boron limits in the tender documents for medium and large membrane desalination plants range between 0.3 and 0.5 mg/L. The World Health Organization (WHO) recommends a maximum boron concentration in the drinking water below 0.3 mg/L as a provisional guideline value, while the Japanese Water Quality Standard for Drinking Water of 1998 tolerates a boron concentration of 1.0 mg/L [2]. Boron concentration in standard seawater composition is approximately 4.5 mg/L and, in general, it is difficult to bring boron content down to WHO levels in one-stage due to its size and charge.

For what concerns arsenic, it is used in a large variety of industries, such as:

- ✓ *chemical industrial, primarily as wood preservatives*, in the form of a compound called *chromated copper arsenate* (CCA). CCA is added to wood used to build houses and other wooden structures. It prevents organisms from growing in the wood and causing it to rot;
- ✓ *agricultural chemicals*. Today agricultural use of arsenic is limited to the insecticides, herbicides, algicides, growth stimulants for plants and animals, for weed control in cotton fields. Prior to the introduction of DDT in the 1940s, most pesticides were made from inorganic arsenic compounds.
- ✓ *Ceramics and glass products*. Arsenic compounds remove dispersed air bubbles and colour in glass manufacturing.
- ✓ *Electronics and nonferrous alloys*. Extremely high-purity arsenic (99.999%) is used to make gallium arsenide (GaAs) or indium arsenide which are employed in the manufacture of semiconductors. GaAs is used in light-emitting diodes (LEDs) and solar cells. Indium arsenide is used to produce infrared devices and lasers. Arsenic is added to *germanium* and *silicon* to make transistors.
  Arsenic serves a variety of other functions in the electronics industry: it is used in the manufacture of microchips, in the processing of gallium arsenic crystal, as a

dopant in silicon wafers, to manufacture arsine gas (which is used to make superlattice materials, lightwave devices and high performance integrated circuits). Arsenic metal also increases corrosion resistance and tensile strength in copper alloys and strengthens posts and grids in lead acid batteries.

Between 1990 and 1995 U.S. consumption of As grew from 20,500 metric tons to 22,300 metric tons. In Massachusetts, As consumption increased 13% between 1990 and 1996. Driving the increase in use was the electronics industry, which did not report any use of arsenic in 1990, but reported almost 73,000 pounds in 1996.

People are exposed to arsenic on a daily basis:

- ✓ residents living near metal smelters or facilities that burn plywood or other arsenic-treated wood products may be exposed to elevated levels of inorganic arsenic;
- ✓ the refuse from discarded electronics products, also known as e-waste (Table 1), often ends up in landfills or incinerators instead of being recycled. That means toxic substances like lead, cadmium, mercury and arsenic that are commonly used in these products, can contaminate the land, water and air.

Table 1: Toxic substances contained in the refuse from discarded electronic products.

Substance	Occurrence in e-waste
Heavy metals and other metals:	
Arsenic	Small quantities in the form of gallium arsenide within light emitting diodes
Barium	Getters in CRT
Beryllium	Power supply boxes which contain silicon controlled rectifiers and x-ray lenses
Cadmium	Rechargeable NiCd-batteries, fluorescent layer (CRT screens), printer inks and toners, photocopying-machines (printer drums)
Chromium VI	Data tapes, floppy-disks
Lead	CRT screens, batteries, printed wiring boards
Lithium	Li-batteries
Mercuri	Fluorescent lamps that provide backlighting in LCDs, in some alkaline batteries and mercury wetted switches
Nickel	Rechargeable NiCd-batteries or NiMH-batteries, electron gun in CRT
Rare Earth elements (Yttrium, Europium)	Fluorescent layer (CRT-screen)
Selenium	Older photocopying-machines (photo drums)
Zinc sulphide	Interior of CRT screens, mixed with rare earth metals
Halogenated compounds:	
PCB (polychlorinated biphenyls)	Condensers, Transformers
TBBA (tetrabromo-bisphenol-A) PBB (polybrominated biphenyls) PBDE (polybrominated diphenyl ethers)	Fire retardants for plastics (thermoplastic components, cable insulation). TBBA is presently the most widely used flame retardant in printed wiring boards and casings.
Chlorofluorocarbon (CFC)	Cooling unit, Insulation foam
PVC (polyvinyl chloride)	Cable insulation
Others:	
Toner Dust	Toner cartridges for laser printers / copiers
Radio-active substances	
Americium	Medical equipment, fire detectors, active sensing element in smoke detectors

Several studies have linked long-term exposure to arsenic in drinking water to cancer of the bladder, lungs, skin, kidney, nasal passages, liver and prostate. Non-cancer effects include cardio-vascular, pulmonary, immunological, neurological and endocrine (e.g. diabetes) disorders. Besides its tumorigenic potential, arsenic has bees shown to be genotoxic [3]. A National Academy of Sciences' report on the potential adverse health effects from arsenic in drinking water at the existing 50 μg/L Maximum Contaminant Level (MCL) prompted the U.S. Environmental Protection Agency (EPA) to change the 50 years old MCL to 10 μg/L (an 80% reduction). This new law has taken effect in January 2006 [4, 5]. The Agency estimates that 5.5% of the nation's 54,000 community water systems and 5.5% of the 20,000 non-community water systems (about 4,100 in all) would need to take measures to achieve compliance [5]. Further, an additional 40 million Americans who obtain their water from private wells, which are not protected by the new standard, may want to invest in new technologies that ensure that their water supply is safe [5].
As a consequence, nowadays, the number of water treatment plants equipped with boron and arsenic removal facilities is growing but, as in the case of boron, also arsenic removal is complicated because of its size and charge.

The objectives of the work presented in this Chapter are: 1) to examine the efficiency of different pressure driven membrane processes for boron and arsenic removal from water; 2) to test experimentally the performance of Membrane Distillation for water purification; 3) to analyse the efficiency of an integrated membrane system for the contaminants removal from water. In the proposed flow sheet, pressure-driven membrane operations have been synergically joined with membrane distillation technology. In order to evaluate the convenience and the feasibility of the proposed integrated membrane system, the characteristic parameters of the process (such as energetic consumption, exergetic efficiency and cost) are compared with those obtained in conventional membrane treatment plants.

2. Boron and arsenic chemistry

Seawater ordinarily contains 1÷8 μg/L of arsenic with an average of 2.6 μg/L [4, 6]. The concentration of arsenic in unpolluted fresh waters typically ranges from 1÷10 μg/L, rising to 100÷5000 μg/L in areas of sulphide mineralization and mining [4, 6]. In natural environment, arsenic is rarely encountered as the free element. It can occur in four oxidation states (-3, 0, +3, +5). Occurrence, distribution, mobility and forms of arsenic rely on the interplay of several geochemical factors, such as pH conditions, reduction-oxidation reactions, distribution of other ionic species [4].
Pentavalent arsenic is normally found in water as arsenic acid which ionizes according to the following equations [7, 8]:

$$H_3AsO_4 \Rightarrow H_2AsO_4^- + H^+ \qquad pK_{a,1}= 2.2,\ K_1 = 5.10^{-3}$$

$$H_2AsO_4^- \Rightarrow HAsO_4^{2-} + H^+ \qquad pK_{a,2}= 7.08,\ K_2 = 4.10^{-5}$$

$$HAsO_4^{2-} \Rightarrow AsO_4^{3-} + H^+ \qquad pK_{a,3}= 11.5,\ K_3 = 4.10^{-10}$$

(where pKa is the pH at which the disassociation of the reactant is 50% complete).

Groundwater is often reducing. In reducing waters, arsenic is found primarily in the trivalent form (As(III)) as same forms of arsenious acid which ionizes according to the equations:

$H_3AsO_3 \Rightarrow H_2AsO_3^- + H^+$ $pK_{a,1}= 9.22, K_1 = 6.10^{-10}$

$H_2AsO_3^- \Rightarrow HAsO_3^{2-} + H^+$ $pK_{a,2}= 12.3, K_2 = 1.10^{-14}$

$HAsO_3^{2-} \Rightarrow AsO_3^{3-} + H^+$

Dissolved As(V) and As (III) have been found to simultaneously exist in many contaminated groundwaters. Experience has shown that trivalent arsenic is difficult to remove from water using the normally available treatment processes. It is usually necessary to change the arsenic to the pentavalent form by adding an oxidant, generally chlorine.

Human activities, geological factors and microbial agents can influence the oxidation state of arsenic in water and can mediate the methylation of inorganic arsenic to form organic arsenic compound [3]. Microorganisms can oxidize arsenite to arsenate, reduce arsenate to arsenite or even to arsine (AsH_3). Bacteria and fungi can reduce arsenate to volatile methylarsines. Marine algae transform arsenate into non-volatile methylated arsenic compounds such as methylarsonic acid ($CH_3AsO(OH)_2$) and dimethylarsinic acid ($(CH_3)_2AsO(OH)$) in seawater. Organic arsenical compounds were reported to have been detected in surface water more often than in ground water.

Methylated forms of arsenic may be present in biologically active waters, however these arsenic forms are generally thought to be unimportant in drinking water sources [9].

In drinking water the two common oxidation states are trivalent (As(III)) and pentavalent (As(V)). Pentavalent arsenic is the thermodynamically stable form of inorganic arsenic in water, particularly in oxygenated conditions and generally predominates in surface water. The ratio of As(V) to As(III) based on thermodynamic calculation should be 10^{26}:1 for seawater at pH 8.1 [6]. In reality, it is 0.1:1 to 10:1. This unexpected high As(III) content is caused at least in part by biological reduction in seawater [6]. Both As(III) and As(V) occur in several forms; at near-neutral pH, the predominant species are H_3AsO_3 for As(III), and $H_2AsO_4^-$ and $HAsO_4^{2-}$ for As(V). It means that at typical pH in natural water (pH 5÷8), As(V) exists as an anion, while As(III) remains as a neutral molecule.

For what concerns boron, its average concentration in raw water is 4.5 mg/L [10]. Boron is usually present in water as boric acid which is not well rejected by RO membranes. The boron rejection performance is increased in the alkali region by the two following effects:

a. *effect of atomic or molecular size.* Boron exists as boric acid in the natural water. It is a weak acid and its dissociation proceeds as shown by the following formulas [11]:

$H_3BO_3 \Leftrightarrow H^+ + H_2BO_3^-$ $pKa = 9.14$

$H_2BO_3^- \Leftrightarrow H^+ + HBO_3^{2-}$ $pKa = 12.74$

$HBO_3^{2-} \Leftrightarrow H^+ + BO_3^{3-}$ $pKa = 13.8$

At high pH values (alkali conditions), dissociation proceeds, ionization takes place and a hydration radius is achieved which is greater than that of the boron molecule. The rejection performance of the RO membrane therefore improves.

b. *Effect of electrical charge of the molecule.* In the alkali region, ionization of boron causes a negative charge and, since the RO membrane also has a negative charge, the two repel each other and the rejection performance of the RO membrane is enhanced.

As normal seawater is in the range of neutral pH (from 7 to 8.5), boron doesn't dissociate and the boron molecular form exists without electrical charge. Therefore, the two effects described above do not occur and the boron rejection by the RO membrane is low. A treatment in which normal seawater would be directly rendered alkali to achieve the boron to dissociation cannot be adopted because the many hardness components contained in the seawater would give scaling problems at high pH levels. Given the above conditions, nowadays, the most parts of seawater desalination plants use RO systems with several pass-stages. At the first pass-stage, the salt in the seawater is removed along with most of the boron. By treating the resulting product water with other boron removal RO membrane elements at ultra-low pressure working at high pH and, eventually, with boron selective resins, the boron concentration is brought to below the regulation value.

3. Pressure Driven Membrane Processes for Pollutants Removal from Water

Membrane filtration is a viable method to remove a wide range of contaminants from water. As described in detail in *Chapter 1*, pressure driven membrane operations can be divided into four overlapping categories of increasing selectivity: Microfiltration (MF), Ultrafiltration (UF), Nanofiltration (NF) and Reverse Osmosis (RO).

In general, driving pressure increases as selectivity increases. Separation is accomplished by MF and UF membranes via mechanical sieving, while capillary flow or solution diffusion is responsible for separation in NF and RO membranes. However, membrane composition combined with solvent and solute characteristics can influence rejection via electrostatic double layer interactions or other hindrances. When a solution containing ions is brought in contact with membranes possessing a fixed surface charge, the passage of ions possessing the same charge as the membrane (co-ion) can be inhibited. This condition is termed Donnen Exclusion. More specifically, when a solution with anionic arsenate is brought in contact with a membrane possessing a fixed negative charge, the rejection of arsenate may be greater than if the membrane is uncharged. Hence, the selection of a membrane possessing a slight negative charge may be advantageous for the removal of arsenic and boron from drinking water.

3.1 Pressure Driven Membrane Processes for Boron Removal. Current situation

Recently Toray [12], Hydranautics [11] and FILMTEC^{TM} [13, 14] have focused attention on the development of RO membranes with high boron-rejection.

The Hydranautics proposes the following RO membranes for the first-pass: SWC3, SWC3+, SWC4 or SWC4+. The boron rejection of these membranes is 89%, 91%, 92% and 93%, respectively, higher than that of the conventional elements. However, these values still do not produce desalted water with boron concentration that satisfy the WHO drinking water quality guidelines. Therefore, as described above, the product water from the first-stage seawater desalination RO membrane is treated to raise its pH to the level of 9.5 and then sent to a second-stage RO membrane for boron removal. Finally, the product water from the second-stage membrane is treated by adding acid to adjusted the pH until the value recommended by WHO. Membranes to be used in the second-stage are, for example, ES20 or ES20B by Hydranautics.

The ultra-low pressure RO membrane ES20B for boron removal has been adopted by a seawater desalination plant in Fukuoka (50,000 m^3/d) and is now on operation since May 2005. The RO membrane SWC4 has been introduced in a seawater desalination plant at Tampa (Florida), which has a production capacity of 100,000 m^3/d and a water production cost of 0.53 $/$m^3$, less than that of a conventional distillation process but still far too high for agricultural use.

Toray proposes instead to use single stage RO operations, with TM820A membranes. The boron rejection in these membrane elements is 94-96%, values that allow to meet only Japanese Water Quality Standard. But in severe condition, for the WHO guideline grade or the Middle East seawater treatment (with the highest boron concentration), rejections between 97 - 99% are needed.

FILMTEC SW30HR LE-400 has a boron rejection performance of 91%. Therefore, a boron concentration less than 1.0 mg/L can usually be achieved with a single pass. For boron removal less than 0.3 mg/L, also in this case, a second pass is required, as well as the use of a boron-selective resin.

More than 40,000 FILMTEC RO membrane elements are contained in the world's largest desalination plant in Ashkelon, Israel, where high boron ion reduction was an important design consideration. In fact, the desalination facility consists of 32 RO treatment trains and uses a multi-stage RO and boron removal procedures capable of delivering a boron removal efficiency of more than 92% [15, 16].

One pass SWRO has been proposed for projects requiring 0.8 to 1.0 mg/L boron concentration in the RO permeate, where boron in the seawater feed is in the order of 4.0-5.0 mg/L and the sea-water temperature range is 18-26°C. The typical water production cost for this concept is in the range of US$0.38-0.52/$m^3$ of product [14].

Seawater desalination systems characterized by two passes with increased pH have been widely proposed for processes where the product boron requirement is between 0.3 and 0.5 mg/L and the boron concentration of the seawater feed ranges between 4.0 and 6.3 mg/L. They have also been used for water temperatures up to 34°C. The typical unit cost for this option is in the range ofUS$0.45-0.55/$m^3$ product water [14].

3.2 Pressure Driven Membrane Processes for Arsenic Removal. Case study.

Two types of membrane processes have been demonstrated to be effective in removing arsenic from water: RO and NF. Moreover, in literature many examples show that both of these processes are more effective in removing As(V) than As(III) (Table 2). Thus, to achieve the best results, the feed water must be treated with an oxidizing agent to

convert As(III) to As(V) in order to obtain substantial arsenic reduction in the permeate, that is the water produced by membrane process.

Table 2: NF membranes rejection (%) for Arsenic removal.

Membrane and manufacturer	Water origin	Rejection (%) As(III)	Rejection (%) As(V)	Reference
NF70 4040B, Film Tec (Dow Chemical)	Pilot studies at various ground-water sites (USA)	50%	99%	[9]
HL-4040F1550, Desal	Idem	20%	99%	[9]
4040-UHA-ESNA Hydranautics	Idem	30%	97%	[9]
ES-10, Aromatic polyamid (Nitto)	Groundwater spiked with 0,6 mg/l As (Japan)	50-89%	90-97%	[17]
NF45 Filmtec (Dow Chemical)	Synthetic water	-	90%	[18]
ES-10, (Nitto Electric Industrial, Japan)	Synthetic water and groundwater	60-80% 60-80%	95% >95%	[19]
NTR-729HF, (PVA), (NittoElectric Industrial, Japan)	Synthetic water and groundwater	10-23% 10-23%	91-94% 95%	[19]
NTR-7250 (PVA), (NittoElectric Industrial, Japan)	Synthetic water and groundwater	10% 10%	86% >90%	[19]

The purpose of this section is to analyse the quantity of arsenic in the fresh water produced by NF and/or RO membrane processes. Arsenic is often measured as total arsenic concentration. However, it is necessary to measure the individual concentrations of arsenic compounds because they have different rejection characteristics and also different toxicity. According to literature, the ratio of As(V) to As(III) should be 4:1 for groundwater and river [19, 20]. Analysing samples from a 65,000 m^3/d water treatment NF plant, Sato et al. [19] have determined As(III) and As(V) rejections and the following conclusions were obtained:

1. arsenic removal efficiency increased slightly (under 4.0%) with the increase in applied pressure for each of the three NF membranes utilized (Table 3). This was attributed to the growth in permeate flux as the applied pressure increased, which resulted in lower arsenic concentration in the permeated water [19, 21].

Table 3: As(III) and As(V) rejections. Applied pressure is 1.1 MPa. Temperature is 20°C. Total arsenic and trivalent arsenic concentrations are about 50 mg/l and 10 mg/l, respectively [19].

Membrane types	As (III) rejection [%]	As (V) rejection [%]
ES-10	80	97.5
NTR-729HF	22	94
NTR-7250	11	86

2. Removal efficiency of As(V) and As(III) was almost the same in both synthetic water and groundwater (Figure 1). Therefore, it can be said that other ions in groundwater have no effect on the removal of As(V) and As(III). Because both As(V) and As(III) removals by NF membranes were not affected by source water composition, it is suggested that NF membrane can be used in any types of waters.

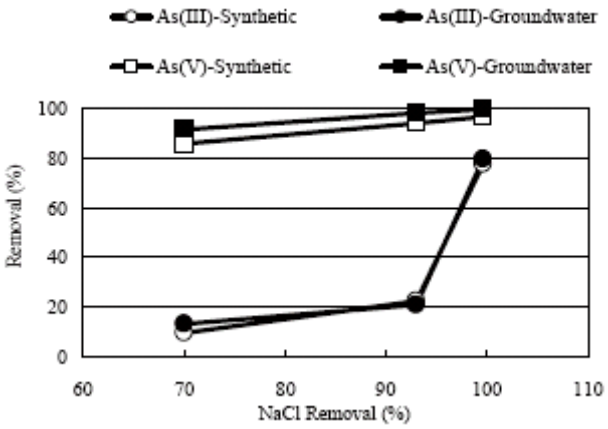

Figure 1: Comparison of synthetic water and groundwater for As removal by three different types of NF membranes (NTR-7250, NTR-729HF and ES-10). Applied pressure is 0.75 MPa.

3. The rejection of As(V) seemed not to be sensitive to the change in operating temperature [21].

4. The As(III) rejection decreases with increasing bulk concentration, an effect that was attributed to its enhanced diffusion and convection through the membrane [22].

By considering the NF membrane modules with the As(III) and As(V) rejection values reported in Table 3 and a ratio of As(V) to As(III) equal to 4:1 [19, 20], Table 4 shows the total permeate arsenic concentration when the feed water is treated by a **NF operation**. According to the table, ES-10 shows an arsenic permeate concentration below 10 ppb (EPA and WHO recommended As limit), at a maximum total As concentration in feed water of about 200 ppb.

Table 4: Permeate arsenic concentration by a single stage NF operation*.

Total As concentration in the feed water [ppb]	Permeate As concentration [ppb]		
	ES-10	NTR-729HF	NTR-7250
50	3	10,2	14,5
100	6	20,4	29
200	12	40,8	58

* The cells reported in grey refer to limit As concentration recommended by EPA and WHO.

As already said, the feed water can be treated **with an oxidizing agent** to convert As(III) to As(V) in order to improve removal efficiencies. For example, chlorine oxidizes approximately 95% of arsenite in arsenate (in less than 5 s at chlorine concentration of 1.0 mg/L); monochloramine at the concentration of 1.0 mg/L oxidizes 45% of As(III) in As(V) [3]. Table 5 shows the total permeate arsenic concentration when the feed water is pre-treated with chlorine before to be sent in a single stage NF operation. According to the table, the membrane ES-10 allows to obtain a permeate

stream with arsenic concentration below 10 ppb at a maximum total As concentration in feed water of about 400 ppb.

Table 5: Permeate arsenic concentration by a single stage NF operation with pre-oxidation.

Total As concentration in the feed water [ppb]	Permeate As concentration [ppb]		
	ES-10	NTR-729HF	NTR-7250
50	1,3	3,4	7,4
100	2,7	6,7	14,8
200	5,4	13,4	29,5
300	8,0	20,2	44,3
400	10,7	26,9	59,0

Table 7 shows the total permeate arsenic concentration when the feed water is treated by a **RO operation**, without and with pre-oxidation. The TFC-ULP reverse osmosis membrane, from Koch Membrane System, has been considered (Table 6).

Table 6: As(III) and As(V) rejections with RO membrane [20].

Membrane RO type	As (III)	As (V)
TFC-ULP	0.925	0.975

Table 7: Permeate arsenic concentration by a single stage RO operation.

Total As concentration in the feed water [ppb]	Permeate As concentration [ppb]	Permeate As concentration with pre-oxidation [ppb]*
50	1.75	1.3
100	3.5	2.6
200	7	5.1
300	10.5	7.7
400	14	10.2

According to the Table 7, the RO membrane employed, without and with the pre-oxidation step, shows an arsenic permeate concentration value below 10 ppb at a maximum total As concentration in feed water of about 300 and 400 ppb, respectively. Therefore, RO membrane allows to treat water with an higher As concentration feed water than NF membrane.

RO and NF membrane processes have both an excellent arsenic removal efficiency. However, an integrated NF/RO membrane system, in which the feed water is firstly treated with a NF unit and its permeate is sent to a RO unit, can become more and more interesting than the single membrane operation. In fact, the integrated system allows to be below the EPA and WHO recommended As limit also treating feed water with As concentration equal to 3000 ppb (Table 8).

Table 8: Permeate arsenic concentration by a NF/RO operation.

Total As concentration in the feed water [ppb]	Permeate As concentration [ppb]		
	ES-10 and TFC-ULP	NTR-729HF and TFC-ULP	NTR-7250 and TFC-ULP
50	0,18	0,65	0,81
100	0,35	1,29	1,62
200	0,70	2,58	3,23
300	1,05	3,87	4,85
400	1,40	5,16	6,46
500	1,75	6,45	8,08
600	2,10	7,74	9,69
700	2,45	9,03	11,31
800	2,80	10,32	12,92
900	3,15	11,61	14,54
1000	3,50	12,90	16,15
2000	7,00	25,80	32,30
3000	10,50	38,70	48,45

4. Integrated Membrane Processes for Water Purification

The possibility of designing innovative processes based on the integration of different membrane operations is becoming quite attractive as a way for increasing the performance of the desalination/purification processes (Table 8). As already stated and proved in the *Chapters 1, 2 and 3*, in the last decade the success of RO technology is also the consequence of the development of other pressure driven membrane operations which often are combined with the RO unit for the pre-treatment or post-treatment steps in order to overcome the limits of the single units.

In this logic, the introduction of MD on RO brine allows to increase the recovery factor of the water treatment plant. Moreover, since MD operates on the principles of vapour-liquid equilibrium, 100% (theoretical) of ions, macromolecules, colloids and other non-volatile components are rejected. As a consequence, MD process can be used for the treatment of polluted water in order to convert it into pure water and in a concentrate containing the substances present in the feed solution.

Therefore, MD can be used also for boron and arsenic removal from water in order to obtain a their substantial reduction in the permeate streams of desalination plants.

A possible integrated membrane system able to remove boron and arsenic from raw/brackish/sea-water is represented in Figure 2.

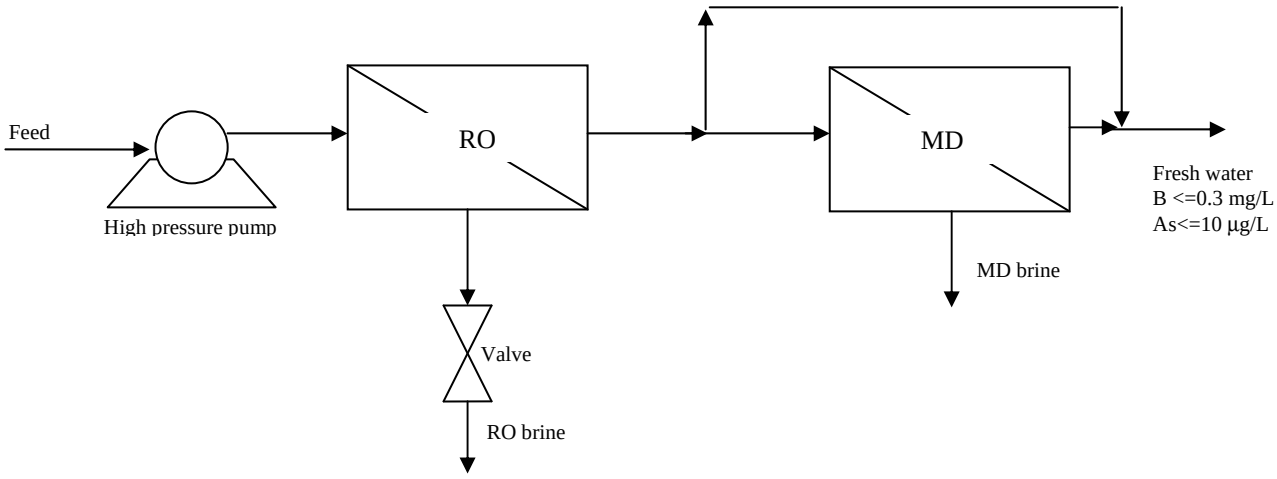

Figure 2: An integrated membrane flow-sheet.

The proposed system is constituted by a Reverse Osmosis step followed by a Membrane Distillation one. Seawater is treated with chemical agents and then it is fed to RO units. In order to achieved the desired boron and arsenic content in the fresh water produced, a fraction of the RO permeate is sent to the MD module.
In the flow sheet, as feed water composition the standard seawater composition with an arsenic concentration equal to 400 ppb (Table 9) has been considered.
Table 10 shows the RO and MD rejection values and performance. They are referred to a SW1 PA and MD020CP-2N Enka Microdyn membrane modules, respectively. The RO and MD feed water flow rates and operation conditions has been taken from [23, 24].

Table 9: Standard seawater composition [25].

Chloride:	19,345 mg/L
Sodium:	10,752 mg/L
Sulphate:	2,701 mg/L
Magnesium:	1,295 mg/L
Calcium:	416 mg/L
Potassium:	390 mg/L
Bicarbonate:	145 mg/L
Boron:	4.5 mg/L
Arsenic:	0.400 mg/L
TDS: 35,000 mg/L	- pH: 8.1

Table 10: Rejection values and recovery factors [23, 24].

Membrane Type	RO	MD
Recovery factor [%]	40.08	77
Rejection values [%]		
HCO_3^-	98.46	≈100%
Na^+	98.92	
Cl^-	98.95	
SO_4^{2-}	99.63	
Ca^{2+}	99.69	
Mg^{2+}	99.56	
As(III) [20]	92.50	
As(V) [20]	97.50	
Boron	90.00	

According to literature, the ratio of As(V) to As(III) considered in the feed has been 4:1 [19, 20].
In Table 11 the achieved fresh water composition is reported. In the proposed system, in order to obtain a boron and arsenic concentration in fresh water equal or less than the recommended values by EPA and WHO, only 36.4% of RO permeate must be treated in the MD unit while, nowadays, in the current water treatment plants, all the 1st stage RO permeate must be treated in the 2nd RO stage [11-14].

Table 11: Fresh water composition.

Ion	Concentration [g/L]
Cl	1.354 E-01
Na	7.741E-02
SO4	6.662E-03
Mg	3.799E-03
Ca	8.597E-04
HCO3	1.489E-03
As(III)	4.000E-06
As(V)	5.333E-06
As (total)	9,333E-06
B	3.000E-04
Total	0.23

Material	Polypropylene
Type	Hollow fiber
No. of fibers	40
Available area [m^2]	0.1
Packing density [%]	70

Table 12: Structural Parameters of an Enka Microdyn MD020CP-2N Module.

5. Evaluation of Membrane Distillation technique for Boron and Arsenic removal from water

In order to test the performance of membrane distillation for total boron and arsenic removal from water, several experimental tests have been carried out.

The used experimental apparatus (Figure 3) employs Enka Microdyn MD020CP-2N membrane module (Table 12). The plant is supplied with centrifugal pumps and with the necessary tools for the control of the most significant parameters of the system: flow rate and temperature. Flow rate control is achieved through Brooks Instruments mass flow-meters, with a capacity of up to 5.7 L/min, placed at the outlet of the pumps on the retentate and permeate lines; four platinum thermocouples (Pt100) disposed at the inlet and outlet of the module on the retentate and permeate lines allow a quantification of the thermal drop.

The estimation of the trans-membrane flux occurs by evaluating weight variations in the distillate tank with a Precisa 6200 DSCS balance.

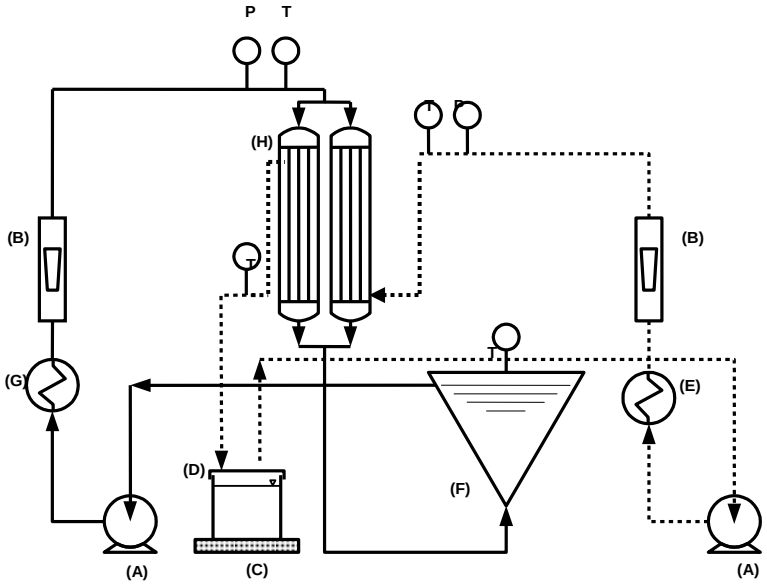

Figure 3: Schematic flow sheet of the lab plant: (A) pump; (B) flow-meter; (C) balance; (D) distillate tank; (E) cooler; (F) feed tank; (G) heater; (H) membrane module; (I) retentate tank.

In order to carry out the experimental tests, synthetic aqueous solutions have been prepared by dissolving the appropriate quantities of chemical reagents in demineralised water also utilized as condensing liquid on the permeate side.

The concentration of arsenic and boron in feed and permeate solutions has been measured with Optima 2100 DV Optical Emission Spectrometer supplied by PerkinElmer precisely. Because it allows to identify the arsenic content in water solution but it does not distinguish between arsenite and arsenate, than two different series of experimental tests have been conducted. At the beginning, only arsenate aqueous solutions and the MD performance for As(V) removal have been investigated. Then, a second series of lab-tests with arsenite solutions have been conducted to check the absence of As(III) in the fresh water obtained by MD process.
Such as chemical reagent has been employed H_3BO_3, $As_2O_5 \cdot 3H_2O$ and As_2O_3 supplied by Sigma-Aldrich.

5.1 Experimental tests

In order to have mass trans-membrane flux from feed to permeate it is necessary a driving force that, in membrane distillation process, is represented by the partial pressure difference across the membrane, which can be imposed by a temperature difference across the membrane.
For this reason, experimental tests varying the following parameters have been conducted:

- concentration of boron and arsenic in feed solution;
- temperature of the solution fed to the membrane module (from 25 to 35°C);
- MD retentate flow rate (from 100 to 250L/h), while MD distillate flow rate was kept constant and equal to 100 L/h.

In literature there are many studies that show as arsenic rejection changes with pH of feed solution in fact, an increase (about 20%) in arsenic (both As III and As V) removal has been observed at pH value rising from 7 to 9 and from 3 to 5 respectively, indicating the importance of finding the optimum operating pH values even for membrane treatments. As already said MD allows 100% (theoretical) rejection of non-volatile components. In any case, in order to verify that and to show if trans-membrane flux changes with pH, it has been chosen to conduct experimental tests at different pH (from 5 to 9).

5.2 Results and discussion

Permeate samples have been withdrawn from the distillate tank every 60 minutes and analysed in order to measure the amount of contaminants passed through the membrane. All the analysed samples have proven the absence of B, As(V) and As(III) in the permeate streams. Therefore, the application of membrane distillation allows to achieve the total boron and arsenic rejection, value not easily reachable with other removal technologies.

The experimental tests have also allowed to test both fluid-dynamic and feed temperature/concentration effect on membrane distillation operation and, in particular, on trend of solvent trans-membrane flux.
For each test, the water fluxes J at different feed temperatures and concentrations have been evaluated and the results are shown in Figures 4 - 6.

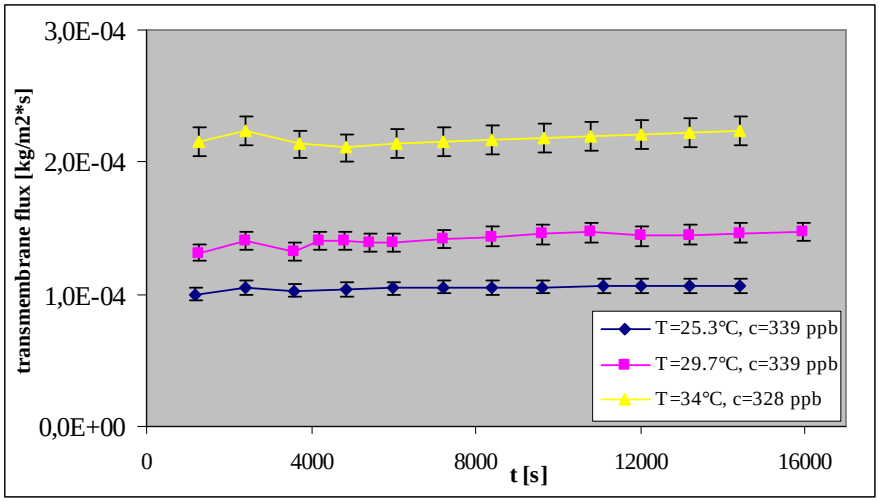

Figure 4: Trans-membrane flux vs time at three different feed temperatures (c=As(V) feed concentration ≈ 339 ppb, feed flow rate=100 L/h).

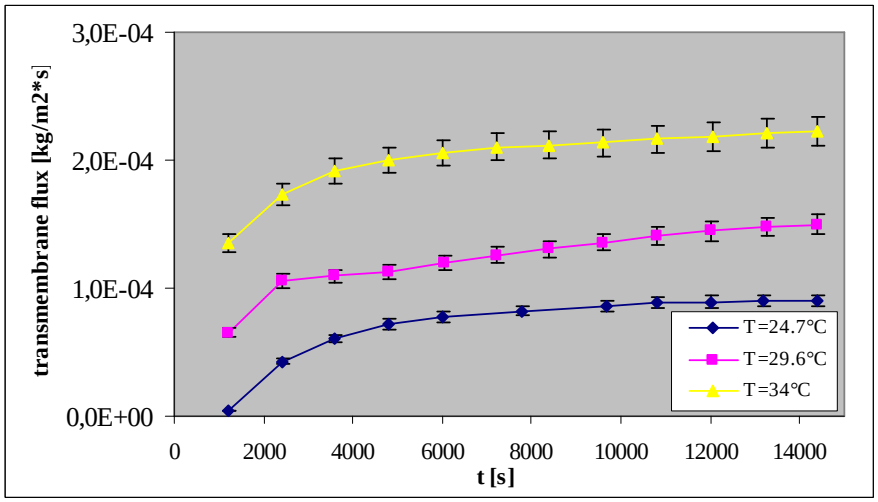

Figure 5: Trans-membrane flux vs time at three different feed temperatures (c=As(V) feed concentration ≈ 1200 ppb, feed flow rate=100 L/h).

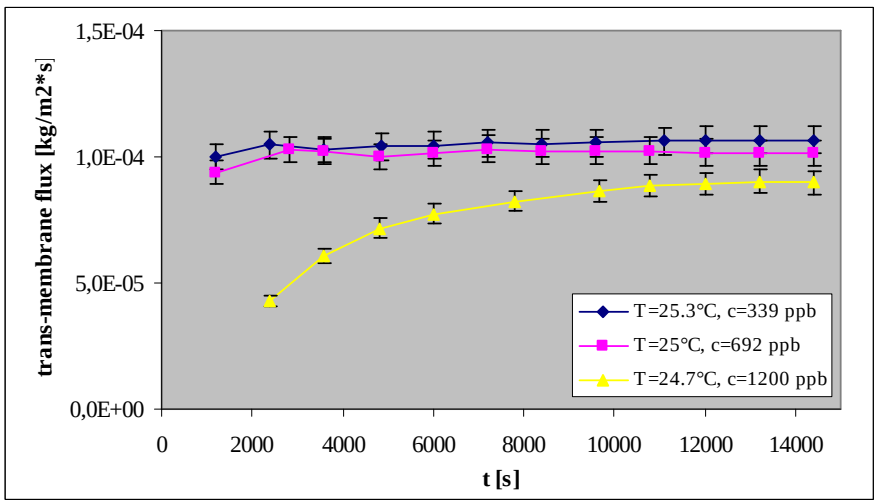

Figure 6: Trans-membrane flux vs time at three different As(V) feed concentrations (feed temperature ≈ 25°C, feed flow rate=100 L/h).

Figures 4 - 6 show that trans-membrane flux increases when feed temperature increases (since MD is a temperature driven membrane operation) and when feed concentration decreases. The latter trend is because concentration influences viscosity: when it increases, vapour pressure and transport coefficients decrease and, as a consequence, polarization phenomena accentuate themselves. However, at steady-state the fluxes are close each other confirming that, in membrane distillation operation, concentration polarization phenomena do not play a significant role.

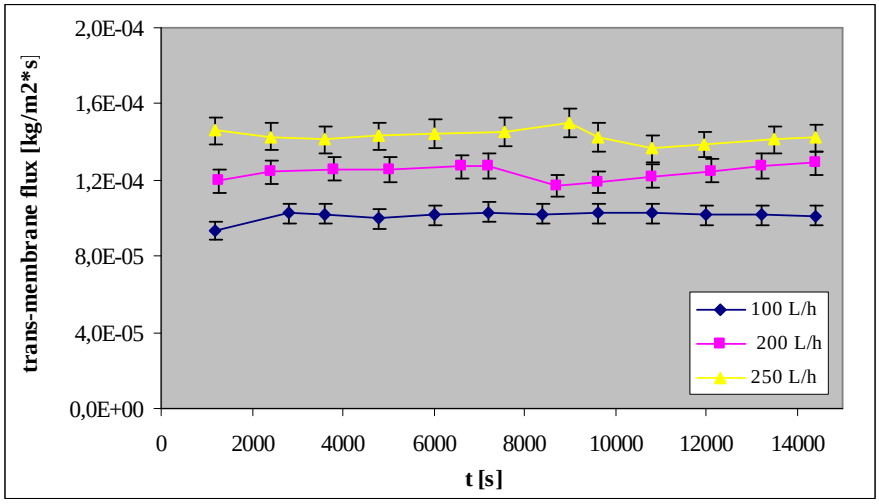

Figure 7: Trans-membrane flux vs time at three different feed flow rates (feed temperature = 25°C, As(V) feed concentration=692 ppb).

Figure 7 shows how water trans-membrane flux increases with retentate flow rate due to the enhancement of transport coefficients.
Analogous results were obtained also with As (III) and B aqueous solutions.

6. Economical Evaluation, Energetic and Exergetic Analysis of four different Membrane-Based Desalination Systems for water purification

From the achieved results through the experimental tests, adoption of membrane distillation system appears a promising process for water purification since it permits to remove completely boron and arsenic from waters.
The main obstacles impeding the implementations of MD processes are, as seen in *Chapter 3*, the relatively high energy consumption, membrane fouling and, as a consequence, high membrane maintenance and replacement cost. In particular, it is necessary to guarantee the hydrophobic character of the MD module.
In order to check if the coupled system RO+MD (described in *Section 4*) can really represent an interesting and economically advantageous alternative to conventional water treatment plants, ***four*** different flow sheets for water treatment have been analysed: the first one is constituted only by the RO unit; in the second, feed water is pre-treated **with an oxidizing agent** to convert As(III) to As(V) in order to improve removal efficiencies and, then, sent to the RO unit (in this work 1.0 mg/L of chlorine was used to oxidize approximately 95% of arsenite in arsenate) [3]. The third flow sheet use RO systems with two pass-stages: at the first pass-stage, the salt in the seawater is

removed along with most of the boron; by treating the resulting product water with other boron removal RO membrane elements working at high pH, the boron concentration is brought to the regulation value (Figure 8). In the forth, a fraction of RO permeate is sent to MD operation (Figure 2).
In all the analyzed flow sheets the same feed flow rate and composition has been used (see Tables 9 and 13).

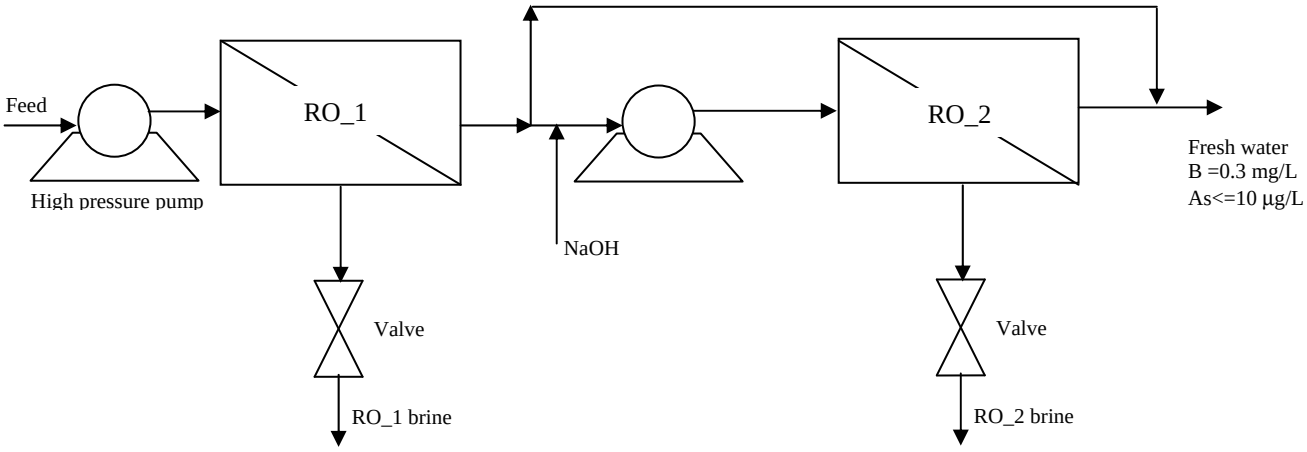

Figure 8: Two RO passes with increased pH.

In the flow sheet with two RO passes (Figure 8), recoveries of 40.1% in the 1st and 85% in the 2nd pass have been considered [14]. Depending on pH value, recovery, Ca and Mg rejection of the membranes, care needs to be taken for $CaCO_3$ and $Mg(OH)_2$ scaling. Anti-scalant use was considered. Moreover, the fraction of first-stage RO permeate sent to the RO second-stage has been optimized in order to obtain a boron and arsenic concentration in the fresh water stream equal to the maximum recommended values.

Table 13 shows energy consumption, product characteristics and desalted water cost for the analysed systems.

Table 13: Product characteristics, energy consumption and desalted water cost for four different flow sheets.

Flow Sheet	RO	RO with pre-oxidation step	RO-RO	RO-MD
Feed flow rate [m^3/h]	1048E+03	1048E+03	1048E+03	1048E+03
Brine flow rate [m^3/h]	628	628	654	666
Brine concentration [g/L]	57.6	57.6	55.4	54.4
Fresh water flow rate [m^3/h]	421	421	395	383
Fresh water concentration [g/L]	0.339	0.339	0.211	0.226
Recovery rate [%]	40.1	40.1	37.6	36.4
As concentration in fresh water [g/L]	1.400E-05	1.020E-05	6.417E-06	9.333E-06
B concentration in fresh water [g/L]	4.500E-04	4.500E-04	3.000E-04	3.000E-04
Elect. energy consumption [KWh/h]	2206	2206	2577	2206
G_V [Kg/h] (c)	/	/	/	9327
Primary Energy (PE) [Mcal/h] (d)	/	/	/	7462
Quantity of energy required per m^3 of fresh water produced [KWh/m^3]	5.24	5.24	6.53	28.4/5.76[b]
Quantity of energy required per m^3 of fresh water produced [KWh/m^3][(a)]	2.69	2.69	3.70	25.6/2.96[b]
Unit cost [$/$m^3$]	0.614	0.616	0.740	0.967/0.797[b]
Unit cost [a] [$/$m^3$]	0.398	0.399	0.50	0.729/0.559[b]
Wu [KJ/h]	7,942E+06	7,942E+06	9,279E+06	7,942E+06
W'u [KJ/h]	0	0	0	4,950E+06
Dex [KJ/h]	-1,972E+04	-1,972E+04	-1,973E+04	1,161E+04
RsTo [KJ/h]	7,962E+06	7,962E+06	9,298E+06	1,288E+07
RsTo [KJ/h][b]	7,962E+06	7,962E+06	9,298E+06	7,930E+06

(a) If Pelton turbine is used as energy recovery device.
(b) If thermal energy is available in the plant or the stream is already at the operating temperature of the MD unit.
(c) The term G_V represents the steam mass flow required to warm up the MD feed flow rate.
(d) PE represents the energy supplied by fuel combustion to produce thermal energy.

The values reported in Table 13 clearly show that only the two integrated systems RO-RO and RO-MD allow to obtain fresh water with boron and arsenic concentration below the WHO and EPA maximum recommended values. Moreover, the achieved desalted water cost for the third flow-sheet with Pelton turbine like energy recovery system is in good agreement with the corresponding values (0.45-0.55 $/$m^3$) found in literature [14]. For what concerns energy consumption and water cost, the system with MD unit (the fourth) has the higher energy demand due to the retentate flow rate which has to be heated. However, in membrane distillation the required operating temperature is much lower than that of a conventional distillation column because it is not necessary to heat

the process liquids above their boiling temperatures. Therefore, low-grade, waste and/or alternative energy sources, such as solar and geothermal energy, can be coupled with MD systems for a cost and energy efficient liquid separation system. As a consequence, if the water streams are already available at the temperature needed for carrying out the MD operation or thermal energy is available in the plant, the energy requirements, the entropic losses and the desalted unit water cost of the RO-MD process decrease reaching competitive values with those of the other processes.
Further improvements in membrane distillation process and, as a consequence, in water cost, can be achieved through the reduction of the high cost of MD membrane modules. This is due to the fact that, currently, there is a lack of commercially available MD units. The membranes used in most of the MD studies are usually manufactured for other processes (i.e. microfiltration) rather than for MD. The need for new membranes, manufactured especially for MD purposes, have been widely accepted by MD investigators, also if the required features to MD membranes are met with the commercially available membranes. The new membranes should have to improve trans-membrane fluxes, through minimizing of boundary layer heat and mass transfer resistances. Moreover, for potential commercial applications of MD technology, larger membrane modules, with the effective required surface area, should have to be investigated.
Merely through a more intensive and focused research effort both in experimentation and modelling, and through the construction of pilot plants for scale-up studies, it will be possible to have, in future, the production and the commercialization of larger modules, expressly designed for MD applications, characterized by a higher trans-membrane flux and, therefore, by a lower total cost of the process.

7. Analysis of water systems through the use of *Metrics*

The proposed flow-sheets have been analyzed also through the use of the following *metrics* (see *Chapter 3 – section 4* for more details about metrics).

1) $\textbf{Mass intensity} = \dfrac{\textbf{Total mass (seawater + reagents)}}{\textbf{Mass of product (fresh water + salts)}}$;

2) $\textbf{Waste Intensity} = \dfrac{\textbf{Total waste}}{\textbf{Mass of product (fresh water + salts)}}$;

3) $\textbf{Energy Efficiency} = \dfrac{\textbf{Total process energy (electrical + thermal)}}{\textbf{Mass of product (fresh water + salts)}}$.

Table 14 shows the value of the quantitative indicators for the proposed membrane systems.

Table 14: Metrics for the three proposed flow-sheets.

	RO	RO-OX	RO-RO	RO-MD
Mass Intensity [kg/kg]	2,495	2,495	2,663	2,744
Waste intensity [kg/kg]	0,0861	0,0861	0,0921	0,0949
Energy efficiency [MJ/kg]	0,0189	0,0189	0,0236	0,1026
Energy efficiency (a) [MJ/kg]				0,0208
Energy efficiency with Pelton turbine [MJ/kg]	0,0097	0,0097	0,0133	0,0925
Energy efficiency with Pelton turbine (a) [MJ/kg]				0,0107
Cost [$/m^3 fresh water]	0,6143	0,6157	0,7396	0,9670
Cost (a) [$/m^3 fresh water]				0,7969
Cost with Pelton turbine [$/m^3 fresh water]	0,398	0,399	0,499	0,729
Cost with Pelton turbine (a) [$/m^3 fresh water]				0,559

(a) if thermal energy is available in the plant or the stream is already at the operating temperature of the MCr unit.

The achieved results agree with those obtained through the exergetic and economic analyses. In fact they show that thermal energy consumption is one of the items that more influences water cost: in the flow sheets without MD unit, the presence of the Pelton wheel, as Electrical Energy Recovery Device, is sufficient to reduce energy consumption and, then, desalted water cost; in the system with MD, instead, thermal energy is the term that more influences energy cost, in fact the introduction of a Pelton wheel leads to a low reduction of the plant energy efficiency and water desalination cost. In order to observe a substantial reduction in plant energy efficiency and water cost, thermal energy has to be already available in the plant.

8. Conclusions

In this work a variety of membrane processes have been evaluated for their ability to reject both boron and arsenic.

The successful application of membrane technology to the As removal from drinking water will depend upon matching the proper membrane to the characteristics of the feed-water: if arsenic in the feed-water is primarily present as As(III), only RO membranes or tight NF membranes appear to be able to sustain high rates of arsenic; pre-oxidation of As(III) to As(V) followed by NF may achieve high rates of arsenic removal; As(V) can be effectively treated by RO and NF; an integrated NF/RO membrane system, in which the feed water is firstly treated with a NF unit and its permeate is sent to a RO unit, allows to obtain permeate streams with As concentration below the maximum recommended limit also treating feed water with As total concentration equal to 3000 ppb.

In the present work also the potentialities of both MD and an integrated membrane desalination system RO-MD have been analyzed. The experimental tests proved that

MD is a promising technology for the total boron and arsenic removal from water. In fact, by treating polluted aqueous solutions with a MD plant, the obtained permeate samples were completely devoid of the dangerous contaminants. MD operation has another important advantage: it allows total B and As removal from water without the use of chemical agents which results in less environmental impact.
The use of energetic, exergetic and economic analyses have shown that, if the water streams are already available at the temperature needed for carrying out the MD operation or thermal energy is available in the plant, the energy consumption and unit water cost of the RO-MD process decrease reaching competitive values with those of the other processes.
From this analysis, adoption of the integrated membrane systems appears an interesting possibility for improving desalination operations and meeting the increasing pure water demand.

Relevant Bibliography

[1] Environmental Protection Agency (EPA). 1975. *Preliminary investigation of effects on the environment of boron, indium, nickel, selenium, tin, vanadium and their compounds*, vol. 1, Boron. US Environmental Protection Agency Rep. 56/2-75-005A.
[2] T. Goto, *State-of-arts Membrane Technology and Its Problems in Future*, International Forum on Water Industry Qingdao 2005, China, July 2005, 38- 49.
[3] R. Y. Ning, Desalination, *Arsenic removal by reverse osmosis*, 143 (2002) 237-241.
[4] Ming-Cheng Shih, *An overview of arsenic removal by pressure-driven membrane processes*, Desalination, 172 (2005) 85-97.
[5] R. D'Aquino, *Clean Drinking Water-A Tall Order*, CEP Magazine, June (2005) 8-11.
[6] B. K. Mandal, K. T. Suzuki, *Arsenic round the world: a review*, Talanta, 58 (2002) 201-235.
[7] E. O. Kartinen, Jr. and C. J. Martin, *An overview of arsenic removal processes*, Desalination, 103 (1995) 79-88.
[8] E. Drioli, M. Romano, *Progress and new perspectives on integrated membrane operations for sustainable industrial growth*, Industrial and Engineering Chemistry Research, 40 (2001) 1277–1300.
[9] P. Brandhuber, G. Amy, *Alternative methods for membrane filtration of arsenic from drinking water*, Desalination 117 (1998) 1-10.
[10] Ambient Water Quality Guidelines for Boron. British Columbia, Water Protection Branch.
[11] Y. Tomi et. al., *Evolution of RO Membrane for Seawater Desalination*, International Forum on Water Industry Qingdao 2005, China, July 2005, 92- 97.
[12] T. Uemura et al., *Recent Progress on RO Membrane Technology*, International Forum on Water Industry Qingdao 2005, China, July 2005, 72- 83.
[13] M. Bush, W. E. Mickols, *Reducing energy consumption in seawater desalination*, Desalination, 165 (2004) 299- 312.

[14] J. Redondo, M. Busch, J.-P. De Witte, *Boron removal from seawater using FILMTEC^{TM} high rejection SWRO membranes*, Desalination, 156 (2003) 229-238.
[15] http://www.water-technology.net/projects/israel/
[16] http://www.dow.com/liquidseps/news/20050927c.htm
[17] T. Urase et al., Desalination 117 (1998)11-18.
[18] E.M. Vrijenhoek et al., Desalination (2000) 262-277.
[19] Sato Y., Kang M., Kamei T., Magara Y., *Performance of nanofiltration for arsenic removal*, Water Research, 2002, 36, 3371- 3377.
[20] *Reverse osmosis membranes remove arsenic and salt from water supplies*, Koch Membrane Systems Inc., Membrane Technology, 140 (2001) 10-11.
[21] H. Saitua et al., Desalination, 172 (2005) 173-180.
[22] S. Velizavor, Reviews in Environmental Science and Bio/technology 3 (2004) 361-380.
[23] A. Criscuoli, E. Drioli, *Energetic and exergetic analysis of an integrated membrane desalination system*, Desalination, 124 (1999) 243-249.
[24] M. Turek, Desalination, 153 (2002) 173-177.
[25] www.usask.ca/geology/classes/geol 206.

General conclusions

The aim of the work presented in this thesis has been to analyze the potentialities of different integrated membrane systems for seawater desalination and to check, experimentally, the performance of membrane crystallization technology particularly for reducing the brine disposal problem and for increasing the recovery factors of the desalination plant.

In order to reach the first goal, seven different flow sheets have been analyzed. In each of them, except for the first (FS1) constituted only by the RO unit, different membrane operations have been integrated: RO operates on NF permeate in FS2; both MF and NF have been introduced for feed water pre-treatment and load reduction to the following reverse osmosis unit in FS3. In the remaining four flow sheets, at the basis process represented by FS3, a membrane crystallizer (MCr) has been added. It has the task to increase the quantity of desalted fresh water combined to solid salts production: MCr operates on NF brine in FS4, on RO brine in FS5, both on RO and NF brine in FS6. In the last flow sheet (FS7), MCr has been introduced on NF brine while membrane distillation (MD) operates on RO brine.

A first comparison of the achieved results has shown a continuous improvement in the quality of the produced desalted water when membrane operations are used as RO pre-treatment (that means shifting from FS1 to FS3):

- ✓ the presence of MF provides an NF/RO feedwater of good quality in view of lower capital and operating cost;
- ✓ the introduction of NF allows to increase up to 52% the recovery factor of the coupled system NF+RO without scaling problems.

The introduction of a MCr unit as RO post-treatment, on one or on both retentate streams, as well as the presence of MD, has increased plant recovery factor so much to reach 92.8% in FS6, higher than that of a RO unit (about 40%) and much higher than that of a typical MSF (about 10%). However, the presence of MD and/or MCr has allowed not only to increase the recovery factor, but also to extract the salts naturally present in the concentrated streams of the desalination plants thus decreasing brine disposal problem and its negative environmental impacts.

Energetic and exergetic analyses have been used in order to establish, respectively, the energy requirements of the membrane integrated systems and their exergetic efficiency evaluated in terms of entropic losses.

From an energetic point of view, FS1, FS2 and FS3 processes use only electrical energy. The introduction of MCr and/or MD (in FS4, FS5, FS6 and FS7) introduces a thermal energy requirement (PE), due to the retentate flow rate which has to be heated and which increases the global energy demand. However, if the water streams are already available at the temperature needed for carrying out the MCr/MD operation or the thermal energy is available in the plant, than the energy requirements of the last four integrated systems decrease, reaching competitive values with those of the other desalination processes.

The exergetic comparison of the proposed systems has shown that, FS1, FS2 and FS3 exergetic efficiencies are interesting because their entropic losses are moderate with respect to the other flow sheets; in the last four cases, instead, the presence of MCr and/or MD increases exergy destruction. In general, higher is the flow rate to heat, higher are the entropic losses; in fact the total exergy destroyed and transformed in

irreversible production of entropy reaches the highest value in FS6 and FS7, where both retentate streams have to be heated. However, in all the proposed flow sheets the entropic losses are reduced when thermal energy is already available in the plant.
The use of exergy destruction distribution has also allowed to identify the sites of greatest losses in the proposed desalination systems. The primary locations of exergy destruction have been (i) the membrane modules in which the saline water is separated into the brine and the permeate and (ii) the throttling valves where the pressure of liquid is reduced. Meanwhile there is nothing that can be done to eliminate or decrease the exergy lost in the membrane module, the most reasonable and practical way to increase efficiency or reduce the power input of the plant significantly has been shown to be replacing the throttling valves on the brine stream by an energy recovery system (like a Pelton turbine or a pressure exchanger system). These devices lead to a reduction of the energy consumption because they transfer the brine pressure to the low-pressure feed water, while discharging the brine at low pressure. The analysis of the alternative design has been based always on the exergy analysis. It has been seen that the process that more gains profit from the use of an ERD is FS1 because is in this system that the turbine or the pressure exchanger, working with the highest RO retentate flow rate, permits to have the major reduction of energetic requirement. Exergetic efficiencies of the integrated systems with MCr unit are lower than those of the systems without MCr unit; this is due to the increase of exergy inlet because of the thermal exergy necessary to heat the retentate streams.
In any case, exergetic efficiency of membrane desalination systems is greater than that of thermal systems (such as MSF) which are highly irreversible and with exergetic efficiencies in the range 1.12 ~ 10.4% due to the high energy consumption.
The economical evaluation of the analyzed flow sheets has been made in order to determine the unit cost of fresh water produced and the gain for the salts sale. The achieved results have shown that fresh water cost is lower than that of thermal desalination processes (about 1.5 $/m^3) and ranges from 0.39 $/m^3 for FS3 with Pelton turbine like energy recovery system, to 0.74 $/m^3 for FS7 if the gain for the salts sale is not considered. The higher water cost in the integrated system with MCr module is due to the thermal demand of the unit and to the annual membrane replacement cost. In fact, only when thermal energy is available in the plant it is possible to observe a significant reduction in water cost. However, through the use of the MCr, the quality and the quantity of produced crystals are high enough that the gain for the salts sale can cover more than entirely the cost of desalination process, particularly in the case of FS6. Therefore, the overall desalination process becomes very attractive also from an economical point of view.
However, the estimation of water cost and energy saving is an important but not a determining factor for the use of these operations. Some other aspects, such as those related to the environmental impact of the desalination plants, must be considered.

The possibility of designing innovative processes based on the integration of different conventional pressure driven membrane separation units with membrane contactor technology is proved to be quite attractive also as a way for increasing the performance of the water purification processes, in particular for boron (B) and arsenic (As) removal from polluted water. The successful application of membrane technology for the

removal of these pollutants from drinking water depends upon matching the proper membrane to the characteristics of the feed-water:

- ✓ if arsenic in the feed-water is primarily present as As(III), only RO membranes or tight NF membranes appear to be able to sustain high rates of arsenic;
- ✓ pre-oxidation of As(III) to As(V) followed by NF may achieve high rates of arsenic removal;
- ✓ As(V) can be effectively treated both by RO and NF;
- ✓ the application of MD allows to achieve the total boron and arsenic removal from water without the use of oxidant agents which results in less environmental impact;
- ✓ the integrated water treatment system constituted by a RO step followed by a MD stage permits to produce fresh water with boron and arsenic concentration equal or less than the recommended values by EPA and WHO when only 36.4% of RO permeate is treated in the MD unit, while the current water treatment plants use RO systems with two pass-stages where all the 1st stage RO permeate must be treated in the 2nd RO stage.

The comparison of four different membrane based systems for water purification (the first constituted only by RO; the second by a pre-oxidation step followed by a RO operation; the third uses RO systems with two pass-stages; the forth constituted by a RO stage followed by MD) has shown that only the two integrated systems RO-RO and RO-MD allow to obtain fresh water with boron and arsenic concentration below the WHO and EPA maximum recommended values. Moreover, if thermal energy is available in the plant, the energy consumption and the desalted unit water cost of the RO-MD process decrease reaching competitive values with those of the other processes. Therefore, adoption of integrated membrane systems appears an interesting possibility not only for improving desalination operations, but also for meeting the increasing pure water demand.

In the present work, an extensive experimental phase has been also carried out in order to check the good operation of the membrane crystallizer and to test its potentialities for the exploitation of some components contained in seawater. The experimental tests have also allowed to test fluid-dynamic effect on membrane crystallization operation and, in particular, on trend of solvent transmembrane flux and crystals growth rate. Crystals distribution has been characterized by the coefficient of variation (CV) and middle diameter d_m. Moreover, the distribution of crystal dimensions, nucleation and growth rate have been studied as a function of the retention time and slurry density. The kinetic parameters, investigated by using a mathematical model for continuous crystallizers of the mixed-suspension or circulating-magma type, have been joined in a power law relation describing the nucleation rate of the salts as a function of the growth rate and magma density.

The evaporative crystallization of sodium chloride and epsomite from aqueous solution of these salts has been used as vehicle for preliminary experimental study. The interest for NaCl and for $MgSO_4 \cdot 7H_2O$ crystallization is due to the fact that they are involved in sea and brackish water desalination processes.

The achieved results have shown that transmembrane flux increases with retentate flow rate and temperature. Therefore, the time for reaching supersaturation and crystals formation decreases when these parameters rise. The obtained CVs are lower than those

from conventional equipments and are therefore characteristic of narrow crystal size distributions and of qualitatively better products. For what concerns the achieved kinetic parameters, they are in substantial agreement with those reported in literature for conventional crystallizers. Of course, also some small discordances are present because of the differences in the hydraulic characteristics of the compared crystallizers and due to the presence, in the MCr, of a membrane that improves the nucleation process.
Moreover, the experimentally determined crystals growth rate has shown that the presence of other ions accelerate kinetic rate of NaCl crystallization while the presence of humic acid (the main component of the Natural Organic Matter contained in waters) in NF retentate inhibits crystals growth rate.
From here the necessity to optimize the pre-treatment steps in order to control the crystallization kinetics that are linked with the nature and the amount of the foreign species existing in the highly concentrated brines emerging from the NF and RO stages. These substances, besides causing fouling on RO membranes, can easily hinder the crystallization kinetics, thus leading either to the cessation of growth or to the production of a product exhibiting inferior, undesired properties.

In conclusion, the use of membrane crystallization on NF and/or RO brine and the choice of a suitable NF/RO pre-treatment can offer the possibility to utilize the added value of the retentate streams of the desalination plants, increasing plant recovery factor, reducing brine disposal problem and its environmental impact, and producing solid materials of high quality, whose structures, sizes, shapes and habits can be adequate to represent a valuable by-product, transforming the traditional brine disposal cost in a new and potential profitable market. It is expected that, in the next future, all the different available membrane operations, from the more traditional pressure driven units (as RO, NF, UF, MF), to the membrane reactors (MBR), to the membrane contactors (Membrane Distillation and Membrane Crystallizer), will be considered for realizing new integrated water production, purification and reuse processes. These systems are able to solve problems from water quality, to brine disposal, to water costs, to recovery factors, etc. The success of this strategy, however, requires the realization of the complete advanced integrated water system following the *3PE* and *Process Intensification* approach along all the lines, from the RO pre-treatment to the RO post-treatment steps.

Attività scientifica del triennio

SCUOLE

1) Partecipazione alla *XXIII EMS Summer School on Membranes, 3-6 September 2006, Prague.*

LISTA PUBBLICAZIONI su RIVISTE INTERNAZIONALI

1) E. Drioli, E. Curcio, G. Di Profio, F. Macedonio, A. Criscuoli, *Integrating Membrane Contactors Technology and Pressure-Driven Membrane Operations for Seawater Desalination: Energy, Exergy and Cost Analysis*, Chemical Engineering Research and Design, 84 (A3) (2006) 209–220.

2) F. Macedonio, E. Curcio, E. Drioli, *Integrated Membrane Systems for Seawater Desalination: Energetic and Exergetic Analysis, Economic Evaluation, Experimental Study*, Desalination, 203 (2007) 260–276.

3) F. Macedonio, G. Di Profio, E. Curcio, E. Drioli, *Integrated Membrane Systems for Seawater Desalination*, Desalination, 200 (2006) 612-614.

4) F. Macedonio, E. Drioli, *Pressure-driven membrane operations and membrane distillation technology integration for water purification*, Desalination, 223 (2008) 396-409.

5) Efrem Curcio, Sulaiman Al-Obaidani, Francesca Macedonio, Gianluca Di Profio, Silvia Gualtieri, and Enrico Drioli, *Advanced Membrane Systems for Seawater Desalination. Kinetics of Salts Crystallization from RO brines Promoted by Polymeric Membranes*, Korean Membrane Journal, Vol. 17. No 2 June, 2007, 93-98.

6) Al Obaidani S. , Curcio E. , Macedonio F. , Di Profio G. , Al Hinai H. , Drioli E. , *Potential of Membrane Distillation in Seawater Desalination: Thermal Efficiency, Sensitivity Study and Cost Estimation*, Journal of Membrane Science, 323 (2008) 85-98.

7) Annarosa Gugliuzza, Marianna Carmela Aceto, Francesca Macedonio, Enrico Drioli, *Water Droplets as Template for Next-Generation Self-Assembled Poly-(etheretherketone) with Cardo Membranes*, J. Phys. Chem B, 112 (34), 10483-10496, 2008.

CAPITOLI di LIBRI

1) Capitolo dal titolo "Integrated Membrane Operations in Water Desalination", facente parte del libro "Peinemann, Pereira Nunes (Eds.:): Membrane Technology, Vol. 4", casa editrice WILEY-VCH Weinheim, *in press.*

LISTA PUBBLICAZIONI su ATTI di CONVEGNI INTERNAZIONALI

1) Partecipazione a *EuroMed 2006 Desalination Strategies in South Mediterranean Countries, May 21-25, 2006, Montpellier, France*, con il seguente lavoro accettato come *presentazione orale* e pubblicato sugli atti del convegno: *Integrated Membrane Systems for Seawater Desalination: Energetic and Exergetic Analysis, Economic Evaluation, Experimental Study,* F. Macedonio, E. Curcio, E. Drioli.

2) Partecipazione a *Advanced Membrane Technology III: Membrane Engineering for Process Intensification, June 11-15, 2006, Cetraro (Calabria), Italy*, con il seguente lavoro accettato come *poster* e pubblicato sugli atti del convegno: *Integrated Membrane Systems for Seawater Desalination,* F. Macedonio, G. Di Profio, E. Curcio, E. Drioli.

3) Partecipazione a *CHISA 2006, 17th International Congress of Chemical and Process Engineering, 27-31 August 2006, Prague, Czech Republic*, con il seguente lavoro accettato come *presentazione orale* e pubblicato sugli atti del convegno: *Membrane-Based Systems for Seawater Desalination: Analysis and Comparison,* E. Drioli, F. Macedonio, E. Curcio, G. Di Profio.

4) Partecipazione a *Network Young MemBrains, 8th Meeting, September 21 – 23, 2006, University of Calabria, Arcavacata di Rende (Italy),* con la seguente *presentazione orale* pubblicata sugli atti del convegno: *Economical Evaluation and Sustainable Metrics: two techniques for evaluating how much a desalination system is a reliable and sustainable desalination process,* F. Macedonio.

5) Partecipazione a *Euromembrane 2006, 24-28 September 2006, Taormina, Italy,* con il seguente lavoro accettato come poster, pubblicato sugli atti del convegno e con cui è stata *vinta la sessione poster*: *Integrated Membrane Systems for Seawater Desalination,* F. Macedonio, G. Di Profio, E. Curcio, E. Drioli.

6) Partecipazione al *5th Italy-Korea Workshop on "Membranes and membrane Processes for Clean Environment", 29-30 September 2006, Giardini Naxos – Taormina- Italia* con la seguente presentazione orale: *Advanced membrane systems for sea water desalination,* Efrem Curcio, Enrico Drioli, Gianluca Di Profio, Sulaiman Al-Obaidani e Francesca Macedonio.

7) Partecipazione a *ATSE National Symposium, Sidney, Australia, 20-21 November, 2006,* con il seguente lavoro accettato come *presentazione orale* e pubblicato sugli atti del convegno: *New Integrated Water Treatments and Production Modes for City Planning,* F. Macedonio, E. Drioli.

8) Partecipazione a *International Conference and Exhibition on Water & Wastewater Treatment (Asia Pro Eco Project Innowa Results), 01-04 April, 2007, Sylhet, Bangladesh,* con il seguente lavoro accettato come *poster* e pubblicato sugli

atti del convegno: *Membrane Distillation Technology for Water Purification*, F. Macedonio, S. I. Mozumder, T. Uddin, A. Criscuoli, E. Drioli.

9) Partecipazione a *Conference on Desalination and the Environment, Halkidki, Greece, April 22-25, 2007*, con il seguente lavoro accettato come *presentazione orale* e pubblicato sugli atti del convegno: *Pressure-driven membrane operations and membrane distillation technology integration for water purification*, Francesca Macedonio, Enrico Drioli.

10) Partecipazione ad *Asian Conference on Desalination & Water Reuse 2007, Qingdao, China, July 4-6, 2007*, con il seguente lavoro accettato come *presentazione orale* e pubblicato sugli atti del convegno: *Progresses in Integrated Membrane Operations for Desalination and Wastewater Treatment*, Enrico Drioli, Francesca Macedonio.

11) Partecipazione ad *Asian Conference on Desalination & Water Reuse 2007, Qingdao, China, July 4-6, 2007*, con il seguente lavoro accettato come *presentazione orale* e pubblicato sugli atti del convegno: *Membrane Distillation as a Viable Optino for Seawater Desalination,* Efrem Curcio, Sulaiman Al-Obaidani, Francesca Macedonio, Gianluca Di Profio, Enrico Drioli.

12) Partecipazione ad *European Congress of Chemical Engineering (ECCE-6), Copenhagen, Denmark, September 16-20, 2007*, con il seguente lavoro accettato come *keynote* e pubblicato sugli atti del convegno: *Progresses on Seawater Desalination and Wastewater Treatment in the Logic of Process Intensification Strategy*, Enrico Drioli, Francesca Macedonio.

13) Partecipazione ad *IMSTEC 07, The 6th International Membrane Science and Technology Conference, University of New South Wales, Sydney, Australia, November 5 - 9, 2007*, con il seguente lavoro accettato come *keynote* e pubblicato sugli atti del convegno: *Integrated Membrane Systems for Water Treatment*, F. Macedonio, E. Curcio, G. Di Profio, E. Drioli.

14) Partecipazione ad *JDA Forum 2007, Tokyo, Japan, November 12th, 2007*, con il seguente lavoro accettato come *presentazione orale* e pubblicato sugli atti del convegno: *Advanced Membrane Research in Desalination and Water Recycle,* Enrico Drioli, Francesca Macedonio.

15) Partecipazione al *All India Conference on "Zero Effluent Discharge-Latest Development in Recycling", Kolkata, India, December 22-23, 2007*, con il seguente lavoro accettato come *presentazione orale* e pubblicato sugli atti del convegno: *Progresses in Membrane Processes for the Rationalization of Industrial Productions and Waste Water Treatment*, Enrico Drioli, Francesca Macedonio.

16) Partecipazione al 5th Chemical Engineering Conference for Collaborative Research in Eastern Mediterranean Countries, Cetraro, Italia, 24-28 Maggio 2008, con il seguente lavoro accettato come *poster* e pubblicato sugli atti del convegno:

Crystals Recovery from NF Retentate Streams through Membrane Crystallizer Devices, F. Macedonio, Ji Xiaosheng, E. Drioli, E. Curcio, G. Di Profio.

17) Partecipazione a "IFMSTED 2008 Asian-Pacific Conference on Desalination & Water Reuse", Qingdao, China, May 28-30, 2008, con il seguente lavoro accettato come *presentazione orale* e pubblicato sugli atti del convegno (pp. 326-329): *MF/NF/RO and Membrane Crystallizers for seawater desalination,* F. Macedonio, E. Curcio, G. Di Profio, E. Drioli.

18) Partecipazione a Membranes in Drinking Water Production and Wastewater Treatment, Toulouse, France, October 20-22, 2008, con il seguente lavoro accettato come *presentazione orale* e pubblicato sugli atti del convegno: *Experimental and economical evaluation of a membrane crystallizer plant,* F. Macedonio, E. Drioli, E. Curcio, G. Di Profio.

LISTA PUBBLICAZIONI su ATTI di CONVEGNI NAZIONALI

1) Partecipazione al Convegno GR.I.C.U. 2008, Le Castella (KR), Italia, 14 - 17 Settembre 2008, con il seguente lavoro accettato come *poster* e pubblicato sugli atti del convegno: ***Applicazione dei Sustainable Metrics per l'Analisi dei Sistemi nella Logica del Process Intensification***, F. Macedonio, E. Drioli.

PREMI

- ✓ Award for poster presentation, ricevuto nel corso della conferenza *Euromembrane 2006, 24-28 September 2006, Taormina, Italy* per il seguente lavoro: *Integrated Membrane Systems for Seawater Desalination,* F. Macedonio, G. Di Profio, E. Curcio, E. Drioli.

ALTRE ATTIVITA' di ORGANIZZAZIONE e RICERCA SCIENTIFICA

- ✓ Coinvolta nelle attività di ricerca nell'ambito del progetto *Membrane-Based Desalination: An Integrated Approach (acronym MEDINA)*, finanziato dall'Unione Europea nell'ambito del 6th Framework Program come Specific Targeted Research Project, presso il Dipartimento di Ingegneria Chimica e dei Materiali, Università della Calabria, Rende (CS).

- ✓ Coinvolta nelle attività di ricerca nell'ambito del progetto *Expanding membrane macroscale applications by exploring nanoscale material properties (acronym NanoMemPro)*, finanziato dall'Unione Europea nell'ambito del 6th Framework Program come NoE, presso l'ITM-CNR c/o Università della Calabria, Rende (CS).